UNIVERSITY OF SOUTHAMPTON

FACULTY OF NATURAL AND ENVIRONMENTAL SCIENCES

School of Ocean and Earth Sciences

On the use of sunlight by the ocean's most abundant inhabitants

by

Samuel Louis Lew

Thesis for the degree of Doctor of Philosophy

July 2015

ABSTRACT

On the use of sunlight by the ocean's most abundant inhabitants

By Samuel Louis Lew

The two most abundant organisms in the ocean, the microbes *Prochlorococcus* (Pro) and SAR11, can harvest and use sunlight in a way that deviates from our conventional understanding of light use, i.e. for photosynthesis. Pro can not only photosynthesise but can also enhance the uptake of dissolved organic material using sunlight through a process called photoheterotrophy. SAR11 is also a photoheterotroph but cannot perform photosynthesis. This thesis aims to explore the importance of photoheterotrophy for Pro and SAR11 growth.

Models of individual Pro and SAR11 cells have been built and parameterised that allow for an investigation into the benefits that photoheterotrophic light use may confer to the growth of these organisms.

The results from the model suggest that the ability to partition harvested solar energy between photosynthesis and photoheterotrophy in Pro can increase growth rate by up to ~50 % relative to an equivalent cell that cannot perform photoheterotrophy. Photoheterotrophy increases Pro growth rate over a broad irradiance range and allows it to grow in nitrogen limiting conditions that are characteristic of the ecosystems it dominates. SAR11 also benefits from the ability to enhance nutrient uptake through photoheterotrophy. The growth rate of SAR11 increases by up to ~20 % relative to an equivalent heterotroph, with the effect being critically dependent on ambient conditions. Photoheterotrophy also significantly influences the processing of carbon and nitrogen by Pro and SAR11.

Despite the significant increases in growth rate that photoheterotrophy provides for Pro, it is of secondary importance for growth compared to the ability to acquire carbon through photosynthesis. Although photoheterotrophy results in significant increases to SAR11 growth rate in certain conditions, the advantages that being small and irregular in shape confer on nutrient harvesting ability and growth outweigh the benefits of photoheterotrophy.

Nevertheless, the results from this thesis suggest that future ecosystem models based on systems dominated by Pro and SAR11 would benefit by including photoheterotrophy.

Table of Contents

List of tables

List of figures

DECLARATION OF AUTHORSHIP

I, **Samuel Louis Lew**

declare that this thesis and the work presented in it are my own and has been generated by me as the result of my own original research.

On the use of sunlight by the ocean's most abundant inhabitants

I confirm that:

1. This work was done wholly or mainly while in candidature for a research degree at this University;
2. Where any part of this thesis has previously been submitted for a degree or any other qualification at this University or any other institution, this has been clearly stated;
3. Where I have consulted the published work of others, this is always clearly attributed;
4. Where I have quoted from the work of others, the source is always given. With the exception of such quotations, this thesis is entirely my own work;
5. I have acknowledged all main sources of help;
6. Where the thesis is based on work done by myself jointly with others, I have made clear exactly what was done by others and what I have contributed myself;
7. None of this work has been published before submission

Signed: .....

Date:.....

Acknowledgements

I would like to express my deepest gratitude to Adrian Martin for his supervision throughout this project. Adrian's endless enthusiasm, patience and knowledge of the marine realm and beyond have been instrumental in the progress of this research. It has been a true privilege to learn and work under his guidance. Many thanks to Mike Zubkov for the opportunity to work within his laboratory group and for the chance to go to sea on board the D369 research cruise. I am also grateful to Tom Anderson for his guidance and advice for the development of the model.

I would also like to express my thanks to friends and family. In particular to my poor old mum for clearing out the spare room and putting me up/putting up with me for the last few months so that I could finish writing this thesis. Thanks mum for your love and support throughout this adventure. To the ladies and gents in the office, Simon, Roz, Katsia, Chris and Sian, thanks for the coffee and cake breaks, fun times and friendship.

I am also grateful to the National Environmental Research Council for funding this project.

Abbreviations

Pro – *Prochlorococcus*

DIN – Dissolved inorganic nitrogen

DIC – Dissolved inorganic carbon

DOC– Dissolved organic carbon

DON - Dissolved organic nitrogen

DOM – Dissolved organic material

CHO - Carbohydrate

AA – Amino acid

ON – Organic nitrogen

OC – Organic carbon

DFAA – Dissolved free amino acids

DEB – Dynamic Energy Budget theory

SU – Synthesising unit

MM – Michaelis-Menten

Chl-a – divinyl chlorophyll-a and chlorophyll-b

PR - Proteorhodopsin

BGE – Bacterial growth efficiency

NRE – Nitrogen regeneration efficiency

CGE – Carbon growth efficiency

β_{opt} – Optimum light investment for maximum growth rate

Chapter 1: Introduction

1.1. General introduction

The ocean's two most abundant inhabitants, the photosynthetic cyanobacteria *Prochlorococcus (Pro)* (Chisholm et al., 1988) and alphaproteobacteria SAR11 (Giovannoni et al., 1990), thrive in and numerically dominate the subtropical gyres (Chisholm et al., 1988, Morris et al., 2002). These regions have characteristically low nutrient concentrations and are often described as ocean deserts. How then do these organisms do so well? And what physiological strategies do they employ that are essential to their success? Perhaps importantly, both use solar energy in a way that diverges from our conventional understanding for how sunlight is used in the ocean. Typically we think of photosynthesis, fixing carbon dioxide and evolving oxygen. Pro and SAR11, however, can use solar energy to enhance the uptake of dissolved organic materials (DOM) through a process termed photoheterotrophy. It is possible that this strategy for nutrient acquisition sets them apart from other non-photoheterotrophic microbes, allowing them to thrive in subtropical ecosystems.

The aim of this study is therefore to answer three questions;

1] How does photoheterotrophy potentially influence Pro and SAR11 growth?

2] What are the consequences of photoheterotrophy for their processing of key elements?

3] How do their other physiological strategies augment photoheterotrophy to assist in their survival?

A modelling approach is employed to answer these questions.

Chapter 1 describes the environment which these organisms dominate. It then provides an overview of photoheterotrophy and introduces the study organisms, Pro and SAR11. Evidence of their photoheterotrophic metabolism will be provided. An argument is then given for why a modelling approach is essential to understand how photoheterotrophy sets them apart from other non-photoheterotrophic microbes and what modelling approach is best suited to this task. Finally the aims of this study are presented.

1.2. Subtropical gyres

The subtropical gyres are the largest ecosystems within each ocean basin. Collectively they cover ~40 % of the planet's surface and are expanding (Polovina et al., 2008). Much of the data available to constrain the model, introduced in Chapter 2, is collected from physiological

studies of Pro and SAR11 in the North Atlantic subtropical gyre (Section 2.3). Results, however, can be generalised to all of the subtropical gyres where Pro and SAR11 abound and photoheterotrophic metabolism is evident (Section 1.3).

Anticyclonic wind systems result in the convergence of surface water and downwelling in the subtropical gyres (Sarmiento, 2013). In these warm subtropical regions, near permanent stratification with minimal seasonal forcing acts to restrict the vertical enrichment of the surface sunlit ocean with deep ocean inorganic nutrients. Vertical nutrient supply would otherwise occur due to vertical mixing as a result of wind driven circulation and buoyancy forcing. The combined influence of downwelling and restricted mixing in the subtropical gyres results in a characteristic low nutrient regime. As a result, regenerated nutrients predominate over "new" nutrients. This has led to the term oligotrophic, from the Greek *oligos* meaning "little" and *trophe* meaning "nourishment". Although seasonal changes in nutrient concentrations are small relative to coastal and temperate systems, the subtropical gyres nevertheless display some intrinsic seasonality in dissolved inorganic nitrogen (DIN) and dissolved organic material (DOM) concentrations that may partially drive seasonal changes in the microbial community structure (Giovannoni and Vergin, 2012). Irradiance intensities in the subtropics are some of the highest on Earth. It is, therefore, perhaps not surprising the microbes have developed strategies to exploit this abundant resource (Béjà and Suzuki, 2008).

1.3. The use of sunlight and photoheterotrophy by marine prokaryotes

Sunlight is the primary source of energy that supports life on Earth. The conversion of solar energy to chemical bond energy through photosynthesis is generally considered to be the primary pathway for solar energy use and has received the most scientific attention. Roughly half of global carbon reduction happens in the oceans, mainly through the activity of photosynthetic single cell eukaryotes and prokaryotes (Field et al., 1998), with Pro making a significant contribution (Zubkov, 2014, Hartmann et al., 2014, Goericke and Welschmeyer, 1993). A growing body of scientific literature, however, demonstrates that the classic view of photosynthesis may be too narrow a definition to explain the importance and diversity of solar energy use in marine prokaryotes. Many of them appear to have evolved mechanisms to harvest and use the sun's energy for enhancing their metabolism that are different from our classic view of photosynthesis (Zubkov, 2009, Béjà and Suzuki, 2008, Zehr and Kudela, 2009, Bryant and Frigaard, 2006, Karl, 2014). Photoheterotrophy is one such mechanism, where sunlight is used as an energy source in addition to the use of organic compounds for carbon and energy (Zubkov, 2009, Béjà and Suzuki, 2008).

Photoheterotrophy is a ubiquitous feature of the oligotrophic subtropical oceans (Church et al., 2004, Church et al., 2006, Mary et al., 2008b, Gómez-Pereira et al., 2012, Evans et al., 2015, Duhamel et al., 2012, Michelou et al., 2007). It is typically assessed by measuring the light-mediated uptake rate of radiolabelled DOM by bulk bacterioplankton populations (Church et al., 2004, Church et al., 2006) or by specific microbial groups, separated using flow cytometry (Mary et al., 2008b, Gómez-Pereira et al., 2012, Evans et al., 2015). Various compounds are used as tracers to assess the importance of heterotrophy for satisfying specific metabolic requirements. For example, nucleotides are used as a measure of nucleic acid synthesis (Church et al., 2004), amino acids are measured for protein synthesis (Gómez-Pereira et al., 2012, Evans et al., 2015, Mary et al., 2008b, Church et al., 2006) and ATP for phosphorous and cellular energy (Evans et al., 2015, Gómez-Pereira et al., 2012, Duhamel et al., 2012).

The marine photoheterotrophic prokaryotes have been divided into three groups. The first contains both the photoautotrophic chlorophyll containing cyanobacteria of the genera *Synechococcus* (Syn) (Waterbury et al., 1979) and Pro. Pro and Syn not only reduce carbon photosynthetically but also operate as heterotrophs and can use solar energy to enhance the uptake of DOM (Mary et al., 2008b, Gómez-Pereira et al., 2012, Evans et al., 2015, Duhamel et al., 2012, Michelou et al., 2007). The second group is the proteorhodopsin containing bacteria, including the most abundant marine prokaryote SAR11 (Giovannoni et al., 2005a, Morris et al., 2002). These cells use a retinal containing opsin which functions as a light driven proton pump (Beja et al., 2000, Beja et al., 2001) generating an electrochemical gradient that can drive ATP synthesis, used for organic molecule uptake and growth (Lami et al., 2009, Gómez-Consarnau et al., 2010, Gómez-Consarnau et al., 2007, Mary et al., 2008b, Gómez-Pereira et al., 2012, Evans et al., 2015). The third group is the bacteriochlorophyll containing bacteria (Shiba et al., 1979, Kolber et al., 2001). Despite the presence of chlorophyll based pigments, these cells cannot reduce carbon dioxide photosynthetically. This group uses solar energy to generate ATP for use in multiple cellular functions including DOM uptake (Yurkov and Beatty, 1998).

Although photoheterotrophic marine prokaryotes within the bacteriochlorophyll containing group are widely distributed and metabolically significant (Béjà and Suzuki, 2008, Kolber et al., 2001, Kolber et al., 2000), Pro and SAR11 are the focus of this study. This is due to their abundance, metabolic significance and the observation that all light stimulated uptake of DOM in the North and South Atlantic subtropical gyre bacterioplankton communities can be attributed to them (Mary et al., 2008a, Gómez-Pereira et al., 2012, Evans et al., 2015). Pro and SAR11 are more fully discussed in Section 1.5.1 and 1.5.2.

Research conducted at Station ALOHA confirmed the presence of photoheterotrophic metabolism in the North Pacific subtropical gyre bacterioplankton communities and that light may play a significant role in not only primary but also secondary production (Church et al., 2004, Church et al., 2006). Light stimulated uptake of leucine appears to function over a broad depth range in these waters. The greatest influence of light on leucine uptake occurred at ~125 m where irradiance is ~ 5 % that found at the surface, and is coincident with the deep chlorophyll maximum (Church et al., 2006). This indicates that dissolved free amino acids (DFAA) and photoheterotrophic metabolism may be more important to bacterioplankton cells at depths where light is limiting and that photosynthetic pigments may be involved in this process (Church et al., 2006).

Differences in the physiological response of populations to irradiance in the upper (5-45 m) and sub-surface (75-125 m) water column was also noted. Surface populations appear better equipped to harvest solar energy for photoheterotrophy at high irradiance with minimal photoinhibition. Populations from deeper in the water column can harvest sufficient solar energy for photoheterotrophy at low irradiance but photo-inhibit at irradiances where surface populations thrive (Church et al., 2004). This photophysiological dynamic closely resembles the adaptive response to vertically changing irradiance in high and low light Pro ecotypes (Moore and Chisholm, 1999, Moore et al., 1998). As Pro dominate these waters numerically (Church et al., 2006) and can effectively compete for DFAA (Zubkov et al., 2003), it was suggested that Pro may play a critical role in the observed photoheterotrophy, although other phototrophic microbes may also play a part. In these microbial populations DFAA uptake plotted against irradiance follows the classic photosynthetic-irradiance non-linear curve suggesting that the observed uptake is a direct photophysiological response (Church et al., 2004). This is discussed in greater detail in Section 1.4.

Physiological analysis of bulk and group specific bacterioplankton populations has demonstrated that photoheterotrophy is also a common feature in both the North (Mary et al., 2008b, Gómez-Pereira et al., 2012) and South Atlantic subtropical gyres (Evans et al., 2015, Michelou et al., 2007). The degree to which light stimulates DFAA uptake is also, like in the North Pacific, critically dependent on irradiance intensity and can occur at low light (Evans et al., 2015). In the South Atlantic subtropical gyre, the rates of light stimulated uptake of ATP, leucine and methionine increase with irradiance intensity although the effect varied with substrate type (Evans et al., 2015). A direct relationship between light enhanced uptake and irradiance could not, however, be established. Increases in the rates of substrate uptake through photoheterotrophic light use were not always proportional to increases in irradiance

intensity, suggesting a threshold for solar energy use in photoheterotrophic metabolism (Evans et al., 2015). Importantly it appears that Pro and SAR11 both account for all light stimulated uptake of DFAAs in these regions. This is discussed in Sections 1.5.1 and 1.5.2.

It should be noted that photoheterotrophy in prokaryotes has been observed in a wide range of environments including temperate productive waters of the North Atlantic (Cottrell et al., 2008, Straza and Kirchman, 2011, Michelou et al., 2007), Arctic ecosystems (Cottrell and Kirchman, 2009) and freshwater lakes (Martinez-Garcia et al., 2012). Photoheterotrophy may therefore have global and regional significance (Paerl, 1991) and should be considered more widely when evaluating the biological and biogeochemical significance of sunlight (Evans et al., 2015).

1.4. Alternative mechanisms for light-stimulated secondary production

It is important to rule out other mechanisms that may result in light stimulated secondary production. Photolytic alteration of organic matter by ultra-violet (UV) radiation has been shown to convert refractory DOM into to labile DOM available for uptake by bacterioplankton (Obernosterer et al., 1999). Church et al. (2004) ruled out this mechanism to explain light-stimulated DFAA uptake as experimental procedures screened ultra-violet radiation. Additionally, Church et al. (2006) argued against this mechanism as light enhanced uptake in their experiments was observed only for leucine and not thymidine. Differential light stimulated uptake by distinct groups within the mixed bacterioplankton samples could not, however, be ruled out (Béjà and Suzuki, 2008). In addition, UV radiation has been shown to convert refractory DOM to labile DOM in the deep euphotic zone and labile DOM to refractory DOM in surface waters (Benner and Biddanda, 1998). It is therefore unlikely that UV conversion of DOM explains light stimulated uptake of DFAA throughout the euphotic zone of subtropical oligotrophic waters.

Tight coupling between primary and secondary bacterial production through the uptake of DOM of photosynthetic origin by heterotrophic or mixotrophic bacterioplankton has also been ruled out (Church et al., 2004, Church et al., 2006). It is unlikely that Pro would respond to light stimulated production of DOM by primary producers as it is one. Additionally, leucine and thymidine uptake should be equally as affected in light but are not (Church et al., 2004). The rapid (within 30 minutes) response of mixed and group specific bacterioplankton to light versus dark incubations suggests that light stimulated uptake of DFAA is a direct photophysiological response (Gómez-Pereira et al., 2012). It is therefore probable that

photoheterotrophic prokaryotes that dominate oligotrophic gyres are responsible for the observed light stimulated secondary production (Church et al., 2004, Church et al., 2006).

1.5. Organisms of interest

1.5.1. *Prochlorococcus*

1.5.1.1. A brief introduction to *Prochlorococcus*

The prokaryotic *Prochlorococcus sp*. are the smallest, most abundant, oxygen-evolving photosynthetic organisms on Earth (Chisholm et al., 1988). They numerically dominate the oligotrophic gyres, have a ubiquitous distribution along a latitudinal band between 40°S (Partensky et al., 1999), and as far as 47°N in studies of the Atlantic Ocean (Zubkov et al., 1998) and occupy depths down to 200 meters at approximately 1 % surface irradiance (Partensky et al., 1999).

Pro are obligate photoautotrophs, using photosynthesis as the primary pathway for carbon acquisition (Zubkov, 2014) although alternative heterotrophic pathways have been suggested (del Carmen Muñoz-Marín et al., 2013). Pro strains utilise various components of the DIN pool for a significant fraction of total cellular nitrogen (Garcia-Fernandez et al., 2004, García-Fernández and Diez, 2004, Casey et al., 2007) but also supplement nitrogen metabolism through the uptake of dissolved organic nitrogen (DON) (Zubkov et al., 2003) photoheterotrophically (Mary et al., 2008b, Gómez-Pereira et al., 2012, Evans et al., 2015). Hence they are mixotrophs.

1.5.1.2. Photoautotrophy in *Prochlorococcus*

It has been argued that the subtropical gyres may account for over 30 % of total marine primary production (Longhurst et al., 1995). Pro are the most abundant (Chisholm et al., 1988) and efficient (Hartmann et al., 2014) photosynthesisers in these ecosystems, contributing significantly (25 % - 80 %) to gyre primary production (Goericke and Welschmeyer, 1993, Liu et al., 1997, Zubkov, 2014, Hartmann et al., 2014, Liu et al., 1999, Liu et al., 1998).

1.5.1.3. Photoheterotrophy in *Prochlorococcus*

Pro strains possess several amino acid transporter systems within a highly streamlined genome (Rocap et al., 2003). This indicates that labile DFAA may be important to Pro survival (Zubkov et al., 2003) otherwise the ability for DFAA uptake would have been lost. Investigations into this mode of nutrient acquisition have demonstrated that Pro operate as photoheterotrophs in the North (Mary et al., 2008b, Gómez-Pereira et al., 2012) and South (Evans et al., 2015) Atlantic subtropical gyres and the North and South Pacific subtropical gyres (Duhamel et al.,

2012). In oligotrophic regions of the Arabian Sea and South Atlantic it is understood that Pro populations account for up to a third of total methionine turnover by total bacterioplankton (Zubkov et al., 2003, Zubkov and Tarran, 2005). Nitrogen assimilation via heterotrophy is an important part of Pro metabolism, and it is clear that Pro are effective competitors within the bacterioplankton community (Zubkov et al., 2003) .

Pro use solar energy to enhance the uptake of a range of DOM materials including leucine (Mary et al., 2008b, Evans et al., 2015, Michelou et al., 2007), methionine (Mary et al., 2008b, Gómez-Pereira et al., 2012) and ATP (Gómez-Pereira et al., 2012, Evans et al., 2015, Duhamel et al., 2012). Depending on the study region and the specific organic nutrient studied, the percentage increase in uptake in the light compared to dark incubations for Pro cells varies between 3 % and 50 %. An average of 20-30 % stimulation appears common (Mary et al., 2008b, Gómez-Pereira et al., 2012).

Depth related changes in the uptake of DFAA in distinct Pro populations can provide insights the importance of light availability for their heterotrophic metabolism. Pro ecotypes vertically partition the water column based partially on their light harvesting physiologies (Moore and Chisholm, 1999, Moore et al., 1998). It has been demonstrated that DFAA uptake in this genus is influenced by depth (Zubkov et al., 2004a). Cell specific methionine uptake rates are 4 times higher in ecotypes experiencing low light at depth (low light (LL) ecotypes) than surface ocean ecotypes experiencing high light (high light (HL) ecotypes), only partially explained by the greater biomass of the former. Population uptake rates showed HL cells consume a quarter of the amino acid pool, decreasing with depth, possibly due to light limiting conditions slowing metabolic activity. LL cells, however, consume half the amino acid pool at depth (Zubkov et al., 2004b). It is estimated that at a Pro population division rate of 0.15 d^{-1}, DFAA might account for 45 % and 75 % of HL and LL biomass, respectively, further highlighting the importance of this resource in nitrogen limiting oceanic regions (Zubkov et al., 2004a).

Ocean microbes respire only a small fraction of DFAAs that are taken up heterotrophically (Hill et al., 2013). It is, therefore, likely that these compounds are primarily used for protein synthesis and influence growth rate. However, it remains to be established quantitatively how the uptake of DFAA through photoheterotrophy influences the growth rate of Pro. This is discussed in greater detail in Section 1.6.

1.5.1.4. Light harvesting and a trade-off for solar energy use in *Prochlorococcus*

Pro have a twin light harvesting photosystem, typical of oxygenic phototrophs, and are capable of directing harvested solar energy to photosynthesis (non-cyclic electron flow) or channelling

this energy to other cellular processes (for example, via cyclic electron flow) (White, 2007). It is understood that some phototrophs with twin photosystems can actively and flexibly regulate (Wilken et al., 2014) and partition (Zehr and Kudela, 2009) harvested solar energy between metabolic processes, conceivably to optimally balance cellular energy to maximise fitness (Zubkov, 2009). As a Pro cell would be limited by the amount of light energy it can harvest using its pigments at a moment in time, directing energy to the uptake DOM would be at the expense of CHO synthesis. It is arguable that a dynamic trade-off for solar energy use exists within the cell, but no direct evidence exists as yet for Pro. The ability of Pro to use harvested solar energy for photosynthesis and to enhance the uptake of nitrogen rich compounds photoheterotrophically, could relieve the limitation of DIN on strictly photoautotrophic growth, explaining the paradox of relatively high phytoplankton production by Pro in nitrogen depleted ecosystems (Zubkov, 2014, Goericke and Welschmeyer, 1993, Paerl, 1991).

1.5.2. SAR11

1.5.2.1. A brief introduction to SAR11

Cells within this ubiquitously distributed clade are the most abundant heterotrophs in the global ocean and exceed the abundance of all other microbes in the oligotrophic subtropical gyres, representing up to 50 % of the total prokaryote community (Morris et al., 2002, Giovannoni et al., 2005b).

The SAR11 clade have complex nutritional requirements (Carini et al., 2012, Tripp, 2013) but are described as obligate heterotrophs with phototrophic capacity (Giovannoni et al., 2005b), and are highly adapted to extreme oligotrophic conditions (Carini et al., 2012). Oceanic SAR11 source carbon through the uptake of organic acids such as pyruvate from the dissolved organic carbon (DOC) pool (Schwalbach et al., 2010, Tripp, 2013), and acquire carbon and nitrogen from DON compounds, primarily DFAA (Malmstrom et al., 2005). It is also highly likely that oceanic SAR11 utilise multiple components from the DIN pool as sources of nitrogen (Sowell et al., 2008).

1.5.2.2. Heterotrophy in SAR11

SAR11 are not only abundant but also highly metabolically active and turnover a large fraction of the DOM pool in oligotrophic (Malmstrom et al., 2004, Mary et al., 2006) and other more productive regions (Mary et al., 2006, Malmstrom et al., 2005). In fact, their processing of multiple components of the DOM pool is often greater than would be expected based on abundance alone (Malmstrom et al., 2005, Malmstrom et al., 2004). For example, in the

oligotrophic Sargasso Sea, SAR11 represent ~25 % of the total prokaryote bacterioplankton community and of this population, 67-85 % are actively assimilating DFAA compared to only 31-35 % of the rest of the prokaryote community (Malmstrom et al., 2004). In addition, although single celled metabolic activity is highly variable, SAR11 individuals appear to be more active than the rest of the bacterioplankton community (Malmstrom et al., 2004). It was estimated that if measurements of DFAA assimilation in SAR11 are representative of their total DOM use, which to first order is reasonable as SAR11 preferentially use DFAA over dissolved organic proteins and other forms of dissolved organic carbon (DOC) (Malmstrom et al., 2005), then as bacterioplankton process roughly 50 % of oceanic primary productivity, SAR11 may process 15-25 % of fixed carbon globally in surface waters (Malmstrom et al., 2004).

1.5.2.3. Photoheterotrophy in SAR11

Light and specifically photoheterotrophic metabolism plays an important part in the acquisition of DOM by SAR11 in the oligotrophic oceans (Evans et al., 2015, Mary et al., 2008b, Gómez-Pereira et al., 2012). SAR11 uses harvested solar energy to enhance the uptake of multiple components of the DOM pool including leucine (Mary et al., 2008, Evans et al., 2015, Michelou et al., 2007), methionine (Mary et al., 2008b, Gómez-Pereira et al., 2012) and ATP (Evans et al., 2015, Gómez-Pereira et al., 2012) in regions of the North and South Atlantic oligotrophic gyres. Uptake of these compounds is typically enhanced by 20-30 % in light incubations compared to dark (Gómez-Pereira et al., 2012, Mary et al., 2008b) but can be as little as 7 %. The percentage increases in uptake are dependent on substrate type (Evans et al., 2015).

It is reasonable to assume that the uptake of DFAA is for use in protein synthesis as little is respired (Hill et al., 2013) and that light enhanced uptake of DFAA may therefore increase SAR11 growth rate. Although one study found that the intrinsic growth rate of SAR11 populations in batch culture grown in continuous darkness was not significantly different to when grown in a light:dark cycle (Giovannoni et al., 2005b); it has been argued that the culture media may have been replete in organic material and that energy demands were already satisfied through oxidative phosphorylation in both light and dark conditions (Zubkov, 2009). Analyses of SAR11 populations in Atlantic coastal waters has shown that their intrinsic growth rate is significantly enhanced in light:dark cycle incubations compared to continuous darkness (Lami et al., 2009). It is yet to be established therefore how photoheterotrophy in SAR11 and specifically the light enhanced assimilation of DOM influences the intrinsic growth rate of populations living in the subtropical gyres.

1.5.2.4. Light harvesting and a trade-off for solar energy use in SAR11

The presence of proteorhodopsin (PR) in SAR11 (Giovannoni et al., 2005a) is probably linked to the ability of the cells to enhance the uptake of DOM in the presence of sunlight (Gómez-Pereira et al., 2012). PR is a light absorbing pigment and is structurally similar to bacteriorhodopsin (Beja et al., 2000). The absorption of a photon of light by PR causes conformational changes in the structure of the pigment and results in the transport or 'pumping' of a proton across the membrane. This generates a potential that drives ATP synthesis via the membrane bound H^+-ATPase (Beja et al., 2001), shown to promote SAR11 survival during starvation conditions (Steindler et al., 2011) and conceivably the active transport of DOM (Zubkov, 2009). PRs can be considered as the prokaryote equivalents to chloroplasts and mitochondria combined (Zubkov, 2009).

It is thought that SAR11 can utilise this proton gradient to enhance the uptake of DOC and/or DON. The argument for this assumption is as follows. It is observed that SAR11 enhances the uptake of DON in the presence of sunlight, relative to dark conditions (Mary et al., 2008b, Gómez-Pereira et al., 2012, Evans et al., 2015). In terms of DOC uptake, uniquely, oceanic strains of SAR11 cannot breakdown glucose, instead utilising organic acids (Schwalbach et al., 2010). As a result, the assumption that DOC (as glucose) is abundant relative to available nitrogen in subtropical ecosystems may not be relevant to SAR11 in terms of bioavailability. In addition to the observation of carbon limited bacterioplankton growth in the Sargasso Sea (Carlson and Ducklow, 1996) where SAR11 dominates the community (Morris et al., 2002), it is conceivable that DOC may at times limit SAR11 growth. The cell may therefore benefit from the ability to enhance DOC uptake photoheterotrophically. As a SAR11 cell would be limited by the amount of energy it can harvest from sunlight by PRs at a moment in time, directing energy to the uptake of one resource would be at the expense of another. A trade-off would therefore exist for the use of harvested solar energy by PRs for the photoheterotrophic uptake of DOC and DON in SAR11.

1.5.3. Achieving similar growth rates using distinct physiological strategies

Pro and SAR11 come from different evolutionary backgrounds (Chisholm et al., 1988, Giovannoni et al., 2005b) and despite significant differences in size and shape (Rappé et al., 2002, Partensky et al., 1999), carbon acquisition strategy (Partensky et al., 1999, Schwalbach et al., 2010), elemental requirements for growth (Bertilsson et al., 2003, Grob et al., 2013), light harvesting system (Partensky et al., 1999, Giovannoni et al., 2005a) and diel growth period (Giovannoni et al., 2005b, Zubkov, 2014), both have remarkably similar specifc growth rates

(Goericke and Welschmeyer, 1993, Malmstrom et al., 2005, Zubkov, 2014, Giovannoni et al., 2005b) and coexist and dominate the subtropical gyres in near equal abundance (Treusch et al., 2009). It is recognised, however, that their ecological niches also overlap, competing for DIN (Garcia-Fernandez et al., 2004, García-Fernández and Diez, 2004, Sowell et al., 2008) and DON and using light photoheterotrophically (Mary et al., 2008a, Gómez-Pereira et al., 2012, Evans et al., 2015). A question asked in this thesis is, how do these physiological differences balance if they have equal growth rates?

1.6. Using a model to explore photoheterotrophy

Examining the influence that photoheterotrophic light use may have on Pro growth rate empirically is challenging. A Pro cell is an obligate phototroph, requiring irradiance to survive. It is therefore not possible to compare population growth rates grown in light:dark and dark:dark cycle incubations to understand the influence of light on heterotrophic metabolism, a method used to determine the influence of photoheterotrophy on SAR11 growth rate (Giovannoni et al., 2005b). Distinguishing between the uses of solar energy in Pro is also problematic due to the difficulties in measuring energy harvesting and storage in bacterioplankton (Zubkov, 2009). Furthermore, controlling the presence/absence of organic material in cultures to test for the influence of heterotrophic uptake on growth alone is not possible using current methods (García-Fernández and Diez, 2004).

For SAR11, investigations in the field (Lami et al., 2009) and culture experiments (Giovannoni et al., 2005b) show varying results for the influence that photoheterotrophic metabolism has on growth rate. In addition, due to the difficulties in quantifying energy harvesting and storage (Zubkov, 2009), changes in the growth rate of SAR11 in the presence/absence of irradiance cannot easily be attributed to specific physiological processes, which may include the light enhanced uptake of DOM (Gómez-Pereira et al., 2012, Mary et al., 2008a, Evans et al., 2015) and/or carbon respiration substituted by phototrophic ATP synthesis (Steindler et al., 2011).

In order to understand the influence that photoheterotrophic resource acquisition has on the growth rate of Pro and SAR11, a modelling approach is therefore ideal. Synthesising available information in a coherent physiological framework can provide a platform for an investigation into how observed changes in resource acquisition through photoheterotrophic light use influences the growth rate of Pro and SAR11 and the consequence for the processing of key elements.

Dynamic energy budget (DEB) theory is a modelling framework that aims to capture the quantitative rules for the uptake and use of resources that are common to individual organisms, based on first principles (Kooijman, 2010). The same basic model structure is, therefore, theoretically applicable to all organisms. Physiological differences between similar organisms are then represented by species specific parameter values and not model structure (Kooijman, 2010). This general theory has been supported by wide spread empirical patterns in nature (Sousa et al., 2010) and well tested in various fields in biology (Kooijman, 2010).

DEB theory provides a "standard" model for an individual that specifies the dynamic change in metabolism throughout the life cycle, related to the uptake of a resource, assimilation into a reserve and then use for maintenance, growth, development, and reproduction (Kooijman, 2010). Chemical stoichiometry associated with transformations between processes are specified based on biochemical theory and adhere to mass conservation laws. Extensions of the standard DEB model have been built to accommodate, for example, multiple resource types and metabolic excretion products (Kooijman, 2010).

A key component of the DEB framework is the synthesising unit (SU), which controls the rate of biochemical reactions depending on the arrival rates of substrates, stoichiometry of the transformation and behaviour of the substrate interaction with the reaction machinery. The specification that production by an SU is determined by arrival rates and not concentrations allows for the treatment of light as a controlling resource analogous to nutrients (Chapter 2). Light energy can, therefore, be directed as a flux to multiple cellular processes through a trade-off framework, i.e. light can be used in both photoautotrophy and/or photoheterotrophy. DEB theory therefore provides an ideal framework to build a model to investigate light stimulated changes in resource acquisition through photoheterotrophy and the influence on Pro and SAR11 growth rate in a physiologically realistic way.

The DEB framework also lends itself to the investigation of the differences in Pro and SAR11 physiology and how they maintain similar growth rates despite their differences. By assuming a similar core model structure, physiological differences are represented by differences in parameter values and not model design. By simply changing a parameter value from that of Pro to SAR11, it can be shown how a difference in physiological strategy influences growth rate.

1.7. Research aim

This thesis aims to extend our understanding of the influence of solar energy in the two most abundant organisms in the subtropical gyre ecosystems, Pro and SAR11. By addressing the three questions posed at the start of this chapter (Section 1.1) specifically, it investigates the influence of photoheterotrophic light use on their growth rate and the influence on the processing of key elements in the subtropical gyres. Chapter 2 describes the model and the parameters used to constrain it. Chapter 3 addresses the influence of photoheterotrophic light use on Pro in multiple environmental settings that represents changes in ambient resources essential to Pro. Chapter 4 address the influence of photoheterotrophic light use on SAR11, also in a range of environments. Chapter 5 analyses the physiological traits of both Pro and SAR11 in order to understand which confer the greatest benefit to growth rate and therefore may be key to their survival and coexistence. Chapter 6 considers the broader implications and directions for future work.

Chapter 2: Methods

2.1. A summary of the model

The model for both *Prochlorococcus* (Pro) and SAR11 is based on Dynamic Energy Budget (DEB) theory (Kooijman, 2010) using aspects of previously published DEB models (Kooijman et al., 2002, Kuijper et al., 2004). The model is parameterised for oligotrophic subtropical Atlantic surface water populations of Pro and SAR11 and run to steady-state. A schematic of the model for both organisms is shown in Figure 2.1. The model is designed to incorporate the fundamental physiology and metabolism shared by Pro and SAR11, whilst maintaining the flexibility to parameterise distinct aspects of their individual physiologies.

A summary of the model structure is as follows. A flux of photons is harvested by a pigment system; divinyl chlorophyll-a and b (chl-a) in Pro and proteorhodopsin (PR) in SAR11. The energy derived from sunlight can be used for two processes by each organism. The first is the acquisition of carbon for energy and synthesis; photoautotrophic dissolved inorganic carbon (DIC) reduction to produce carbohydrate (CHO) in Pro, and photoheterotrophic dissolved organic carbon (DOC) uptake in SAR11. CHO and DOC contain carbon but no nitrogen. The second is the acquisition of dissolved organic nitrogen (DON) by both Pro and SAR11. This contains both carbon and nitrogen. The partitioning of harvested light energy between these two processes controls a trade-off that assumes the use of light energy to enhance one processes is at the cost of the other. Pro is entirely dependent on available light energy to facilitate DIC reduction and DON uptake. SAR11 can uptake DOC and DON in the dark but uptake is greater with sunlight. Both organisms can uptake dissolved organic nitrogen (DIN) to combine with a source of carbon (CHO in Pro and DOC in SAR11) to synthesis amino acids (AA). This process does not involve light. The sum of DON and AA produce an organic nitrogen (ON) flux that contains both carbon and nitrogen. The remaining CHO/DOC flux after AA synthesis produces an organic carbon (OC) flux containing carbon but no nitrogen. ON and OC are used by the cell to satisfy maintenance as a priority with the remainder available for growth.

The model fluxes are given relative to one mole of carbon biomass, i.e. units are mol C $(\text{mol C})^{-1}$ hr^{-1}. The model represents fluxes at a moment in time. Growth leads to no change in the model.

2.2. The model description

Where parameterisations for resource acquisition processes are specific to an organism this is stated and described below. Otherwise, the use of substrates for maintenance and growth and the manner in which the model has been constructed and parameterised is assumed to be the same for both organisms. All parameters and variables are listed in Table 2.1 at the end of this chapter.

2.2.1. The use of light energy for the acquisition of substrates

The following sections describe the phototrophic metabolism used by both Pro and SAR11. It must be noted however that SAR11 can also uptake substrate in the absence of sunlight, whereas Pro cannot. The model structure facilitating substrate uptake by SAR11 in the dark will be presented in Section 2.2.5. Each component of the model and its description is given for both Pro and SAR11 physiologies. Where parameter values differ for Pro and SAR11, this is noted (Table 2.1).

2.2.1.1. Light harvesting

It is well documented that phototrophy (measured as electron turnover) levels off at high photosynthetically active radiation (PAR) resulting in a hyperbolic relationship between energy yields and irradiance (Kirchman and Hanson, 2012). This is observed for both a chlorophyll based pigment systems (MacKenzie et al., 2004) and PR (Walter et al., 2007). It is therefore assumed that electron fluxes vary with irradiance in a Michaelis-Menten (MM) type functional form (known in DEB theory as a one-substrate synthesising unit, 1-SU), and the fraction of the maximum flux is expressed as;

$$f_L = \frac{\dot{J}_{L,F}}{\dot{J}_{L,FK} + \dot{J}_{L,F}} \qquad [2.2.1.1a]$$

where $\dot{J}_{L,F}$ is the solar irradiance and $\dot{J}_{L,FK}$ is the half saturation irradiance, both with units µmol photons m^{-2} s^{-1}. The half saturation constant values are different for Pro and SAR11 but both are assumed to receive the same flux of incident irradiance (Section 2.3.1, Table 2.1).

2.2.1.2. Partitioning energy harvested from sunlight

Harvested light energy is partitioned between carbon acquisition (CHO synthesis in Pro and DOC uptake in SAR11) and DON uptake (in both Pro and SAR11) through a single parameter (β)

that varies between 0 and 1. When β = 0, all light energy is entirely invested in carbon acquisition and when β = 1, all light energy is invested in DON uptake. As such,

$$f_{L\beta} = \frac{\dot{J}_{L,F}\beta}{\dot{J}_{L,FK} + \dot{J}_{L,F}\beta} \quad [2.2.1.2a]$$

and

$$f_{L(1-\beta)} = \frac{\dot{J}_{L,F}(1-\beta)}{\dot{J}_{L,FK} + \dot{J}_{L,F}(1-\beta)} \quad [2.2.1.2b]$$

where Equation 2.2.1.2a directs harvested light energy to DON uptake and Equation 2.2.1.2b directs light energy to carbon acquisition. Each destination for solar energy can, therefore, saturate independently.

2.2.1.3. Using light energy for carbon acquisition

The photoautotrophic production of CHO in Pro requires sources of both DIC and light. Photoheterotrophic DOC uptake in SAR11 requires sources of DOC and light. The uptake of single substrates (DIC and DOC) is taken to follow a MM-type function. The MM function that describes the uptake of DIC or DOC is given as,

$$f_C = \frac{1}{1 + {x_C}^{-1}}, \qquad x_C = \frac{X_C}{K_C} \quad [2.2.1.3a]$$

where f_C is the fraction of the maximum uptake for DIC or DOC uptake, X_C is the ambient concentration of DIC or DOC and K_C is the half saturation constant for DIC or DOC uptake, describing the concentration at which half the maximum uptake rate is attained. The ambient concentration X_C is not the same for DIC and DOC, nor is the half saturation constant K_C and therefore K_C. The specific values are presented in Section 2.3.1 and Table 2.1. The same notation is used for photoheterotrophic DOC uptake in SAR11 and photoautotrophic DIC reduction in Pro as both are modelled in the same way. Their maximum rates of carbon acquisition are, however, different (Section 2.3.1, Table 2.1).

Light and DIC/DOC are complementary to each other, i.e. one cannot be used to generate a product without the other being present (ignoring uptake in the dark by SAR11 for now). They are assumed to be processed in parallel, meaning that an increase in the abundance of one can increase the use of the other (Kooijman et al., 2002). The rate of carbon acquisition ($\dot{J}_{C,U}$) by both Pro and SAR11 is represented using an SU given as,

$$\dot{J}_{C,U} = \dot{J}_{C,Um} \frac{(1 + {z_C}^{-1} + {z_L}^{-1}) - (z_C + z_L)^{-1}}{1 + {z_C}^{-1}{f_C}^{-1} + {z_L}^{-1}{f_{L(1-\beta)}}^{-1} - \left(z_C f_C + z_L f_{L(1-\beta)}\right)^{-1}} \quad [2.2.1.3b]$$

where $\dot{J}_{C,Um}$ is the maximum rate of carbon acquisition and z_C and z_L are parameters that weight the relative contribution of DIC/DOC and light to the acquisition process, respectively (Troost et al., 2005, Kooijman et al., 2002). The flux $\dot{J}_{C,U}$ is given in units of mol C (mol C)$^{-1}$ hr^{-1}. z_C and z_L are identical for Pro and SAR11, discussed in Section 2.3.1. The maximum rate of carbon acquisition ($\dot{J}_{C,Um}$) is different for Pro and SAR11. In Pro it is the maximum rate of photosynthetic CHO synthesis and in SAR11 it is the maximum rate of DOC uptake (Section 2.3.1, Table 2.1). In both organisms this product flux contains carbon but no nitrogen. This flux can be used for both the synthesis of AA and maintenance and growth, discussed below in Section 2.2.2.

2.2.1.4. Using light energy for DON uptake

The same formulation for complementary substrates processed in parallel, is used to represent the rate of light enhanced DON uptake ($\dot{J}_{DON,U}$) in Pro and SAR11, given as,

$$\dot{J}_{DON,U} = \dot{J}_{DON,Um} \frac{(1 + {z_{DON}}^{-1} + {z_L}^{-1}) - (z_{DON} + z_L)^{-1}}{1 + {z_{DON}}^{-1}{f_{DON}}^{-1} + {z_L}^{-1}{f_{L\beta}}^{-1} - \left(z_{DON} f_{DON} + z_L f_{L\beta}\right)^{-1}} \quad [2.2.1.4a]$$

where $\dot{J}_{DON,Um}$ is the maximum rate of light enhanced DON uptake and z_{DON} is a parameter that weights the relative contribution of the incident flux of DON to the uptake process. The maximum rate of light enhanced DON uptake ($\dot{J}_{DON,Um}$) is not the same for Pro and SAR11 (Section 2.3.1, Table 2.1). f_{DON} represents how DON is taken up, given as,

$$f_{DON} = \frac{1}{1 + {x_{DON}}^{-1}}, \qquad x_{DON} = \frac{X_{DON}}{K_{DON}} \quad [2.2.1.4b]$$

where f_{DON} is the fraction of the maximum uptake rate for DON, X_{DON} is the ambient DON concentration and K_{DON} is the saturation constant describing the concentration at which half the maximum uptake rate is achieved. These parameters are considered to be the same for both Pro and SAR11 (Section 2.3.1). The flux $\dot{J}_{DON,U}$ is given in units of mol C (mol C)$^{-1}$ hr^{-1}. It contains both carbon and nitrogen. The nitrogen flux (mol N (mol C)$^{-1}$ hr^{-1}) is given by dividing $\dot{J}_{DON,U}$ by the C:N of ambient DON (φN).

2.2.2. Amino acid biosynthesis

Pro and SAR11 both possess similar genes required for the synthesis of AA and have the capacity to transport DIN across their outer membrane (Kettler et al., 2007, Sowell et al., 2008). DIN is assimilated via the sequential activity of two enzymes, glutamine synthetase (GS) and glutamate synthase (GOGAT), in a system known as the GS-GOGAT pathway, utilised by both Pro and SAR11 (Kettler et al., 2007, Sowell et al., 2008). An identical representation of the synthesis of AA is employed for both Pro and SAR11, with the caveat that the source of carbon differs.

In the present model DIN from the ambient pool is combined with a carbon source to create AA. A similar representation to that used for photoautotrophy and photoheterotrophy is used for AA synthesis.

Bacteria take up nitrogen in stoichiometrically balanced proportions relative to available carbon when DIN is the only growth substrate (Goldman and Dennett, 1991, Goldman et al., 1987, Goldman and Dennett, 2000). The rate of DIN uptake in the model will be given as the rate at which nitrogen is assimilated into AA. The rate at which DIN becomes available for assimilation is given as,

$$\dot{J}_{DIN,U} = \dot{J}_{DIN,U_m} \frac{1}{1 + x_{DIN}{}^{-1}}, \qquad x_{DIN} = \frac{X_{DIN}}{K_{DIN}} \qquad [2.2.2a]$$

where $\dot{J}_{DIN,U_m}$ is the maximum rate, X_{DIN} is the concentration of DIN in the ambient pool and K_{DIN} is the ambient concentration that supports half the maximum rate. The maximum rate parameter is not the same for Pro and SAR11 and will be fitted according to the protocol discussed in Section 2.3.1. The half saturation constant (K_{DIN}) is the same for both organisms, and both experience the same concentration of ambient DIN (X_{DIN}) (Section 2.3.1, Table 2.1). The units of DIN uptake are in mol N (mol C)$^{-1}$ hr^{-1}.

The parameter α is the fraction of the carbon flux directed to maintenance and growth. The fraction of the carbon flux made available for the synthesis of AA is (1- α). The parameter α is given as,

$$\alpha = \frac{\dot{J}_{DON,U} + \dot{J}_{AA,S}}{\dot{J}_{DON,Um} + \dot{J}_{AA,Sm}} \qquad [2.2.2b]$$

where $\dot{J}_{DON,Um}$ and $\dot{J}_{AA,Sm}$ are the maximum rates of DON uptake and AA synthesis, respectively. $\dot{J}_{AA,S}$ is the rate of AA synthesis (discussed below), which is added to the rate of

DON uptake ($\dot{J}_{DON,U}$) to produce the total flux of organic nitrogen (ON), which contains both carbon and nitrogen, available for maintenance and growth.

When bacteria grow on DIN as the sole nitrogen source, they appear not to generate DIN as a metabolic waste product (Goldman and Dennett, 1991, Goldman et al., 1987, Goldman and Dennett, 2000). For simplicity, it is therefore assumed that DIN is assimilated into AA with 100 % efficiency. The cost of synthesis is paid for through CHO/DOC mobilisation, resulting in carbon dioxide production. The pathway for the construction of AA is given by,

$$n_C^{GS} C + n_N^{GS} DIN \rightarrow \square A + n_{CO_2}^{GS} CO_2 \quad [2.2.2c]$$

Coefficients (n) describe how a unit of amino acid (AA) is synthesised by combining carbon materials (C) and DIN at a specified C:N ratio. The notation GS corresponds to the GS-GOGAT pathway. The synthesised flux $\dot{J}_{AA,S}$ and $\dot{J}_{DON,U}$, are both assumed to have a fixed and identical C:N. The coefficients n are given by,

$$n_N^{GS} = \frac{1}{\varphi ON} \quad [2.2.2d]$$

$$n_C^{GS} = \frac{1}{\psi C_{AA}} \quad [2.2.2e]$$

$$n_{CO_2}^{GS} = \frac{1}{\psi C_{AA}} - 1 \quad [2.2.2f]$$

where φON is the C:N of AA (and DON) in mol C (mol N)$^{-1}$ and ψC_{AA} is efficiency with which C (CHO/DOC) is used to synthesise AA (Section 2.3.1, Table 2.1).

Amino acid synthesis is modelled as arising from the dynamics of four linked binding states. This can be considered as a proxy for a set of enzymes that have two binding sites that can accept C (CHO/DOC) and DIN fluxes, respectively. The four possible states are an unbound state ($\theta_{..}$), a C bound state ($\theta_{.C}$), a DIN bound state ($\theta_{DIN.}$) and a state where both substrates are bound ($\theta_{DI\square C}$). When both substrates are bound in the fourth state, an AA is formed. The total number of binding states remains constant. AA formation is therefore dependent on both the arriving fluxes of substrates and the relative abundance of each state. The equations for the four binding states are,

$$\frac{d}{dt}\theta_{..} = \theta_{DINC}\dot{J}_{AA,Sm} - \left(\frac{\dot{J}_{DIN,U}}{n_N^{GS}} + \frac{\dot{J}_{C,U}}{n_C^{GS}}(1-\alpha)\right)\theta_{..} \quad [2.2.2g]$$

$$\frac{d}{dt}\theta_{.C} = -\frac{\dot{J}_{DIN,U}}{n_N^{GS}}\theta_{.C} + \frac{\dot{J}_{C,U}}{n_C^{GS}}(1-\alpha)\theta.. \quad [2.2.2h]$$

$$\frac{d}{dt}\theta_{DIN.} = -\frac{\dot{J}_{C,U}}{n_C^{GS}}(1-\alpha)\theta_{DIN.} + \frac{\dot{J}_{DIN,U}}{n_N^{GS}}\theta_{..} \quad [2.2.2i]$$

$$\frac{d}{dt}\theta_{DINC} = \frac{\dot{J}_{DIN,U}}{n_N^{GS}}\theta_{.C} + \frac{\dot{J}_{C,U}}{n_C^{GS}}(1-\alpha)\theta_{DIN.} - \theta_{DINC}\dot{J}_{AA,Sm} \quad [2.2.2j]$$

where $\dot{J}_{AA,Sm}$ is the maximum rate of AA synthesis and each θ represents the fractions of all binding states in that state. Note that the probabilities of each substrate binding to the AA synthesis machinery are assumed to be equal. Binding probability parameters are both set to equal 1 and are therefore omitted from Equations 2.2.2g-j). The rate of AA synthesis ($\dot{J}_{AA,S}$) is therefore given as,

$$\dot{J}_{AA,S} = \theta_{DINC}\dot{J}_{AA,Sm} \quad [2.2.2k]$$

The flux $\dot{J}_{AA,S}$ divided by the C:N of AA (φON) gives the rate of DIN uptake in mol N (mol C)$^{-1}$ hr^{-1}, given that DIN is assumed to be assimilated with 100 % efficiency, as discussed. Note that Equation 2.2.2a only describes the rate at which DIN is made available for AA synthesis. The difference between Equation 2.2.2a and Equation 2.2.2k (when the latter is converted to mol N (mol C)$^{-1}$ hr^{-1} units), provides a measure of the rejected flux of DIN that cannot be assimilated into AA, given as,

$$\dot{J}_{AA,R} = \dot{J}_{DIN,U} - \frac{\dot{J}_{AA,S}}{\varphi ON} \quad [2.2.2l]$$

Flux $\dot{J}_{AA,R}$ is rejected from the cell.

The rate of carbon dioxide release through costs associated with AA synthesis is given as,

$$\dot{J}_{CO_2,S} = n_{CO_2}^{GS}\dot{J}_{AA,S} \quad [2.2.2m]$$

As discussed, this flux is added to the light enhanced flux of DON ($\dot{J}_{DON,U}$) to produce the total ON flux ($\dot{J}_{ON}$) available for maintenance and growth, given as,

$$\dot{J}_{ON} = \dot{J}_{DON,U} + \dot{J}_{AA,S} \quad [2.2.2n]$$

If there is insufficient DIN available to combine with the incident C (CHO/DOC) flux in the required C:N, a fraction of the C (CHO/DOC) flux is rejected and made available for

maintenance and growth. The total OC flux ($\dot{J}_{OC}$) arriving at maintenance, containing carbon and no nitrogen, is therefore given as,

$$\dot{J}_{OC} = \dot{J}_{C,R} + \alpha \dot{J}_{C,U} \quad [2.2.2o]$$

and

$$\dot{J}_{C,R} = (1-\alpha)\dot{J}_{C,U} - n_C^{GS}\dot{J}_{AA,S} \quad [2.2.2p]$$

where $1-\alpha \dot{J}_{C,U}$ is the original fraction of the CHO/DOC flux made available for AA synthesis and $n_C^{GS}\dot{J}_{AA,S}$ is the gross carbon flux used in AA synthesis.

2.2.3. Reactions for the utilisation of substrates in maintenance and growth

The following section defines the use of substrates for maintenance and growth which are considered to be the same for both Pro and SAR11. The model uses the formulation given by Kuijper et al. (2004), which describes the synthesis of biomass for a crustacean, which follows similar principles to that of a bacterium for the use of organic carbon (OC) and organic nitrogen (ON). Somatic maintenance must be met prior to the allocation of metabolites to growth. Maintenance includes the production of biomass that is lost via protein turnover and other costs associated with energetic expenditure. Maintenance results in zero net biomass production. Mass and energy are effectively lost from the cell.

Maintenance and growth can be met using both the ON and OC fluxes (Goldman and Dennett, 1991, Goldman et al., 1987, Goldman and Dennett, 2000). The OC flux contains carbon only and therefore cannot be used for biomass synthesis without the ON flux. The ON flux, however, contains carbon and nitrogen and therefore can be used for biomass synthesis on its own and/or in combination with the OC flux. It is assumed that maintenance and growth conform to the same elemental stoichiometry i.e. the same C:N. Two pathways of resource utilisation for maintenance and growth are possible, given as:

$$n_{ON}^{D} ON \rightarrow X + n_{CO_2}^{D} CO_2 + n_{NH_4^+}^{D} NH_4^+ \quad [2.2.3a]$$

$$n_{ON}^{S} ON + n_{OC}^{S} OC \rightarrow X + n_{CO_2}^{S} CO_2 \quad [2.2.3b]$$

Equation 2.2.3a balances the production of biomass (X) from ON alone (gaining energy through ON deamination, hence denoted by D). Equation 2.2.3b balances the production of

biomass from ON and OC (gaining energy through OC mobilisation whilst sparing ON mobilisation, allowing for its complete assimilation into biomass, hence denoted by S). The sparing pathway is considered energetically preferential over the deamination pathway as it releases only carbon waste products (Equation 2.2.3a) rather than both carbon and nitrogen (2.2.3b).

The efficiencies of synthesis using the two pathways are defined in Equations 2.2.3a and 2.2.3b by coefficients n. These are the yield coefficients, which are based on theoretical efficiencies of biomass production (Calow, 1977) and known C:N ratios of ON and biomass (Section 2.3.2, Table 2.1).

2.2.3.1. Stoichiometric balancing with the yield coefficients

The following equations define the stoichiometry through which equations 2.2.3a and 2.2.3b balance using assumed C:N of biomass (φX) and ON (φON). If the efficiencies through which the deamination (D) (Equation 2.2.3b) and sparing (S) (Equation 2.2.3a) reactions proceed are known (ψOC and ψON) i.e. the amount of each substrate used to produce one unit of biomass is known, then the yield coefficients can be written as,

$$n_{ON}^{D} = \frac{1}{\psi ON} \quad [2.2.3.1a]$$

$$n_{CO_2}^{D} = \frac{1}{\psi ON} - 1 \quad [2.2.3.1b]$$

$$n_{NH_4^+}^{D} = \frac{1}{\psi ON.\varphi ON} - \frac{1}{\varphi X} \quad [2.2.3.1c]$$

$$n_{ON}^{S} = \frac{\varphi ON}{\varphi X} \quad [2.2.3.1d]$$

$$n_{OC}^{S} = \frac{1}{\psi OC} - \frac{\varphi ON}{\varphi X} \quad [2.2.3.1e]$$

$$n_{CO_2}^{S} = \frac{1}{\psi OC} - 1 \quad [2.2.3.1f]$$

These formulae provide stoichiometric balance of Equations 2.2.3a and 2.2.3b.

2.2.3.2. Representation of maintenance

The deamination and sparing reactions merge the potentially limiting ON and OC fluxes to support maintenance at a fixed C:N. The equations used mimic the biochemical interactions in the enzyme-substrate complex, allowing quantification of the product flux based on the likelihood of an interaction occurring between the enzyme and substrate and the substrate supply rate (Kooijman, 1998).

Multiple binding states are possible for maintenance, which accepts fluxes of OC and ON. Figure 2.2 shows the four different binding states; $\theta_{..}$ is unbound or free, $\theta_{.OC}$ has an organic carbon (OC) molecule bound, $\theta_{ON.}$ has an organic nitrogen (ON) molecule bound and θ_{ONOC} is an SU with both molecule types bound. As discussed there are two possible pathways to meet maintenance and growth; the ON only pathway (deamination) and the ON and OC pathway (sparing). Therefore, the binding states $\theta_{ON.}$ and θ_{ONOC} can both be considered to synthesise material for maintenance.

The maintenance requirements are assumed to be fixed for the organism and therefore are not dependent on the size of uptake fluxes. The maintenance term k_M defines the rate at which maintenance takes place and is thus a fixed parameter. Maintenance is carried out when substrates which were bound are released as maintenance product (X) leaving an unbound state ($\theta_{..}$). The maintenance term (k_M) is therefore the rate at which the unbound state is created (Equation 2.2.3.2a) with units mol C (mol C)$^{-1}$ hr^{-1}.

Binding affinities ($\rho_{Substrate\ flux}^{Reaction\ pathway}$) define the statistical likelihood of the substrate binding for each reaction pathway. Figure 2.2 illustrates the manner in which substrates bind and satisfy maintenance via the two pathways.

The binding of an ON molecule can result in maintenance synthesis via the deamination pathway. However, if an OC molecule has already been bound to the SU then the sparing pathway proceeds once an ON molecule has also bound. The binding affinity values satisfy $0 \leq \rho \leq 1$. The sparing pathway is favoured over the deamination pathway, which is represented in the binding affinities by setting $\rho_{ON}^{D} \leq \rho_{ON}^{S}$ and $\rho_{ON}^{D} \leq \rho_{OC}^{S}$ i.e. the probability of an ON molecule binding to a $\theta_{.OC}$ state or an OC molecule binding to a $\theta_{..}$ state is greater than the probability of an ON molecule binding to a $\theta_{..}$ state (Section 2.3.2.1, Table 2.1).

The differential equations for the binding states for maintenance are,

$$\frac{d}{dt}\theta_{..} = k_M - \left(\frac{\rho_{ON}^D}{n_{ON}^D}\dot{J}_{ON} + \frac{\rho_{OC}^S}{n_{OC}^S}\dot{J}_{OC}\right)\theta.. \quad [2.2.3.2a]$$

$$\frac{d}{dt}\theta_{.OC} = \frac{\rho_{OC}^S}{n_{OC}^S}\dot{J}_{OC}\theta.. - \frac{\rho_{ON}^S}{n_{ON}^S}\dot{J}_{ON}\,\theta_{.OC} \quad [2.2.3.2b]$$

$$\frac{d}{dt}\theta_{ON.} = \frac{\rho_{ON}^D}{n_{ON}^D}\dot{J}_{ON}\,\theta.. - k_M\frac{\theta_{ON.}}{\theta_{ON.} + \theta_{ONOC}} \quad [2.2.3.2c]$$

$$\frac{d}{dt}\theta_{ONOC} = \frac{\rho_{ON}^S}{n_{ON}^S}\dot{J}_{ON}\,\theta_{.OC} - \,k_M\frac{\theta_{ONOC}}{\theta_{ON.} + \theta_{ONOC}} \quad [2.2.3.2d]$$

In Equations 2.2.3.2c and 2.2.3.2d the sum of the two dissociation rates is fixed because k_M, the parameter that specifies the maintenance requirement is fixed. Therefore, the relative contributions of each pathway to satisfy maintenance are proportional to the relative abundances of $\theta_{ON.}$ and θ_{ONOC} at steady state.

The fractions determining how maintenance is met are,

$$\Omega_{ON.} = \frac{\theta_{ON.}}{\theta_{ON.} + \theta_{ONOC}} \quad [2.2.3.2e]$$

$$\Omega_{ONOC} = \frac{\theta_{ONOC}}{\theta_{ON.} + \theta_{ONOC}} \quad [2.2.3.2f]$$

which can be used to calculate the amounts of ON and OC used in maintenance as,

$$\dot{J}_{ON,M} = k_M\left(n_{ON}^S\Omega_{ONOC} + n_{ON}^D\Omega_{ON.}\right) \quad [2.2.3.2g]$$

$$\dot{J}_{OC,M} = k_M n_{OC}^S\Omega_{ONOC} \quad [2.2.3.2h]$$

$$\dot{J}_M = k_M \quad [2.2.3.2i]$$

and $\dot{J}_M$ is the maintenance rate set by the fixed maintenance rate parameter k_M.

In this demand driven maintenance system, OC has to be delivered at a rate to match its consumption in maintenance, which is the rate of consumption of biomass via the sparing route (Equation 2.2.3b) ($k_M\Omega_{ONOC}$) multiplied by the amount of organic carbon material (n_{OC}^S) needed to produce one unit of maintenance product X, given as Equation 2.2.3.2h. The

argument also applies to Equation 2.2.3.2g and formation of ammonium (Equation 2.2.3.2j) and carbon dioxide (Equation 2.2.3.2k) metabolic products.

$$\dot{J}_{NH_4^+,M} = k_M n^D_{NH_4^+} \Omega_{ON.} \quad [2.2.3.2j]$$

$$\dot{J}_{CO_2,M} = k_M \left(n^D_{CO_2} \Omega_{ON.} + n^S_{CO_2} \Omega_{ONOC} \right) \quad [2.2.3.2k]$$

2.2.3.3. Growth

After maintenance has been 'paid' the remainder of the ON and OC fluxes are available for growth. Thus, subtracting the maintenance flux ($j_{ON,M}$ or $j_{OC,M}$) from the fluxes $\dot{J}_{ON}$ and $\dot{J}_{OC}$ gives the fluxes of compounds available for growth.

$$\dot{J}^{.g}_{ON,G} = \dot{J}_{ON} - \dot{J}_{ON,M} \quad [2.2.3.3a]$$

$$\dot{J}^{.g}_{OC,G} = \dot{J}_{OC} - \dot{J}_{OC,M} \quad [2.2.3.3b]$$

Note that under starvation conditions, i.e. when fluxes $\dot{J}_{ON}$ and $\dot{J}_{OC}$ are cumulatively or individually in the case of $\dot{J}_{ON}$ below that required to satisfy maintenance, negative values drive the growth SU system. Therefore, results only consider scenarios when maintenance has been satisfied.

Growth in the model has identical kinetics to maintenance with respect to chemical stoichiometry, yield coefficients and binding affinity and therefore follows the pattern illustrated in Figure 2.2. This assumes that the same proportion of ON and OC materials used to maintain the organism are used to build new biomass. However, the flux of metabolites to growth is controlled by what is available after maintenance, i.e. growth is supply driven.

As for maintenance, four binding states are possible. However, as it is assumed that biomass is formed as soon as an ON is bound to either pathway, the fractions of states $\theta_{ON.}$ and θ_{ONOC} remain at zero. This is based on the assumption that the creation of biomass when $\theta_{ON.}$ and θ_{ONOC} are created is much faster than the binding to those states. The relative abundances of binding states $\theta_{..}$ and $\theta_{.OC}$, therefore, control the ratio of fluxes through the deamination and sparing pathways to growth. The manner in which the relative abundance of binding states $\theta_{..}$ and $\theta_{.OC}$ change with time is given as:

$$\frac{d}{dt}\theta_{..} = \frac{\rho_{ON}^{S}}{n_{ON}^{S}} j_{ON,G}^{.g} \theta_{.OC} - \frac{\rho_{OC}^{S}}{n_{OC}^{S}} j_{OC,G}^{.g} \theta_{..} \quad [2.2.3.3c]$$

$$\frac{d}{dt}\theta_{.OC} = \frac{\rho_{OC}^{S}}{n_{OC}^{S}} j_{OC,G}^{.g} \theta_{..} - \frac{\rho_{ON}^{S}}{n_{ON}^{S}} j_{ON,G}^{.g} \theta_{.OC} \quad [2.2.3.3d]$$

The steady state values of $\theta_{..}$ and $\theta_{.OC}$ are used to specify the magnitude of bound compounds that can be used in growth.

ON can be used down one of two pathways. The fraction sent down each pathway is given by the relative number of binding states $\theta_{..}^{*}$ and $\theta_{.OC}^{*}$ and the associated affinity,

$$j_{ON,G} = j_{ON,G}^{.g} \left(\rho_{ON}^{D} \theta_{..}^{*} + \rho_{ON}^{S} \theta_{.OC}^{*} \right) \quad [2.2.3.3e]$$

$$j_{OC,G} = \frac{\rho_{OC}^{S} n_{OC}^{S}}{n_{ON}^{S}} j_{ON,G}^{.g} \theta_{.OC}^{*} \quad [2.2.3.3f]$$

The flux of OC to growth needs to be specified relative to the ON flux via the sparing pathway as OC materials alone cannot satisfy growth. Using the ratio of the OC yield relative to the ON yield via the sparing pathway ($\frac{n_{OC}^{S}}{n_{ON}^{S}}$) gives the relative proportion of OC to ON in the growth flux when multiplied by the flux of ON to growth $j_{ON,G}^{.g}$.

The same principle is used to quantify the ammonium release flux in the deamination pathway (Equation 2.2.3.3g) and the respiration fluxes in the sparing and deamination pathway (Equation 2.2.3.3h) from growth generated due to the inefficiency of substrate use, given as,

$$j_{NH_4^+,G} = j_{ON,G}^{.g} \frac{\rho_{ON}^{D} \, n_{NH_4^+}^{D}}{n_{ON}^{D}} \, \theta_{..}^{*} \quad [2.2.3.3g]$$

$$j_{CO_2,G} = j_{NF,G}^{.g} \left(\frac{\rho_{ON}^{D} \, n_{CO_2}^{D}}{n_{ON}^{D}} \, \theta_{..}^{*} + \frac{\rho_{ON}^{S} n_{CO_2}^{S}}{n_{ON}^{S}} \, \theta_{.OC}^{*} \right) \quad [2.2.3.3h]$$

The total amount of biomass produced per hour is given by,

$$j_{X,G} = j_{ON,G}^{.g} \left(\frac{\rho_{ON}^{D}}{n_{ON}^{D}} \, \theta_{..}^{*} + \frac{\rho_{ON}^{S}}{n_{ON}^{S}} \theta_{.OC}^{*} \right) \quad [2.2.3.3i]$$

The units of the growth rate (Equation 2.2.3.3i) are in mol C (mol C)$^{-1}$ hr^{-1}. The growth rates for Pro and SAR11 in Chapters 3-5 are also specified as rates per day. Pro, an obligate phototroph

grows only during 12 hours of daylight. The hourly rate for Pro is therefore multiplied by 12. SAR11 grows in the light and the dark. The light enhanced rate of growth per hour is multiplied by 12 and the rate of growth in the dark is multiplied by 12. The sum of these two rates gives the daily growth rate for SAR11. The light dark (L:D) cycle that SAR11 grows under is therefore 12:12 (Section 2.2.5).

The fluxes of ON and OC left over after maintenance and growth i.e. that are in excess to stoichiometrically balanced growth are released from the cell, given as,

$$\dot{J}_{ON,R} = (\dot{J}_{ON} - \dot{J}_{ON,M} - \dot{J}_{ON,G}) \quad [2.2.3.3j]$$

$$\dot{J}_{OC,R} = (\dot{J}_{OC} - \dot{J}_{OC,M} - \dot{J}_{OC,G}) \quad [2.2.3.3k]$$

2.2.4. Growth efficiency

The bacterial growth efficiency (BGE) is calculated as the rate of new growth relative to total carbon demand which is defined as the sum of new growth and total respiration.

$$BGE = \frac{\dot{J}_{X,G}}{\dot{J}_{X,G} + \dot{J}_{CO_2,S} + \dot{J}_{CO_2,M} + \dot{J}_{CO_2,G}} \quad [2.2.4a]$$

2.2.5. SAR11 uptake without light: heterotrophic metabolism

In order to modify the model to incorporate resource uptake in the absence of sunlight, two constraints need to be satisfied. Firstly, uptake rates used to constrain the model during the day measured empirically at an irradiance of 500 µmol photons m^{-2} s^{-1} need to be maintained. Secondly, the cell must still uptake resources even when irradiance is reduced to zero. The ratio of light to dark DON uptake in SAR11 has been observed to be 1.23 (Mary et al., 2008) (Section 2.3.1) and this value is used to constrain the new model formulation. For simplicity, the ratio of light to dark uptake rates is constrained to be 1.23 at β = 1, where all light is invested in DON uptake.

In the current model formulation, the uptake of DOC and DON is dependent upon irradiance through the parallel processing of complementary substrates. For simplicity the functional response for light harvesting is modified to provide the capacity for nutrient uptake and growth in the absence of sunlight. The original functional response for light harvesting

(Equation 2.2.1.1a) is replaced with Equation 2.2.5a below. The new functional response for light harvesting f_{Light}^{new} is given as;

$$f_{Light}^{new} = \frac{I + Io}{I + Io + K_{new}} \quad [2.2.5a]$$

Io and K_{new} are defined in Equations 2.2.5e and 2.2.5f, respectively, below. When irradiance I equals zero, f_{Light}^{new} is given as;

$$f_{Dark} = \frac{Io}{Io + K_{new}} \quad [2.2.5b]$$

When irradiance is 500 µmol photons^{-2} s^{-1} f_{Light}^{new} is given as;

$$f_{Light}^{new} = \frac{500 + Io}{500 + Io + K_{new}} \quad [2.2.5c]$$

In order to satisfy the requirement that the functional response for light harvesting is the same at 500 µmol photons^{-2} s^{-1}, and so maintaining the constrained uptake rates, f_{Light}^{new} must equal the original functional response for light harvesting, given as;

$$f_{Light}^{new} = \frac{500 + Io}{500 + Io + K_{new}} = \frac{500}{500 + \dot{J}_{L,FK}} \quad [2.2.5d]$$

where $\dot{J}_{L,FK}$ is the original half saturation constant value of 2700 µmol photons^{-2} s^{-1}. Using Equation 2.2.5b to eliminate K_{new} from Equation 2.2.5d gives,

$$Io = \frac{\dot{J}_{L,FK}}{\left[\frac{1}{f_{Dark}} - 1 - \frac{\dot{J}_{L,FK}}{500}\right]} \quad [2.2.5e]$$

$f_{Dark}$is tuned using the model. The value of $f_{Da\square k}$ is the functional response value that allows SAR11 to uptake DON at night. When irradiance is increased from 0 to 500 µmol photons m^{-2} s^{-1}, the rates of DON uptake during the day and night are at a ratio 1.23, in accordance with observations (Mary et al., 2008a) at β = 1 when f_{Dark} = 0.097. Equation 2.2.5e can then be substituted into equation 2.2.5b to get,

$$K_{new} = \dot{J}_{L,FK}\left[1 + \frac{Io}{500}\right] \quad [2.2.5f]$$

All parameters values are given in Table 2.1. The model is run at an irradiance of 500 µmol photons m^{-2} s^{-1} to give the diurnal growth rate. Another model is run in parallel at 0 µmol photons m^{-2} s^{-1} to give the nocturnal growth rate. The sum of both nocturnal and diurnal growth, each over 12 hours, gives the complete diel growth rate for 24 hours.

2.2.6. Simulation settings

The coupled differential equations were solved using the Runge-Kutta fourth order method. The model was run with a time step of 0.05 hours for 300 hours. The Powersim Studio 8 platform was used to code the model.

2.3. Model parameters

Parameter values where possible were sourced from the literature. Where not available, parameters were tuned to data from the literature.

2.3.1. Parameters for the kinetics of resource acquisition

The kinetics for the uptake of individual resources is modelled using the Michaelis-Menten parameterisation. Therefore, up to three pieces of information are required to describe the uptake of each resource; the ambient resource concentration, the concentration where half the maximum rate of the resource uptake is attained, and the maximum rate of uptake.

2.3.1.1. Light harvesting (Pro and SAR11)

Irradiance: 500 µmols photons m^{-2} s^{-1}. This value is used as it is the experimental irradiance used to obtain known maximum rate values (Section 2.3.1.4) used in this study (Mary et al., 2008b).

Half-saturation flux for light harvesting in Pro: 40 µmol photons m^{-2} s^{-1}. Taken from observations of chlorophyll based light harvesting in cyanobacteria (MacKenzie et al., 2004, Kirchman and Hanson, 2012).

Half-saturation flux for light harvesting in SAR11: 2700 µmol photons m^{-2} s^{-1}. Taken from observations of PR based light harvesting (Walter et al., 2007, Kirchman and Hanson, 2012).

2.3.1.2. Photosynthetic carbon reduction (Pro only)

DIC concentration: 2000 µM. The total global average dissolved carbon dioxide concentration in the global ocean has been calculated on the Geotechnical Ocean Sections Study (Takashi et

al., 1981). For simplicity it is assumed that the global average is relevant to oligotrophic gyre DIC concentration.

Half saturation constant for DIC uptake: 500 μM. The sensitivity of DIC reduction is largely dependent on the enzyme RUBISCO, which has a low affinity for its substrate, resulting in a high half-saturation constant (Falkowski and Raven, 2013). The value used here is that used by Kooijman et al. (2002) in a similar DEB model of a mixotrophic protist. Protist photosynthetic systems were gained through horizontal gene transfer from cyanobacteria, such that both still retain similar twin light harvesting complexes (White, 2007). Therefore assuming the same half-saturation constant for DIC uptake seems a reasonable first estimate.

2.3.1.3. Uptake of DOC (SAR11 only), DON and DIN (Pro and SAR11)

Defining ambient concentrations for DOC, DON and DIN is problematic. We are only starting to understand which specific components of each pool are used by each organism and the little information we have on the size of each generalised ambient pool is highly variable. In addition, knowledge of the kinetics of nutrient uptake in relation to changing resource concentrations are limited (del Carmen Muñoz-Marín et al., 2013) and so obtaining accurate half saturation constants is difficult.

Uptake uses a Michaelis-Menten representation and so the half saturation constant defines the shape of the saturating curve and therefore the nature of the cells response to changing ambient conditions. Both Pro and SAR11 use the same high affinity ABC-cassette transporters (Kettler et al., 2007, Sowell et al., 2008) and so may have a similar response to changing ambient nutrient conditions. The half saturation constants for DOC, DON and DIN are therefore considered to be the same for Pro and SAR11.

For simplicity the maximum ambient concentrations for DOC, DON and DIN are 1 and each nutrient's half saturation constant is 0.2, which produces a similar shaped curve to that observed for glucose uptake in Pro, which is the only information available (del Carmen Muñoz-Marín et al., 2013). Ambient conditions in each experiment (X) are given as the concentration of DOC, DON and DIN relative to the half saturation constant estimate (Section 2.3.2) (K) as X/K. The maximum ambient nutrient condition experienced by Pro and SAR11 in each experiment is therefore 5 and are referred to as non-limiting conditions. The sensitivity of results to changes in the ambient conditions is explored for each experiment from X/K of 5 to 0.

2.3.1.4. The maximum rates of uptake and synthesis

The maximum rates of uptake and synthesis have not been empirically determined for natural populations for Pro and SAR11. Measurements of uptake and synthesis from field studies used to parameterise the model are, therefore, considered as maximum rates. These "maximum rates" are not available for every resource from empirical analyses for Pro and SAR11 and, therefore, some need to be estimated as described in Section 5.2.1.

A key assumption for the estimation of the maximum rate parameters is that both Pro and SAR11 grow at 0.20 d^{-1}. The requirement that both Pro and SAR11 grow at the same rate is explained in Section 5.1. The growth rate of 0.20 d^{-1} is within ranges observed for both organisms (Goericke and Welschmeyer, 1993, Zubkov, 2014, Rappe et al., 2002, Giovanonni et al., 2005a).

Estimates for the maximum DON uptake rate (Mary et al., 2008b), and a maximum CHO synthesis rate (Jardillier et al., 2010) are available for Pro but the maximum DIN uptake rate is not. In order to estimate this rate, it is assumed that DIN, DON and CHO satisfy all of Pro's carbon and nitrogen requirements. The estimated maximum rate of DIN uptake is therefore that required to supplement the nitrogen sourced from DON, allowing Pro to grow at 0.20 d^{-1}. This is achieved by increasing the parameter that defines the maximum uptake rate of DIN until the growth rate 0.20 d^{-1} is achieved for single value of light energy investment β.

For SAR11, an estimate for the maximum uptake rate of DON is available (Mary et al., 2008b) but not for the maximum uptake rates of DOC and DIN. For consistency in order to get parameter values for all these rates a scaling method is employed. The maximum rates of DIN and DON uptake are estimated by assuming that these rates will scale according to the differences in surface area to volume ratio (SA:V) between Pro and SAR11. The details of this method are given in Section 5.2.1. The estimated and measured values for the maximum rate of DON uptake are compared in Section 2.3.1.5. The maximum rate of DOC uptake is estimated by assuming that DOC supplements the fluxes of DIN and DON in order for SAR11 to grow at a rate of 0.20 d^{-1}. The maximum rate of DOC uptake parameter is increased until this growth rate is achieved for a single value of β.

The ambient conditions used to constrain the maximum rates are all at the maximum investigated in this thesis. Irradiance is therefore 500 µmols photons m^{-2} s^{-1}, DIC is 2000 µM and all other substrates are set to 1, with an X/K of 5. Conversions from cell specific to biomass specific uptake rates were calculated by assuming 16 fg C $cell^{-1}$ in Pro and 8 fg C $cell^{-1}$ in SAR11 (Grob et al., 2013).

2.3.1.5. Maximum uptake rate for DON

Pro: 0.0030 mol C (mol C)$^{-1}$ hour^{-1}. Amino acids are a significant source of nitrogen for Pro (Zubkov et al., 2003, Zubkov and Tarran, 2005) and therefore used as proxy for DON uptake. Leucine uptake rates are known for Pro (Mary et al., 2008b, Gómez-Pereira et al., 2012). The mole percentage composition of leucine in bacteria protein has been determined by Simon and Azam (1989). A maximum DON uptake rate $\dot{J}_{DON,Um}$, of 0.003 mol C (mol C)$^{-1}$ hr^{-1}, is calculated assuming all other amino acids scale with leucine uptake according to their relative abundance in bacteria protein.

SAR11: 0.0063 mol C (mol C)$^{-1}$ hr^{-1}. This value is calculated using the same method to that used for Pro by scaling the uptake rate of leucine, known for SAR11 (Mary et al., 2008a).

SAR11: 0.0084 mol C (mol C)$^{-1}$ hr^{-1}. This value was obtained through scaling the DON uptake rate in Pro to SAR11 by assuming differences in uptake are linearly proportional to any change in the cells SA:V. This value is 1.33 fold greater than that measured by Mary et al. (2008a) and within the studies measurement variability. This value is used for consistency with the approach used to estimate the maximum rate of DIN uptake in SAR11 (Section 2.3.1.7).

2.3.1.6. Maximum rate of carbon acquisition

Pro (CHO synthesis): 0.080 mol C (mol C)$^{-1}$ hr^{-1}. It is assumed for simplicity that the maximum rate of CHO synthesis is equal to the maximum rate of carbon dioxide assimilation. The above parameter value is estimated from assimilation rate measurements using carbon-14 uptake experiments (Jardillier et al., 2010). The rate of assimilation is based on internal quota of assimilated radio-isotopic tracer. This value may not include any CHO excreted from the cell, which can be up to 40 % of fixed carbon in Pro (Bertilsson et al., 2005, Karl et al., 1998). The value may be lower than the true gross photosynthetic carbohydrate flux. Direct empirical measurements of the gross carbohydrate flux are unavailable for Pro. The value used probably lies somewhere between the net and gross CHO synthesis rate and seems a reasonable compromise.

SAR11 (DOC uptake): 0.023 mol C (mol C)$^{-1}$ hr^{-1}. This value is found by tuning the model to fit a growth rate of 0.20 d^{-1}, supplementing the DIN and DON fluxes (as discussed in Section 2.3.1.4).

2.3.1.7. Maximum rate of DIN uptake

Pro: 0.0022 mol N (mol C)$^{-1}$ hr^{-1}. This value is the required maximum rate needed to supplement the known uptake rates of DON uptake and CHO synthesis in order for Pro to grow at 0.20 d^{-1}.

SAR11: 0.0057 mol N (mol C)$^{-1}$ hr^{-1}. This value has been obtained through scaling the maximum DIN uptake rate in Pro according to differences in the two cells' SA:V (Section 5.2.1).

2.3.1.8. Maximum rate of amino acid synthesis

Pro: 0.053 mol C (mol C)$^{-1}$ hour^{-1}. It is assumed that the maximum rate of AA synthesis is constrained by the flux of available CHO and reflecting the efficiency of AA synthesis, which is 67 % (De Vries et al., 1974). As the rate of maximum rate of CHO synthesis is 0.080 mol C (mol C)$^{-1}$ hr^{-1} (Jardillier et al., 2010), this value is multiplied by 0.67 to give the above maximum rate of AA synthesis.

SAR11: 0.015 mol C (mol C)$^{-1}$ hr^{-1}. This value was obtained in the same manner as the maximum rate of AA synthesis in Pro but using the maximum rate of DOC uptake. The same efficiency in the synthesis process is assumed for Pro and SAR11.

Conversion efficiency from carbon compounds (CHO/DOC) to AA: 1.5 mol C (mol C)$^{-1}$. AA synthesis is paid for through CHO/DOC mobilisation when DIN is the only nitrogenous growth substrate (Goldman and Dennett, 1991, Goldman et al., 1987, Goldman and Dennett, 2000). The cost has been calculated using the biochemistry of conversion reactions involved in AA synthesis reaction chains (De Vries et al., 1974). It is assumed that the summation of all the steps in reaction chains yields an overall balance for the synthesis of an AA (De Vries et al., 1974). As a first estimate, the reaction chain has been calculated for the synthesis of leucine, which requires a total of 1.5 carbon molecules for the synthesis of 1 leucine molecule (De Vries et al., 1974). Therefore the carbon conversion efficiency for AA synthesis is 67 %. The same value is assumed for Pro and SAR11 as both cells use the same synthesis machinery (Sowell et al., 2008, Kettler et al., 2007).

C:N of synthesised amino acids: 4.3 mol C (mol N)$^{-1}$. The AA composition and relative abundance in bacteria biomass has been determined for coastal Atlantic waters (Simon and Azam, 1989). The average C:N ratio of bacterial AA, based on their relative abundance in bacterial protein, has been calculated to represent the average C:N ratio of AA synthesised by the organism, which is 4.3 (Simon and Azam, 1989). Although oceanic bacterioplankton populations have a higher C:N ratio than coastal populations (Fukuda et al., 1998) differences

are assumed to be negligible for the sake of this parametrisation. It is a requirement in the model that the C:N of ambient DON is the same as the C:N of synthesised AA. This is because biomass is synthesised in a fully stoichiometrically balanced framework using the known C:N ratio of substrate relative to the C:N ratio of cell biomass. Because mixed oceanic bacterioplankton where Pro and SAR11 abound can select individual AAs specifically suited for metabolism (Zubkov et al., 2008), it is assumed that the DON taken up will have the same C:N as synthesised AA.

2.3.1.9. Flux ratios

Flux ratios: A value of 10 for the flux ratios, z_L, z_C and z_{DON}, is taken from a previously published DEB model of a mixotrophic protest (Kooijman et al., 2002). These parameters control the contribution of each compound to the production process in the photoautotrophy and photoheterotrophy SUs (Equations 2.2.1.3 and 2.2.1.4), which is assumed to be equal for all substrates.

2.3.2. Maintenance and growth

Maintenance rate: 0.0021 mol C (mol C)$^{-1}$ hr^{-1}. This value is the turnover rate of leucine in Pro cells in the subtropical North Atlantic (Hill et al., 2013). There is no other information available quantifying biomass turnover for maintenance biomass for Pro and SAR11. Therefore, this rate is assumed for both organisms.

Organic carbon (OC) conversion efficiency: 0.96 (sparing pathway, Equation 2.2.3a) (mol C (mol C)$^{-1}$)

Organic nitrogen (OC) conversion efficiency: 0.96 (deamination pathway, Equation 2.2.3b) (mol C (mol C)$^{-1}$)

The conversion efficiencies have been calculated by Calow (1977) and are considered the 'best possible' efficiency of a unicell. The calculations are based on the requirement of energy for polymerisation of monomers using ATP, the efficiency of aerobic systems and the efficiency of transferring energy from ATP to polymeric linkages (Calow, 1977).

DON C:N: 4.3 mol C (mol N)$^{-1}$. The value for this parameter is the same as the C:N of AA and the full justification is given in Section 2.3.1.8.

Biomass C:N of Pro: 9.2 mol C (mol N)$^{-1}$. The C:N ratio of Pro biomass has been determined using measurements of the elemental composition of six strains of Pro by X-ray microanalysis (Bertilsson et al., 2003).

Biomass C:N of SAR11: 5 mol C (mol N)$^{-1}$. The C:N ratio of SAR11 biomass has been determined using measurements of the elemental composition of individual cells from natural populations using X-ray microanalysis (Grob et al., 2013).

2.3.2.1. Binding probabilities

Binding probability of organic nitrogen (ON) to $\theta_{..}$: 0.95

Binding probability of organic nitrogen (ON) to $\theta_{.OC}$: 1

Binding probability of organic carbon (OC) to $\theta_{..}$: 1

In the model, the ON and OC fluxes are delivered to the maintenance and growth machinery. The use of these metabolites for maintenance and growth and the relative influence of the deamination and sparing pathways on synthesis is dependent on the rate of ON and OC delivery and the likelihood of substrates binding to enzymes for synthesis. The likelihood is set by the binding affinity parameters (Section 2.2.3.2). To tune the values for the binding affinity parameters the model was fit to data of Goldman et al. (1987). This experimental work provided data for the change in the growth efficiency of a mixed bacterioplankton population with different ambient substrate C:N, set using different relative DON and DOC concentrations. Goldman et al. (1987) defined carbon growth efficiency (CGE) as the ratio of particulate carbon to total available carbon. The nitrogen regeneration efficiency (NRE) was defined as the relative amount of released ammonium to total nitrogen.

For the purpose of parameter tuning it was assumed that maintenance and growth are satisfied by heterotrophic DON and DOC uptake, i.e. the kinetics of maintenance and growth are based on that of a heterotrophic bacterial cell growing on DOC and DON only. The rate of uptake in the model is not only dependent on ambient substrate concentrations but also upon the maximum rate of substrate uptake, which conceptually represents the number of membrane transporters for each substrate and substrate handling time (Aksnes and Egge, 1991). We do not have this information for the study by Goldman et al. (1987) and therefore assume the same quantity of transporters for DOC and DOC. CGE and NRE were fitted according to changes in the ambient pools only. The experimental conditions of Goldman et al. (1987) were recreated in this study by changing the ambient concentration of DOC and DON. A maintenance rate for the study by Goldman et al. (1987) was not calculated. The rate of 0.0021 mol C (mol C)$^{-1}$ hr^{-1} (Section 2.3.2) is used as a first estimate. The model fit is shown in Figure 2.2.

The theory behind the relative values for the binding probabilities is in accordance with that given by Kuijper et al. (2004). In short, a high affinity is set for the binding of ON to $\theta_{.OC}$ and OC to $\theta_{..}$ favouring the sparing pathway.

To first order the model follows the patterns of bacterioplankton CGE and NRE. It is reassuring that at low substrate C:N, i.e. carbon limitation, the model fits the data well. Where the C:N increases, i.e. increased carbon availability, NRE is over predicted. The absence of maximum uptake rates of DOC and DON uptake from the Goldman et al. (1897) study required to constrain the model may partially explain the poor model fit at high C:N. These maximum rates are set to be equal for the purpose of tuning the binding affinity parameters and, therefore, an equal density of membrane transporters for DOC and DON is assumed, as discussed. If this is not the case for every experimental substrate C:N, then the uptake rates of DOC and DON at the simulated substrate C:N may not represent that which occurred in the experiments by Goldman et al. (1987). This may influence the relative delivery of OC and ON to maintenance and growth, the rate of ammonium release and therefore NRE.

It has been suggested that nitrogen recycling is likely in bacterial cells (Goldman and Dennett, 2000). The current model formulation does not consider nitrogen recycling. It is possible that the absence of a recycling mechanism in the model may contribute to the over prediction of ammonium regeneration efficiency at high substrate C:N. A nitrogen recycling mechanism would presumably increase the potential for ammonium assimilation where carbon is non-limiting (high substrate C:N) and reduced the rate of ammonium release.

2.4. Sensitivity analysis

Sensitive model parameters are evaluated in order to quantify how variation in model output can be apportioned to sources of physiological variation and parameter uncertainty. Sensitivity analysis is conducted by evaluating the relative change in model output divided by a relative change in a parameter value, known as normalised sensitivity (S), given as

$$S = \frac{V_C - V_S}{P_C - P_S}$$

where V_S and P_S is the standard variable quantity and standard parameter value, respectively. V_C is the changed variable quantity as a result of the changed parameter value P_C. Parameter values are changed individually by ±20 %. Sensitivity analyses are conducted for all parameters relative to key processes of interest which are listed for Pro and SAR11 in Table 3.1 and Table 4.1, respectively. Sensitivity analyses are conducted for key processes of interested at the

optimum light investment for maximum growth rate for both Pro and SAR11 in specified ambient conditions.

2.5. Summary of the approach

Models have been built and parametrised that describe the physiology and metabolism of individual Pro and SAR11 cells. Each model has the ability to partition harvested solar energy between resource acquisition pathways. This allows for an analysis of how photoheterotrophic light use influences the growth and processing of carbon and nitrogen in Pro and SAR11, investigated separately in Chapters 3 and 4, respectively. The influence of photoheterotrophic light use on the growth and metabolism of Pro and SAR11 is first explored using the default parameter sets (Table 2.1), referred to as non-limiting conditions. Ambient resources are then decreased individually in subsequent experiments in order to investigate the importance of photoheterotrophy for Pro and SAR11 growth under resource limiting conditions. A detailed description of the experimental approach is given for the analyses of Pro and SAR11 in Sections 3.2 and 4.2, respectively.

Note that for Pro, the non-limiting conditions specified by the default parameter set are not saturating for ambient DIN (Figure 3.8). This is because the maximum rate of DIN uptake has been estimated using the model and the use of DIN saturates at a higher maximum rate of DIN uptake. For simplicity and continuity with the other experiments the default parameter set will still be referred to as non-limiting conditions with the caveat that the use of DIN is not saturating in Pro.

The model framework has the flexibility to parameterise for the distinct physiologies of Pro and SAR11 in order to understand how their unique strategies influences their growth rate, investigated in Chapter 5. The approach used is discussed in detail in Section 5.2. The strategy provides a means of quantifying the relative importance of each investigated physiological trait for Pro and SAR11 growth and critically for this thesis, photoheterotrophic resource acquisition. Only the default parameter set and, therefore, non-limiting conditions are used for this investigation.

A full sensitivity analysis is conducted according to the method given in Section 2.4 for the Pro and SAR11 default parameter sets and in resource limiting conditions, provided in the Appendices Sections 3.8 and 4.8, respectively.

2.6. Tables

Table 2.1 All of the model parameters and variables for both Pro and SAR11 with a brief description and units. The arrow (←) indicates that the values for SAR11 are the same as for Pro.

Symbol	Description	Pro	SAR11	Units
X_{DON}	Concentration of ambient dissolved organic nitrogen	0-1	←	-
X_{DOC}	Concentration of ambient dissolved organic carbon	0-1	←	-
X_{DIN}	Concentration of ambient dissolved inorganic nitrogen	0-1	←	-
X_{DIC}	Concentration of ambient dissolved inorganic carbon	2000	n/a	µM
$\dot{J}_{L,F}$	Irradiance	0-500	←	µmols photons m^{-2} s^{-1}
K_{DON}	Half saturation constant for dissolved organic nitrogen	0.2	←	-
K_{DOC}	Half saturation constant for dissolved organic carbon	n/a	0.2	-
K_{DIN}	Half saturation constant for dissolved inorganic nitrogen	0.2	←	-
K_{DIC}	Half saturation constant for dissolved inorganic carbon	500	n/a	µM
$\dot{J}_{L,FK}$	Half saturation flux for light	40	2700	µmols photons m^{-2} s^{-1}
$\dot{J}_{DON,Um}$	Maximum rate of dissolved organic nitrogen uptake	0.003	0.0084	mol C (mol C)$^{-1}$ hr^{-1}
$\dot{J}_{DIN,Um}$	Maximum rate of dissolved inorganic nitrogen uptake	0.0022	0.0057	mol N (mol C)$^{-1}$ hr^{-1}
$\dot{J}_{C,Um}$	Maximum rate of carbohydrate synthesis or DOC uptake	0.080	0.023	mol C (mol C)$^{-1}$ hr^{-1}
$\dot{J}_{AA,Sm}$	Maximum rate of amino acid synthesis	0.053	0.015	mol C (mol C)$^{-1}$ hr^{-1}
X	Growth biomass	Variable	←	mol C (mol C)$^{-1}$
n_C^{GS}	CHO/DOC used per amino acid produced	1.5	←	mol C (mol C)$^{-1}$
n_N^{GS}	DIN used per amino acid produced	0.23	←	mol N (mol C)$^{-1}$
$n_{CO_2}^{GS}$	CO_2 formed per amino acid produced	0.5	←	mol C (mol C)$^{-1}$
n_{ON}^{D}	Organic nitrogen (ON) used per biomass unit formed via the deamination route	1.04	←	mol C (mol C)$^{-1}$
$n_{CO_2}^{D}$	CO_2 formed per biomass unit produced via the deamination route	0.04	←	mol C (mol C)$^{-1}$
$n_{NH_4^+}^{D}$	NH_4^+ formed per biomass unit produced via the deamination route	0.05	0.14	mol N (mol C)$^{-1}$
n_{ON}^{S}	Organic nitrogen (ON) used per biomass unit formed via the sparing route	0.47	0.86	mol C (mol C)$^{-1}$
n_{OC}^{S}	Organic carbon (OC) used per biomass unit formed via the sparing route	0.57	0.18	mol C (mol C)$^{-1}$
$n_{CO_2}^{S}$	CO_2 formed per biomass unit produced via the sparing route	0.04	←	mol C (mol C)$^{-1}$
ρ_{ON}^{D}	Binding probability of organic nitrogen (ON) to $\theta_{..}$	0.95	←	-
ρ_{ON}^{S}	Binding probability of organic nitrogen (ON)to $\theta_{.ON}$	1	←	-
ρ_{OC}^{S}	Binding probability of organic carbon (OC) to $\theta_{..}$	1	←	-
θ_{xy}	Fraction of SUs in state xy	Variable	←	-
k_M	Maintenance turnover rate	0.0021	←	mol C (mol C)$^{-1}$ hr^{-1}
ψC_{AA}	CHO/DOC yield efficiency of amino acid synthesis	0.67	←	mol C (mol C)$^{-1}$
ψON	Organic nitrogen (ON) yield efficiency: deamination route	0.93	←	mol C (mol C)$^{-1}$

ψOC	Organic carbon yield efficiency: sparing route	0.93	←	mol C (mol C)$^{-1}$
φON	C:N of organic nitrogen (ON) (DON and AA)	4.3	←	mol C (mol N)$^{-1}$
φX	C:N of biomass	9.2	5	mol C (mol N)$^{-1}$
$\Omega_{ON.}$	Steady-state binding state for the D-route	Variable	←	-
Ω_{ONOC}	Steady state binding state for the S-route	Variable	←	-
α	Trade-off parameter for the CHO/DOC flux	Variable	←	-
β	Trade-off parameter for light use	0≤β≤1	←	-
z_C	Flux ratio for CHO/DOC synthesis/uptake	10	←	-
z_N	Flux ratio for DON uptake	10	←	-
z_L	Flux ratio for light harvesting	10	←	-
$j_{DON,U}$	Rate of DON uptake	Variable	←	mol C (mol C)$^{-1}$ hr^{-1}
$j_{DIN,U}$	Rate of DIN uptake	Variable	←	mol N (mol C)$^{-1}$ hr^{-1}
$j_{DIN,R}$	Rate of DIN rejection for AA SU	Variable	←	mol N (mol C)$^{-1}$ hr^{-1}
$j_{C,S}$	Rate of CHO synthesis/DOC uptake	Variable	←	mol C (mol C)$^{-1}$ hr^{-1}
$j_{AA,S}$	Rate of amino acid synthesis	Variable	←	mol C (mol C)$^{-1}$ hr^{-1}
$j_{AA,R}$	Rejected CHO/DOC flux from amino acid synthesis SU	Variable	←	mol C (mol C)$^{-1}$ hr^{-1}
$j_{CO_2,AA}$	CO_2 produced at amino acid synthesis	Variable	←	mol C (mol C)$^{-1}$ hr^{-1}
j_{OC}	Total organic carbon (OC) flux sent to maintenance and growth	Variable	←	mol C (mol C)$^{-1}$ hr^{-1}
j_{ON}	Total organic nitrogen (ON) flux sent to maintenance and growth	Variable	←	mol C (mol C)$^{-1}$ hr^{-1}
$j_{ON,M}$	Organic nitrogen (ON) flux used for maintenance	Variable	←	mol C (mol C)$^{-1}$ hr^{-1}
$j_{OC,M}$	Organic carbon (OC) flux used for maintenance	Variable	←	mol C (mol C)$^{-1}$ hr^{-1}
$j_{NH_4^+,M}$	NH_4^+ produced in maintenance	Variable	←	mol N (mol C)$^{-1}$ hr^{-1}
$j_{CO_2,M}$	CO_2 produced in maintenance	Variable	←	mol C (mol C)$^{-1}$ hr^{-1}
$j_{X,M}$	Biomass produced in maintenance	Variable	←	mol C (mol C)$^{-1}$ hr^{-1}
$j_{ON,G}^{g}$	Organic nitrogen (ON) flux assigned to growth	Variable	←	mol C (mol C)$^{-1}$ hr^{-1}
$j_{OC,G}^{g}$	Organic carbon (OC) flux assigned to growth	Variable	←	mol C (mol C)$^{-1}$ hr^{-1}
$j_{ON,G}$	Organic nitrogen (ON) flux used for growth	Variable	←	mol C (mol C)$^{-1}$ hr^{-1}
$j_{OC,G}$	Organic carbon (OC) flux used for growth	Variable	←	mol C (mol C)$^{-1}$ hr^{-1}
$j_{NH_4^+,G}$	NH_4^+ produced in growth	Variable	←	mol N (mol C)$^{-1}$ hr^{-1}
$j_{CO_2,G}$	CO_2 produced in growth	Variable	←	mol C (mol C)$^{-1}$ hr^{-1}
$j_{X,G}$	Growth rate	Variable	←	mol C (mol C)$^{-1}$ hr^{-1}
$j_{ON,R}$	Organic nitrogen (ON) flux in excess to growth	Variable	←	mol C (mol C)$^{-1}$ hr^{-1}
$j_{OC,R}$	Organic carbon (OC) flux in excess to growth	Variable	←	mol C (mol C)$^{-1}$ hr^{-1}
f_{Dark}	Functional response for SAR11 uptake in the dark	n/a	0.097	-
K_{new}	Half saturation irradiance for the SAR11 dark model	n/a	6430	µmols photons m^{-2} s^{-1}
Io	Irradiance for the SAR11 dark model	n/a	691	µmols photons m^{-2} s^{-1}

2.7. Figures

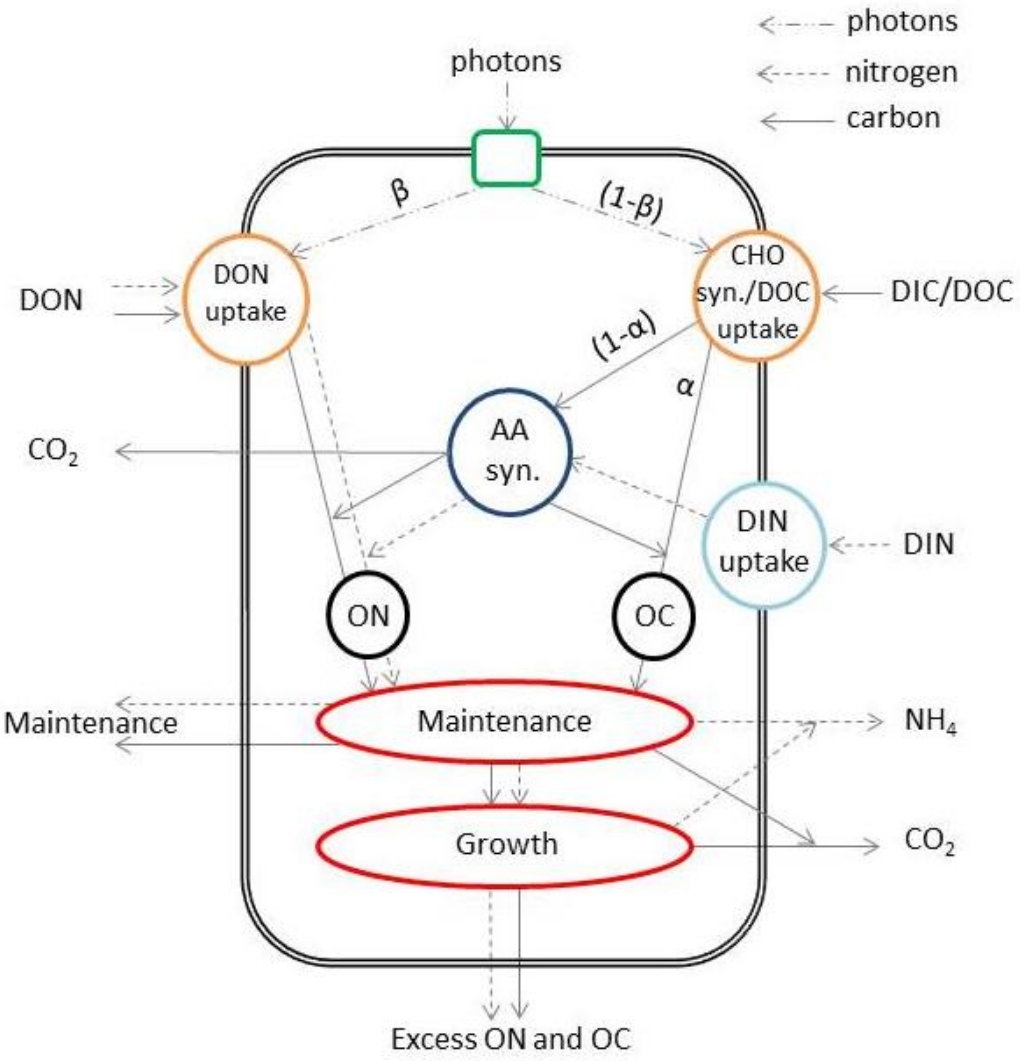

Figure 2.1 Schematic of the model. The green box represents light harvesting pigments: divinyl-chlorophyll-a in Pro and proteorhodopsin in SAR11. The partitioning of harvested light energy between CHO synthesis/DOC uptake and DON uptake is controlled by the parameter β. CHO in Pro, synthesised through DIC reduction, and DOC in SAR11 are partitioned between AA synthesis (dark blue circle) and maintenance and growth (red circles) using the parameter α. DIN is taken up (light blue circle) and bound to CHO/DOC to synthesise AA (dark blue circle) which is added to the flux of DON. The organic nitrogen flux (ON), which contains carbon and nitrogen (DON and AA fluxes) and organic carbon flux (OC), which contains carbon but no nitrogen (CHO/DOC fluxes remaining after AA synthesis) (black circles) are available for the cell to satisfy maintenance as a priority and then growth (red circles). Carbon dioxide is respired at AA synthesis and maintenance and growth. Ammonium is released at maintenance and growth. Maintenance biomass is assumed to be lost from the cell along with OC and ON that are in excess to stoichiometric requirements for growth.

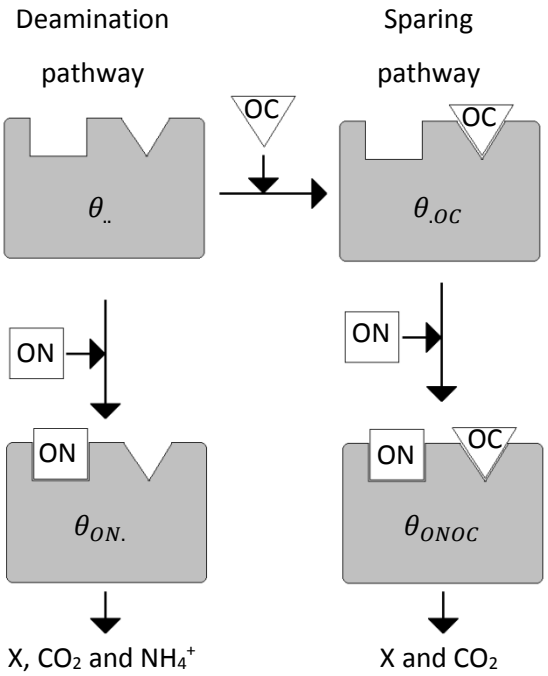

Figure 2.2 Schematic detailing the four binding states for maintenance and growth and the products formed via the deamination (Equation 2.2.3a) (left) and sparing (Equation 2.2.3b) (right) pathways. ON corresponds to an organic nitrogen molecule and OC corresponds to the organic carbon molecule. θ_{xy} corresponds to binding states. Figure adapted from Kuijper et al. (2004)

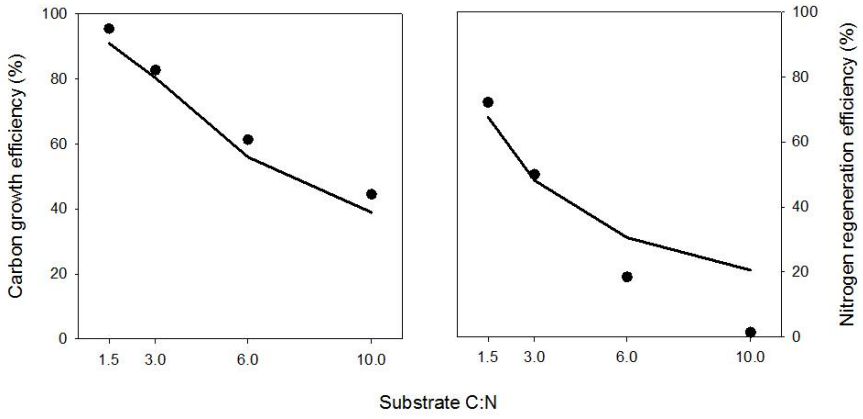

Figure 2. 3 Model fit (line) to data of Goldman et al. (1987) (circles) for carbon growth efficiency and nitrogen regeneration efficiency for tuning the binding efficiencies.

Chapter 3: The use of sunlight in *Prochlorococcus*

3.1 Chapter overview and rationale

Chapter 1 described how the most abundant photosynthetic organism in the ocean, the cyanobacteria *Prochlorococcus* (Pro) (Partensky et al., 1999), can also enhance its uptake of dissolved organic material (DOM) in the presence of sunlight (Michelou et al., 2007, Mary et al., 2008b, Gómez-Pereira et al., 2012), a mode of resource acquisition termed photoheterotrophy. Pro not only play a critical role in open ocean carbon fixation (Zubkov, 2014, Goericke and Welschmeyer, 1993) but also dominate the uptake of DOM (Michelou et al., 2007, Mary et al., 2008b, Gómez-Pereira et al., 2012, Zubkov et al., 2003, Zubkov et al., 2004b, Zubkov and Tarran, 2005) and therefore play an important part in the cycling of organic matter in the microbial food web. The ability to partition the use of harvested solar energy between photosynthesis and photoheterotrophy may increase the growth rate of Pro and alter our understanding of the role of this abundant organism in the processing of carbon and nitrogen in the open ocean. The aim of this chapter is to investigate the influence of photoheterotrophic light use on the growth rate of Pro and its influence on key physiological processes.

3.2 Approach

The focus of this study is the specific growth rate of Pro and in particular the maximum growth rate that can be achieved by optimally partitioning harvested solar energy between photosynthesis and photoheterotrophy. The growth rate is defined as the quantity of carbon invested in new biomass per day (Section 2.2.3.3). The influence of the multiple uses of harvested solar energy on the uptake and fate of carbon and nitrogen is also evaluated. All fluxes considered are listed in Table 3.1. A schematic summary of the model is shown in Figure 3.1. The model description, formulae and parameter values can be found in Chapter 2.

The impact of partitioning light energy between photosynthesis and photoheterotrophy on growth rate is explored through four experiments. Each experiment investigates a different influence of the ambient environment. In the first experiment, the growth rate of a Pro cell that can use light energy for photosynthesis and photoheterotrophy is compared to a baseline cell type that cannot direct light energy to enhance DON uptake, growing by photoautotrophy alone. All ambient conditions in the first experiment are assumed to be non-limiting. The dynamics of the baseline photoautotrophy model and the multiple light use model are then compared at multiple ambient DIN (Experiment 2), DON (Experiment 3) and irradiance

(Experiment 4) conditions in order to understand how a changing ambient environment influences the importance of photoheterotrophic light use for Pro growth rate, and its use of carbon and nitrogen. A quantitative evaluation of the key processes of interest, listed in Table 3.1, is undertaken for each experiment. Experimental conditions are given in Table 3.2 and outlines of the four experiments are given below.

Experiment 1: The first experiment analyses the influence of multiple solar energy uses on Pro growth and metabolism relative to a cell that can only perform photosynthesis. The model allowing photosynthetic and photoheterotrophic light use is referred to as Pro-PH and the baseline model growing by photoautotrophy alone is called Pro-PA. Both cells harvest light and nutrients for 12 hours out of a 24 hour growth period and growth is only possibly during daylight hours. A 12:12 light:dark cycle is therefore assumed and is used for all experiments. The parameter representing how light energy is allocated, β, varies between 0 and 1. As β tends to zero more light energy is invested in photosynthesis at the expense of photoheterotrophy, and as β tends to one, more light energy is invested in photoheterotrophy at the expense of photosynthesis. Irradiance and ambient nutrient conditions are given in Table 3.2. and explained in Section 2.3.1. Optimal light investment for maximum growth rate, referred to as β_{opt}, in addition to suboptimal β are investigated in the first experiment. This is in order to understand what processes constrain the optimum. The suboptimum analysis is only undertaken for Experiment 1 as it is assumed that Pro would optimally balance the use of solar energy to maximise growth rate and, therefore, the behaviour at β_{opt} is of primary interest.

Experiment 2: The second experiment is designed to analyse how ambient DIN influences the use of harvested solar energy by comparing the dynamics of Pro-PA and Pro-PH at multiple ambient DIN from 0 to 5 (X/K). All other ambient conditions are kept constant as in Experiment 1 (Table 3.2). For each value of DIN (X/K) only the behaviour at β_{opt} is investigated.

Experiment 3: The third experiment investigates how ambient DON influences solar energy use by comparing the dynamics Pro-PA and Pro-PH at multiple ambient DON from 0 to 5 (X/K). Again all other ambient conditions are kept constant (Table 3.2) as in Experiment 1 and only the behaviour at $\beta_{o\square t}$ is evaluated.

Experiment 4: The fourth experiment analyses how irradiance intensity influences the use of harvested solar energy by comparing the behaviour of Pro-PA and Pro-PH at multiple irradiances from 0 to 500 µmol photons m^{-2} s^{-1}. All other nutrients are constant (Table 3.2) and once again only the behaviour at β_{opt} is evaluated.

3.3 Results

3.3.1 Experiment 1: non-liming conditions (the default parameter set)

3.3.1.1 Growth rate and the uptake of carbon and nitrogen at β_{opt}

The Pro-PH model has been fitted to a growth rate of 0.20 mol C (mol C)$^{-1}$ d^{-1}, as discussed in Section 2.3.1.4. In order to grow at this rate Pro-PH needs to invest 38 % of harvested solar energy in photosynthesis with the remaining 62 % invested in photoheterotrophy (β_{opt} = 0.62) (Figure 3.2). Pro-PA can only invest solar energy in photosynthesis (β = 0) and grows at 0.137 mol C (mol C)$^{-1}$ d^{-1}. The growth curves of Pro-PA and Pro-PH, therefore, intersect at β = 0 where both growth via photoautotrophy only. The difference in growth rate between Pro-PA and Pro-PH is 0.063 mol C (mol C)$^{-1}$ d^{-1}, i.e. the ability to partition harvested solar energy between photosynthesis and photoheterotrophy allows Pro-PH to grow 46.0 % faster than Pro-PA in non-limiting conditions (Figure 3.2).

The effect of directing solar energy away from photosynthetic CHO synthesis is inconsequential for its rate of production as light use for its production is saturating, decreasing by only 0.8 % from 7.83 x10^{-2} mol C (mol C)$^{-1}$ hr^{-1} in Pro-PA to 7.77 x 10^{-2} mol C (mol C)$^{-1}$ hr^{-1} Pro-PH (Figure 3.2). The trade-off for solar energy does not significantly influence the rate of AA production either (and therefore DIN assimilation), decreasing by only 0.3 % from 6.73 x 10^{-3} mol C (mol C)$^{-1}$ hr^{-1} in Pro-PA to 6.71 x 10^{-3} mol C (mol C)$^{-1}$ hr^{-1} in Pro-PH. The solar energy trade-off, therefore, does not significantly affect carbon availability for AA synthesis. The OC flux is not changed significantly as the rates of CHO and AA synthesis aren't affected by photoheterotrophic light use, decreasing by 0.9 % from 6.83 x 10^{-2} mol C (mol C)$^{-1}$ hr^{-1} in Pro-PA to 6.77 x 10^{-2} mol C (mol C)$^{-1}$ hr^{-1} in Pro-PH (Figure 3.2). Photoheterotrophy facilitates a DON uptake rate of 2.94 x 10^{-3} mol C (mol C)$^{-1}$ hr^{-1} in Pro-PH (Figure 3.2). Supplementing the AA flux with DON produces an ON delivery rate to maintenance and growth of 9.64 x 10^{-3} mol C (mol C)$^{-1}$ hr^{-1}, which is 43.4 % greater than in Pro-PA (6.73 x 10^{-3} mol C (mol C)$^{-1}$ hr^{-1}) (Figure 3.2), providing Pro-PH with the increased nitrogen required to grow 46.0 % faster.

Photoheterotrophy increases the total rate of nitrogen uptake by 43.4 %, from 1.56 x 10^{-3} mol N (mol C)$^{-1}$ hr^{-1} in Pro-PA to 2.24 x 10^{-3} mol N (mol C)$^{-1}$ hr^{-1} in Pro-PH (Figure 3.3). DON accounts for 30.0 % of total nitrogen uptake, with the remaining 70.0 % from DIN in Pro-PH (Figure 3.2). The total carbon uptake rate, however, is not changed significantly through photoheterotrophic light use, increasing only by 3.0 % from 7.83 x 10^{-2} mol C (mol C)$^{-1}$ hr^{-1} in Pro-PA to 8.36 x 10^{-2} mol C (mol C)$^{-1}$ hr^{-1} in Pro-PH (Figure 3.3). Photosynthetically generated CHO accounts for 96.4 % of total carbon uptake, with the remaining 3.6 % sourced from DON (Figure 3.2).

3.3.1.2 The fate of carbon and nitrogen at β_{opt}

Photoheterotrophic light use results in a small increase in the percentage of the total carbon flux assimilated into biomass from 15 % in Pro-PA to 21 % in Pro-PH, whilst the change in total carbon uptake rate is minimal (Figure 3.3). The ability to enhance nitrogen acquisition via photoheterotrophic DON uptake, increases carbon assimilation and reduces the rate of excess carbon release by 5.3 % from 6.09 x 10^{-2} mol C (mol C)$^{-1}$ hr^{-1} in Pro-PA to 5.77 x 10^{-2} mol C (mol C)$^{-1}$ hr^{-1} in Pro-PH (Figure 3.4), which accounts for 77 % of the total carbon flux in Pro-PA and 71 % of the total carbon flux in Pro-PH (Figure 3.3). Maintenance is fixed, accounting for ~ 3 % of the total carbon flux in both cell types. Respiration through AA synthesis is unchanging, accounting for ~4 % of the total carbon flux. Respiration at maintenance and growth accounts for less than 1 % of the total carbon flux in both cell types (Figure 3.3, 3.4). The small increase in the fraction of carbon assimilated into biomass is a result of the decline in the rate of excess carbon release (Figure 3.3).

The majority of the total nitrogen flux is assimilated into biomass, the percentage of which is similar for both cell types; 79 % in Pro-PA and 81 % in Pro-PH (Figure 3.3). The maintenance rate is the same for both cell types yet accounts for a smaller percentage of the total nitrogen flux in Pro-PH (11 %) than Pro-PA (15 %), due to the greater total rate of nitrogen uptake in the former (Figure 3.3). Photoheterotrophic light use increases the rate of ammonium release by 103.0 % from 0.80 x 10^{-4} mol N (mol C)$^{-1}$ hr^{-1} in Pro-PA to 1.63 x 10^{-4} mol N (mol C)$^{-1}$ hr^{-1} in Pro-PH (Figure 3.4). However, this flux accounts for only 5 % and 7 % of the total nitrogen flux in Pro-PA and Pro-PH, respectively (Figure 3.3). The difference partially offsets the change in the percentage used in maintenance and the influence on nitrogen assimilation. The rate of excess nitrogen release increases by 30.8 % from 3.25 x 10^{-4} mol N (mol C)$^{-1}$ hr^{-1} in Pro-PA to 4.21 x10^{-4} mol N (mol C)$^{-1}$ hr^{-1} in Pro-PH (Figure 3.4), and represents ~1 % of the total nitrogen flux for both cell types (Figure 3.3).

3.3.1.3 Growth rate and the uptake and fate of carbon and nitrogen at suboptimum β

The dynamics of suboptimum β have been evaluated by default for β = 0 (i.e. Pro-PA) in the previous analysis of Pro-PA and Pro-PH. The suboptimum at β = 1 will be evaluated in order to understand what processes reduce growth rate this side of the optimum. Investing all harvested solar energy in the uptake of DON (β = 1) gives a growth rate of 8.71 x 10^{-3} mol C (mol C)$^{-1}$ d^{-1}, 4.4 % that of Pro-PH at β_{opt} (0.20 mol C (mol C)$^{-1}$ d^{-1}) (Figure 3.2).

When all harvested solar energy is invested in DON uptake (β = 1), the cell depends on DON for all energy, carbon and nitrogen (Figure 3.5b). The cell does not synthesise CHO

(Figure 3.5c) and therefore cannot assimilate DIN into AA (Figure 3.5d). The flux OC is zero (Figure 3.5e). The ON flux is made up entirely of DON and is 30.6 % of the ON flux at β_{opt} (Figure 3.5f). Total carbon uptake rate is 2.95 x 10^{-3} mol C (mol C)$^{-1}$ hr^{-1} and the total nitrogen uptake rate is 6.85 x 10^{-4} mol N (mol C)$^{-1}$ hr^{-1}, 3.5 % and 30.6 % that found at β_{opt}, respectively (Figure 3.7).

Nitrogen assimilation into biomass is significantly reduced at β = 1 at only 12 % of the total nitrogen flux, compared to 81 % at β_{opt} (Figure 3.7). The rate of ammonium release whilst growing exclusively on DON is 127.6 % greater than at β_{opt}. The release rate increases from 1.63 x 10^{-4} mol N (mol C)$^{-1}$ hr^{-1} at β_{opt} where it accounts for 7 % of the total nitrogen flux to 3.71 x 10^{-4} mol N (mol C)$^{-1}$ hr^{-1} at β = 1 where it accounts for 54 % of the total nitrogen flux (Figure 3.6d, 3.7). In addition, as a result of the reduced rate of total nitrogen uptake, relative to β_{opt}, maintenance accounts for 33 % of the total nitrogen flux at β = 1 compared to 11 % at β_{opt} (Figure 3.7). Excess nitrogen only accounts for ~1 % percent of total nitrogen in both cell types.

A slightly greater percentage of the total carbon flux is assimilated into biomass at β = 1 than at β_{opt} (25 % at β = 1 and 21 % at β_{opt}). The rate of excess carbon release, however, changes significantly and accounts for only 1 % total carbon uptake compared to 71 % at β_{opt} (Figure 3.7). The rate of excess carbon release is 1.99 x 10^{-5} mol C (mol C)$^{-1}$ hr^{-1}, just 0.03 % the rate at β_{opt} (Figure 3.6e). Because of the significantly reduced rate of total carbon uptake (Figure 3.7), 70 % of the total carbon flux is used to satisfy the fixed maintenance requirements, compared to only 3 % at β_{opt} (Figure 3.7). The different dynamics of excess carbon release and maintenance largely offset each other resulting in a similar percentage of assimilated carbon at β = 1 and β_{opt}.

3.3.2 Experiment 2: The effect of ambient DIN

3.3.2.1 Growth rate and the uptake of carbon and nitrogen

Photoheterotrophic light use can not only enhance growth rate during non-limiting conditions (Section 3.3.1) but also relieve DIN limitation of photoautotrophic growth (Figure 3.8a) by facilitating DON uptake in Pro-PH (Figure 3.8d), with a negligible influence on CHO synthesis (Figure 3.8e) and AA synthesis (therefore DIN assimilation) (Figure 3.8c) relative to Pro-PA.

As ambient DIN decreases, the growth rate of Pro-PH decreases from 0.20 to 0.05 mol C (mol C)$^{-1}$ d^{-1}, with a growth rate at zero ambient DIN which is 75 % less than when ambient DIN is at a maximum (5 X/K) (Figure 3.8a). Pro-PA grows at 0.137 mol C (mol C)$^{-1}$ d^{-1} when DIN

is at a maximum but cannot grow between an ambient DIN of 0.125 (X/K) and zero. In these conditions, Pro-PH growth rate varies between at 0.07 mol C (mol C)$^{-1}$ d^{-1} and 0.05 mol C (mol C)$^{-1}$ d^{-1} (Figure 3.8a).

In order to maintain the maximum possible growth rate as ambient DIN decreases, Pro-PH needs to invest an increasing fraction of harvested solar energy in the uptake of DON (Figure 3.8b). β_{opt} shifts from 0.62 at maximum DIN (5 X/K) to 0.87 at limiting DIN (DIN = 0.02 to zero (X/K)). Although an increasing fraction of solar energy is invested in DON uptake as ambient DIN declines, there is no appreciable change in its rate of uptake, remaining at 2.94 x 10^{-3} mol C (mol C)$^{-1}$ hr^{-1} between maximum and zero DIN (Figure 3.8c). In these conditions (Table 3.2) DON uptake is saturated. At the ambient DIN (DIN = 0.125 to zero (X/K)) where Pro-PA cannot grow, satisfying maintenance only (Figure 3.8a), the additional contribution of DON to the ON flux in Pro-PH, increases its rate of delivery to maintenance and growth by 348.0 % relative to Pro-PA, from 8.46 x 10^{-4} mol C (mol C)$^{-1}$ hr^{-1} to 3.79 x 10^{-3} mol C (mol C)$^{-1}$ hr^{-1} (Figure 3.8d). Redirecting solar energy to enhance DON uptake has a negligible influence on the rate of CHO synthesis as ambient DIN declines, which decreases no more than 3.3 % from 7.83 x 10^{-3} mol C (mol C)$^{-1}$ hr^{-1} in Pro-PA at DIN = 0.125 to 7.57 x 10^{-3} mol C (mol C)$^{-1}$ hr^{-1} in Pro-PH when DIN is limiting (DIN = 0.02 to zero (X/K) (Figure 3.8e). Photoheterotrophic light use has no influence on the rate of AA synthesis in these conditions as its carbon source is not affected by the trade-off. Unsurprisingly its rate of production decreases to zero at zero ambient DIN (Figure 3.8c). The OC flux left over after AA synthesis decreases by only 2.7 %, from 7.70 x 10^{-2} mol C (mol C)$^{-1}$ hr^{-1} in Pro-PA to 7.57 x10^{-2} mol C (mol C)$^{-1}$ hr^{-1} in Pro-PH when DIN is limiting (Figure 3.8f).

3.3.2.2 The fate of carbon and nitrogen

At ambient DIN (DIN = 0.125 (X/K)) where the growth rate of Pro-PA is zero, the vast majority of the cell's total carbon flux is in excess (96 %) released at a rate of 7.61 x 10^{-2} mol C (mol C)$^{-1}$ hr^{-1} (Figure 3.9c and 3.10). The remaining carbon (4 %) is used and respired in the synthesis of maintenance biomass (Figure 3.10). Practically all nitrogen, however, is used and released as ammonium to satisfy maintenance, with a negligible amount in excess (Figure 3.10). The increase in the rate of ON delivery to maintenance and growth in Pro-PH via photoheterotrophic DON uptake, in conditions that do not allow Pro-PA to grow (DIN = 0.125 (X/K) (Figure 3.8d) allows the cell to assimilate 7 % of the total carbon flux into new growth, leaving 89 % in excess released at 7.07 x 10^{-2} mol C (mol C)$^{-1}$ hr^{-1} (Figure 3.9c and 3.10). The remaining 4 % is used and respired in the synthesis of maintenance biomass (Figure 3.10). At DIN = 0.125 (X/K), 70 % of nitrogen is now assimilated in Pro-PH, with 29 % used and released

as ammonium to satisfy maintenance. The rate of ammonium release increases by up to 138.5 %, from 1.35 x 10^{-5} mol N (mol C)$^{-1}$ hr^{-1} in Pro-PA to 3.22 x 10^{-5} mol N (mol C)$^{-1}$ hr^{-1} in Pro-PH (Figure 3.9e), accounting however for only 5 % and 4 % of the total nitrogen flux, respectively (Figure 3.10). Excess nitrogen release represents less than 1 %.

At zero ambient DIN, Pro-PH releases the vast majority (92 %) of the total carbon flux as excess at a rate of 7.23 x 10^{-2} mol C (mol C)$^{-1}$ hr^{-1} (Figure 3.9c, Figure 3.10). Only 5 % of the total carbon flux can be assimilated with the remaining 3 % used and respired for maintenance (Figure 3.10). 62 % of the total nitrogen flux can be assimilated at zero DIN, with 37 % used to for maintenance, 4 % of which is released as ammonium at a rate of 2.43 x 10^{-5} mol N (mol C)$^{-1}$ hr^{-1} (Figure 3.9e). Only 1 % is in excess.

3.3.3 Experiment 3: the effect of ambient DON

3.3.3.1 Growth rate

As ambient DON declines the growth rate of Pro-PH decreases from 0.20 mol C (mol C)$^{-1}$ d^{-1} at maximum DON to 0.137 mol C (mol C)$^{-1}$ d^{-1} at 0.005 DON (X/K) (Figure 3.11a), the latter is the same rate of growth as Pro-PA. Pro-PH must invest an increasing fraction of harvested solar energy in the synthesis of CHO to grow at the maximum rate as ambient DON decreases (Figure 3.11b). β_{opt} shifts from the optimum of 0.62 at maximum DON, to 0 at 0.005 to zero (X/K) ambient DON (Figure 3.11b). The dynamics and magnitude of the key processes of interested are therefore akin to that discussed in Experiment 1 (Figures 3.11, 3.12 and 3.13) which compares the dynamics of Pro-PA and Pro-PH at β_{opt} in non-limiting conditions. A description of the differences between the dynamics of Pro-PA and Pro-PH will therefore not be given here again.

3.3.4 Experiment 4: the effect of irradiance

3.3.4.1 Growth rate and the uptake of carbon and nitrogen

With decreasing irradiance Pro-PH invests less solar energy in photoheterotrophy in preference for photosynthesis (Figure 3.14b) and the growth rates of Pro-PA and Pro-PH decrease and consequently converge at low light (Figure 3.14a). The changing trade-off dynamics reduces the availability of DON for growth in Pro-PH (Figure 3.14d) but with minimal influence on AA synthesis (Figure 3.14c) and therefore DIN assimilation. However, photoheterotrophic light use decreases carbon reduction in certain irradiance conditions relative to Pro-PA (Figure 3.14e).

As irradiance declines the growth rates of Pro-PA and Pro-PH decrease from 0.137 and 0.20 mol C (mol C)$^{-1}$ d^{-1} at saturating irradiance (500 µmol photons m^{-2} s^{-1}), respectively, to zero at 0.12 µmol photons m^{-2} s^{-1} (Figure 3.14a). The growth strategies of both cell types converges at 1.8 µmol photons m^{-2} s^{-1} growing by photoautotrophy only at a rate of 0.11 mol C (mol C)$^{-1}$ d^{-1} (Figure 3.14a). At this irradiance, Pro-PA grows 20 % slower than at saturating irradiance and Pro-PH grows 45 % slower than at saturating irradiance. Between 1.8 and 500 µmol photons m^{-2} s^{-1}, the growth rate of Pro-PH is, therefore, more sensitive to changes in irradiance than Pro-PA, and below, photoheterotrophic light use is of no benefit to the cell (Figure 3.14a).

Pro-PH needs to invest an increasing fraction of harvested solar energy in the synthesis of CHO as irradiance decreases to maintain the maximum growth rate (Figure 3.14b). β_{opt} shifts from the 0.62 at saturating irradiance, to 0 at limiting irradiance (1.8 µmol photons m^{-2} s^{-1} to darkness) (Figure 3.14b). The growth rate of Pro-PH is more sensitive to changes in light level than Pro-PA between saturating and limiting irradiance primarily because of the significant decline in the cells ON flux, decreasing by 37.2 % from 9.64 x 10^{-3} mol C (mol C)$^{-1}$ hr^{-1} to 6.05 x 10^{-3} mol C (mol C)$^{-1}$ hr^{-1} (Figure 3.14d). For the most part this is due to the decreasing solar energy investment in DON uptake as irradiance decreases (Figure 3.14b, d) and not because of any significant change in the rate of AA synthesis (Figure 3.14c). The rate of DON uptake decreases by 100 % from 2.94 x 10^{-3} mol C (mol C)$^{-1}$ hr^{-1} to zero between 500 and 1.8 µmol photons m^{-2} s^{-1} (Figure 3.14d). However, photoheterotrophy has a negligible effect on the rate of AA synthesis (no greater than 2.7 % less in Pro-PH relative to Pro-PA). Although the OC flux drops significantly, the rate of delivery decreases by ~73 % for both cell types as irradiance decreases (Figure 3.14f). Between 500 and 1.8 µmol photons m^{-2} s^{-1}, the rate of CHO synthesis decreases by ~65 % for both cell types. Interestingly, the trade-off for solar energy results in a decrease of CHO synthesis in Pro-PH relative to Pro-PA by up to 22.0 %, with the greatest difference at ~10 µmol photons m^{-2} s^{-1} (Figure 3.14e). The trade-off for solar energy decreases carbon reduction in Pro-PH relative to Pro-PA by no less than 15.0 % between 3 and 30 µmol photons m^{-2} s^{-1}. The 15.0 % boundary is arbitrary, used only to demonstrate a range of irradiances where photoheterotrophic light use may influence the rate of CHO synthesis.

The growth rate of Pro-PA is insensitive to changes in irradiance between 500 and 1.8 µmol photons m^{-2} s^{-1} primarily because although the CHO production rate decreases by up to ~65 % (Figure 3.14e) and OC by ~73 % (Figure 3.14f), the rate of AA synthesis, and therefore the ON flux, is largely unchanging, decreasing by only 9.8 % from 6.71 x 10^{-3} mol C (mol C)$^{-1}$ hr^{-1} to 6.05 x 10^{-3} mol C (mol C)$^{-1}$ hr^{-1} between saturating and limiting light (500 and 1.8 µmol photons m^{-2} s^{-1}) (Figure 3.14c). AA synthesis is maintained in Pro-PA (and Pro-PH) despite the

significant decrease in the rate of CHO synthesis (carbon source for AA) because the majority of synthesised CHO is in excess to stoichiometric requirements for growth (Figure 3.16).

3.3.4.2 The fate of carbon and nitrogen

Maintenance and carbon dioxide release account for an increasingly greater percentage of the total carbon flux as irradiance declines for both Pro-PA and Pro-PH as light limits the synthesis of CHO and therefore the cell's primary source of carbon (Figure 3.16). However, the significant decrease in the rate of excess carbon release (Figure 3.15c) and its fraction of the total carbon flux means Pro-PA and Pro-PH use carbon more efficiently in low compared to high irradiance conditions (Figure 3.16). The percentage of carbon assimilated by Pro-PA and Pro-PH at 1.8 µmol photons m^{-2} s^{-1} (limiting irradiance where photoheterotrophy is no longer of use to Pro-PH) is ~33 %, whilst at saturating irradiance Pro-PA assimilates 15 % and Pro-PH assimilates 21 % of the total carbon flux (Figure 3.16). Photoheterotrophic light use does not significantly influence the rate of total carbon dioxide release as irradiance decreases (Figure 3.15d) but carbon dioxide does makes up an increasing fraction of the total carbon flux, up to 13 % in Pro-PA and Pro-PH at 1.8 µmol photons m^{-2} s^{-1}, compared to ~5 % in both cell types at saturating irradiance (Figure 3.16). Maintenance also makes up an increasing fraction of the total carbon flux as irradiance decreases, accounting for up to ~10 % in Pro-PA and Pro-PH at 1.8 µmol photons m^{-2} s^{-1} compared to just ~3 % in both cell types at saturating irradiance (Figure 3.16). The percentage of the total carbon flux used for maintenance continues to increase as irradiance declines further. The rate of excess carbon release, however, decreases significantly as irradiance declines (Figure 3.15c) and makes up 44 % of the total carbon flux at 1.8 µmol photons m^{-2} s^{-1} compared to 77 % in Pro-PA and 71 % in Pro-PH at saturating irradiance (Figure 3.16). The rate of excess carbon release continues to decrease further with decreasing irradiance. Photoheterotrophic light use reduces the rate of excess carbon release by up to 33.0 % in Pro-PH relative to Pro-PA, the biggest difference being at ~10 µmol photons m^{-2} s^{-1} (Figure 3.16).

Both cell types assimilate less nitrogen at low irradiance compared to saturating irradiance because of the increase in the percentage of nitrogen used to satisfy maintenance, and released as ammonium (Figure 3.16). Pro-PA and Pro-PH both assimilate ~80 % total nitrogen at saturating irradiance whereas nitrogen assimilation at limiting irradiance (1.8 µmol photons m^{-2} s^{-1}) is ~70 % (Figure 3.16). Nitrogen assimilation declines further with decreasing irradiance. Within the region of irradiance (500 and 1.8 µmol photons m^{-2} s^{-1}) where photoheterotrophy increases growth rate, ammonium release is over 100 % greater in Pro-PH relative to Pro-PA, the biggest difference being at saturating irradiance (Figure 3.15f). OC:ON is

lower in Pro-PH than Pro-PA between 500 and 1.8 µmol photons m^{-2} s^{-1} (Figure 3.17), attributed to the significantly greater rate of DON uptake (Figure 3.14d), and lower rate of CHO synthesis (Figure 3.14e). As a result, biomass synthesis occurs through the use of ON as a source of energy to a greater extent in Pro-PH than Pro-PA, and Pro-PH releases ammonium at a greater rate (Figure 3.15e). Excess nitrogen never accounts for more than ~3 % of total nitrogen for either cell type at any irradiance.

3.3.5. Results summary

The ability to partition harvested solar energy between photosynthesis and photoheterotrophy in Pro results in significant increases to the cell's specific growth rate. In non-limiting conditions Pro grows 46 % faster when it directs light to DON uptake compared to an equivalent photoautotroph. The use of solar energy for the uptake of DON allows Pro to grow to DIN limiting conditions that would inhibit the growth on a cell that is incapable of photoheterotrophy. The trade-off for solar energy use functions over a broad irradiance range. At low light (~1 µmol photons^{-2} s^{-1}), however, the benefit that photoheterotrophy confers to growth rate is diminished. At irradiance intensities of 3-30 µmol photons^{-2} s^{-1}, directing solar energy away from photosynthesis for photoheterotrophic DON uptake results in a significant decline in the rate of carbon fixation by up to ~20 %. As a result Pro releases significantly less DOC into the surrounding water. In these irradiance conditions, Pro not only competes with other bacterioplankton for valuable nitrogen resources through photoheterotrophy but the trade-off for light use also restricts the availability of additional growth substrates for these competitors.

3.4 Discussion

3.4.1 Growth rate

The present investigation is the first to demonstrate that the use of harvested solar energy in Pro, trading off photosynthetic CHO synthesis for photoheterotrophic DON uptake, can increase the specific growth rate of the cell (Figures 3.2, 3.8a, 3.11a, 3.14a). When conditions are non-limiting, photoheterotrophic light use allows Pro to grow almost 50 % faster than an equivalent photoautotrophic cell (Figure 3.2). In DIN limiting conditions, which are characteristic of the oligotrophic ecosystems that Pro dominate (Capone, 2000, Karl, 2002, Zehr and Kudela, 2011) and known to limit Pro growth (Graziano et al., 1996), photoheterotrophic light use allows Pro to grow in an environment that would otherwise inhibit the growth of the cell growing by photoautotrophy only (Figure 3.8a). Pro occupies an irradiance range of over 3 orders of magnitude, the broadest of any phototroph, and thrives down to a depth of 200m (Partensky et al., 1999). Here it is shown that the ability to use light

energy to enhance DON uptake, may function over a broad irradiance range (Figure 3.14) indicating that photoheterotrophy may be critical for Pro survival throughout the organism' illuminated habitat.

Variability in field estimates of Pro growth rates, from 0.15 d^{-1} to 1 d^{-1} (Partensky et al., 1999, Zubkov et al., 2000), may be linked to temporal fluctuations in nitrogen availability (Graziano et al., 1996) and irradiance (Zinser et al., 2007, Moore et al., 1998, Moore and Chisholm, 1999) and specifically the ability to use light energy photoheterotrophically where DON is available (Figures 3.2, 3.8a, 3.11a, 3.14a). High light intensities and high DON concentrations relative to DIN are characteristic of the surface oligotrophic waters where Pro abounds (Capone, 2000, Karl, 2002, Zehr and Kudela, 2011). Such conditions may select for the use of solar energy for processes in addition to that of photosynthesis, at least partially driving the distribution of Pro. Pro are referred to as a "federation" of diverse cells, sustaining broad distribution, stability and abundance along ocean gradients, including light and nutrient availability both vertically and horizontally (Biller et al., 2015, Garcia-Fernandez et al., 2004, García-Fernández and Diez, 2004, Tolonen et al., 2006). The present analysis shows that along these gradients, photoheterotrophic light use may function in facilitating a significant increase in growth rate. This may in part drive the distribution of Pro in the ocean. Other factors such as grazing, viral activity, temperature, and competition may also be important in structuring Pro communities (reviewed by Biller et al., 2015). A proposal for an extension of the present analysis to address how competition influences multiple light uses in Pro and coexistence with other photoheterotrophic bacteria, namely SAR11, is given in Section 6.3.

Designing experimental protocols to determine the influence of photoheterotrophic resource acquisition on Pro growth rate in order to validate the model results is challenging. Testing for the influence of heterotrophic nutrient uptake on growth rate in Pro is problematic as addition of organic substrates to culture media can result in the growth of contaminating bacteria, which can outcompete photoautotrophic cells (Garcia-Fernandez et al., 2004). In addition, Pro release a complex range of organic substrates (Karl et al., 1998, Marañón et al., 2004, Bertilsson et al., 2005, Kujawinski, 2011), which may serve as growth rate enhancing nutrients via heterotrophic uptake, making it difficult to regulate for the presence/absence of DOM in experimental controls. Experiments that compare the growth rates of populations in light:dark and dark:dark growth cycles are used for understanding the influence of photoheterotrophic light use on facultative phototrophs such as SAR11 (Giovannoni et al., 2005a). These kinds of studies are of no use for obligate phototrophs such as Pro as they require a light:dark cycle in order to survive. The presented model is nevertheless a powerful

tool with which to test conceptual ideas for the influence of photoheterotrophic resource acquisition on the growth rate of Pro, where current methodological limitations restrict determination through empirical analysis.

3.4.2 Optimum light investment for maximum growth rate

The trade-off framework is a useful tool to navigate the carbon and nitrogen acquisition parameter space to find the optimum balance of harvested solar energy to maximise growth rate. If Pro can optimally balance the use of harvested solar energy to maximise growth rate, then the parameter β represents the physiological plasticity of an individual Pro cell for dynamic light use with time, allowing it to navigate along β through a changing ambient environment, maximising growth rate at β_{opt}. There is no empirical data with which to compare the behaviour of β_{opt} in the model. However, in support of the presented trade-off framework concept, there is a growing body of literature demonstrating pathways for harvested solar energy in cyanobacteria, other than linear electron flow to carbon dioxide reduction (Bailey et al., 2008, Zehr and Kudela, 2009, Battchikova et al., 2011, McDonald et al., 2011, Cardol et al., 2011, Ogawa and Mi, 2007). In addition, evidence is building that demonstrates solar energy enhances photoheterotrophic carbon, nitrogen (Michelou et al., 2007, Mary et al., 2008b, Gómez-Pereira et al., 2012) and phosphate (Gómez-Pereira et al., 2012, Duhamel et al., 2012) acquisition in Pro. Zubkov (2009) wrote that it is conceivable that the flexibility to regulate and balance cellular energy could drive organism selection in the ocean, inspiring the β concept.

This kind of trade-off framework has also been used to represent the diversity of microbial populations, allowing the simulated environment to choose the best balance of traits (for example, light and nutrient harvesting ability), to maximise a certain variable, often growth rate (Follows et al., 2007), simulating the principles of natural selection (reviewed by Follows and Dutkiewicz, 2010). If Pro is completely inflexible in the use of solar energy, or limitations exist on the degree to which solar energy is partitioned between processes, then each value of β may correspond to a different physiological strategy for different individuals. Tremendous diversity is documented for Pro, with a complex range of ecotypes that are highly adapted to different environmental regimes, (reviewed by Biller et al., 2015). If such diversity exists for the balance of solar energy invested in physiological processes in Pro, then future work should consider a full evaluation of the suboptimum trait space in a variable environment, with each value of β representing different individuals using harvested solar energy differently. However, due to the absence of any data with which to constrain the dynamics of β, the evaluation of the optimum (β_{opt}) is a useful first step towards

understanding the influence of photoheterotrophic light use on processing of carbon and nitrogen by Pro.

The specific value of β_{opt} may not represent the actual percentage of harvested solar energy invested CHO synthesis and/or DON uptake. Although the present study uses field data to constrain synthesis and uptake rates (Section 2.3.1), there is no physiological detail included in the model on the energy requirement for photosynthesis and photoheterotrophy and the quantity of energy harvested for any given irradiance. This detail could be incorporated by merging the presented DEB model with the bioenergetic model presented by Kirchman and Hanson (2012), which quantifies net energy acquisition via phototrophy through a cyanobacterial photosystem. This will be discussed in greater detail in Section 6.3. In addition, the use of harvested solar energy for photoheterotrophic uptake of phosphorus (Gómez-Pereira et al., 2012, Duhamel et al., 2012) and ATP synthesis (White, 2007) may further influence the balance of light energy investment and therefore β_{opt}.

3.4.3 The uptake of DIN

Understanding the dynamics of DIN in the oligotrophic ocean is critical as it is considered a major limiting nutrient for primary production (Capone, 2000, Karl, 2002, Zehr and Kudela, 2011), the growth of Pro (Graziano et al., 1996) and depending on DIN chemical species and source the export of carbon to the deep ocean (Johnson and Lin, 2009). The results from the model suggest that the ability to use harvested solar energy for photoheterotrophy does not significantly affect the uptake and assimilation of DIN into AA in Pro in any of the conditions investigated (Figure 3.2, 3.8c, 3.11c, 3.14c).

The present study suggests that a Pro cell using light energy to facilitate photoheterotrophic DON uptake, may obtain 70 % of nitrogen from DIN and the remaining 30 % from DON when conditions are non-limiting at β_{opt} (Figure 3.2). In order to estimate the rate of DIN uptake in Pro, which is absent from the literature, it is assumed that the cell must supplement known rates of carbon and nitrogen acquisition via CHO synthesis and DON uptake with DIN in order to grow at 0.20 d^{-1}. Measurements of the rate of CHO synthesis (Jardillier et al., 2010, Zubkov, 2014), DON uptake (Michelou et al., 2007, Mary et al., 2008b, Gómez-Pereira et al., 2012, Zubkov et al., 2003, Zubkov et al., 2004b, Zubkov and Tarran, 2005) and growth rate (Partensky et al., 1999, Zubkov et al., 2000) are highly variable indicating that the present study cannot be by any means conclusive as all rates may vary independently. For this reason it is not meaningful yet to conduct multiple investigations into the contribution of DIN (and DON) to the Pro nitrogen budget for different parametrisations of uptake. That said the

rate of DIN uptake in the model is also estimated for a Pro cell growing at 0.40 d^{-1}, which may represent a value closer to an average for a Pro cell (Partensky et al., 1999, Zubkov et al., 2000) (all other parameters remaining unchanged (Appendix Figure 3.1)). In this case, Pro sources 85 % of nitrogen from DIN and remaining 15 % from DON. Other studies suggest that between 55 % and 90 % of nitrogen may be source from DIN in surface ocean Pro, with estimates depending critically on the assumed specific rate of growth (Zubkov et al., 2003, Zubkov et al., 2004b). Reassuringly the estimates here fall within this range. Future work would ideally measure a series of parameters in a single empirical study in order to constrain the present model, discussed in greater detail in Section 6.3.

It is assumed here that the only DIN form used by Pro is ammonium (Section 2.3.1.8). To first order this may be reasonable as all Pro isolates can assimilate ammonium (López-Lozano et al., 2002, Moore et al., 2002, Garcia-Fernandez et al., 2004), ammonium transporters are expressed over a wide range of ambient conditions (Lindell et al., 2002), expression of transporters for other DIN species are repressed when ammonium is available (Herrero et al., 2001) and other forms of DIN such as nitrate and nitrite are expensive to reduce (Garcia-Fernandez et al., 2004). However, whilst some Pro strains cannot reduce nitrate and nitrite (Moore et al., 2002) many can (Martiny et al., 2009, Berube et al., 2014, Casey et al., 2007). This is linked to different environmental regimes such as light and nitrogen availability (Garcia-Fernandez et al., 2004, García-Fernández and Diez, 2004). A sensitivity analysis (Appendix Tables 3.1-3.4) shows that the rate of AA synthesis (therefore DIN assimilation) and growth rate are only sensitive to the efficiency of AA synthesis (therefore DIN species) at very low irradiances where Pro grows on DIN as the only nitrogen source and light and therefore carbon is limiting. In all other ambient conditions ample carbon is available and in excess (Figure 3.3, 3.9c, 3.12c). Variability in DIN species used by Pro may not influence the conclusions drawn here but may be important for understanding Pro growth in the deep euphotic zone where it is abundant (Giovannoni and Vergin, 2012) and light and therefore carbon is limiting (Figure 3.16).

3.4.4 The uptake of DON

The ability to use harvested solar energy to facilitate the uptake of DON may be critical for Pro growth and survival in oligotrophic ecosystems over a wide range of DIN (Figure 3.8a), DON (Figure 3.11a) and irradiance (Figure 3.14a) conditions.

An important result found here is that the ability to use solar energy to facilitate DON uptake allows Pro to survive in DIN conditions that do not support the growth of an equivalent

photoautotroph (Figure 3.8a). Photoheterotrophic DON uptake may, therefore, relieve DIN limitation of Pro growth in oceanic subtropical gyres. The importance of DIN as a nitrogen source for Pro (Figure 3.2) means that although taking up DON facilitates an increased rate of growth, a decrease in ambient DIN still results in a significant decrease in Pro growth rate (Figure 3.8a), supported by the observation that DIN limiting conditions can restrict Pro growth (Graziano et al., 1996). Amino acid uptake has been suggested to be key for Pro survival in oceanic gyres (Zubkov et al., 2003). Here it is shown that photoheterotrophic light use may also be essential to Pro survival in these regions. Pro thrive and uptake DON across horizontal (Zubkov and Tarran, 2005) and vertical (Zubkov et al., 2004b) gradients in ambient DIN concentrations and it is possible that photoheterotrophy may be essential to survival in such gradients. Selection criteria may be for the uptake of different nitrogen sources such as DON, facilitated and/or enhanced through photoheterotrophic light use, in part driving the distribution of Pro.

The model shows that Pro at low light are more likely to grow via strict autotrophy, which is interesting given that DIN, specifically nitrate, is the dominant source of nitrogen at depth in subtropical oceanic gyres and that DON is more abundant at the surface (Biller et al., 2015). However, it has been shown that Pro ecotypes living at the bottom of the euphotic zone, uptake DON at a greater rate per cell than Pro ecotypes living nearer the surface (Zubkov et al., 2004b). Pro ecotypes are separated vertically according to their ability to harvest available solar energy (Moore and Chisholm, 1999, Moore et al., 1998) and nutrients (Garcia-Fernandez et al., 2004, García-Fernández and Diez, 2004) but the parametrisation for light harvesting and nitrogen acquisition in the model is that of surface ocean Pro (Section 2.3.1). Ecotype diversity (Biller et al., 2015) may therefore not be captured in the present model. Differences in ecotype light harvesting capacity can be captured by changing the half saturation constant for irradiance. The greater sensitivity that low light (LL) ecotypes have for irradiance relative to high light (HL) ecotypes can be set by have a smaller half saturation constant for irradiance for the LL cells than the HL cells. This is consistent with observations of ecotype growth rate response to different irradiances (Moore and Chisholm, 1999, Moore et al., 1998).

3.4.5 The synthesis of carbohydrate

Pro is the most abundant photosynthetic organism on Earth (Partensky et al., 1999, Chisholm et al., 1988), contributing significantly to open ocean primary production (Goericke and Welschmeyer, 1993, Liu et al., 1997, Zubkov, 2014, Hartmann et al., 2014, Liu et al., 1999, Liu et al., 1998). It is therefore critical that we understand how photoheterotrophic light use may

influence carbon reduction in Pro. The result from the model demonstrate that at low irradiance intensities, the use of light energy for photoheterotrophy, trading-off CHO synthesis for DON uptake (where available), may result in a decrease in CHO synthesis and therefore carbon dioxide reduction by up to 22 % relative to an equivalent cell that cannot use light photoheterotrophically (Figure 3.14e). Variability in the measurements of carbon reduction for Pro (Goericke and Welschmeyer, 1993, Liu et al., 1997, Zubkov, 2014, Hartmann et al., 2014, Liu et al., 1999, Liu et al., 1998) may be partially explained by photoheterotrophic light use at low irradiance levels if DON availability is transient. This may be important for understanding measurements of carbon reduction at the deep chlorophyll maximum in oligotrophic subtropical where Pro account for a significant percentage (20-80 %) of total carbon reduction (Goericke and Welschmeyer, 1993). Despite the observation that carbon fixation is typically low in oligotrophic subtropical gyres relative to more productive waters, these regions span over 40 % of the planet's surface and may account for 30 % total marine primary production (Longhurst et al., 1995). Photoheterotrophic light use may be critical for understanding variability in the measurements of carbon fixation at low irradiance in oceanic gyres. Accuracy in such measurements are important for our understanding of metabolic balance (Duarte et al., 2013, Williams et al., 2013) and the ability of the oceans to respond to anthropogenic carbon dioxide release.

Sensitivity analysis suggests than the rate of CHO synthesis in Pro-PH is sensitive to the half saturation irradiance flux in low irradiance conditions (1.8 and 10 µmols photons m^{-2} s^{-1}), and that if its value is changed to represent a Pro cell adapted to low light conditions, the rate of CHO synthesis would increase significantly (Appendix Table 3.3 and 3.4). This, in addition to the previous statement that accurate detail on light energy harvesting is not built into the model (Section 3.4.2), suggests that reliable interpretations of the influence of photoheterotrophic light use on CHO synthesis at low light may have to wait until ecotype light harvesting and light energy as a currency are incorporated in the model. The results presented may, however, reflect the response of surface ocean Pro ecotypes to diel variations in irradiance.

3.4.6 Respired carbon dioxide

The balance between carbon reduction and respiration is a key to understanding the ocean's role in atmospheric carbon sequestration and therefore climate change (Ducklow and Doney, 2013). Photosynthetic cyanobacteria not only reduce carbon but also respire it (White, 2007), and due to the abundance of Pro (Partensky et al., 1999) it is important to know the role that it plays in oceanic carbon dioxide release. Yet measurements of oceanic respiration often only

consider carbon dioxide release from the heterotrophic bacterial community (Del Giorgio et al., 2011) and therefore neglect the photosynthetic communities role in respiration. However, methods for measuring respiration as total oxygen consumption will include the role of primary producers (Ducklow and Doney, 2013).

The model quantifies the rate of carbon dioxide release through the synthesis of amino acids and biomass (Section 2.2). The results suggest that there is no reason to expect that photoheterotrophic light use in Pro influences measurements of carbon dioxide release in the open ocean to any significant degree. Carbon dioxide release, however, accounts for up to 5 % of the total carbon flux in Pro (Pro-PA and Pro-PH) when CHO synthesis is saturated. As Pro contributes significantly to carbon reduction in the surface open ocean (Zubkov, 2014, Goericke and Welschmeyer, 1993), the release of up to 5 % fixed carbon as carbon dioxide may still be important for the role of Pro in metabolic balance. However, significant uncertainties exist in measuring carbon reduction and respiration, (reviewed by Ducklow and Doney, 2013). Specifically, up to 40 % of fixed carbon in Pro may be released as DOC (Karl et al., 1998), creating uncertainty in the interpretation of measurements as gross or net production. With such uncertainties, although the release of 5 % fixed carbon as carbon dioxide may represent a significant flux in the carbon cycle, it may not be a priority for refining the debate on metabolic balance at this point in time, based on current methods.

3.4.7 The release of excess organic carbon

Photosynthetic organisms release a complex suite of organic substrates, through a variety of mechanisms, that serve as growth media for heterotrophic and mixotrophic microbes (Kujawinski, 2011). In the oligotrophic subtropical gyres, the release of DOC substrates from dominant photosynthesisers such as Pro (Bertilsson et al., 2005, Karl et al., 1998), may be critical carbon resources for (photo)heterotrophs such as SAR11, known to be able to utilise organic carbon substrates released from Pro (Bertilsson et al., 2005, Carini et al., 2013).

In situations where irradiance saturates the rate of CHO synthesis (Experiment 1-3), excess carbon release accounts for between 71 % (non-limiting conditions) and 92 % (DIN limiting conditions) of the total carbon flux. It is observed that Pro release up to 40 % of fixed carbon as excess in oligotrophic subtropical waters where it dominates (Karl et al., 1998), significantly less than shown here (Figure 3.3, 3.10, 3.13, 3.16). The rate of excess carbon release and percentage of total carbon in the present study is greatly reduced when the model is fit to a growth rate of 0.40 d^{-1}, representing only ~45 % of total carbon in non-limiting conditions (Appendix Figure 3.1). This indicates that the chosen growth rate of 0.20 d^{-1} for the

present parameter set may be too low, and 0.40 d^{-1} is more of a representative average growth rate of Pro with which to constrain the model. This reiterates the previous statements (Section 3.4.3) that parameters to constrain a model such as this would ideally be measured in a single empirical study.

When irradiance is limiting, photoheterotrophic light use may result in a decrease in the release of excess carbon by up to 22 % when DON is available for uptake (Figure 3.15c). This may be important as photoheterotrophy may not only increase the ability of Pro to compete with other heterotrophic microbes for DON but the trade-off may further limit the availability of DOC for these heterotrophs. The importance of photoheterotrophy on competition between Pro and SAR11 could be addressed using a model chemostat, discussed in greater detail in Section 6.3.

In low irradiance conditions that result in the 22 % decrease in the rate of excess carbon release via photoheterotrophic light use, its release rate is sensitive to the half saturation irradiance, and if changed to represent a Pro cell adapted to low light conditions, the rate of excess carbon release would increase (Appendix Tables 3.3 3.4). The diversity in light harvesting strategies found in Pro ecotypes that stratify in the water column according to light regime may not be captured in the presented model, suggesting that dynamics at low irradiance may not necessarily represent low light ecotypes.

3.4.8 The release of ammonium

The model releases between ~6 % and ~35 % of the total nitrogen flux as ammonium depending on environmental conditions, the greatest of which being when irradiance is limiting. Photoheterotrophic light use also results in significant increases in ammonium release compared to an equivalent photoautotroph, which is again highly dependent on ambient conditions (Figure 3.4, 3.9e, 3.15e). However, the release of ammonium in the model may be in error. When CHO synthesis is saturated (Experiment 1-3), and therefore carbon is not limiting in the model, Pro releases up to 7 % of the total nitrogen flux as ammonium (Figure 3.3). Research on heterotrophic bacterial communities does however show that bacterioplankton will not release ammonium when an ample carbon source is available (Goldman and Dennett, 1991, Goldman et al., 1987, Goldman and Dennett, 2000). The release of ammonium through the deamination of ON in the model is dependent on the efficiency of synthesis and the difference between the C:N of ON and the C:N of biomass (Section 2.3). The C:N of Pro biomass is almost double that of the bacterioplankton in the study used to constrain the model, meaning that any fraction of synthesis via the use of ON only results in large

fraction of nitrogen being removed from ON in order to stoichiometrically balance synthesis, which cannot be verified using the data to which the model is fitted (Section 2.3.2.1).

Ammonium release increases with decreasing irradiance (Figure 3.15, 3.3.4.3) where the cell increasingly depends on DIN as a source of nitrogen (Figure 3.14c, d). It is highly unlikely that synthesised AA using DIN, which is an energetically expensive processes (De Vries et al., 1974), will be used as a source of energy and mobilised, resulting in such a high percentage of the total nitrogen flux being release as ammonium (Figure 3.16). The model structure is chosen to be generic to allow comparison of the metabolisms and physiologies of Pro and SAR11 (Section 5.1). However, it is likely that such a simplification should be treated with care in regard to the release of ammonium. Model development is therefore required to resolve this issue, discussed in greater detail in Section 6.3.

3.4.9 Maintenance

Photoheterotrophic light use does not result in any significant changes to the percentages of carbon and nitrogen required to satisfy maintenance demands for Pro. As DIN and irradiance becoming limiting the importance of the maintenance rate for carbon and nitrogen assimilation increases and becomes a significant constraint on Pro growth. However, the rate of maintenance biomass turnover in Pro is not well understood and here based on the turnover rate of leucine (Section 2.3.2). A greater understanding of the maintenance requirements for Pro would be useful modelling Pro growth.

3.5 Summary

The ability to partition harvested solar energy between photosynthesis and photoheterotrophy in Pro can significantly increase its growth rate, allowing it to survive on DON in DIN limiting conditions that restrict the growth of an equivalent photoautotroph. Photoheterotrophy functions over a broad range of irradiances being less influential at low light. Photoheterotrophic light use does not appear to influence the ability of Pro to assimilate DIN in any conditions investigated. At low irradiance carbon reduction may be significantly decreased where DON is available for uptake. In similar conditions both the ability to uptake DON photoheterotrophically and resulting reduced excess carbon flux may increase competitive pressure on other heterotrophic microbes. Due to the significance of the changes in growth rate observed here, it is reasonable to assume that the ability to partition energy from sunlight between photosynthesis and photoheterotrophy in Pro may be critical for survival, influencing the distribution of Pro in subtropical oligotrophic ecosystems.

3.6 Tables

Table 3.1 Table detailing the key processes of interest, a description of each process, chemical forms, associated elements, units and equation reference.

Key processes of interest	Description	Chemical form and associated elements	Units	Equation reference
Growth rate	Allocation of biomass to new growth	Organic containing carbon and nitrogen with a C:N of 9.2	mol C (mol C)$^{-1}$ d^{-1}	2.2.3.3i
Light investment	Use of harvested light energy for the synthesis of carbohydrate (CHO) and the uptake of DON to maximise growth rate	-	-	2.2.1.2a, 2.2.1.2b
Carbohydrate (CHO) synthesis	The rate of photosynthetic carbohydrate synthesis	Organic containing carbon only	mol C (mol C)$^{-1}$ hr^{-1}	2.2.1.3b
Dissolved organic nitrogen (DON) uptake	The rate of photoheterotrophic DON uptake	Organic containing carbon and nitrogen at a C:N of 4.3	mol C (mol C)$^{-1}$ hr^{-1}	2.2.1.4a
Amino acid (AA) synthesis	The rate of AA synthesis using CHO and DIN	Organic containing carbon and nitrogen at a C:N of 4.3	mol C (mol C)$^{-1}$ hr^{-1}	2.2.2k
ON (organic nitrogen) delivery to maintenance and growth	The rate that ON (sum of DON and AA) is delivered to maintenance and growth	Organic containing carbon and nitrogen at a C:N of 4.3	mol C (mol C)$^{-1}$ hr^{-1}	2.2.2m
OC (organic carbon) delivery to maintenance and growth	The rate that OC (CHO remaining after AA synthesis) is delivered to maintenance and growth	Organic containing carbon only	mol C (mol C)$^{-1}$ hr^{-1}	2.2.2n
Maintenance	The synthesis of biomass for use in general cell functioning that does not contribute to new growth	Organic containing carbon and nitrogen with a C:N of 9.2	mol C (mol C)$^{-1}$ hr^{-1}	2.2.3.2i
Respiration at AA synthesis	The production of carbon dioxide due to costs in the synthesis of amino acids (AA) paid for by CHO mobilisation	Inorganic carbon	mol C (mol C)$^{-1}$ hr^{-1}	2.2.2l
Respiration at maintenance and growth	The production of carbon dioxide through costs in transport and synthesise associated with maintenance and growth	Inorganic carbon	mol C (mol C)$^{-1}$ hr^{-1}	2.2.3.2k, 2.2.3.3h
Ammonium release at maintenance and growth	Ammonium that has been released through the deamination of ON for maintenance and growth	Inorganic nitrogen	mol N (mol C)$^{-1}$ hr^{-1}	2.2.3.2j, 2.2.3.3g
Excess OC	CHO that has been synthesised by the cell but is in excess to stoichiometric requirements for growth	Organic containing carbon only	mol C (mol C)$^{-1}$ hr^{-1}	2.2.3.3k
Excess ON	ON that has been taken up /synthesised by the cell but is in excess to stoichiometric requirements for growth	Organic containing carbon and nitrogen at C:N of 4.3	mol C (mol C)$^{-1}$ hr^{-1}	2.2.3.3j

Table 3.2 Ambient conditions for experiments 1-5. (X/K) is the ratio of the ambient nutrient concentration to the nutrient's half saturation constant, explained in Section 2.3.1.2.

Environmental factor	Exp. 1	Exp. 2	Exp. 3	Exp. 4
Irradiance (μmols photons m^{-2} s^{-1})	500	500	500	0-500
DIN (X/K)	5	0-5	5	5
DON (X/K)	5	5	0-5	5

3.7 Figures

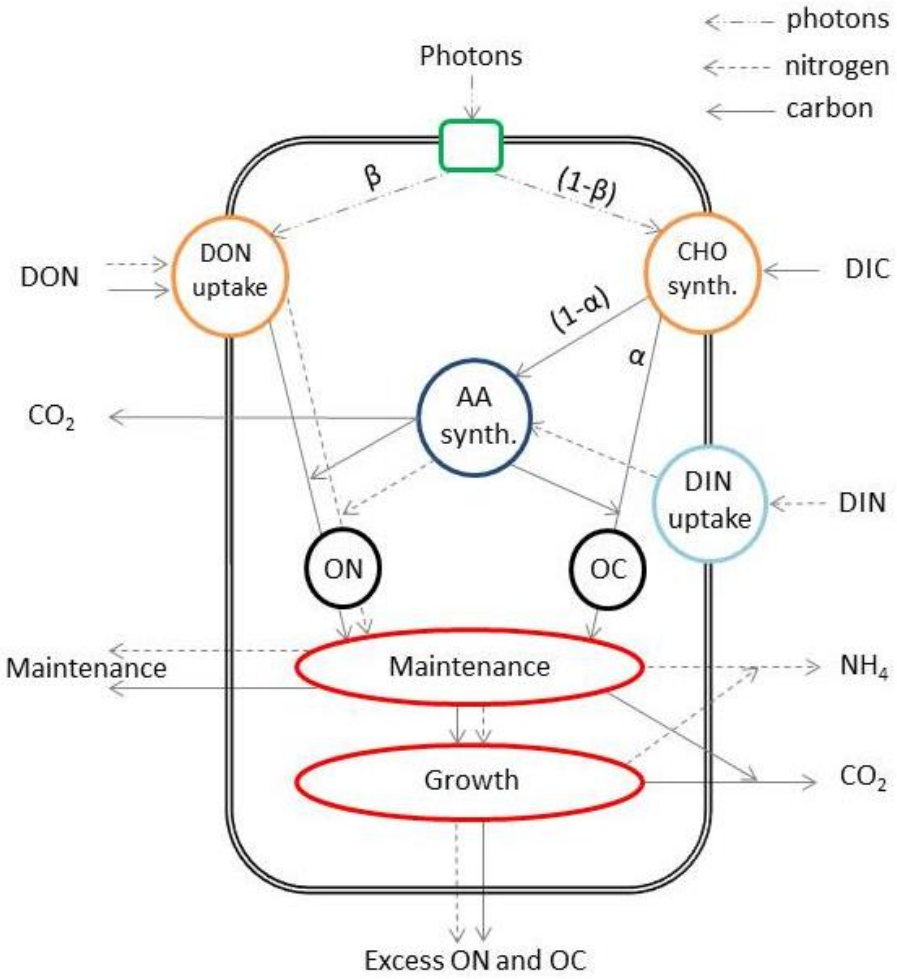

Figure 3.1 Schematic of the Pro model. The green square represents the chlorophyll-based light harvesting system. Harvested light energy is partitioned between photoautotrophic carbohydrate (CHO) synthesis and photoheterotrophic DON uptake (orange circles) using the parameter β. CHO is partitioned between amino acid (AA) synthesis (dark blue circle) and maintenance and growth (red circles) using the parameter α. DIN is taken up (light blue circle) and bound CHO to synthesise AA (dark blue circle) which is added to the flux of DON. The organic nitrogen (ON) (sum of DON and AA) and organic carbon (OC) (CHO remaining after AA synthesis) fluxes (black circles) are available for the cell to satisfy maintenance as a priority and then growth (red circles). Carbon dioxide is respired at AA synthesis and maintenance and growth. Ammonium is released at maintenance and growth. Maintenance biomass is excreted from the cell along with ON and OC that are in excess to stoichiometric requirements for growth.

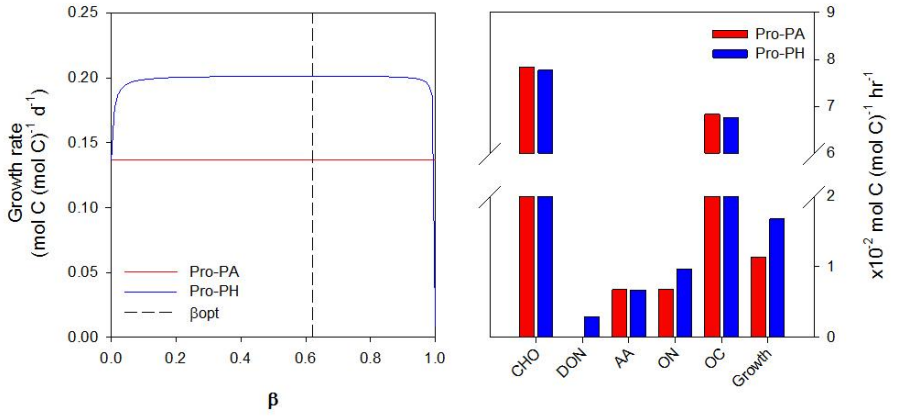

Figure 3.2 The variation of Pro-PH growth rate with β and the growth rate of Pro-PA (left). The vertical dashed line shows the position of β_{opt}. The uptake of carbon and nitrogen and growth rate of Pro-PA and Pro-PH per hour (right) at β_{opt}.

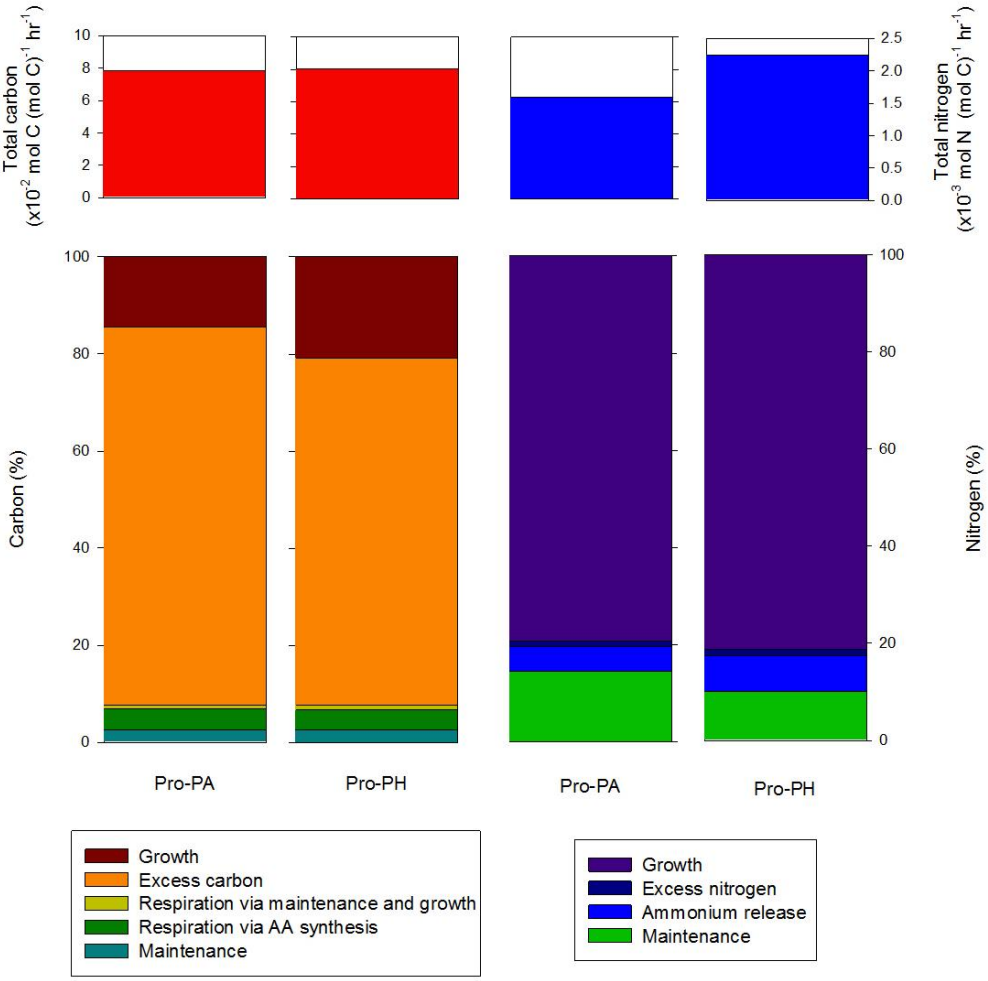

Figure 3.3 The total (top) and fate of (bottom) of carbon (left) and nitrogen (right) in Pro-PA and Pro-PH at β_{opt}. Processes are specified in the keys at the bottom of the figure.

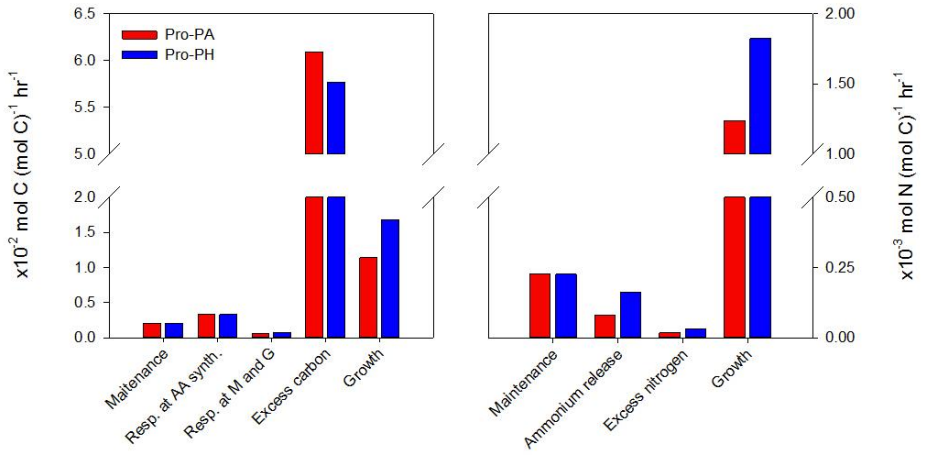

Figure 3.4 The fate of carbon (left) and nitrogen (right) for Pro-PA and Pro-PH at β_{opt}. M and G represent maintenance and growth, respectively.

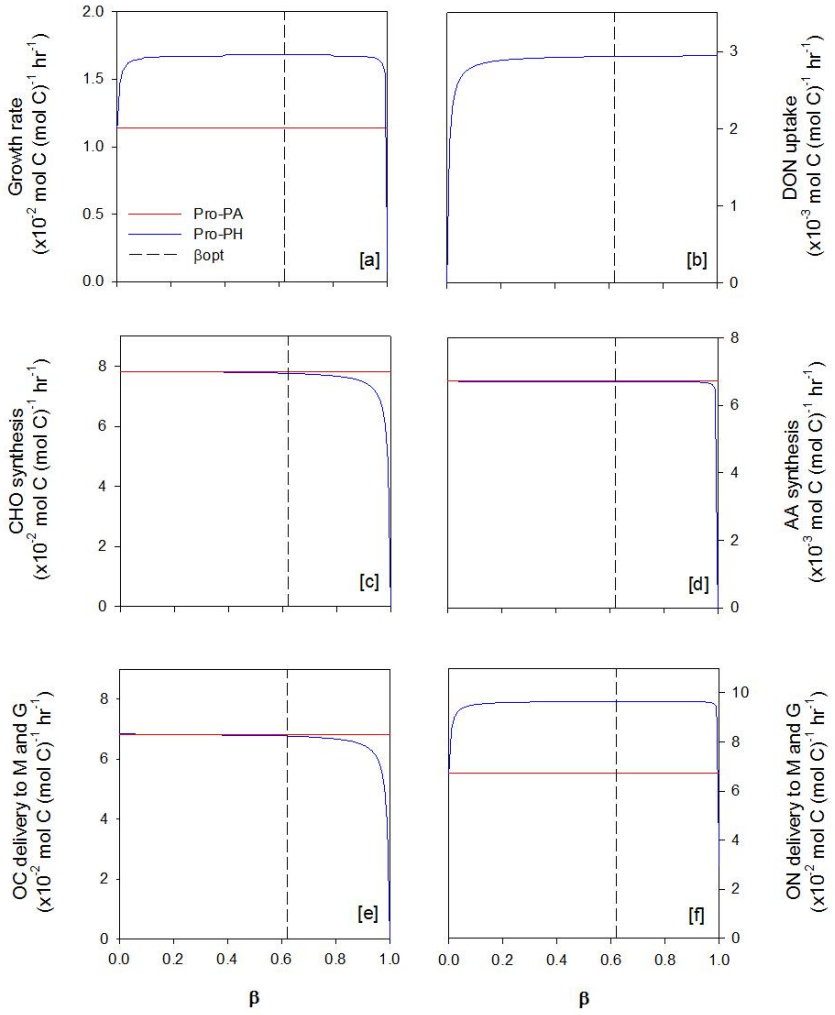

Figure 3.5 The rate of growth (a) and uptake of carbon and nitrogen (b-f) with β. The vertical dashed line shows the position of β_{opt}. M and G represent maintenance and growth, respectively.

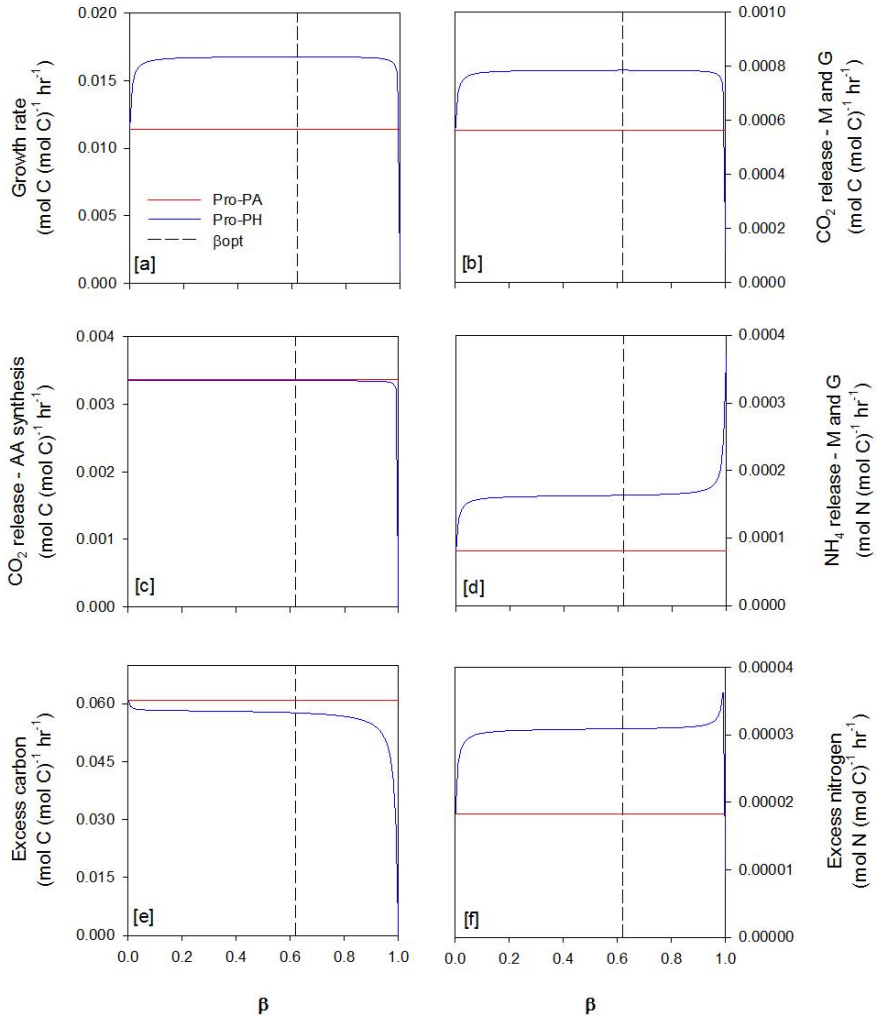

Figure 3.6 The rate of growth (a) fate of carbon and nitrogen (b-f) with β. The vertical dashed line shows the position of β_{opt}. M and G represent maintenance and growth, respectively.

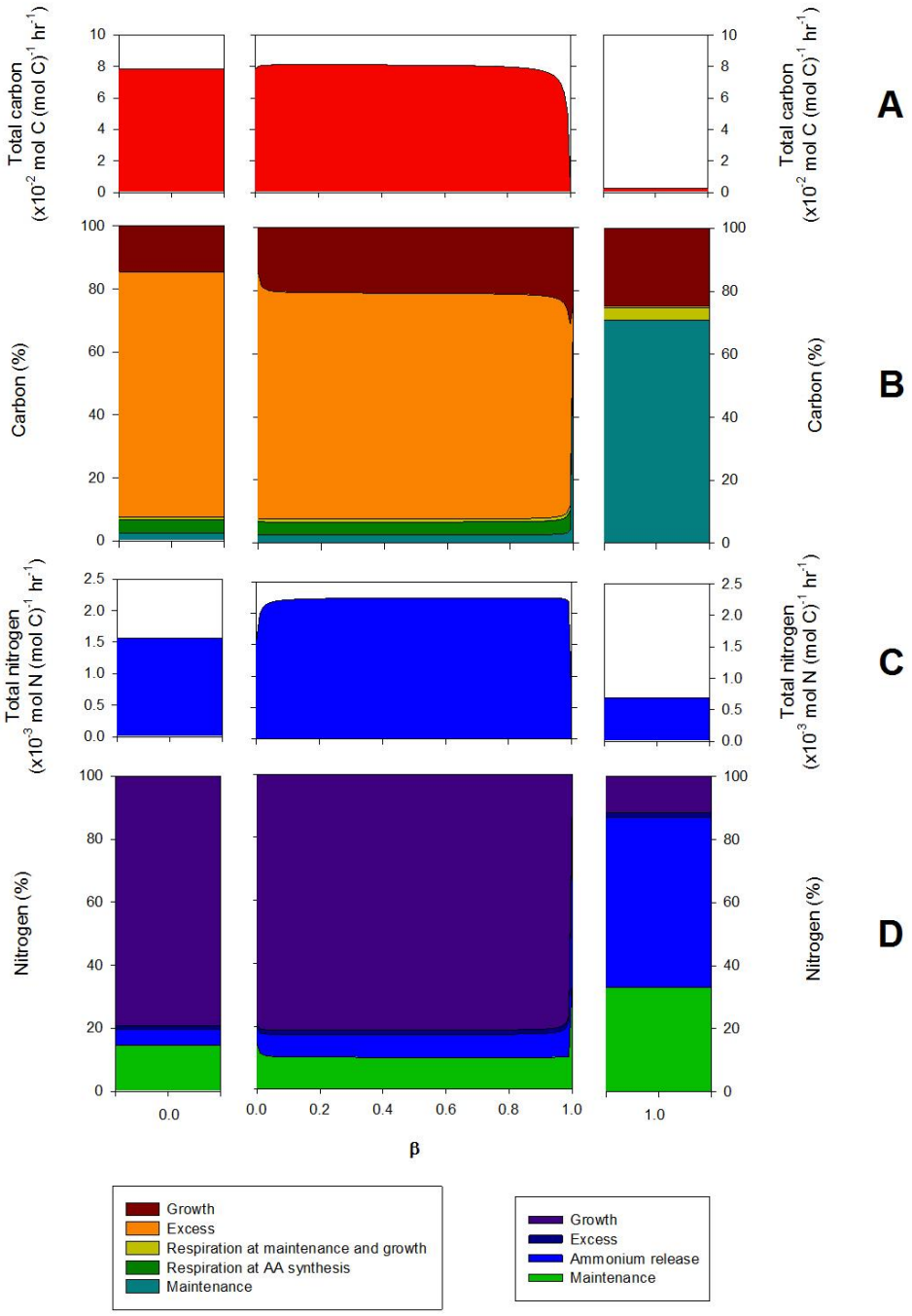

Figure 3.7 The total (panels A and C) and fate of (panels B and D) of carbon (panels A and B) and nitrogen (panels C and D) with β. Processes are specified in the keys at the bottom of the figures. Results for β = 0 and β = 1 are expanded.

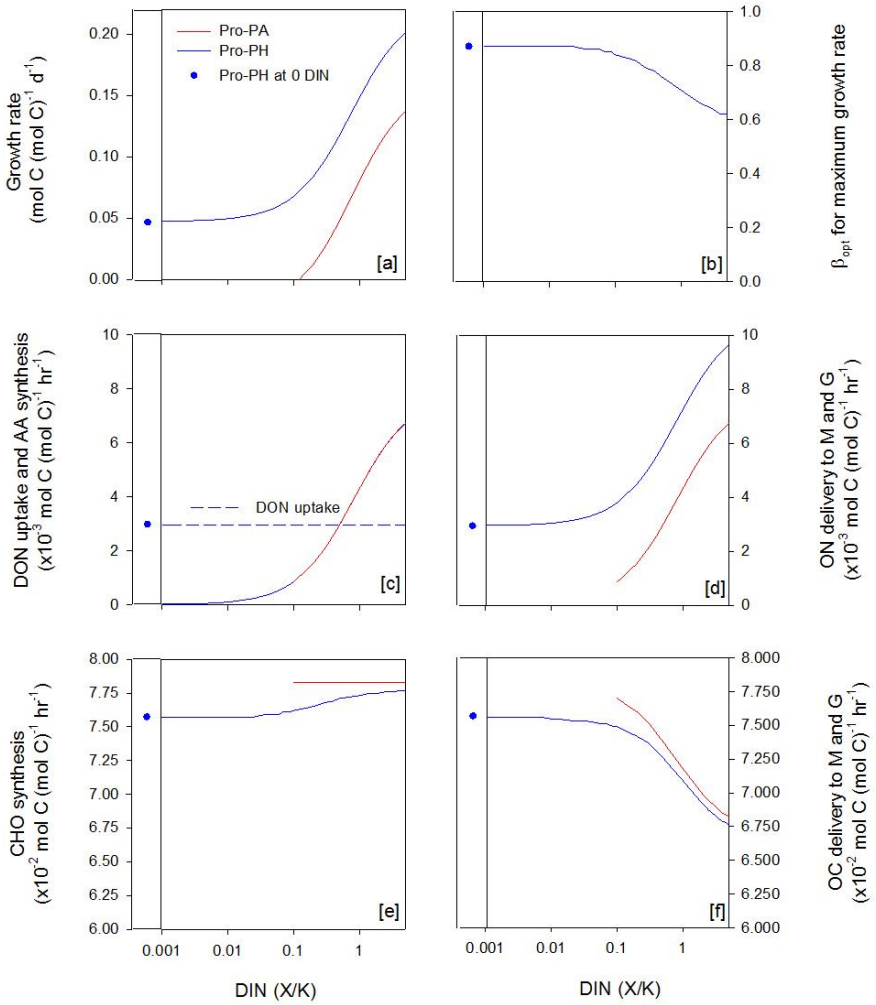

Figure 3.8 The change in growth rate (a), β_{opt} (b), and the uptake of carbon and nitrogen (c-f) at multiple ambient DIN (X/K) for Pro-PA and Pro-PH at β_{opt}. The vertical solid line separates data at zero DIN (X/K). M and G represent maintenance and growth, respectively.

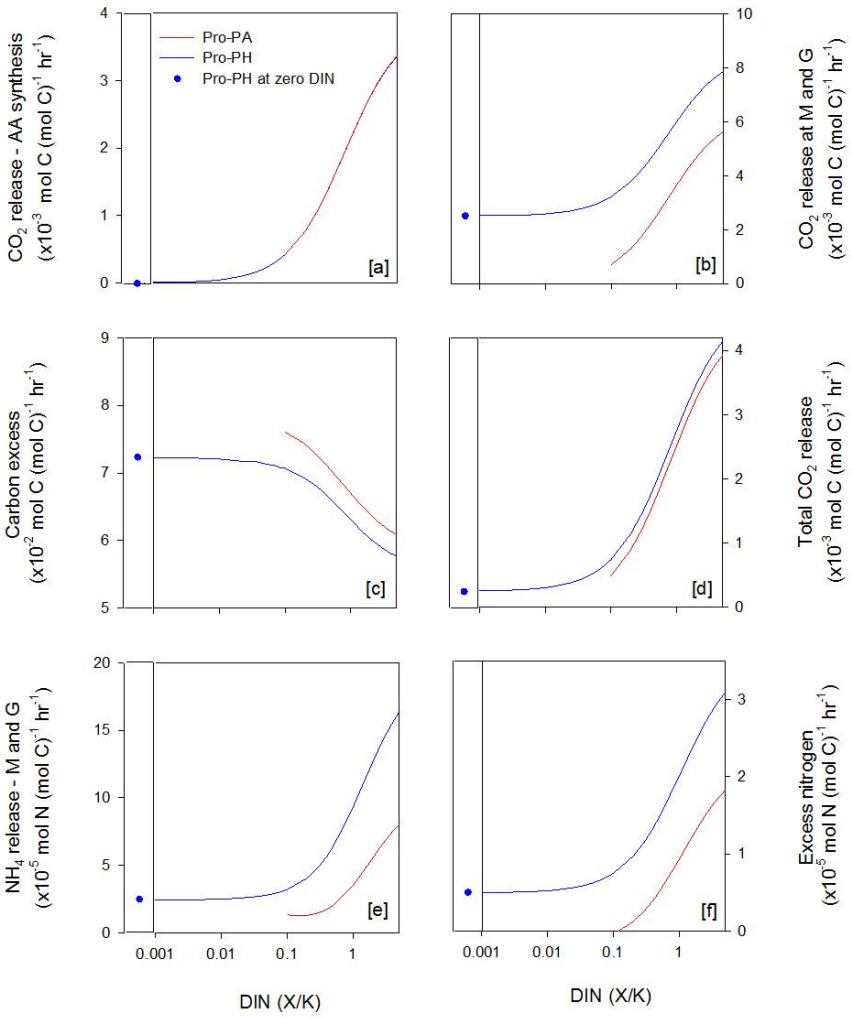

Figure 3.9 The fate of carbon (a-d) and nitrogen (e-f) at multiple ambient DIN (X/K) for Pro-PA and Pro-PH at β_{opt}. The vertical solid line separates data at zero DIN (X/K). M and G represent maintenance and growth, respectively.

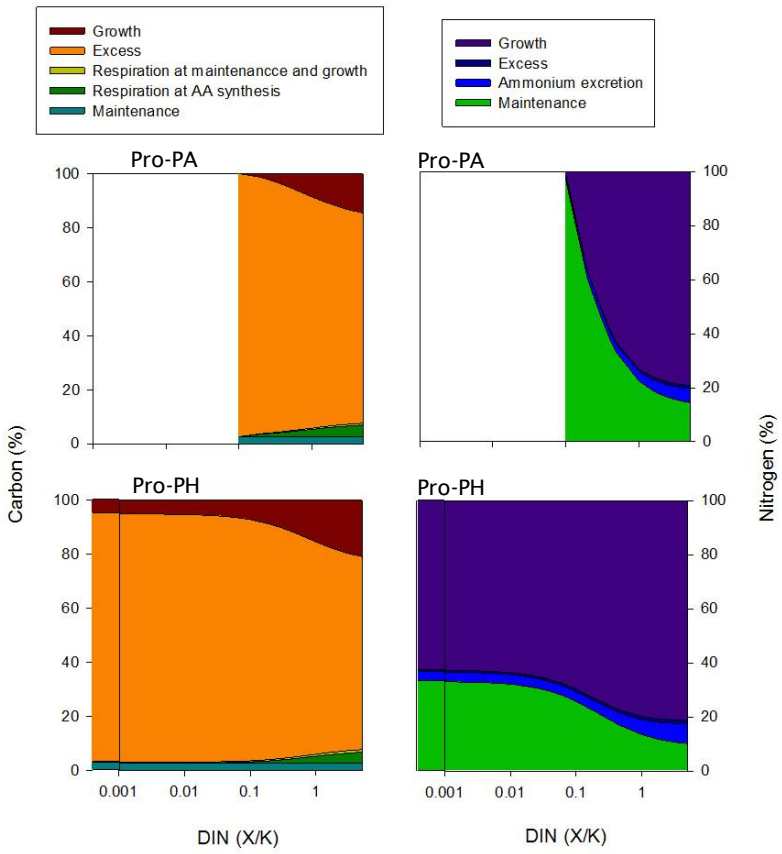

Figure 3.10 The fate of carbon (left) and nitrogen (right) as percentages of the total carbon and nitrogen fluxes at multiple ambient DIN (X/K) for Pro-PA (top) and Pro-PH (bottom). The vertical solid line separates data at zero DIN (X/K).

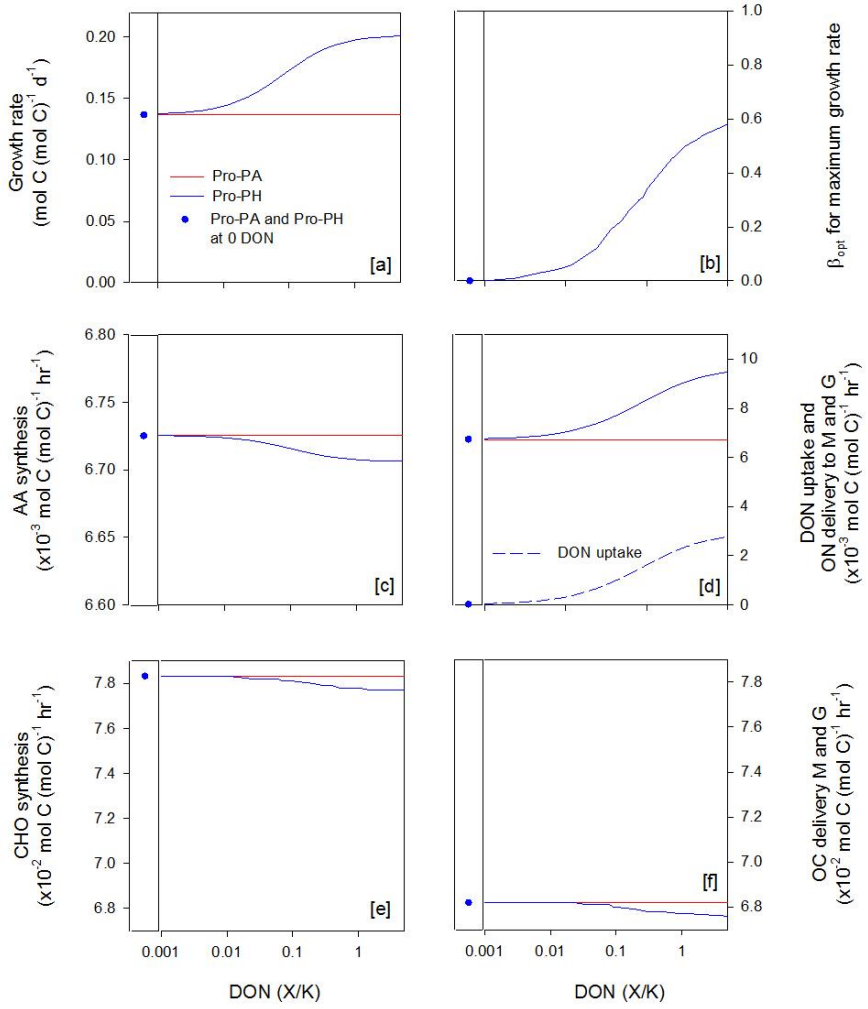

Figure 3.11 The change in growth rate (a), β_{opt} (b), and the uptake of carbon and nitrogen (c-f) at multiple ambient DON (X/K) for Pro-PA and Pro-PH at β_{opt}. The vertical solid line separates data at zero DON (X/K). M and G represent maintenance and growth, respectively.

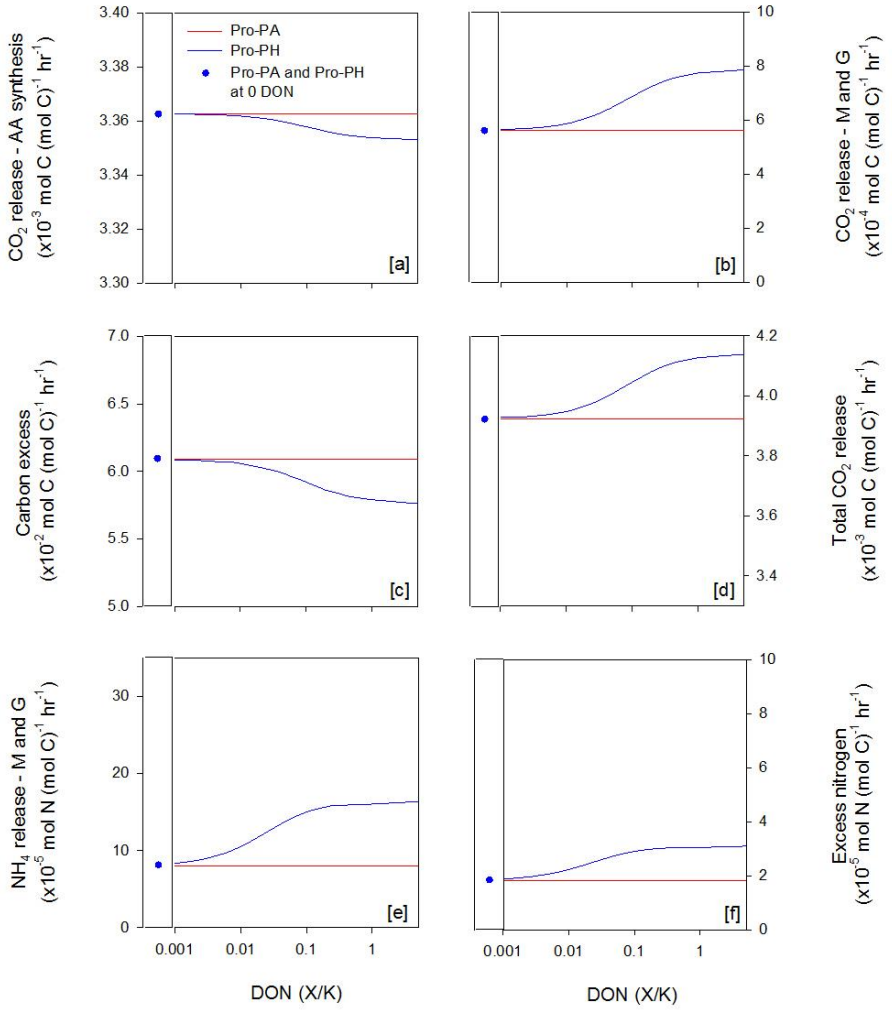

Figure 3.12 The fate of carbon (a-d) and nitrogen (e-f) at multiple ambient DON (X/K) for Pro-PA and Pro-PH at β_{opt}. The vertical solid line separates data at zero DON (X/K). M and G represent maintenance and growth, respectively.

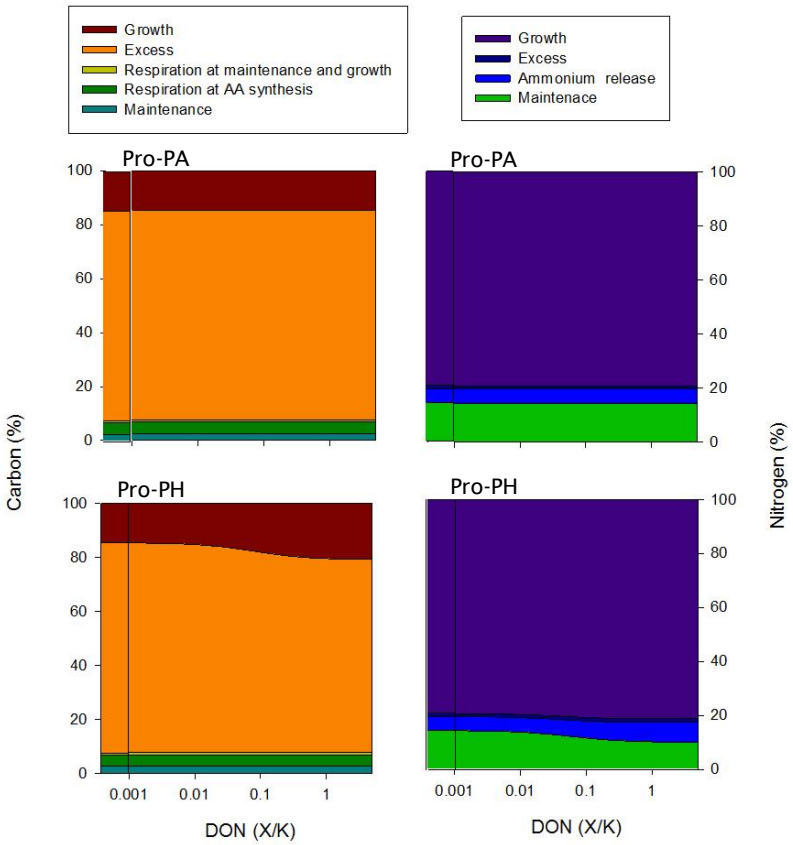

Figure 3.13 The fate of carbon (left) and nitrogen (right) as percentages of the total carbon and nitrogen fluxes at multiple ambient DON (X/K) for Pro-PA (top) and Pro-PH (bottom). The vertical solid line separates data at zero DON (X/K).

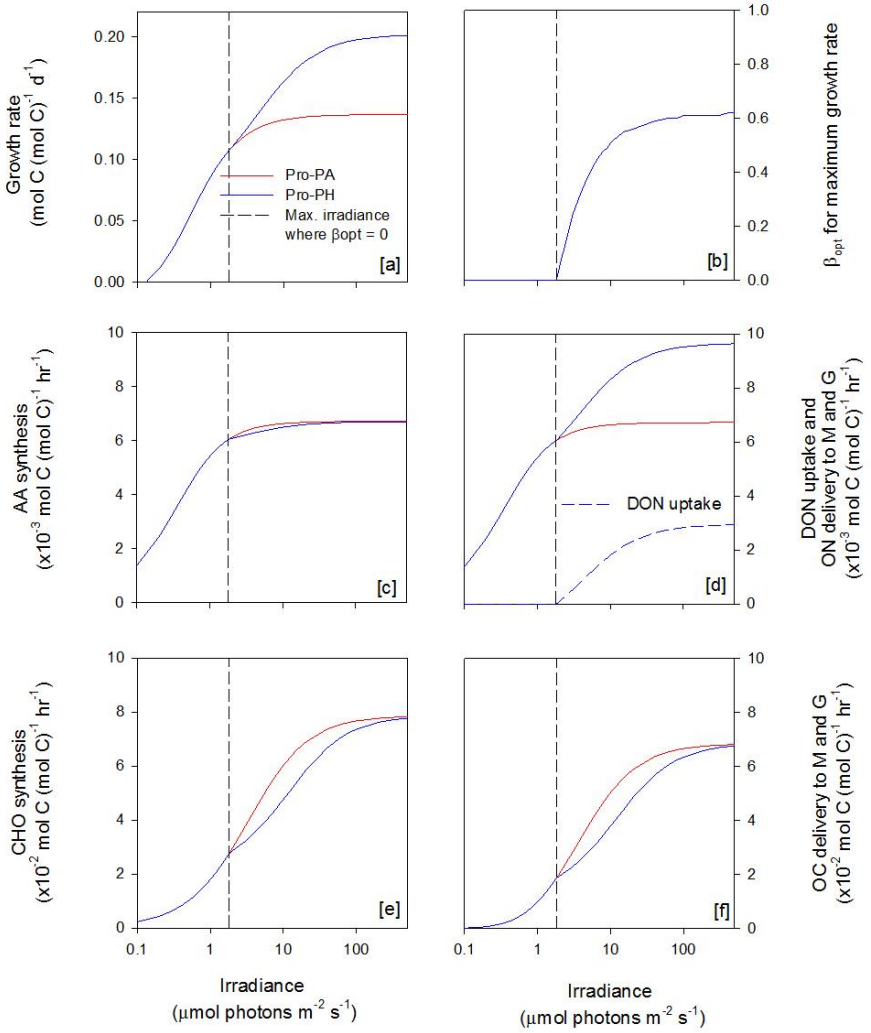

Figure 3.14 The change in growth rate (a), β_{opt} (b), and uptake of carbon and nitrogen (c-f) at multiple irradiances for Pro-PA and Pro-PH at β_{opt}. The vertical dashed line defines the maximum irradiance where β_{opt} is zero. M and G represent maintenance and growth, respectively.

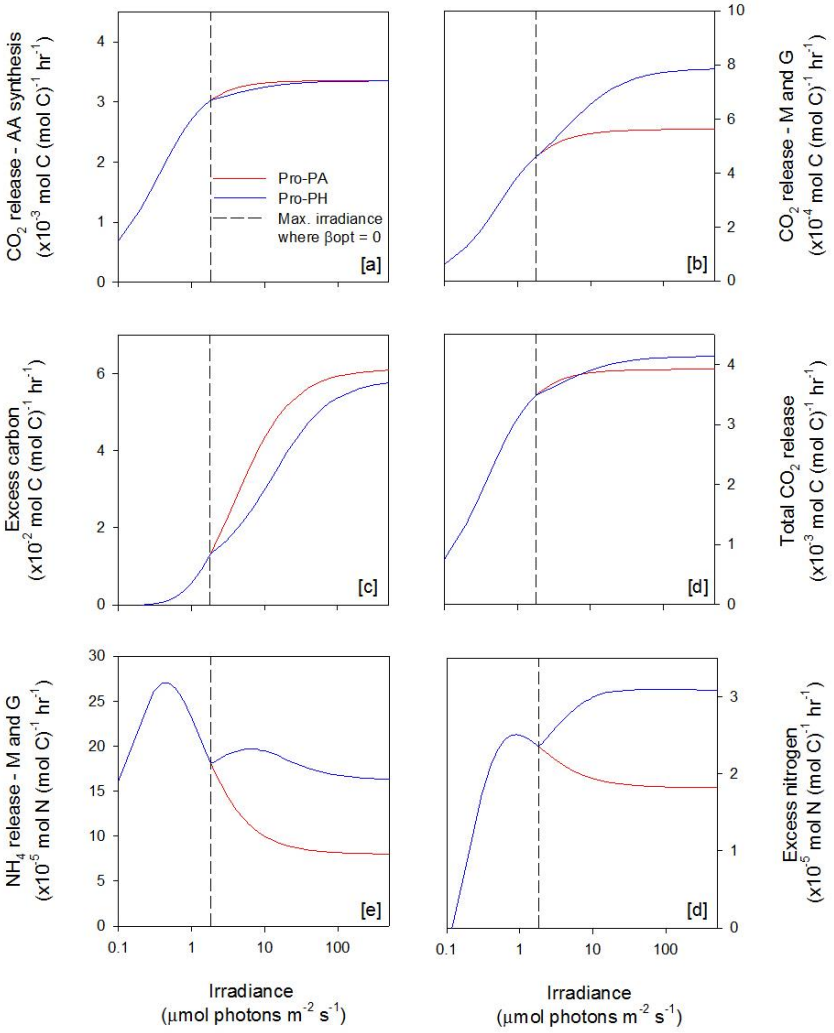

Figure 3.15 The fate of carbon (a-d) and nitrogen (e-f) at multiple irradiances for Pro-PA and Pro-PH at β_{opt}. The vertical dashed line defines the maximum irradiance where β_{opt} is zero. M and G represent maintenance and growth, respectively.

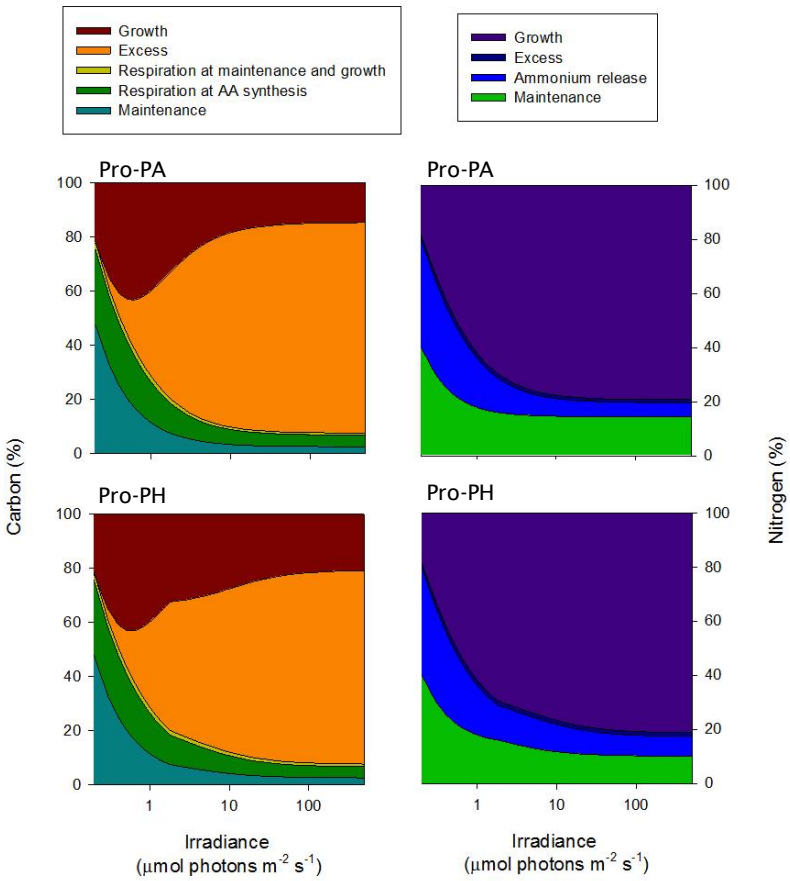

Figure 3.16 The fate of carbon (left) and nitrogen (right) as percentages of the total carbon and nitrogen fluxes at multiple irradiances for Pro-PA (top) and Pro-PH (bottom).

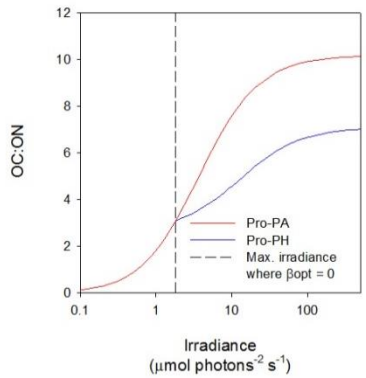

Figure 3.17 The ratio of OC to ON delivered to maintenance and growth at multiple irradiances. The vertical dashed line defines the maximum irradiance where β_{opt} is zero.

3.8. Appendix Tables

Appendix Table 3. 1 Sensitivity analysis for Pro-PH at β_{opt} (0.82) in non-limiting conditions (Experiment 1). – and + for each parameter corresponds to a -20 % or +20 % change in each parameter.

Parameter	Growth rate	Excess carbon	Excess nitrogen	NH_4 release M and G	CO_2 release AA	CO_2 release M and G	AA synth.	DON uptake	CHO synth.
DIN half sat. -	-0.10	0.04	-0.15	-0.20	-0.14	-0.09	-0.14	0.00	0.00
DIN half sat. +	-0.10	0.04	-0.14	-0.19	-0.13	-0.08	-0.13	0.00	0.00
CO_2 half sat. -	0.00	0.02	0.00	-0.01	0.00	0.00	0.00	0.00	0.01
CO_2 half sat. +	0.00	-0.02	0.00	0.01	0.00	0.00	0.00	0.00	-0.01
DON half sat. -	0.00	0.00	-0.01	-0.01	0.00	0.00	0.00	-0.01	0.00
DON half sat. +	0.00	0.00	-0.01	-0.01	0.00	0.00	0.00	-0.01	0.00
Light half sat. -	-0.01	-0.04	0.01	0.02	0.00	0.00	0.00	-0.01	-0.03
Light half sat. +	-0.01	-0.04	0.01	0.02	0.00	0.00	0.00	-0.01	-0.03
Flux ratio -	-0.03	-0.08	-0.01	0.02	0.00	-0.02	0.00	-0.06	-0.07
Flux ratio +	-0.02	-0.06	0.00	0.02	0.00	-0.02	0.00	-0.05	-0.05
Max. DIN -	0.62	-0.24	0.88	1.13	0.86	0.55	0.86	0.00	0.00
Max. DIN +	0.55	-0.22	0.87	1.18	0.79	0.49	0.79	0.00	0.00
Max. CHO -	0.15	1.31	-0.37	-1.06	0.06	0.14	0.06	0.00	1.00
Max. CHO +	0.10	1.32	-0.26	-0.73	0.04	0.09	0.04	0.00	1.00
Max. DON -	0.31	-0.05	0.44	0.57	0.00	0.28	0.00	1.00	0.00
Max. DON +	0.31	-0.05	0.45	0.60	0.00	0.28	0.00	1.00	0.00
Max AA -	0.11	-0.05	0.17	0.23	0.16	0.10	0.16	0.00	0.00
Max AA +	0.08	-0.03	0.12	0.17	0.11	0.07	0.11	0.00	0.00
AA syn. eff -	0.06	0.20	0.01	-0.06	-3.68	0.05	0.06	0.00	0.00
AA syn. eff. +	0.03	0.14	0.00	-0.04	-2.51	0.03	0.04	0.00	0.00
C:N ON -	-0.35	0.06	0.23	-2.80	0.86	-0.31	0.86	0.00	0.00
C:N ON +	-0.28	0.04	0.14	-1.86	0.79	-0.25	0.79	0.00	0.00
C:N X -	0.94	-0.29	0.73	2.33	0.00	0.84	0.00	0.00	0.00
C:N X +	0.85	-0.26	0.66	2.42	0.00	0.75	0.00	0.00	0.00
ON eff-	0.08	0.00	0.02	-0.89	0.00	-1.60	0.00	0.00	0.00
OC eff-	0.17	0.33	-0.65	-1.76	0.00	-1.36	0.00	0.00	0.00
Maintenance -	-0.12	0.00	-0.16	-0.07	0.00	0.01	0.00	0.00	0.00
Maintenance +	-0.12	0.00	-0.16	-0.07	0.00	0.01	0.00	0.00	0.00

Appendix Table 3. 2 Sensitivity analysis for Pro-PH at β_{opt} (0.87) in DIN-limiting conditions (Experiment 2). – and + for each parameter corresponds to a -20 % or +20 % change in each parameter.

Parameter	Growth rate	Excess carbon	Excess nitrogen	NH_4 release M and G	CO_2 release AA	CO_2 release M and G	AA synth.	DON uptake	CHO synth.
DIN half sat. -	-	-	-	-	-	-	-	-	-
DIN half sat. +	-	-	-	-	-	-	-	-	-
CO_2 half sat. -	0.00	-0.01	0.00	0.01	-	0.00	-	0.00	-0.01
CO_2 half sat. +	0.00	-0.01	0.00	0.01	-	0.00	-	0.00	-0.01
DON half sat. -	-0.02	0.00	-0.02	-0.01	-	-0.01	-	-0.01	0.00
DON half sat. +	-0.02	0.00	-0.02	-0.01	-	-0.01	-	-0.01	0.00
Light half sat -	-0.01	-0.04	-0.01	0.01	-	-0.01	-	-0.01	-0.04
Light half sat +	-0.01	-0.04	-0.01	0.01	-	-0.01	-	-0.01	-0.04
Flux ratio -	-0.09	-0.07	-0.09	-0.03	-	-0.06	-	-0.06	-0.07
Flux ratio +	0.04	0.03	0.04	0.01	-	0.03	-	0.03	0.03
Max. DIN -	0.00	0.00	0.00	0.00	-	0.00	-	0.00	0.00
Max. DIN +	0.00	0.00	0.00	0.00	-	0.00	-	0.00	0.00
Max. CHO -	0.04	1.04	-0.12	-0.60	-	0.02	-	0.00	1.00
Max. CHO +	0.02	1.05	-0.08	-0.41	-	0.02	-	0.00	1.00
Max. DON -	1.52	-0.05	1.65	0.97	-	1.00	-	1.00	0.00
Max. DON +	1.51	-0.05	1.75	1.23	-	0.99	-	1.00	0.00
Max. AA -	-	-	-	-	-	-	-	-	-
Max. AA +	-	-	-	-	-	-	-	-	-
AA syn. eff -	-	-	-	-	-	-	-	-	-
AA syn. eff +	-	-	-	-	-	-	-	-	-
C:N ON -	-1.74	0.10	-0.80	-4.03	-	-1.14	-	0.00	0.00
C:N ON +	-1.20	0.07	-0.65	-2.06	-	-0.78	-	0.00	0.00
C:N Biomass -	1.44	-0.08	0.80	1.77	-	0.94	-	0.00	0.00
C:N Biomass +	1.40	-0.08	0.66	1.78	-	0.91	-	0.00	0.00
ON eff -	0.08	0.00	0.08	-1.49	-	-0.79	-	0.00	0.00
OC eff -	0.06	0.10	-0.21	-1.09	-	-0.80	-	0.00	0.00
Maintenance -	-0.47	0.10	-0.88	-0.81	-	-0.89	-	0.00	0.00
Maintenance +	-0.60	-0.10	-0.44	1.38	-	0.70	-	0.00	0.00

Appendix Table 3. 3 Sensitivity analysis for Pro-PH at β_{opt} (0.46) in light-limiting (10 µmol photons m^{-2} s^{-1}) conditions (Experiment 4). – and + for each parameter corresponds to a -20 % or +20 % change in each parameter.

Parameter	Growth rate	Excess carbon	Excess nitrogen	NH_4 release M and G	CO_2 release AA	CO_2 release M and G	AA synth.	DON uptake	CHO synth.
DIN half sat. -	-0.10	0.07	-0.18	-0.23	-0.13	-0.09	-0.13	0.00	0.00
DIN half sat. +	-0.10	0.07	-0.17	-0.21	-0.12	-0.09	-0.12	0.00	0.00
CO_2 half sat. -	0.00	0.00	0.00	0.00	0.00	0.00	0.00	0.00	0.00
CO_2 half sat. +	0.00	0.00	0.00	0.00	0.00	0.00	0.00	0.00	0.00
DON half sat. -	0.00	0.00	0.00	0.00	0.00	0.00	0.00	0.00	0.00
DON half sat. +	0.00	0.00	0.00	0.00	0.00	0.00	0.00	0.00	0.00
Light half sat. -	-0.23	-0.81	0.00	0.20	-0.05	-0.20	-0.05	-0.59	-0.53
Light half sat. +	-0.20	-0.66	0.01	0.20	-0.05	-0.17	-0.05	-0.48	-0.44
Flux ratio -	-0.06	-0.22	0.00	0.06	-0.02	-0.05	-0.02	-0.15	-0.15
Flux ratio +	-0.04	-0.15	0.00	0.05	-0.01	-0.04	-0.01	-0.10	-0.10
Max. DIN -	0.66	-0.46	1.06	1.28	0.80	0.57	0.80	0.00	0.00
Max DIN +	0.56	-0.39	1.03	1.32	0.71	0.48	0.71	0.00	0.00
Max. CHO -	0.30	1.51	-0.36	-0.94	0.14	0.26	0.14	0.00	1.00
Max. CHO+	0.20	1.57	-0.28	-0.69	0.09	0.17	0.09	0.00	1.00
Max. DON -	0.19	-0.04	0.28	0.35	0.00	0.16	0.00	1.00	0.00
Max. DON +	0.19	-0.04	0.29	0.36	0.00	0.16	0.00	1.00	0.00
Max. AA -	0.13	-0.09	0.22	0.29	0.16	0.11	0.16	0.00	0.00
Max. AA +	0.09	-0.06	0.16	0.21	0.12	0.08	0.12	0.00	0.00
AA syn. eff. -	0.16	0.36	0.06	-0.01	-3.53	0.13	0.14	0.00	0.00
AA syn. eff. +	0.10	0.26	0.03	-0.02	-2.48	0.08	0.09	0.00	0.00
C:N ON -	-0.21	0.01	0.30	-2.42	0.80	-0.18	0.80	0.00	0.00
C:N ON +	-0.20	0.02	0.13	-1.76	0.71	-0.17	0.71	0.00	0.00
C:N Biomass -	0.88	-0.47	0.89	2.32	0.00	0.76	0.00	0.00	0.00
C:N Biomass +	0.75	-0.40	0.77	2.32	0.00	0.64	0.00	0.00	0.00
ON eff.-	0.12	0.00	0.03	-0.87	0.00	-2.41	0.00	0.00	0.00
OC eff.-	0.25	0.50	-0.74	-1.65	0.00	-2.54	0.00	0.00	0.00
Maintenance -	-0.14	-0.01	-0.20	-0.11	0.00	0.02	0.00	0.00	0.00
Maintenance +	-0.14	-0.01	-0.20	-0.11	0.00	0.02	0.00	0.00	0.00

Appendix Table 3. 4 Sensitivity analysis for Pro-PH at β_{opt} Pro-PA (β = 0) in light-limiting (1.8 µmol photons m^{-2} s^{-1}) conditions (Experiment 4). – and + for each parameter corresponds to a -20 % or +20 % change in each parameter.

Parameter	Growth rate	Excess carbon	Excess nitrogen	NH_4 release M and G	CO_2 release AA	CO_2 release M and G	AA synth.	DON uptake	CHO synth.
DIN half sat. -	-0.11	0.11	-0.21	-0.26	-0.11	-0.09	-0.11	-	0.00
DIN half sat. +	-0.11	0.10	-0.20	-0.24	-0.11	-0.09	-0.11	-	0.00
CO_2 half sat. -	0.00	0.00	0.00	0.00	0.00	0.00	0.00	-	0.00
CO_2 half sat. +	0.00	0.00	0.00	0.00	0.00	0.00	0.00	-	0.00
DON half sat.	0.00	0.00	0.00	0.00	0.00	0.00	0.00	-	0.00
DON half sat.	0.00	0.00	0.00	0.00	0.00	0.00	0.00	-	0.00
Light half sat.	-0.28	-1.40	0.16	0.47	-0.13	-0.22	-0.13	-	-0.77
Light half sat.	-0.27	-1.03	0.12	0.41	-0.13	-0.22	-0.13	-	-0.59
Flux ratio -	-0.06	-0.28	0.03	0.10	-0.03	-0.05	-0.03	-	-0.16
Flux ratio +	-0.04	-0.19	0.02	0.07	-0.02	-0.04	-0.02	-	-0.11
Max. DIN -	0.75	-0.72	1.27	1.49	0.73	0.61	0.73	-	0.00
Max DIN +	0.58	-0.57	1.20	1.49	0.62	0.47	0.62	-	0.00
Max. CHO -	0.49	1.72	-0.21	-0.73	0.24	0.40	0.24	-	1.00
Max. CHO+	0.35	1.84	-0.20	-0.60	0.16	0.28	0.16	-	1.00
Max. DON -	0.00	0.00	0.00	0.00	0.00	0.00	0.00	-	0.00
Max. DON +	0.00	0.00	0.00	0.00	0.00	0.00	0.00	-	0.00
Max. AA -	0.16	-0.15	0.29	0.37	0.16	0.13	0.16	-	0.00
Max. AA +	0.11	-0.11	0.21	0.27	0.11	0.09	0.11	-	0.00
AA syn. eff. -	0.32	0.54	0.22	0.14	-3.36	0.26	0.24	-	0.00
AA syn. eff. +	0.21	0.41	0.13	0.08	-2.45	0.17	0.16	-	0.00
C:N ON -	-0.09	-0.11	0.46	-2.03	0.73	-0.07	0.73	-	0.00
C:N ON +	-0.14	-0.04	0.19	-1.65	0.62	-0.11	0.62	-	0.00
C:N Biomass -	0.87	-0.63	1.01	2.33	0.00	0.70	0.00	-	0.00
C:N Biomass	0.70	-0.51	0.85	2.29	0.00	0.57	0.00	-	0.00
ON eff.-	0.16	-0.01	0.05	-0.86	0.00	-2.97	0.00	-	0.00
OC eff.-	0.31	0.65	-0.75	-1.59	0.00	-2.35	0.00	-	0.00
Maintenance	-0.20	-0.02	-0.28	-0.15	0.00	0.03	0.00	-	0.00
Maintenance	-0.20	-0.02	-0.27	-0.14	0.00	0.03	0.00	-	0.00

3.9. Appendix Figure

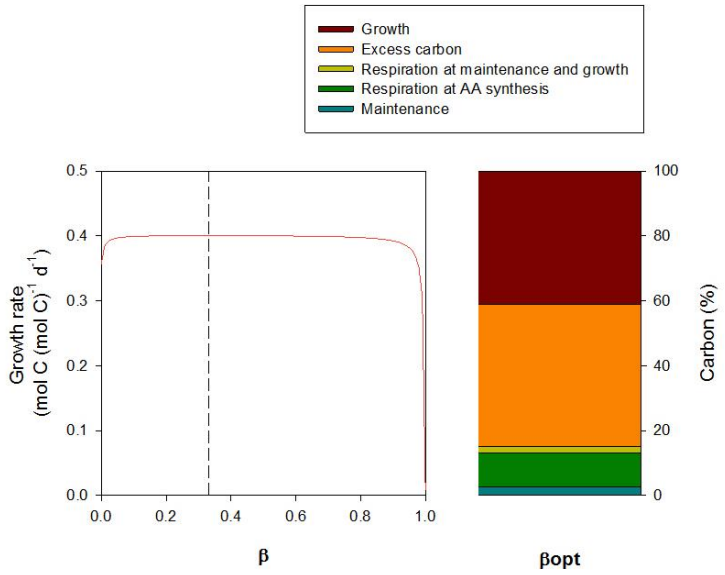

Appendix Figure 3. 1 The growth rate of Pro-PH fitted to 0.40 d^{-1} with β (left). The vertical dashed line shows the position of β_{opt}. The fate of carbon at β_{opt} with processes specified in the key at the top of the figure (right).

Chapter 4: The use of sunlight in SAR11

4.1. Chapter overview and rationale

Chapter 1 described how the most abundant heterotrophic bacteria in the ocean, the alphaproteobacterial clade SAR11, can enhance its uptake of DOM in the presence of sunlight (Mary et al., 2008b, Gómez-Pereira et al., 2012, Steindler et al., 2011), most likely using the light harvesting proton pump proteorhodopsin (Giovannoni et al., 2005a). SAR11 dominates the uptake of multiple components of the DOM pool, including DOC and DON (Alonso and Pernthaler, 2006, Mary et al., 2008b, Gómez-Pereira et al., 2012, Malmstrom et al., 2005, Malmstrom et al., 2004). Photoheterotrophically enhanced uptake of DOM may increase the growth rate of SAR11 and alter our conventional understanding of heterotrophic metabolism and associated key processes in the open ocean. The aim of this chapter is to investigate the influence of photoheterotrophic light use on the growth rate of SAR11 and its impact on physiological processes involving carbon and nitrogen.

4.2. Approach

The cell's specific growth rate is the main focus of this study. In particular the maximum growth rate that can be achieved when SAR11 grows photoheterotrophically, through optimal light energy investment. The growth rate is defined as the amount of carbon invested in new biomass per day (Section 2.2.3.3). The impact of photoheterotrophic light use on the uptake and fate of carbon and nitrogen is also evaluated. These fluxes are listed in Table 4.1. A schematic summary of the model is shown in Figure 4.1. A model description, formulae and parameter values can be found in Chapter 2.

The impact of photoheterotrophy on the growth rate of SAR11 is explored through four experiments. Each experiment investigates a different influence of ambient environment. First the influence of photoheterotrophy on growth rate is compared to a baseline organism that cannot enhance substrate uptake in the presence of sunlight but is otherwise identical to SAR11. Ambient conditions in the first experiment are assumed to be non-limiting. The dynamics of the baseline and photoheterotrophy SAR11 models are then compared at multiple ambient DIN (Experiment 2), DON (Experiment 3) and DOC (Experiment 4) conditions in order to establish how a changing ambient environment influences the importance of photoheterotrophy for SAR11 growth rate and its use of carbon and nitrogen. A quantitative evaluation of the key processes of interest, listed in Table 4.1, is undertaken for each experiment. Ambient conditions explored in experiments 1-4 are given in Table 4.2. Optimal

light investment for maximum growth rate, β_{opt}, as well as either side of the optimum are investigated in the first experiment. The evaluation of suboptimal light investment can provide an understanding of the constraints on growth either side of the optimum. The suboptimum analysis is only undertaken for Experiment 1 because henceforth it is assumed that SAR11 would balance solar energy optimally for maximum growth rate and the behaviour at β_{opt} is, therefore, of primary interest. The influence of different irradiances on SAR11 growth rate is not evaluated because the change in growth rate between the maximum irradiance studied and darkness is small (Section 4.3.1). The outline of each experiment is given below.

Experiment 1: The first experiment analyses the influence of photoheterotrophy on growth rate relative to a cell type growing by heterotrophy alone. The model used to represent photoheterotrophic resource acquisition is referred to as SAR11-PH, and the model used for the baseline is called SAR11-H. Sunlight is available for photoheterotrophy for 12 hours out of the 24 hour growth period. Therefore, SAR11-PH differs from SAR11-H in that it can enhance substrate uptake in the presence of sunlight for half of the daily growth period. The irradiance used for Experiment 1 is 500 µmol photons m^{-2} s^{-1}. This corresponds to the irradiance used during empirical analyses (Mary et al., 2008b), used to constrain the model. Nutrient conditions are kept constant (Table 4.2). The parameter representing how light energy is allocated, β, can vary between 0 and 1. As β tends to zero, more light energy is invested in DOC uptake at the expense of DON. As β tends to one, more light energy is invested in DON uptake instead of DOC.

Experiment 2: The second experiment is used to analyse how ambient DIN conditions influences photoheterotrophy by comparing the dynamics of SAR11-PH and SAR11-H at multiple of ambient DIN (X/K) from 0 to 5. All other ambient nutrient conditions and irradiance are held constant as in Experiment 1 (Table 4.2) and only the behaviour at β_{opt} is evaluated.

Experiment 3:.The third experiment is designed to analyse how ambient DON conditions influences photoheterotrophy by comparing the dynamics of SAR11-PH and SAR11-H at multiple ambient DON (X/K) from 0 to 5. All other ambient nutrient conditions and irradiance are as in Experiment 1 (Table 4.2) and again only the behaviour at β_{opt} is evaluated.

Experiment 4: The fourth experiment analyses the influence of ambient DOC on photoheterotrophy by comparing the dynamics of SAR11-PH and SAR11-H at multiple ambient DOC (X/K) from 0 to 5. All other ambient nutrient conditions and irradiance are held constant (Table 4.2) and only the behaviour at β_{opt} is evaluated.

4.3. Results

4.3.1. Experiment 1: non-liming conditions (the default parameter set)

4.3.1.1. Growth rate and the uptake and use of carbon and nitrogen at β_{opt}

The SAR11-PH model has been fitted to a growth rate of 0.20 mol C (mol C)$^{-1}$ d^{-1}, as discussed in Section 2.3.1.4. SAR11-PH must invest 82 % of harvested solar energy in DON uptake with the remaining 18 % invested in the uptake of DOC (β_{opt} = 0.82) for the maximum growth rate to be achieved when ambient conditions are non-limiting (Figure 4.2). At β_{opt} the difference in the maximum rate of growth between SAR11-H and SAR11-PH is 0.012 mol C (mol C)$^{-1}$ d^{-1}. Photoheterotrophy enhances SAR11-PH growth rate by 6.4 % relative to that of SAR11-H (Figure 4.2).

Photoheterotrophy enhances the DOC uptake rate in SAR11-PH by 5.0 % at β_{opt} relative to that of SAR11-H, increasing from 13.9 x 10^{-3} mol C (mol C)$^{-1}$ hr^{-1} to 14.6 x 10^{-3} mol C (mol C)$^{-1}$ hr^{-1}. These fluxes account for 75 % and 72 % of total carbon uptake in SAR11-H and SAR11-PH, respectively (Figure 4.2). Although DOC is the carbon source used for the synthesis of AA, the influence of light enhanced DOC uptake on the rate of AA synthesis and therefore DIN assimilation is negligible (-0.5 % in SAR11-PH relative to SAR11-H). AA is produced at a rate of 4.2 x 10^{-3} mol C (mol C)$^{-1}$ hr^{-1} in both SAR11-H and SAR11-PH (Figure 4.2).

Photoheterotrophy enhances the DON uptake rate in SAR11-PH by 20.1 % at β_{opt} relative to that of SAR11-H. Its rate of uptake increases from 4.73 x 10^{-3} mol C (mol C)$^{-1}$ hr^{-1} to 5.68 x 10^{-3} mol C (mol C)$^{-1}$ hr^{-1} and makes up the remaining 25 % and 28 % of total carbon uptake for SAR11-H and SAR11-PH, respectively. DON and AA together both make up the organic nitrogen (ON) flux that is available for maintenance and growth, which increases by 10.4 % in SAR11-PH relative to SAR11-H, from 8.92 x 10^{-3} mol C (mol C)$^{-1}$ hr^{-1} to 9.85 x 10^{-3} mol C (mol C)$^{-1}$ hr^{-1} (Figure 4.2). DON and DIN make up 53 % and 47 % of the total ON flux in SAR11-H and 58 % and 42 % in SAR11-PH, respectively. The organic carbon (OC) flux available for maintenance and growth (i.e. DOC remaining after AA synthesis) also increases by 10.4 %, from 7.86 x 10^{-3} mol C (mol C)$^{-1}$ hr^{-1} to 8.89 x 10^{-3} mol C (mol C)$^{-1}$ hr^{-1}. This increase in the delivery of both ON and OC to maintenance and growth allows SAR11-PH to grow at a 13.0 % faster rate than SAR11-H during day light (Figure 4.2). This increase in growth rate afforded by photoheterotrophic DOC and DON uptake over the 12 hour sunlit day allows SAR11-PH to grow at a rate 6.4 % greater than SAR11-H over 24 hours (Figure 4.2).

4.3.1.2. Fate of carbon and nitrogen at β_{opt}

The total uptake rate of carbon and nitrogen increases by 9.4 % and 10.4 %, respectively, in SAR11-PH relative to SAR11-H (Figure 4.3). With these increases the relative fate of carbon and nitrogen does not change significantly (Figure 4.3). This is because although photoheterotrophic light use increases DON uptake to a greater extent than DOC, the increases in the delivery of ON and OC to maintenance and growth are the same (Figure 4.2). As a result, the stoichiometry of synthesis is similar between SAR11-H and SAR11-PH and the relative fate of carbon and nitrogen is largely unchanging (Figure 4.3). SAR11-PH grows at a faster rate than SAR11-H because it uptakes more DOC and DON and not because there is a change in the relative fates of carbon and nitrogen.

SAR11-H and SAR11-PH assimilate a similar percentage of the total carbon flux into new biomass at 42 % and 44 %, respectively. Although the rate of excess carbon release increases by 11 % (Figure 4.4), it accounts for ~33 % of the total carbon flux in both cell types and is the largest component of non-growth carbon. The fate of maintenance carbon is unchanging as it is fixed and the same for both SAR11-H and SAR11-PH, representing 11 % of the total carbon flux in SAR11-H and 10 % in SAR11-PH. Carbon respired through AA synthesis changes in proportion to the change in the rate of AA production, which is negligible (Figure 4.2, 4.4) but represents 11 % of total carbon in SAR11-H and 10 % in SAR11-PH (Figure 4.3). The rate of carbon dioxide release from maintenance and growth increases by 10 % in SAR11-PH relative to SAR11-H (Figure 4.4). However, this flux only represents ~3 % of total carbon in SAR11-PH and SAR11-H (Figure 4.3).

Growth accounts for the majority of the total nitrogen flux in SAR11-PH and SAR11-H at 78 % and 76 %, whilst maintenance accounts for 18 % and 20 %, respectively (Figure 4.3). The consequence of the increase in growth rate through photoheterotrophy for the fate of nitrogen is that ammonium release and excess nitrogen increase by 13 % and 14 % in SAR11-PH relative to SAR11-H, respectively (Figure 4.4). However, ammonium release accounts for less than 3 % and excess nitrogen less than 1 % of the total nitrogen flux in both cell types (Figure 4.3).

4.3.1.3. Growth rate and the uptake and use of carbon and nitrogen at suboptimum β

Suboptimal β still allows for an increased rate of growth relative to SAR11-H (Figure 4.2). Relative to SAR11-H, investing all harvested light energy in DON uptake (β = 1) increases growth rate by 6.0 % and investing all harvested light energy in DOC uptake (β= 0) increases

growth rate by 3.9 % (Figure 4.2). The growth curves of SAR11-H and SAR11-PH do not intersect at any point on the axis β as the photoheterotrophy model (SAR11-PH) always provides additional (light enhanced) resources relative to the heterotrophy model (SAR11-H). Although the choice of how to invest harvested solar energy in either DOC or DON uptake has a minimal influence on growth rate in non-limiting conditions, the dynamics of suboptimum β are evaluated to understand what processes reduce growth rate relative to β_{opt}.

SAR11-PH growth rate is at a maximum of 8.89 x 10^{-3} mol C (mol C)$^{-1}$ hr^{-1} at β_{opt}= 0.82 (Figure 4.5a). For values of β greater than 0.82, the cell's growth rate decreases. It is 8.87 x 10^{-3} mol C (mol C)$^{-1}$ hr^{-1} at β = 1, 99.0 % that found at β_{opt} (Figure 4.5a). At β = 1, the rate of DON uptake in SAR11-PH is 3.0 % greater than at β_{opt} (Figure 4.5b). The rate of DOC uptake at β = 1 is the same for SAR11-H and SAR11-PH, which is 95.2 % that found at β_{opt} (Figure 4.5c). Although DOC, the carbon source for AA synthesis, is taken up at the same rate in SAR11-H and SAR11-PH at β = 1, SAR11-PH invests less DOC in AA synthesis, because it has more DON (Figure 4.5b). The rate of AA production in SAR11-PH is 96.6 % that found at β_{opt} (Figure 4.5d). Despite the different dynamics of DON uptake and AA synthesis, the delivery of ON to maintenance and growth are the same in SAR11-PH at β_{opt} and β = 1 (Figure 4.5f). However, the delivery of OC to maintenance and growth is 93.6 % that found at β_{opt} (Figure 4.5e). The small decrease in SAR11-PH growth rate for values of β greater than 0.82 is due to a decrease in available OC. Growth rate is limited by carbon for values of β between 0.82 and 1, relative to β_{opt}.

As β tends to zero from β_{opt} at 0.82, the growth rate of SAR11-PH decreases and at β = 0 is 8.45 x 10^{-3} mol C (mol C)$^{-1}$ hr^{-1}, which is 95.1 % of the maximum growth rate at β_{opt} (Figure 4.5a). At β = 0, the rate of DOC uptake is at a maximum, which is 17.1 % greater than that found at β_{opt} (Figure 4.5c). As a result, the rate of AA synthesis is also at a maximum at β = 0, 12.6 % greater than the rate of synthesis at β_{opt} (Figure 4.5d). However, the rate of DON uptake decreases as β approaches zero and is the same for SAR11-H and SAR11-PH at β = 0 (Figure 4.5b). As a result, despite the maximum rate of AA synthesis occurring at β = 0, the rate of ON delivery is 83.3 % that found at β_{opt} in SAR11-PH (Figure 4.5f). Although the rate of OC delivery to maintenance and growth is at a maximum at β = 0, which is 19.5 % greater than at β_{opt} (Figure 4.5e), the decline in the rate of ON delivery limits the rate of growth. Growth rate is nitrogen limited for values of β between 0.82 and 0, relative to β_{opt}.

4.3.1.4. The fate of carbon and nitrogen at suboptimum β

The decrease in growth rate for values of β greater than β_{opt} (0.82 to 1) is because of a reduction in the delivery OC to maintenance and growth (Figure 4.5e). As a result, a greater fraction of biomass is synthesised via the processing of ON. Synthesis through the use of ON for energy results in the release of ammonium, which increases as β tends to 1 (Figure 4.6d). As the degree of carbon limitation increases as β tends to 1, nitrogen excess tends towards a maximum (Figure 4.6f) and carbon excess tends towards a minimum (Figure 4.6e). This decrease in excess carbon is the only significant change in the fate of carbon as a percentage of the total carbon flux, which results in a greater percentage of total carbon being used for growth (Figure 4.7). Although respiration through AA synthesis decreases as β tends to 1, this does not alleviate the limitation of carbon on synthesis.

As β tends to 0, SAR11-PH growth rate is limited by nitrogen relative to β_{opt}. The high flux of OC relative to ON for values of β less than β_{opt} (Figure 4.5e and f) means a greater fraction of synthesis occurs through sourcing energy and carbon from OC, sparing the mobilisation of ON and allowing for its direct assimilation. As the use of ON for energy declines so does the release of ammonium, which is at a minimum at β = 1 (Figure 4.6d). Nitrogen excess is at a minimum (Figure 4.6f). A large fraction of carbon is in excess, due to the relative nitrogen limitation, and its rate of release tends towards a maximum at β = 0 (Figure 4.6e).

4.3.1.5. Bacterial growth efficiency

The bacterial growth efficiency (BGE) of SAR11-PH is 78 % at β_{opt} compared to 76 % in SAR11-H (Figure 4.8). The higher BGE of SAR11-PH is a result of the increased rate of growth despite the fact that the rate of AA synthesis is the same in both cell types (Figure 4.2). As AA synthesis is the primary source of carbon dioxide in the modelled cell (Figure 4.3 and 4.4), SAR11-PH has higher growth efficiency than SAR11-H.

As β tends to 0, SAR11-PH increasingly depends on DIN as a source of nitrogen (Figure 4.5d), which has a higher cost on carbon for assimilation, resulting in higher respiration rates (Figure 4.6b) and lower BGE than that found at β_{opt} (Figure 4.8). As β tends to 1, SAR11-PH invests less solar energy in DOC uptake, the source of carbon for AA synthesis, its rate of production decreases (Figure 4.5d), along with the rate of respiration released through AA synthesis (Figure 4.6b), and BGE tends towards a maximum (Figure 4.8).

4.3.2. Experiment 2: The effect of ambient DIN

4.3.2.1. Growth rate and the uptake and use of carbon and nitrogen

As ambient DIN decreases, the growth rate of SAR11-PH decreases from 0.20 d^{-1} to 0.094 d^{-1} and for SAR11-H from 0.188 d^{-1} to 0.079 d^{-1} (Figure 4.9a). Photoheterotrophy increases the growth rate of SAR11-PH by up to 18.6 % relative to SAR11-H, the largest difference being at zero ambient DIN. Growth on only DOC and DON can support a growth rate that is 47.0 % in SAR11-PH and 42.0 % in SAR11-H of that achieved when ambient substrates are non-limiting (Figure 4.9a).

With decreasing ambient DIN, SAR11-PH needs to invest an increasing fraction of harvested solar energy in the uptake of DON to maintain maximum growth rate. β_{opt} shifts from 0.82 at saturating DIN (DIN of 5 (X/K)), to β_{opt} = 1 when DIN is limiting (DIN of 0.5 to zero (X/K)) (Figure 4.9b). As DIN reaches these limiting conditions, photoheterotrophic light use increases the rate of DON uptake to 5.82 x 10^{-3} mol C (mol C)$^{-1}$ hr^{-1} in SAR11-PH, 23.0 % greater than SAR11-H at 4.73 x 10^{-3} mol C (mol C)$^{-1}$ hr^{-1} (Figure 4.9c). Under these conditions solar energy is not invested in the uptake of DOC, the rate of which is therefore the same for SAR11-H and SAR11-PH at 1.37 x 10^{-2} mol C (mol C)$^{-1}$ hr^{-1} (Figure 4.9e). Photoheterotrophy has a negligible influence on AA synthesis with declining ambient DIN (Figure 4.9c). The rate of AA synthesis does however decline to zero for both SAR11-H and SAR11-PH at zero ambient DIN and therefore does not contribute to ON. Photoheterotrophy has the greatest effect on growth rate at zero ambient DIN because ON delivery to maintenance and growth increases by 23.0 % due to the light enhanced rate of DON uptake (Figure 4.9d). As less DOC is used to synthesise AA with decreasing ambient DIN, the rate of OC delivery to maintenance and growth increases, being equal for SAR11-H and SAR11-PH when DIN is absent at 1.37 x 10^{-2} mol C (mol C)$^{-1}$ hr^{-1} (Figure 4.9f).

4.3.2.2. The fate of carbon and nitrogen

DIN limitation has a significant influence on the capacity of SAR11 to assimilate carbon (Figure 4.11). Between saturating and limiting DIN, the percentage of the total carbon flux assimilated into new biomass decreases from 42 % to 18 % in SAR11-H and from 44 % to 24 % in SAR11-PH (Figure 4.11). As ambient DIN declines the rate of excess carbon release increases by 89.6 % in SAR11-PH, from 0.67 x 10^{-2} mol C (mol C)$^{-1}$ hr^{-1} at saturating DIN to 1.27 x 10^{-2} mol C (mol C)$^{-1}$ hr^{-1} at zero DIN (Figure 4.10c). Photoheterotrophy and the resulting increase in the ON flux (Figure 4.9d) means SAR11-PH can assimilate a greater percentage of carbon into new biomass at limiting DIN, which increasing from 18 % to 24 % when ambient DIN is zero (Figure 4.11). As

a result, excess carbon release accounts for 70 % of the total carbon flux in SAR11-H but only 65 % in SAR11-PH at zero DIN. As carbon uptake is unchanging with decreasing DIN for each cell type, the percentage of carbon used for maintenance is the same as when DIN is saturating, accounting for 11 % in SAR11-H and 10 % in SAR11-PH. Although carbon dioxide release through maintenance and growth increases by up to 22.8 %, with the greatest increase occurring when DIN is absent (Figure 4.10b), in these conditions this flux represents roughly 1 % of total the carbon flux in both cell types (Figure 4.11). Respiration though AA synthesis is the primary source of carbon dioxide and is not changed through photoheterotrophic light use but does decline with decreasing availability ambient DIN (Figure 4.11). Total carbon dioxide release is not significantly influenced by photoheterotrophy when ambient DIN decreases (Figure 4.10d).

As ambient DIN declines to zero, the percentage of the total nitrogen flux assimilated into new biomass decreases from 76 % to 60 % in SAR11-H and from 78 % to 67 % in SAR11-PH (Figure 4.11). Maintenance accounts for an increasing and majority percentage of the total nitrogen flux as ambient DIN decreases, up to 38 % in SAR11-H and 31 % in SAR11-PH, with the maximum at zero ambient DIN, explaining the decline in nitrogen assimilation into new biomass (Figure 4.11). At zero ambient DIN photoheterotrophy increases the percentage of the total nitrogen flux assimilated into biomass, from 60 % in SAR11-H to 67 % in SAR11-PH. This is due primarily to the increase in nitrogen uptake via light enhanced DON acquisition (Figure 4.9c), which reduces the percentage of the total nitrogen flux used for the fixed maintenance requirements (Figure 4.11). Although photoheterotrophy increases the rate of ammonium release by up to 39.6 % (Figure 4.10e) and excess nitrogen by up to 39.1 % (Figure 4.10f), with the biggest difference occurring when DIN is absent, these fluxes account for a minor component of the total nitrogen flux (Figure 4.11). For both SAR11-PH and SAR11-H, ammonium release and excess nitrogen represents ~1 % of the total nitrogen flux when DIN is absent (Figure 4.11).

4.3.2.3. Bacterial growth efficiency

BGE increases with decreasing ambient DIN for both cell types (Figure 4.12) as the major source of carbon dioxide release, AA synthesis, decreases to zero (Figure 4.11). BGE increases from 78 % to ~94 % in SAR11-H and from 76 % to ~94 % in SAR11-PH. Photoheterotrophy does not affect BGE when DIN becomes limiting because no carbon dioxide is released through AA synthesis and release through the synthesis of biomass represents only 1 % of the total carbon flux (Figure 4.12).

4.3.3. Experiment 3: The effect of ambient DON

4.3.3.1. Growth rate and the uptake of carbon and nitrogen

As ambient DON decreases, the growth rate of SAR11-PH decreases from 0.20 d^{-1} to 0.089 d^{-1}, whilst SAR11-H growth rate declines from 0.0188d^{-1} to 0.081 d^{-1} (Figure 4.13a). SAR11-PH can grow on just DOC and DIN at 44.5 % the rate achieved when DON is saturating and SAR11-H can grow at 43.1 % of the rate. The growth rate of SAR11-PH is up to 9.9 % greater than that of SAR11-H as DON varies, with the greatest difference being at zero ambient DON (Figure 4.13a).

SAR11-PH needs to invest an increasing fraction of harvested solar energy in the uptake of DOC as ambient DON decreases for the maximum growth rate to be achieved (Figure 4.13b). β_{opt} = 0.82 when DON is abundant (DON (X/K) of 5) and shifts to β_{opt} = 0 when DON is limiting (DON (X/K) of 0.06 to zero) (Figure 4.13b). At limiting DON (DON (X/K) of 0.06 to zero), photoheterotrophy increases the uptake rate of DOC to 1.69 x 10^{-2} mol C (mol C)$^{-1}$ hr^{-1}, which is 23.4 % greater than SAR11-H at 1.37 x 10^{-2} mol C (mol C)$^{-1}$ hr^{-1} (Figure 4.13e). This allows SAR11-PH to increase the rate of AA synthesis by up to 11.0 % to 5.34 x 10^{-3} mol C (mol C)$^{-1}$ hr^{-1}, relative to SAR11-H at 4.81 x 10^{-3} mol C (mol C)$^{-1}$ hr^{-1}, the largest different occurring at zero ambient DON (Figure 4.13c). AA makes up the entire flux ON at zero DON, which increases by 11.0 % (Figure 4.13d). The remainder of the OC flux is directed to maintenance and growth at a rate 36.9 % faster in SAR11-PH at 0.89 x 10^{-2} mol C (mol C)$^{-1}$ hr^{-1}, compared to SAR11-H at 0.65 x 10^{-2} mol C (mol C)$^{-1}$ hr^{-1} (Figure 4.13e). Photoheterotrophic DOC uptake allows for a growth rate increase of 9.9 % in SAR11-PH relative to SAR11-H at zero ambient DON (Figure 4.13a).

4.3.3.2. The fate of carbon and nitrogen

DON limitation significantly affects the percentage of the total carbon flux assimilated into new biomass, decreasing from 42 % to 25 % in SAR11-H and 44 % to 24 % in SAR11-PH (Figure 4.15). The percentage of the total carbon flux in growth declines with decreasing DON because of the increase in excess carbon release, carbon respiration through AA synthesis and the increased fraction of the total carbon flux needed to satisfy maintenance. Although photoheterotrophy does not significantly change the percentage of the total carbon flux assimilated as ambient DON decreases, the magnitude of the carbon fluxes are significantly affected. Photoheterotrophic light use increases the rate of excess carbon release by up to 46.3 % from 0.54 x 10^{-2} mol C (mol C)$^{-1}$ hr^{-1} in SAR11-H to 0.79 x 10^{-2} mol C (mol C)$^{-1}$ hr^{-1} in SAR11-PH (Figure 4.14c), with the greatest difference at zero ambient DON. Excess carbon accounts for the largest percentage of the total carbon flux at zero DON, 41 % in SAR11-H and 47 % SAR11-PH (Figure 4.15). Total carbon dioxide release in SAR11-PH increases by up to 11.4

% relative to SAR11-H with decreasing ambient DON (Figure 4.14d). The greatest difference occurs at zero DON, with a rate of release that increases from 2.63 x 10^{-3} mol C (mol C)$^{-1}$ hr^{-1} in SAR11-H to 2.93 x 10^{-3} mol C (mol C)$^{-1}$ hr^{-1} in SAR11-PH (Figure 4.14d), accounting for 19 % and 17 % of the total carbon flux, respectively (Figure 4.15). The primary source of carbon dioxide release is AA synthesis, accounting for up to 16 % of the total carbon flux in SAR11-PH and 18 % in SAR11-H (Figure 4.15). Although carbon dioxide release increases through maintenance and growth and is greater in SAR11-PH by up to 11.0 % relative to SAR11-H (Figure 4.14b), it represents only 1 % of the total carbon flux for both cell types (Figure 4.15). Because of the decline in DON uptake and therefore carbon, maintenance accounts for an increasing percentage of the total carbon flux as DON declines, 15 % in SAR11-H and 12 % in SAR11-PH at zero DON.

The percentage of nitrogen assimilated declines with decreasing DON from 76 % to 61 % in SAR11-H and 78 % to 64 % in SAR11-PH (Figure 4.15). With the decrease in DON uptake, less nitrogen is taken into the cell and an increasing fraction is used in maintenance for both cell types, up to 36 % in SAR11-H and 33 % in SAR11-PH (Figure 4.15). The release of ammonium and excess nitrogen both decrease with declining ambient DON but are not significantly affected by photoheterotrophic light use (Figure 4.14 e and f). They represent roughly 2 % and 1 % of the total nitrogen flux, respectively (Figure 4.15).

4.3.3.3. Bacterial growth efficiency

Photoheterotrophy does not significantly influence BGE when ambient DON decreases. BGE does, however, decrease from 76 % to 58 % for SAR11-H and from 78 % and 56 % in SAR11-PH when ambient DON decreases (Figure 4.16). At zero ambient DON, BGE is lowest for both cell types as they are dependent on DIN for all nitrogen, which is assimilated into AA at a high cost in carbon resulting in higher respiration rates (Figure 4.14a).

4.3.4. Experiment 4: The effect of ambient DOC

4.3.4.1. Growth rate and the uptake of carbon and nitrogen

As ambient DOC decreases the growth rate of SAR11-PH decreases from 0.20 d^{-1} to 0.068 d^{-1} and that of SAR11-H from 0.188 d^{-1} to 0.056 d^{-1} (Figure 4.17a). When ambient DOC is zero growth is entirely dependent on DON, which can support 34.0 % (in SAR11-PH) and 29.8 % (in SAR11-H) of the growth rate achieved when ambient conditions are saturating (Figure 4.17a). Photoheterotrophy in SAR11-PH enhances growth rate by up to 21.4 % relative to SAR11-H, with the greatest difference being at zero ambient DOC.

In order to grow at the maximum rate as ambient DOC decreases, SAR11-PH needs to invest an increasing fraction of harvested solar energy in the uptake of DON (Figure 4.17b). β_{opt} shifts from 0.82 when DOC is saturating (DOC (X/K) = 5) to β = 1 when DOC is limiting ((X/K) = 0.1 to zero) (Figure 4.17b). The uptake rate of DON when DOC decreases to limiting conditions ((X/K) = 0.1 to zero) is enhanced by 23.0 % from 4.73 x 10^{-3} mol C (mol C)$^{-1}$ hr^{-1} in SAR11-H to 5.82 x 10^{-3} mol C (mol C)$^{-1}$ hr^{-1} in SAR11-PH (Figure 4.17c). Under the same conditions, DOC uptake in SAR11-PH approaches that of SAR11-H as no solar energy is invested in its uptake, both decreasing from 1.20 x 10^{-2} mol C (mol C)$^{-1}$ hr^{-1} to zero when DOC is absent (Figure 4.17e). Photoheterotrophy has a minimal influence on the synthesis rate of AA as ambient DOC decreases and production stops when ambient DOC is zero (Figure 4.17c). At zero ambient DOC when the effect of photoheterotrophy on growth rate is greatest, the increase in growth rate is through an increase in ON delivery to maintenance and growth by 23.0 % (Figure 4.17d), which is comprised entirely of DON.

4.3.4.2. The fate of carbon and nitrogen

As ambient DOC decreases the percentage of the total carbon flux assimilated increases from 44 % to 57 % in SAR11-PH and from 42 % to 50 % in SAR11-H (Figure 4.19). The ability to enhance DON uptake increases carbon uptake and a smaller percentage of the total carbon flux is used for maintenance in SAR11-PH relative to SAR11-H. When DOC is absent, maintenance uses the majority of the total carbon flux, accounting for 44 % in SAR11-H and 36 % in SAR11-PH. Excess carbon release is not enhanced by photoheterotrophy because the cell does not invest solar energy in DOC uptake with declining ambient DOC (Figure 4.18c). As ambient DOC declines and the OC flux available for maintenance and growth decreases, the flux of excess carbon also declines to 2-3 % in both cell types (Figure 4.18d). Although carbon dioxide release through maintenance and growth does increase in SAR11-PH relative to SAR11-H (Figure 4.18b) it is only a minor component of the total carbon flux (~4 %) (Figure 4.19). The primary source of carbon dioxide, AA synthesis, is not changed and therefore total carbon dioxide release is relatively unaffected and declines to zero when DOC is absent (Figure 4.18a).

As ambient DOC becomes limiting, resulting in a decrease in DIN assimilation (Figure 4.17c) and therefore total nitrogen uptake, the percentage of the total nitrogen flux assimilated decreases from 76 % to 42 % in SAR11-H and from 78 % to 49 % in SAR11-PH. Maintenance uses a significant percentage of the total nitrogen flux as ambient DOC decreases, accounting for 38 % of the total nitrogen flux in SAR11-H and 31 % in SAR11-PH at zero ambient DOC. The ability to increase nitrogen uptake through photoheterotrophy reduces

the fraction of the total nitrogen flux used in maintenance, allowing SAR11-PH to use more for growth. The decrease in the available OC flux for maintenance and growth as ambient DOC declines (Figure 4.18f) increases the cells dependency on ON as a source of energy (Figure 4.17d), resulting in an increase in the rate of ammonium release. Photoheterotrophic light use increases the rate of ammonium release in SAR11-PH by up to 22.5 % relative to SAR11-H, as ambient DOC decreases, with the largest difference at zero DOC (Figure 4.18e). Ammonium release increases from 18.7 x 10^{-5} mol N (mol C)$^{-1}$ hr^{-1} in SAR11-H to 22.9 x 10^{-5} mol N (mol C)$^{-1}$ hr^{-1} in SAR11-PH at zero DOC (Figure 4.18e), accounting for 17 % of the total nitrogen flux in both cell types (Figure 4.19). Although excess nitrogen release increases by up to 42.3 % through photoheterotrophic light use with the greatest change at zero DOC (Figure 4.18f), the flux represents ~3 % of the total nitrogen flux for both SAR11-H and SAR11-PH (Figure 4.19).

4.3.4.3. Bacterial growth efficiency

Decreasing ambient DOC limits carbon available for the assimilation of DIN into AA. Accordingly the synthesis of AA declines and respiration through this process decreases, resulting in an increase in BGE for both cell types from 76 % to 91 % in SAR11-H and from 78 % to 94 % in SAR11-PH (Figure 4.20). The increase in BGE through photoheterotrophic light use is small and never is greater than 3 %.

4.3.5. Results summary

Photoheterotrophic light use in SAR11 results in significant increases to the cells specific growth rate. Such benefits are only noteworthy during nutrient DIN and DOC limiting conditions, where growth rate is enhanced by up to ~20 %. The requirements of carbon and nitrogen for maintenance during nutrient limitation are significant, which photoheterotrophy partially relieves. Photoheterotrophic light use results in significant increases in respiratory carbon dioxide release during DON limitation, when the cell is increasingly dependent on DIN as a source of nitrogen, which is expensive to assimilate. When DOC limits the growth of SAR11, photoheterotrophic light use increase growth rate significantly and consequently the rate of ammonium release is enhanced by up to 22.5 %.

4.4. Discussion

4.4.1. Photoheterotrophic light use and growth rate

The present study shows that photoheterotrophic resource acquisition can enhance growth rate by 6.4 % when all substrates are non-limiting (Figure 4.2). The greatest benefit of photoheterotrophy to growth rate, however, is when ambient DOC is limiting (Figure 4.17a) (21.4 %) followed by DIN (Figure 4.9a) (18.6 %) and to a lesser extent when DON is limiting (Figure 4.13a) (9.9 %). Light enhanced growth rate has been observed for natural populations of SAR11 (Lami et al., 2009) and other PR containing bacteria (Gómez-Consarnau et al., 2007) but without specification of ambient nutrient conditions.

Batch cultures of SAR11 (Steindler et al., 2011) and other PR containing bacteria (Gómez-Consarnau et al., 2010) that have been exposed to light:dark and dark:dark cycles have been shown to survive substrate limiting conditions (stationary phase) with a light phase for longer periods of time than in continuous darkness but with no influence on growth rate. Phototrophic processes other than photoheterotrophically enhanced substrate uptake, such as light mediated ATP production to substitute carbon respiration (Steindler et al., 2011) and other energy spilling pathways (Del Giorgio and Cole, 1998), may be critical during starvation conditions found during stationary phase, but are not considered here.

Giovannoni et al. (2005a) demonstrated that the presence of a light phase in batch culture compared to continuous dark generally has no influence on SAR11 growth rate in non-limiting conditions (exponential phase). It has been suggested however, that the SAR11 culture may be replete with organic material, satisfying the energy demands of cells in light and dark conditions (Zubkov, 2009). Giovannoni et al. (2005a) did note that in some experiments cells grew better in the light but results were variable.

Are such increases in growth rate related to photoheterotrophy ecologically relevant and do they influence the distribution of SAR11? SAR11 are ubiquitously distributed along horizontal (Morris et al., 2002) and vertical gradients (Field et al., 1997) of nutrients. It is likely that photoheterotrophic light use increases their competitive ability for limiting resources and growth rate relative to non-photoheterotrophic microbes and functions in governing their distribution in the ocean. The use of a single cell model in the present study restricts full evaluation of the interactions of the SAR11 population with physical and other chemical forcing agents, in addition to the influence of competition for shared resources with other microbes such as Pro. A proposal for a chemostat model to address the influence of changes in

growth rate through photoheterotrophy and the influence on competition for shared nutrient pools is discussed in Section 6.3.

Energetic arguments that compare net solar energy harvesting to cellular maintenance energy requirements imply that proteorhodopsin based photoheterotrophy may influence the distribution of PR containing microbes such as SAR11. High light intensities (≥ 800 µmol photons m^{-2} s^{-1}) and high densities of proteorhodopsin units in membranes may result in solar energy harvesting that exceeds maintenance requirements (Kirchman and Hanson, 2012). Such light intensities are representative of experimental conditions where photoheterotrophy increases nutrient uptake in SAR11 cells (Gómez-Pereira et al., 2012). High PR densities in SAR11 membranes are however yet to be measured (Giovannoni et al., 2005a, Kirchman and Hanson, 2012).

The assumed maintenance energy requirements are important for the conclusions drawn by Kirchman and Hanson (2012). In the present study, growth rate is sensitive to changes in the maintenance rate, the sensitivity of which increases as substrates become limiting (Appendix Tables 4.1-4.4). Neither study use observed maintenance rates specific to SAR11 as such measurements are absent from the literature. Understanding the maintenance requirements of SAR11 is therefore important in determining the influence of photoheterotrophy on their distribution.

4.4.2. Optimum light investment for maximum growth rate

We do not have any observational evidence with which to compare the behaviour of β_{opt} in the model. The ability to partition cellular energy could drive organism selection in the ocean (Zubkov, 2009). The parameter β can be considered to represent the physiological plasticity of an individual SAR11 cell for the use of harvested solar energy. A population of SAR11 could navigate along β with time through fluctuating ambient conditions, maximising growth rate at β_{opt}.

This kind of trade-off framework has been used to represent the diversity of populations, allowing the modelled environment to select the best combination of parameter values or traits to maximise a certain property, often growth rate (for example Follows et al., 2007). Such a conceptual approach is motivated by the principles of natural selection (reviewed by Follows and Dutkiewicz, 2010). The present study can also be seen from this perspective, with each value of β corresponding to a different physiological strategy for different individuals. Populations of SAR11, each with a different value of β, would

interchangeably have β_{opt} in fluctuating ambient conditions. In such a situation the full β trait space would represent diverse populations of SAR11. Future work could consider this alternative theory for how light is partitioned within SAR11 and evaluate suboptimum β in addition to β_{opt} in changing ambient conditions.

The specific value of β_{opt} might not represent the actual percentage of harvested solar energy invested in DOC and/or DON uptake for any given environment. The use of harvested solar energy for photoheterotrophic uptake of dissolved organic phosphorus (Gómez-Pereira et al., 2012, Duhamel et al., 2012) and ATP synthesis (Gómez-Consarnau et al., 2010) may influence the balance of light energy investment and therefore the specific value of β_{opt}. This will be discussed in greater detail in Section 6.3.

4.4.3. The uptake of DIN

Understanding the dynamics of DIN acquisition and metabolism in the subtropical gyres is important as it is considered a major limiting nutrient for microbial growth. While it has been demonstrated that SAR11 are capable of assimilating DIN (Sowell et al., 2008), the present study may be the first attempt at investigating the contribution of DIN to a SAR11 cell's nitrogen budget.

A photoheterotrophic SAR11 cell may need to source 42 % of cellular nitrogen from DIN (47 % in in a non-photoheterotrophic SAR11 cell) in order to grow at the maximum rate when ambient substrates are saturating (Figure 4.2). This estimate is dependent on the growth rate per day, (Section 2.3.1.4) and the scaling method used to gain an estimate for the theoretical maximum rates of DIN and DON uptake (with the maximum uptake rate of DON estimate being comparable to field estimates) (Section 5.2.1). The scaling method is critiqued in Section 5.4. According to observations an assumed growth rate of 0.20 d^{-1} is reasonable (Rappé et al., 2002, Giovannoni et al., 2005b, Malmstrom et al., 2005). Measured rates of DON uptake are, however, variable (Mary et al., 2008a, Gómez-Pereira et al., 2012, Evans et al., 2015). Until parallel measurements of growth rate and uptake are made in a single empirical study it is difficult to assess variation in the contribution of DIN (and DON) to SAR11 the nitrogen budget as all parameters can theoretically vary independently. The present study should therefore not be considered an absolute representation of the SAR11 nitrogen budget. However, the estimates are a first attempt at understanding the contribution of DIN to SAR11 growth and they allow for an evaluation of the influence of photoheterotrophy on the dynamics of resource acquisition with changing ambient fields.

When ambient conditions are non-limiting, photoheterotrophic light use does not appear to reduce the requirement of DIN for growth (Figure 4.2). However, the ability to enhance the uptake of DOC photoheterotrophically may enhance DIN assimilation into AA when DON limits growth (Figure 4.13c), even if the concentration of DIN is unchanging (Table 4.2). The results from the model suggests that increasing the delivery of DOC to the AA synthesis machinery when ON declines, increases the cells capacity to assimilate DIN into AA by up to 11.0 % (Figure 4.13c). The effect is greatest when ambient DON is zero, where the increase in growth rate is by up to 9.9 % (Figure 4.13a).

In cases when ambient DON is limiting SAR11 growth relative to DIN and DOC, the ability to enhance the assimilation of DIN into AA indirectly through photoheterotrophically enhanced DOC uptake, may have important consequences for competition for nitrogen resources in oligotrophic gyre ecosystems. Primary production is limited by DIN in oligotrophic ecosystems and evidence suggests that bacteria out-compete phytoplankton for DIN, due to their smaller size and increased surface area to volume ratio (Suttle et al., 1990). The DIN form of ammonium is preferred by cells on an energetic basis over nitrate and nitrite as it is in the chemical form required for AA synthesis (White, 2007). The ability to enhance the assimilation of ammonium when SAR11 uses light energy photoheterotrophically may further increase competitive pressure on phytoplankton for limiting DIN, forcing these primary producers to utilise resources, such as nitrate, which is expensive to assimilate due to the additional cost of reduction. In situations where new nitrate fuels new production, which may be a rare case in gyres with limited vertical mixing, as new production balances export, it is possible that photoheterotrophic light use in SAR11 might partially mediate the export of carbon to the deep ocean in oligotrophic ecosystems if cells are DON limited. Alternatively the increased competitive ability for DIN in SAR11 through photoheterotrophy may modify ambient conditions such that other DIN competitors such as Pro are at a competitive advantage if they the ability to uptake DON photoheterotrophically.

SAR11 can transport and assimilate less reduced forms of DIN, such as nitrate and nitrite (Sowell et al., 2008). If a fraction of DIN used by SAR11 is made up of less reduced forms of DIN, the cost for synthesising AA may be underestimated in the model as it is based on the assimilation of ammonium into AA. Growth rate is sensitive to the cost of AA synthesis when DON limits growth (Appendix table 4.3). The increase in growth rate through photoheterotrophic light use when DON limits growth (Figure 4.13a) may therefore be over-estimated in the present analysis if SAR11 assimilates substantial fractions nitrate and/or

nitrite instead of ammonium. Determining DIN sources readily used by SAR11 is therefore important in understanding constraints on SAR11 growth rate.

4.4.4. The uptake of DON

SAR11 frequently dominate the uptake of DON compounds in oligotrophic subtropical gyres (Malmstrom et al., 2005, Malmstrom et al., 2004, Mary et al., 2008b, Gómez-Pereira et al., 2012) demonstrating the importance of SAR11 as competitors and processors of organic material.

The ability to enhance DON uptake photoheterotrophically may increase growth rate by up to 18.6 % when DIN is limiting (Figure 4.9a) and 21.4 % at limiting DOC (Figure 4.17a). Photoheterotrophic light use in SAR11, specifically for the uptake of DON, may be essential for survival when DIN and DOC (Carlson and Ducklow, 1996) are limiting in oligotrophic ecosystems where SAR11 dominate (Morris et al., 2002). The ability to direct solar energy to the uptake of DON may also increase SAR11's competitive ability for the limiting concentrations of nitrogen.

Results presented here suggest that DON may account for just over half of a cell's cellular nitrogen requirements and a quarter of its carbon requirements when substrates are saturating (Figure 4.2). DON is therefore a critical source of not just nitrogen but also of carbon in oligotrophic ecosystems.

The chemical species and energetic status of DON may be critical for the growth of SAR11. Sensitivity analysis suggests that the growth rate of SAR11 is sensitive to the C:N of DON (Appendix Tables 4.1-4.3) and the efficiency with which it is assimilated into biomass (Appendix Table 4.4). In the model, the C:N of DON is that of bacterial protein, which assumes that SAR11 can select specific components of the DON pool best suited for metabolism (Mary et al., 2008b) and that SAR11 protein is the same as that of coastal populations from which the bacterial protein was characterised (Section 2.3.1.8). Knowledge of the nature of SAR11 protein and the specific components of the DON pool that are assimilated would be important for understanding constraints on SAR11 growth rate when analysed using the presented model.

4.4.5. The uptake of DOC

Photoheterotrophic DOC uptake results in an increase in growth rate of up to 9.9 % when DON is limiting (Figure 4.13a). The influence of light enhanced DOC uptake on DIN assimilation has

already been discussed (Section 4.4.3). Light enhanced DOC uptake also significantly enhances the delivery of OC to maintenance and growth (Figure 4.13f), contributing to the ability of SAR11 to increase growth rate by up to 9.9 % if DON is limiting growth (Figure 4.13a).

The model demonstrates that SAR11 could use harvested light energy to enhance the uptake of DOC during non-limiting (Figure 4.2) and DON limiting conditions (Figure 4.13e) suggesting that if DOC metabolism measurements for SAR11 (Alonso and Pernthaler, 2006, Malmstrom et al., 2005) are made in such conditions then neglecting to consider photoheterotrophic metabolism would underestimate the SAR11 contribution to DOC turnover.

The model results suggest that DOC may be the primary carbon source for SAR11 accounting for roughly 75 % when ambient conditions are saturating (Figure 4.13). Limiting concentrations of ambient DOC, which have been documented for the oligotrophic Sargasso Sea (Carlson and Ducklow, 1996) where SAR11 numerically dominates the bacterioplankton community (Morris et al., 2002), results in a growth rate that is approximately 30 % of that possible when substrates are saturating (Figure 4.17a). Although nitrogen is often considered the primary limiting resource in oligotrophic ecosystems, the availability of this carbon substrate is a critical factor for SAR11 survival in subtropical oligotrophic gyres.

4.4.6. Carbon dioxide respired

The results from the model indicate that photoheterotrophic resource acquisition may influence our understanding of carbon dioxide release in regions of the ocean where SAR11 dominate. The degree to which it is influenced is highly dependent on ambient conditions, more specifically DON availability (Figure 4.14d).

In the model, carbon dioxide is released through costs incurred in maintenance, growth and the synthesis of AA. Conditions under which these processes are significantly influenced through photoheterotrophic light use may therefore change our understanding of carbon dioxide release in SAR11. Under DON limiting conditions, growth rate and AA synthesis are enhanced when SAR11 acquires resources photoheterotrophically and total carbon dioxide release increases by up to 11.4 % relative to an equivalent heterotroph when DON becomes limiting (Figure 4.13d), primarily through costs in the synthesis of AA (Figure 4.14a and 4.15). If respiration measurements are made in regions of the ocean where SAR11 dominate, and DON limitation increases the dependency of the cell on AA synthesis using DOC and DIN, the model demonstrates that the failure to consider the dynamics of photoheterotrophic metabolism

may result in an underestimation of carbon dioxide release or may account for a degree of variation between measurements of respiration. That respiration through this dominant bacterial clade is highly dependent on environmental conditions suggests that measurements of respiration in the ocean should be made in parallel with an evaluation of those conditions.

Respiration rates in the model are sensitive to the efficiency with which AA are synthesised (Appendix Tables 4.1 and 4.3). The efficiency with which AA are synthesised is parameterised by assuming ammonium is the only chemical species of DIN taken up from the ambient pool. Therefore any costs of DIN reduction, through the use of nitrate and nitrite, are ignored. SAR11 can however transport nitrate and nitrite (Sowell et al., 2008), and therefore when DIN assimilation incurs additional costs of reduction, respiration may be enhanced and therefore underestimated in the present study.

4.4.7. Bacterial growth efficiency

Metabolic balance, the balance between respiration and primary production, in the open ocean is a matter of debate (Ducklow and Doney, 2013). If all organisms respire all fixed carbon dioxide then the system is assumed to be in metabolic balance. If the open ocean is net autotrophic (Williams et al., 2013) it will act as a sink for carbon dioxide. whereas if the open ocean is net heterotrophic (Duarte et al., 2013) it will be a source. Reconciling which side of the balance the ocean is on is critical for our knowledge of the capacity of the ocean to sequester atmospheric carbon dioxide and therefore to respond to anthropogenic carbon dioxide release. Variations in measurements and significant methodological uncertainties in quantifying primary production and respiration currently complicate finding a definite solution to this argument (Ducklow and Doney, 2013).

The results from the model suggest that photoheterotrophic resource acquisition has a negligible influence on BGE for SAR11 (Figure 4.8 4.12, 4.16, 4.20). However, BGE is strongly dependent upon ambient conditions and the substrates used. The range of BGE values reported in this study is between 56 % to 94 % when SAR11 grows heterotrophically. The lowest BGE estimates are found when DON limits growth (Figure 4.16). In these conditions, SAR11 increasingly depends on DIN as a source of nitrogen, which is assimilated at a high cost in carbon, resulting in high respiration rates (Figure 4.14a). As a result, BGE decreases as ambient DON declines. The sensitivity of respiration to the efficiency of AA synthesis and therefore DIN species assimilated (discussed above in Section 4.4.6) is also important for BGE (Appendix Table 4.3). Higher estimates of BGE are found when DOC and DIN are limiting, restricting the synthesis of AA (Figures 4.12 and 4.20). In such cases respiration in the model is

via production of maintenance and growth biomass only, which releases only a small quantity of carbon dioxide (Figure 4.10b, 4.18b).

Measurements of BGE in oligotrophic ecosystems such as the Atlantic subtropical gyres where SAR11 dominate are typically between 1 and 10 % (Hansell et al., 1995, Alonso and Pernthaler, 2006, Del Giorgio et al., 2011). This model predicts much higher BGE. This indicates that if field measurements are correct, respiration through the synthesis of AA and maintenance and growth biomass is only a fraction of total carbon dioxide release in SAR11. If we assume, for simplicity that a BGE of 10 % is representative of oligotrophic waters, then, using our estimates of BGE (56 % - 94 %) (heterotrophic BGE for direct comparison to measurements that do not consider dynamics of photoheterotrophy), between 46 % and 84 % of total carbon may be respired through processes other than AA synthesis, maintenance and growth in SAR11.

Low BGE in oligotrophic ecosystems indicates that maintenance requirements may be high in regions of the ocean with low concentrations of nutrients (Del Giorgio and Cole, 1998). Energy requiring processes relevant to oligotrophic ecosystems, which may be paid for through organic carbon mobilisation resulting in the respiration of carbon dioxide, includes the cost for transporting nutrients into the cell up the strong concentration gradient (Mårdén et al., 1987). and the cost of maintaining diverse transport systems (Morita, 1997, Sowell et al., 2008). However, such shifts in energetic costs have not been measured in natural populations of open ocean bacterioplankton. The transport of substrates in the model has an efficiency that does not change with decreasing concentrations of ambient nutrients (Section 2.3.2). BGE is however sensitive to changes in this efficiency parameter in all experimental conditions (Appendix Tables 4.1-4.4). Transport costs have been incorporated into a similar bioenergetic model, by assuming costs increase as the ambient pool decreases relative to a constant internal cellular pool concentration (Vallino et al., 1996). However, predictions of BGE in this study were also significantly higher than field estimates. Incorporating transport costs into the present studies may prove useful in development of a model that can represent metabolic costs in addition to biomass synthesis and possibly refine BGE predictions. However, accurate predictions of BGE will require a greater understanding of maintenance processes in bacterioplankton.

It is also important to note that we do not consider all potential uses of harvested light energy that may affect respiration in the model. It has been demonstrated that SAR11 can substitute the use of DOM for energy, which results in carbon respiration, for direct

phototrophic ATP synthesis (Gómez-Consarnau et al., 2010), which may increase BGE if respiration rates decline as a consequence.

4.4.8. Ammonium release

The results from the model suggest that the release of ammonium is never a significant fraction of the total nitrogen flux as long as a readily available source of DOC is present (Figure 4.3, 4.11, 4.15). Ammonium release never represents more than 3 % of the total nitrogen flux taken up by the cell if DOC is available, regardless of whether DIN and/or DON are limiting.

It has been demonstrated that ammonium release will only occur from bacterial cells when the available source of organic carbon (here DOC) has been exhausted and if DON is the only source of nitrogen available to the cell (Goldman and Dennett, 1991, Goldman et al., 1987, Goldman and Dennett, 2000). Currently, the flux of AA and DON are summed to produce the flux of ON available for maintenance and growth and therefore AA (synthesised using DOC) may be mobilised as an energy resource. Bacterial cells are unlikely to synthesise a compound using DOC, with an efficiency of 67 % per mole of carbon synthesised (De Vries et al., 1974) and then to use this molecule as a source of energy. Despite this model limitation it is reassuring that ammonium release never exceeds 3 % of the total nitrogen flux and when DIN and DON limit growth is less than 1 % of the total nitrogen flux. This model limitation is therefore not considered to influence the results significantly.

The model is of use in evaluating the release of ammonium when DOC is limiting the growth of SAR11 and the influence that photoheterotrophic light use may have upon its rate of release. The imposition of DOC limitation demonstrates that ammonium release increases as DOC limits the cells capacity for ON sparing (for both SAR11-H and SAR11-PH) (Figure 4.18e). When DOC is absent ammonium release represents a significant fraction of total nitrogen in both cell types (Figure 4.20). The increase in DON uptake through photoheterotrophic light use at zero ambient DOC increases the release of ammonium by up to ~20 % relative to an equivalent heterotroph (Figure 4.18e). In regions of the oligotrophic ocean where carbon limitation has been demonstrated and SAR11 dominate, such as the Sargasso Sea (Carlson and Ducklow, 1996, Morris et al., 2002), photoheterotrophic light use may therefore be important in mediating the regeneration of nitrogen.

4.4.9. The importance of maintenance for carbon and nitrogen assimilation

Maintenance makes up a significant fraction of the total carbon flux when DOC and DON are limiting (Figure 4.16, 4.20). The most dominant loss term of the total nitrogen flux in SAR11 is

the fraction used to satisfy maintenance, irrespective of the degree of nutrient limitation (Figure 4.5, 4.12, 4.16, 4.20). Photoheterotrophic resource acquisition reduces the fraction of total carbon and nitrogen used for maintenance, increasing the fraction than can be used for growth. Photoheterotrophic light use is important for increasing the efficiency with which carbon and nitrogen are used by SAR11 in nutrient depleted subtropical gyre ecosystems.

The importance of resolving the maintenance requirements of bacterial cells in subtropical gyres in terms of respired carbon dioxide and BGE has been discussed in Section 4.4.7. The use of carbon and nitrogen to form maintenance biomass is also a significant constraint on growth, which photoheterotrophic light use partially relieves.

We do not have detailed knowledge on the rate of maintenance biomass turnover in SAR11 or more generally bacterial cells. The maintenance rate in the present study is based on the turnover of leucine in open ocean bacterioplankton (Hill et al., 2013). The results from the model suggest that understanding the maintenance requirements of SAR11 is a priority for more accurately modelling the influence of photoheterotrophic light use on the cells growth rate.

4.5. Summary

The aim of Chapter 4 was to investigate the influence of photoheterotrophic light use on the growth rate of SAR11 and the impact on key physiological processes involving carbon and nitrogen. The results show that photoheterotrophic light use may significantly increase the growth rate of SAR11 and may assist in allowing these cells to dominate the bacterial communities in oligotrophic subtropical gyre ecosystems. The influence of photoheterotrophic nutrient uptake on growth rate is critically dependent on the relative availability of ambient resources and the effect is only of significance when DON and DIN are limiting. Photoheterotrophy also results in higher rates of respiration and ammonium regeneration than would be expected if heterotrophic production were not influenced by solar energy. SAR11 uses a significant fraction of carbon and nitrogen for maintenance. Photoheterotrophy partially relieves this constraint on growth rate.

4.6. Tables

Table 4.1 Table detailing key processes of interest, a short description of each process, chemical forms, associated elements, units and equation references.

Key processes of interest	Description	Chemical form and associated elements	Units	Equation reference (Chapter 2)
Growth rate	Allocation of biomass to new growth	Organic containing carbon and nitrogen with a C:N of 5	mol C (mol C)$^{-1}$ d^{-1}	2.2.3.3i
Light investment	Use of harvested light energy for the acquisition of DOC and DON to maximise growth rate	-	-	2.2.1.2a, 2.2.1.2b
Dissolved organic carbon (DOC) uptake	The rate of DOC uptake, which is subject to enhancement through photoheterotrophy	Organic containing carbon only	mol C (mol C)$^{-1}$ hr^{-1}	2.2.1.3b
Dissolved organic nitrogen (DON) uptake	The rate of DON uptake, which is subject to enhancement through photoheterotrophy	Organic containing carbon and nitrogen at C:N of 4.3	mol C (mol C)$^{-1}$ hr^{-1}	2.2.1.4a
Amino acid (AA) synthesis	The rate of AA synthesis using DOC and dissolved organic nitrogen (DIN)	Organic containing carbon and nitrogen at C:N of 4.3	mol C (mol C)$^{-1}$ hr^{-1}	2.2.2k
ON (organic nitrogen) delivery to maintenance and growth	The rate that ON (sum of DON and AA) is delivered to maintenance and growth	Organic containing carbon and nitrogen at C:N of 4.3	mol C (mol C)$^{-1}$ hr^{-1}	2.2.2m
OC (organic carbon) delivery to maintenance and growth	The rate that OC (DOC remaining after AA synthesis) is delivered to maintenance and growth	Organic containing carbon only	mol C (mol C)$^{-1}$ hr^{-1}	2.2.2n
Maintenance	The synthesis of biomass for use in general cell functioning that does not contribute to new growth	Organic containing carbon and nitrogen with a C:N of 5	mol C (mol C)$^{-1}$ hr^{-1}	2.2.3.2i
Respiration at AA synthesis	The production of carbon dioxide due to costs in the synthesis of AA	Inorganic carbon	mol C (mol C)$^{-1}$ hr^{-1}	2.2.2l
Respiration at maintenance and growth	The production of carbon dioxide through costs in transport and synthesise associated with maintenance and growth	Inorganic carbon	mol C (mol C)$^{-1}$ hr^{-1}	2.2.3.2k, 2.2.3.3h
Ammonium release at maintenance and growth	Ammonium that has been released through the deamination of ON for maintenance and growth	Inorganic nitrogen	mol N (mol C)$^{-1}$ hr^{-1}	2.2.3.2j, 2.2.3.3g
Excess OC	DOC that has been taken up by the cell but is in excess to stoichiometric requirements for growth	Organic containing carbon only	mol C (mol C)$^{-1}$ hr^{-1}	2.2.3.3k
Excess ON	ON that has been taken up/synthesised by the cell but is in excess to stoichiometric requirements for growth	Organic containing carbon and nitrogen at C:N of 4.3	mol C (mol C)$^{-1}$ hr^{-1}	2.2.3.3j

Table 4.2 Ambient conditions for Experiments 1-5. (X/K) is the ratio of the ambient nutrient concentration to the nutrient's half saturation constant, explained in Section 2.3.1.

Environmental factor	Exp. 1	Exp. 2	Exp. 3	Exp. 4
Irradiance (μmols photons m^{-2} s^{-1})	0 and 500	500	500	500
DIN (X/K)	5	0-5	5	5
DON (X/K)	5	5	0-5	5
DOC (X/K)	5	5	5	0-5

4.7. Figures

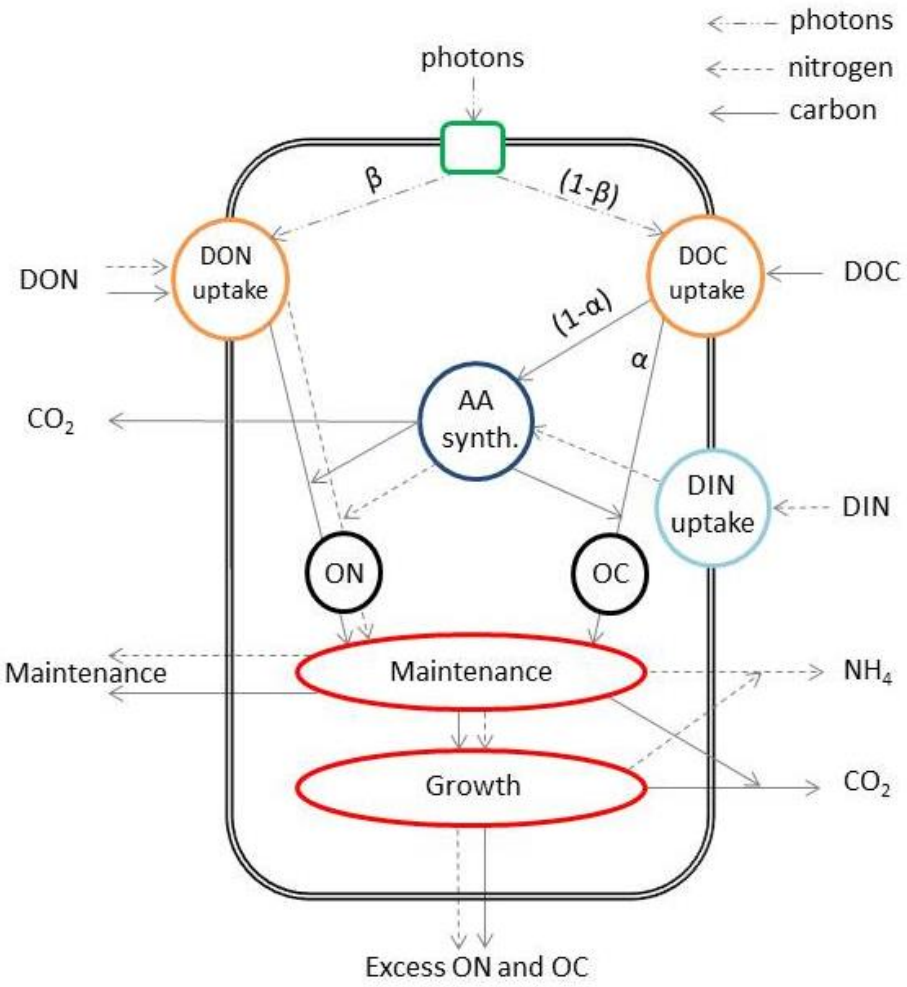

Figure 4.1 Schematic of the SAR11 model. The green square represents the proteorhodopsin light harvesting system. Harvested light energy is partitioned between photoheterotrophic DON and DOC uptake (orange circles) using the parameter β. DOC is partitioned between amino acid (AA) synthesis (dark blue circle) and maintenance and growth (red circles) using the parameter α. DIN is taken up (light blue circle) and bound DOC to synthesise AA (dark blue circle) which is added to the flux of DON. The organic nitrogen (ON) (sum of DON and AA) and organic carbon (OC) (DOC remaining after AA synthesis) fluxes (black circles) are available for the cell to satisfy maintenance as a priority and then growth (red circles). Carbon dioxide is respired at AA synthesis and maintenance and growth. Ammonium is released at maintenance and growth. Maintenance biomass is excreted from the cell along with ON and OC that are in excess to stoichiometric requirements for growth.

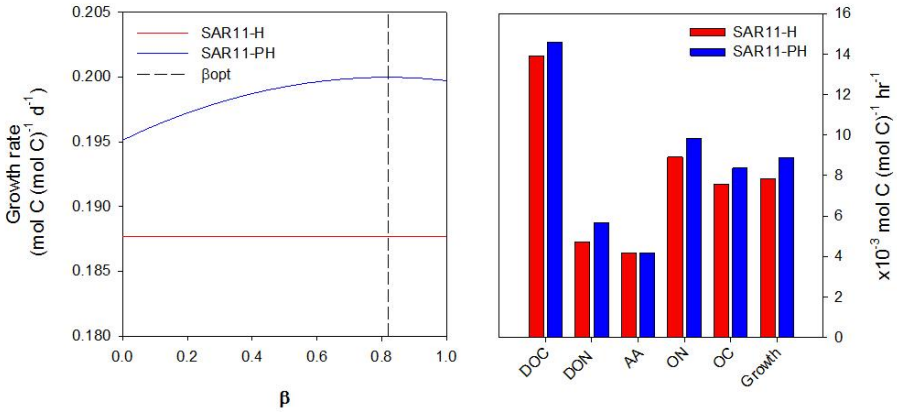

Figure 4.2 The variation of SAR11-PH growth rate with β and the growth rate of SAR11-H per day (left). The vertical dashed line shows the position of β_{opt}.The uptake of carbon and nitrogen and growth rate of Pro-PA and Pro-PH per hour at β_{opt} (right).

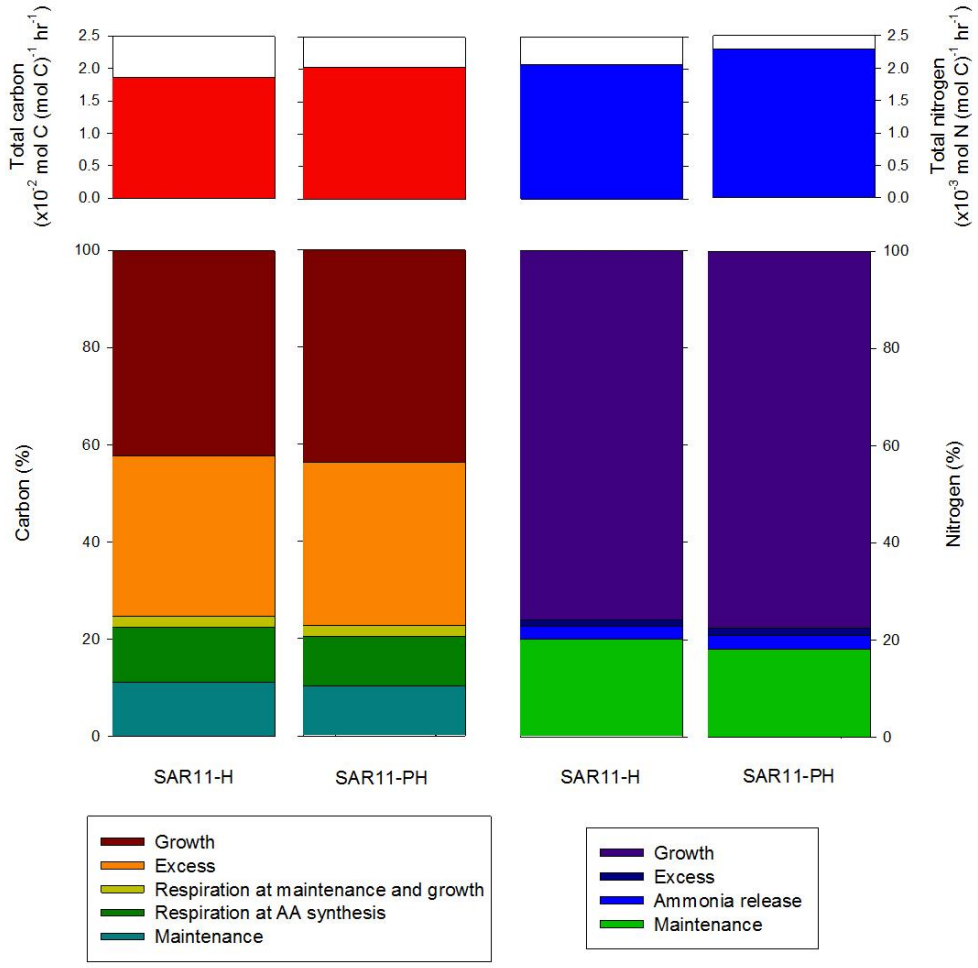

Figure 4.3 The total (top) and fate of (bottom) of carbon (left) and nitrogen (right) in SAR11-H and SAR11-PH at β_{opt}. Processes are specified in the keys at the bottom of each figure. M and G represent maintenance and growth, respectively.

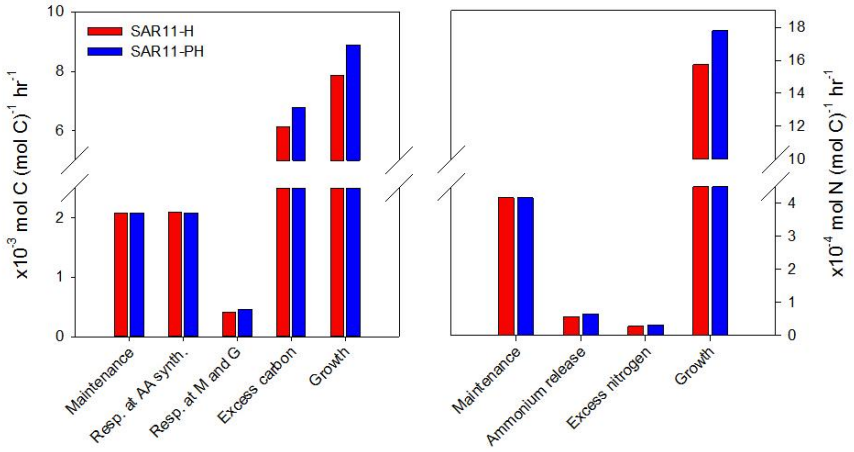

Figure 4.4 The fate of carbon (left) and nitrogen (right) for SAR11-H and SAR11-PH at β_{opt}. M and G represent maintenance and growth, respectively.

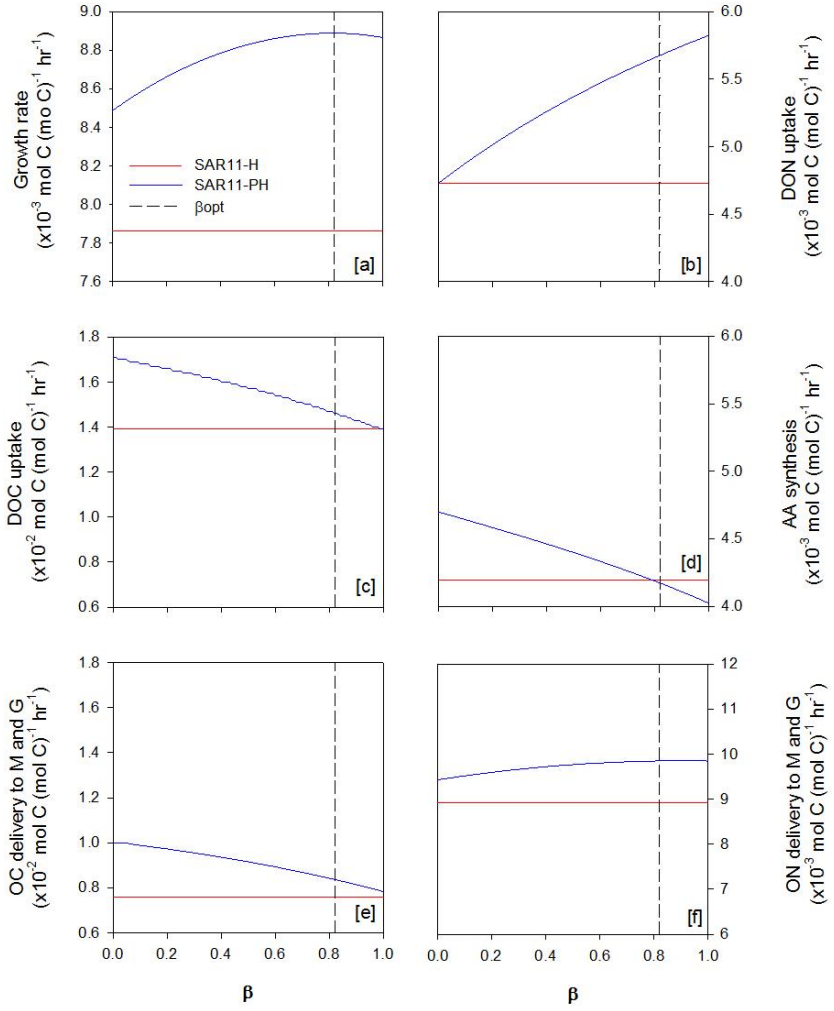

Figure 4.5 The rate of growth (a) and uptake of carbon and nitrogen (b-f) for SAR11-H and SAR11-PH with β. The vertical dashed line shows the position of β_{opt}. M and G represent maintenance and growth, respectively.

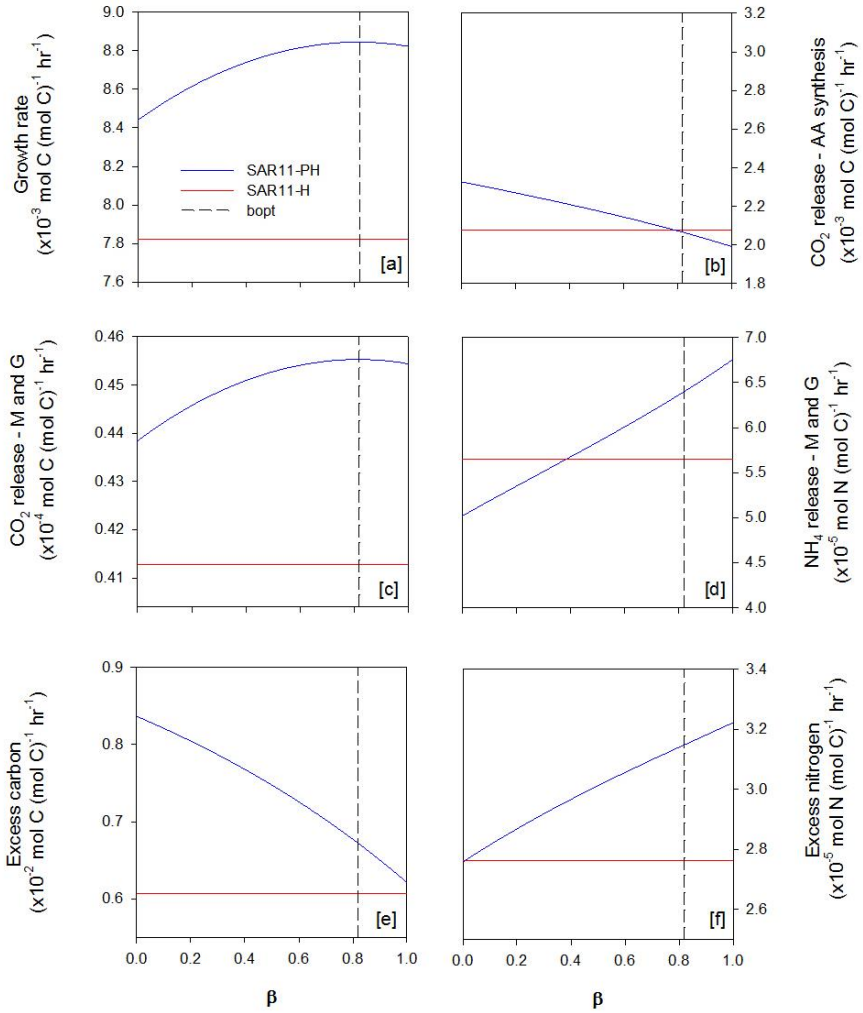

Figure 4.6 The growth rate (a) and fate of carbon and nitrogen (b-f) for SAR11-H and SAR11-PH with β. The vertical dashed line shows the position of β_{opt}. M and G represent maintenance and growth, respectively.

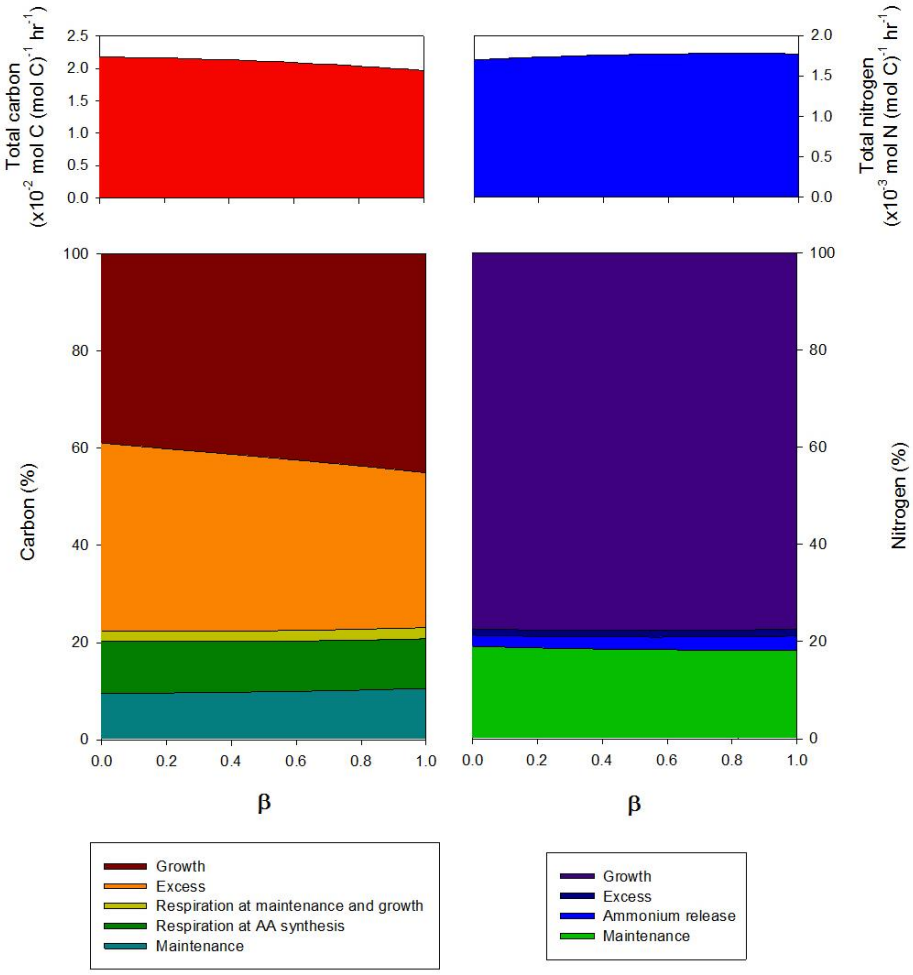

Figure 4.7 The total (top) and fate of (bottom) of carbon (left) and nitrogen (right) in SAR11-H and SAR11-PH with β. Processes are specified in the keys at the bottom of the figure.

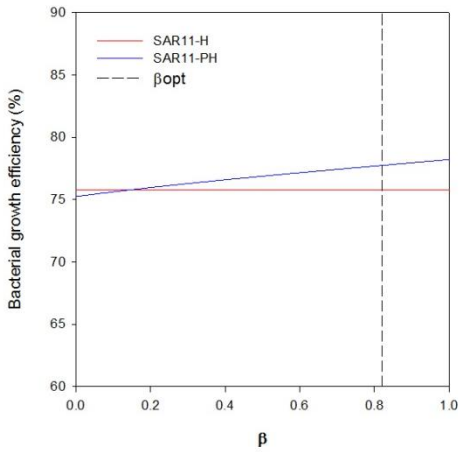

Figure 4.8 Bacterial growth efficiency of SAR11-H and SAR11-PH with β. The vertical dashed line shows the position of β_{opt}.

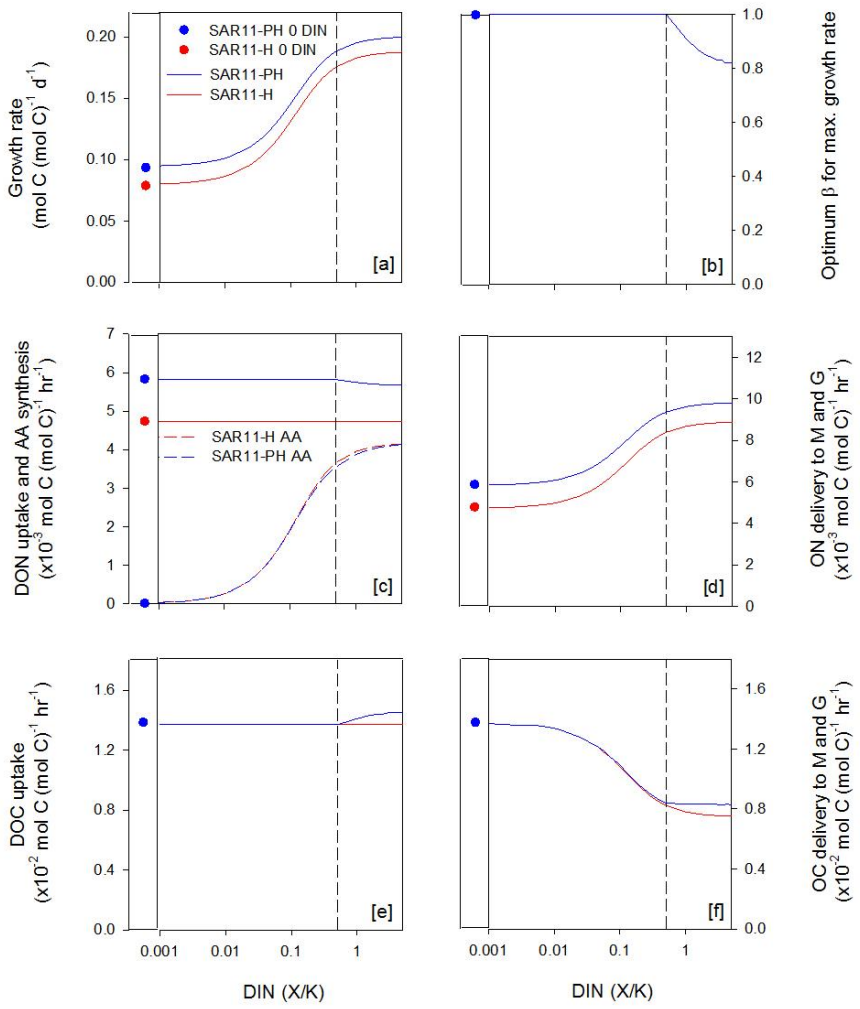

Figure 4.9 The change in growth rate (a), β_{opt} (b), and uptake of carbon and nitrogen (c-f) at multiple ambient DIN (X/K) for SAR11-H and SAR11-PH-PH at β_{opt}.The vertical dashed line corresponds to ambient maximum DIN where β_{opt} = 1. The vertical solid line separates DIN equals zero (X/K). M and G represent maintenance and growth, respectively.

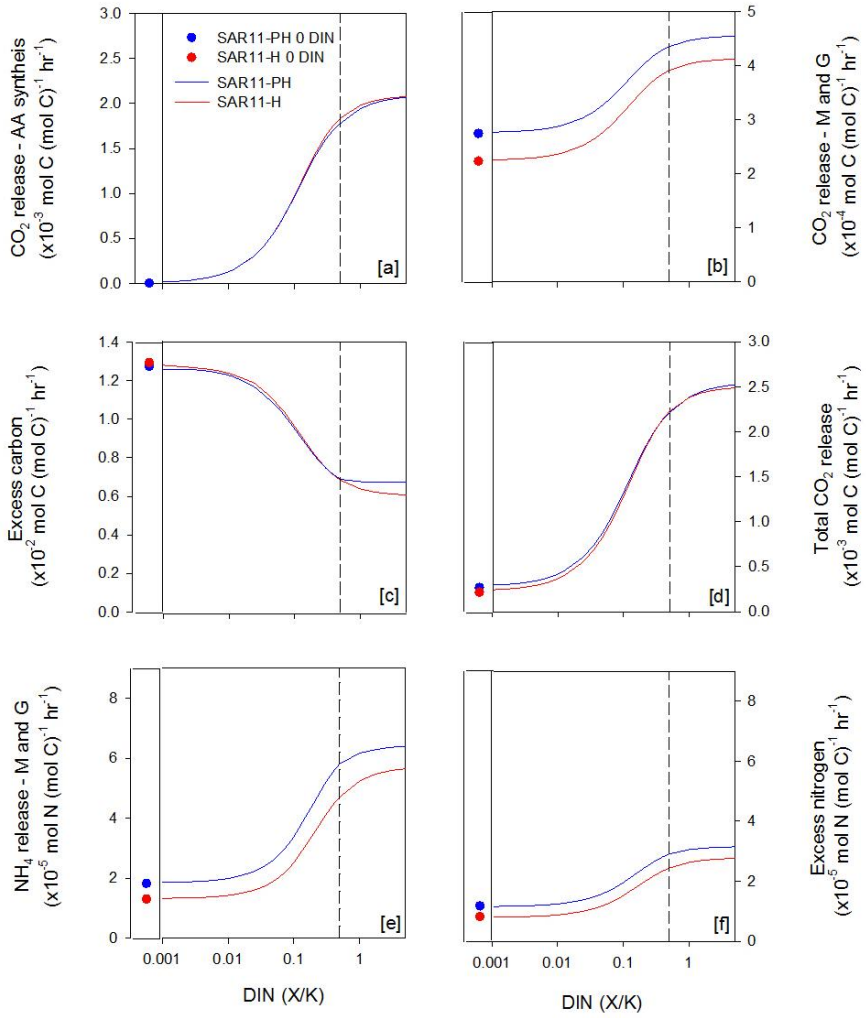

Figure 4.10 The fate of carbon (a-d) and nitrogen (e and f) at multiple ambient DIN (X/K) for SAR11-H and SAR11-PH at β_{opt}. The vertical dashed line corresponds to the maximum ambient DIN where β_{opt} = 1. The vertical solid line separates DIN equals zero (X/K). M and G represent maintenance and growth, respectively.

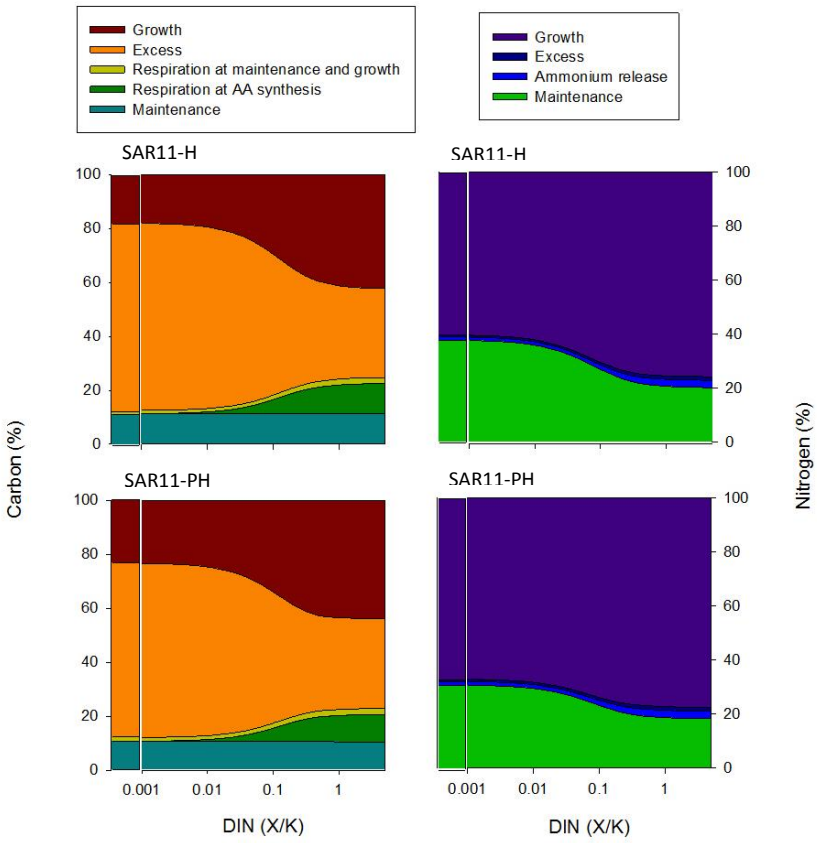

Figure 4.11 Carbon (left) and nitrogen (right) metabolic fluxes at multiple ambient DIN (X/K). for SAR11-H (top) and SAR11-PH (bottom). The vertical solid line separates data at zero DIN (X/K).

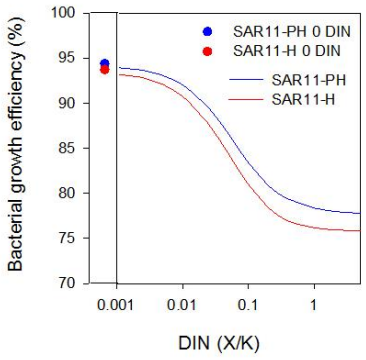

Figure 4.12 Bacterial growth efficiency of SAR11-H and SAR11-PH. The vertical solid line separates DIN equals zero (X/K).

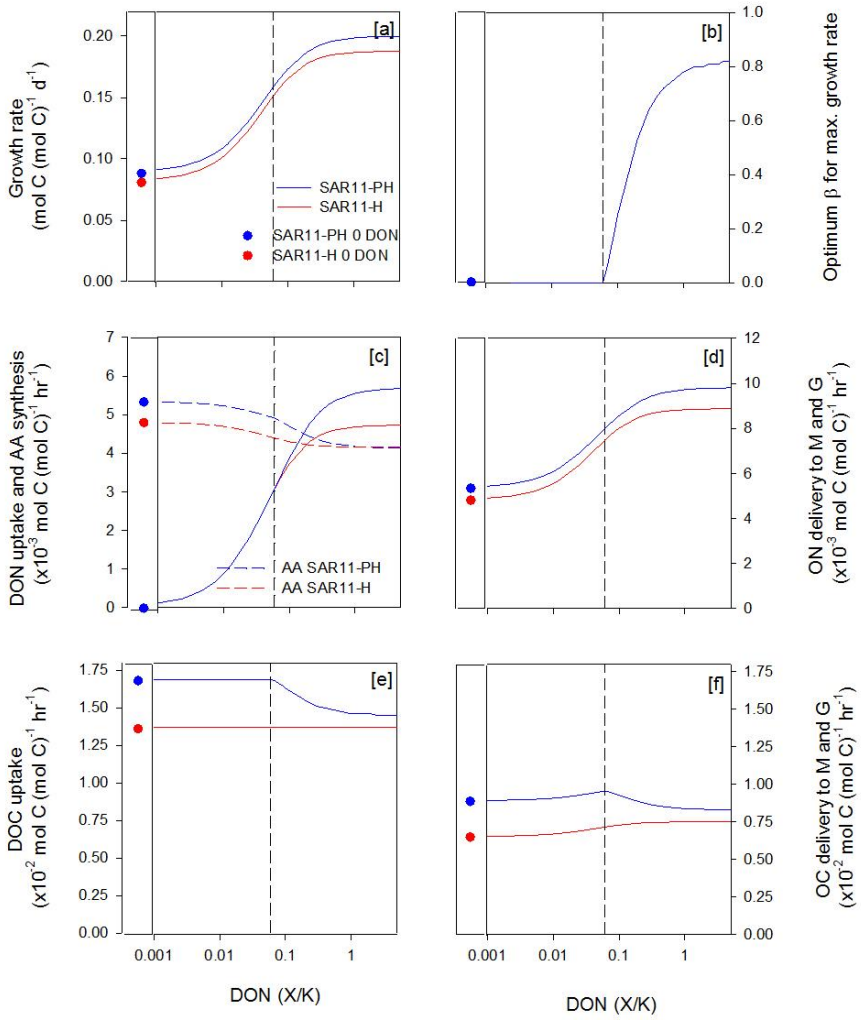

Figure 4.13 The change in growth rate (a), β_{opt} (b), and uptake of carbon and nitrogen (c-f) at multiple ambient DON (X/K) for SAR11-H and SAR11-PH at β_{opt}.The vertical dashed line corresponds to ambient maximum DON where $\beta_{o\square t}$ = 1. The vertical solid line separates DON equals zero (X/K). M and G represent maintenance and growth, respectively.

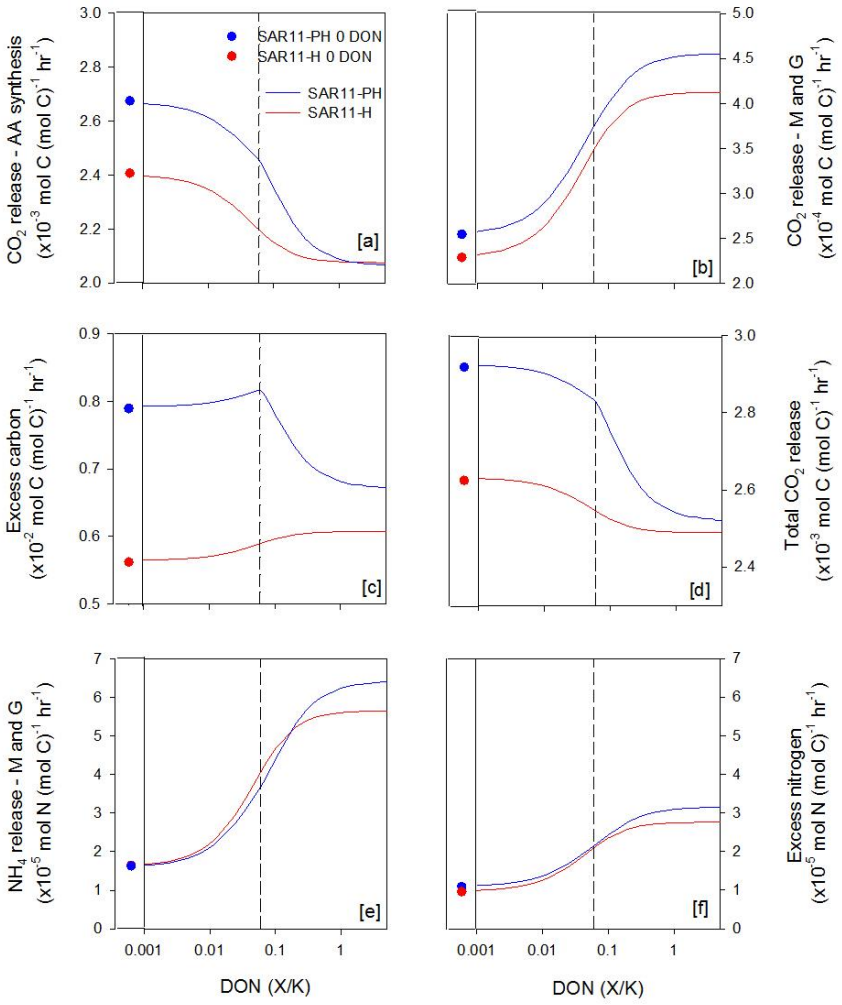

Figure 4.14 The fate of carbon (a-d) and nitrogen (e-f) at multiple ambient DON (X/K) for SAR11-H and SAR11-PH at β_{opt}. The vertical dashed line corresponds to the maximum concentration of DON where β_{opt} = 1. The vertical solid line separates DON equals zero (X/K). M and G represent maintenance and growth, respectively.

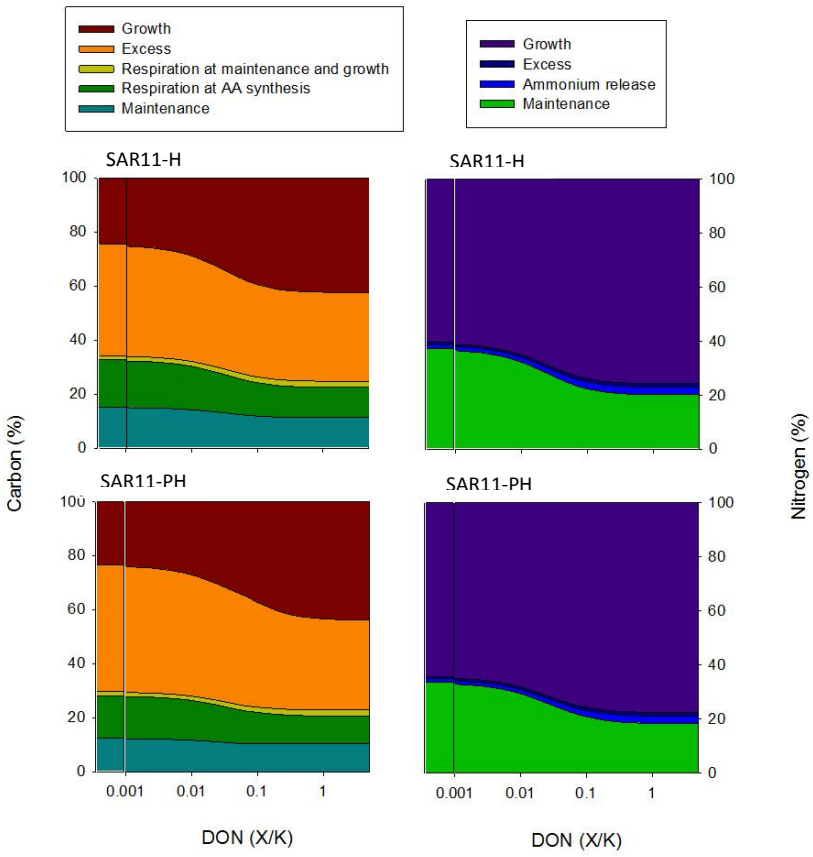

Figure 4.15 Carbon (left) and nitrogen (right) metabolic fluxes at multiple ambient DON (X/K) for SAR11-H (top) and SAR11-PH (bottom). The vertical solid line separates data at zero DON (X/K).

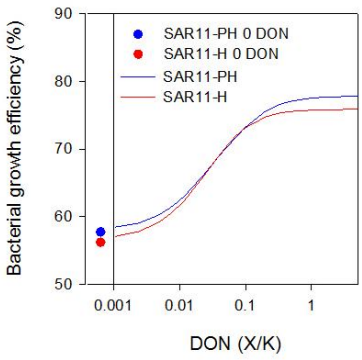

Figure 4.16 Bacterial growth efficiency for SAR11-H and SAR11-PH. The vertical solid line separates DON equals zero (X/K).

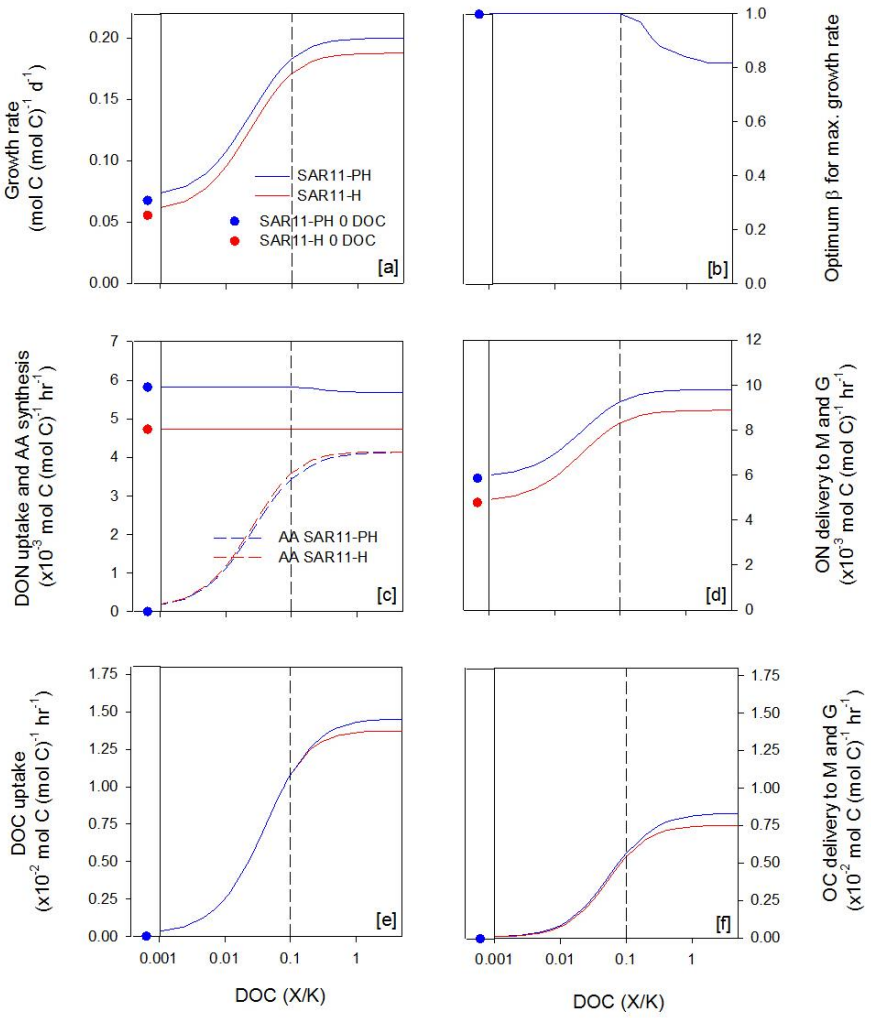

Figure 4.17 The change in growth rate (a), β_{opt} (b), and uptake of carbon and nitrogen (c-f) at multiple ambient DOC (X/K) for SAR11-H and SAR11-PH-PH at β_{opt}.The vertical dashed line corresponds to ambient maximum DOC where β_{opt} = 1. The vertical solid line separates DOC equals zero (X/K). M and G represent maintenance and growth, respectively.

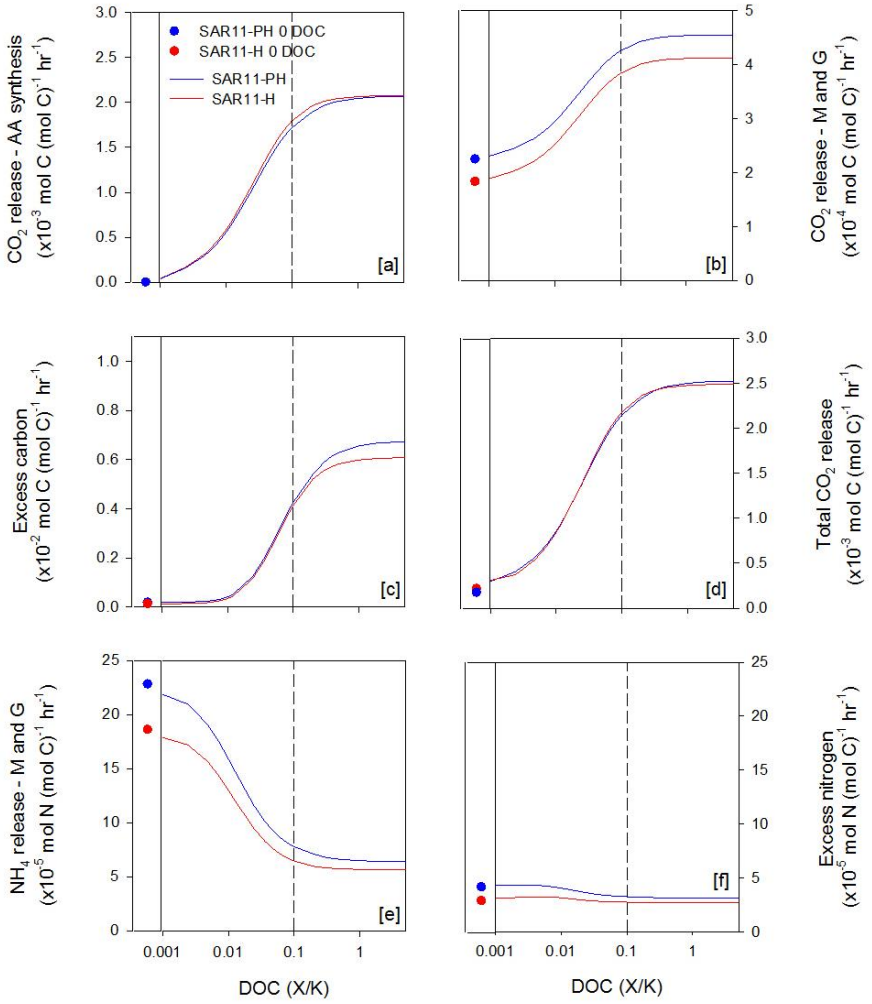

Figure 4.18 The fate of carbon (a-d) and nitrogen (e-f) at multiple ambient DOC (X/K) for SAR11-H and SAR11-PH at β_{opt}. The vertical dashed line corresponds to the maximum concentration of DOC where β_{opt} = 1. The vertical solid line separates DOC equals zero (X/K). M and G represent maintenance and growth, respectively.

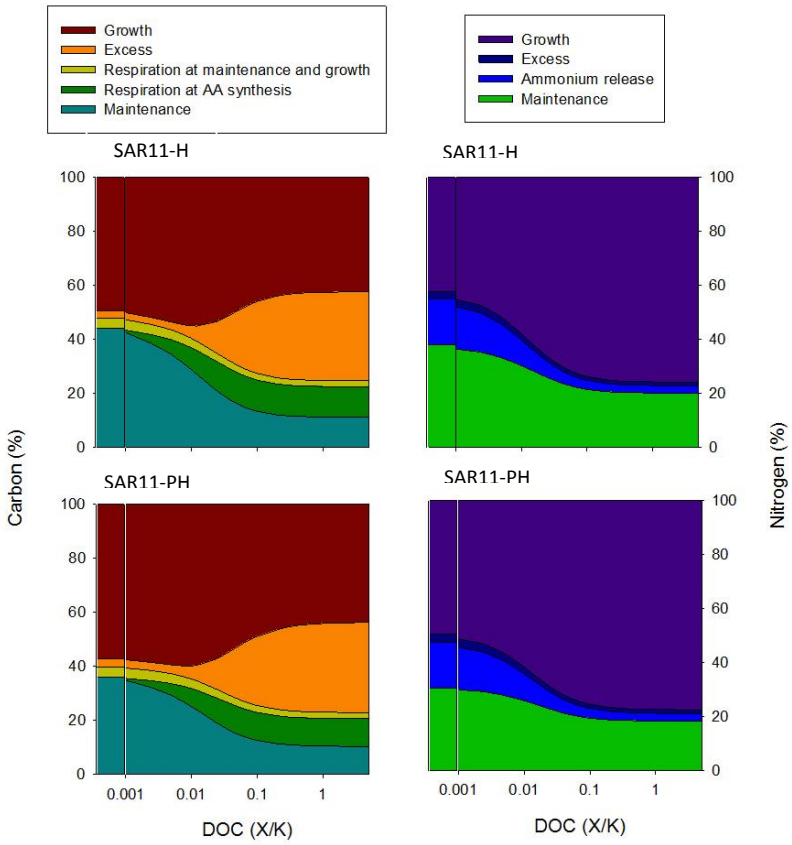

Figure 4.19 Carbon (left) and nitrogen (right) metabolic fluxes at multiple ambient DOC (X/K) for SAR11-H (top) and SAR11-PH (bottom). The vertical solid line separates data at zero DOC (X/K).

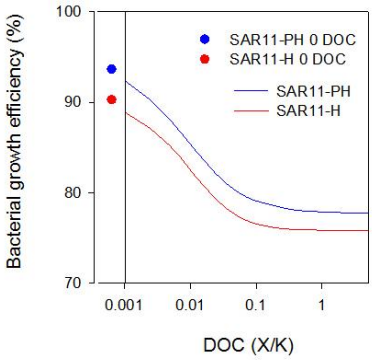

Figure 4.20 Bacterial growth efficiency for SAR11-H and SAR11-PH. The vertical solid line separates DOC equals zero (X/K).

4.8. Appendix Tables

Appendix Table 4. 1 Sensitivity analysis for SAR11-PH at β_{opt} in non-limiting conditions (Experiment 1). – and + for each parameter corresponds to a -20 % or +20 % change in each parameter.

Para.	Growth rate	BGE	Excess carbon	Excess nitrogen	NH_4 release M and G	CO_2 release AA	CO_2 release M and G	AA synth.	DON uptake	CHO synth.
DIN half sat.-	0.00	0.00	0.01	-0.01	-0.01	-0.01	0.00	-0.01	0.00	0.00
DIN half sat.+	-0.01	0.00	0.01	-0.01	-0.01	-0.01	0.00	-0.01	0.00	0.00
DOC half sat.-	0.00	0.00	0.00	0.00	0.00	0.00	0.00	0.00	0.00	0.00
DOC half sat.+	0.00	0.00	0.00	0.00	0.00	0.00	0.00	0.00	0.00	0.00
DON half sat.-	0.00	0.00	0.00	0.00	0.00	0.00	0.00	0.00	0.00	0.00
DON half sat.+	0.00	0.00	0.00	0.00	0.00	0.00	0.00	0.00	0.00	0.00
Light half sat.-	-0.12	-0.04	-0.25	-0.23	-0.20	-0.01	-0.19	-0.01	-0.32	-0.14
Light half sat.+	-0.10	-0.04	-0.18	-0.20	-0.18	0.00	-0.16	0.00	-0.28	-0.10
Flux ratio -	-0.13	-0.01	-0.24	-0.09	-0.03	-0.05	-0.10	-0.05	-0.14	-0.14
Flux ratio +	-0.09	-0.01	-0.16	-0.06	-0.02	-0.04	-0.07	-0.04	-0.09	-0.10
Max. DIN -	0.04	-0.01	-0.08	0.08	0.11	0.08	0.03	0.08	0.00	0.00
Max. DIN +	0.02	0.00	-0.05	0.04	0.07	0.05	0.02	0.05	0.00	0.00
Max. DOC -	0.39	-0.05	1.50	-0.09	-0.70	0.62	0.30	0.62	0.00	1.00
Max. DOC +	0.32	-0.03	1.61	-0.05	-0.52	0.53	0.25	0.53	0.00	1.00
Max. DON -	0.63	0.15	-0.03	0.84	1.00	-0.09	0.52	-0.09	1.00	0.00
Max. DON +	0.63	0.12	-0.03	0.89	1.08	-0.09	0.52	-0.09	1.00	0.00
Max. AA-	0.25	-0.05	-0.51	0.46	0.65	0.51	0.20	0.51	0.00	0.00
Max. AA+	0.21	-0.04	-0.42	0.42	0.62	0.42	0.16	0.42	0.00	0.00
AA synth. eff -	0.35	0.52	0.38	0.31	0.24	-2.70	0.26	0.62	0.00	0.00
AA synth. eff +	0.29	0.48	0.31	0.26	0.21	-2.26	0.22	0.53	0.00	0.00
C:N ON -	-0.81	-0.14	1.13	-2.24	-19.11	0.08	-0.64	0.08	0.00	0.00
C:N ON +	-0.84	-0.19	1.19	-2.06	-4.98	0.05	-0.67	0.05	0.00	0.00
C:N X+	0.70	0.12	-1.01	1.95	11.53	0.00	0.56	0.00	0.00	0.00
ON eff. -	0.17	0.17	0.00	0.04	-4.81	0.00	-3.35	0.00	0.00	0.00
OC eff. -	0.22	0.80	1.23	-2.02	-4.92	0.00	-21.40	0.00	0.00	0.00
Maintenance -	-0.24	-0.05	-0.01	-0.30	-0.16	0.00	0.01	0.00	0.00	0.00
Maintenance +	-0.24	-0.05	-0.01	-0.29	-0.15	0.00	0.01	0.00	0.00	0.00

Appendix Table 4. 2 Sensitivity analysis for SAR11-PH at β_{opt} in DIN-limiting conditions (Experiment 2). – and + for each parameter corresponds to a -20 % or +20 % change in each parameter.

Para.	Growth rate	BGE	Excess carbon	Excess nitrogen	NH_4 release M and G	CO_2 release AA	CO_2 release M and G	AA synth.	DON uptake	CHO synth.
DIN half sat.-	-	-	-	-	-	-	-	-	-	-
DIN half sat.+	-	-	-	-	-	-	-	-	-	-
DOC half sat.-	0.00	0.00	0.00	0.00	0.00	-	0.00	-	0.00	0.00
DOC half sat.+	0.00	0.00	0.00	0.00	0.00	-	0.00	-	0.00	0.00
DON half sat.-	0.00	0.00	0.00	-0.01	-0.01	-	0.00	-	0.00	0.00
DON half sat.+	0.00	0.00	0.00	-0.01	-0.01	-	0.00	-	0.00	0.00
Light half sat.-	-0.28	-0.01	0.03	-0.59	-0.59	-	-0.33	-	-0.34	0.00
Light half sat.+	-0.25	-0.01	0.03	-0.51	-0.49	-	-0.29	-	-0.30	0.00
Flux ratio -	-0.21	0.00	-0.15	-0.20	-0.12	-	-0.13	-	-0.13	-0.15
Flux ratio +	-0.15	0.00	-0.10	-0.14	-0.08	-	-0.09	-	-0.09	-0.10
Max. DIN -	0.00	0.00	0.00	0.00	0.00	-	0.00	-	0.00	0.00
Max. DIN +	0.00	0.00	0.00	0.00	0.00	-	0.00	-	0.00	0.00
Max. DOC -	0.02	0.00	1.08	-0.22	-0.92	-	0.01	-	0.00	1.00
Max. DOC +	0.01	0.00	1.08	-0.15	-0.63	-	0.01	-	0.00	1.00
Max. DON -	1.51	0.04	-0.08	1.64	1.50	-	0.99	-	1.00	0.00
Max. DON +	1.50	0.02	-0.08	1.78	1.86	-	0.98	-	1.00	0.00
Max. AA-	-	-	-	-	-	-	-	-	-	-
Max. AA+	-	-	-	-	-	-	-	-	-	-
AA synth. eff -	-	-	-	-	-	-	-	-	-	-
AA synth. eff +	-	-	-	-	-	-	-	-	-	-
C:N ON -	-1.52	-0.02	0.54	-1.81	-19.81	-	-0.97	-	0.00	0.00
C:N ON +	-1.18	-0.03	0.42	-1.24	-4.95	-	-0.77	-	0.00	0.00
C:N X+	1.24	0.02	-0.44	1.46	11.48	-	0.79	-	0.00	0.00
ON eff. -	0.10	0.10	0.00	0.07	-5.16	-	-1.65	-	0.00	0.00
OC eff. -	0.11	1.19	0.54	-1.19	-4.98	-	-26.57	-	0.00	0.00
Maintenance -	-0.52	-0.02	0.00	-0.54	0.03	-	0.00	-	0.00	0.00
Maintenance +	-0.53	-0.03	0.00	-0.53	0.05	-	0.00	-	0.00	0.00

Appendix Table 4. 3 Sensitivity analysis for SAR11-PH at β_{opt} in DON-limiting conditions (Experiment 3). – and + for each parameter corresponds to a -20 % or +20 % change in each parameter.

Para.	Growth rate	BGE	Excess carbon	Excess nitrogen	NH_4 release M and G	CO_2 release AA	CO_2 release M and G	AA synth.	DON uptake	CHO synth.
DIN half sat.-	-0.02	0.00	0.02	-0.04	-0.05	-0.02	-0.02	-0.02	-	0.00
DIN half sat.+	-0.02	0.00	0.02	-0.04	-0.05	-0.02	-0.02	-0.02	-	0.00
DOC half sat.-	0.00	0.00	-0.01	0.00	0.00	0.00	0.00	0.00	-	0.00
DOC half sat.+	0.00	0.00	-0.01	0.00	0.00	0.00	0.00	0.00	-	0.00
DON half sat.-	-	-	-	-	-	-	-	-	-	-
DON half sat.+	-	-	-	-	-	-	-	-	-	-
Light half sat.-	-0.13	-0.03	-0.54	-0.18	0.04	-0.16	-0.16	-0.16	-	-0.34
Light half sat.+	-0.12	-0.03	-0.47	-0.17	0.03	-0.15	-0.15	-0.15	-	-0.30
Flux ratio -	-0.11	-0.01	-0.21	-0.07	0.01	-0.06	-0.06	-0.06	-	-0.13
Flux ratio +	-0.08	-0.01	-0.15	-0.05	0.01	-0.04	-0.05	-0.04	-	-0.09
Max. DIN -	0.19	0.03	-0.15	0.27	0.39	0.14	0.13	0.14	-	0.00
Max. DIN +	0.11	0.02	-0.09	0.17	0.26	0.08	0.08	0.08	-	0.00
Max. DOC -	0.88	0.14	1.53	0.64	-0.05	0.54	0.54	0.54	-	1.00
Max. DOC +	0.73	0.09	1.64	0.48	-0.12	0.43	0.44	0.43	-	1.00
Max. DON -	0.07	0.01	-0.05	0.10	0.13	0.05	0.05	0.05	-	0.00
Max. DON +	0.06	0.01	-0.05	0.09	0.12	0.04	0.04	0.04	-	0.00
Max. AA-	0.61	0.09	-0.47	0.81	1.04	0.42	0.40	0.42	-	0.00
Max. AA+	0.48	0.06	-0.38	0.72	1.03	0.34	0.32	0.34	-	0.00
AA synth. eff -	0.86	1.25	0.52	0.86	0.75	-2.85	0.53	0.54	-	0.00
AA synth. eff +	0.71	1.26	0.42	0.71	0.63	-2.31	0.43	0.43	-	0.00
C:N ON -	-1.25	-0.47	0.61	-1.90	-20.64	0.14	-0.80	0.14	-	0.00
C:N ON +	-1.10	-0.51	0.54	-1.43	-4.94	0.08	-0.70	0.08	-	0.00
C:N X+	1.19	0.41	-0.63	1.87	13.18	0.00	0.78	0.00	-	0.00
ON eff. -	0.11	0.10	0.00	0.05	-5.20	0.00	-1.54	0.00	-	0.00
OC eff. -	0.15	0.87	0.80	-1.52	-5.68	0.00	-26.53	0.00	-	0.00
Maintenance -	-0.54	-0.20	0.00	-0.63	-0.38	0.00	0.01	0.00	-	0.00
Maintenance +	-0.55	-0.22	0.00	-0.61	-0.33	0.00	0.01	0.00	-	0.00

Appendix Table 4. 4 Sensitivity analysis for SAR11-PH at β_{opt} in DOC-limiting conditions (Experiment 4). – and + for each parameter corresponds to a -20 % or +20 % change in each parameter.

Para.	Growth rate	BGE	Excess carbon	Excess nitrogen	NH_4 release M and G	CO_2 release AA	CO_2 release M and G	AA synth.	DON uptake	CHO synth.
DIN half sat.-	-	-	-	-	-	-	-	-	-	-
DIN half sat.+	-	-	-	-	-	-	-	-	-	-
DOC half sat.-	-	-	-	-	-	-	-	-	-	-
DOC half sat.+	-	-	-	-	-	-	-	-	-	-
DON half sat.-	0.00	0.00	0.02	-0.01	0.00	-	0.00	-	0.00	-
DON half sat.+	0.00	0.00	0.02	-0.01	0.00	-	0.00	-	0.00	-
Light half sat.-	-0.32	-0.01	1.48	-0.54	-0.33	-	-0.33	-	-0.34	-
Light half sat.+	-0.28	-0.01	1.76	-0.48	-0.30	-	-0.29	-	-0.30	-
Flux ratio -	-0.24	0.00	0.64	-0.21	-0.13	-	-0.13	-	-0.13	-
Flux ratio +	-0.16	0.00	0.49	-0.15	-0.09	-	-0.09	-	-0.09	-
Max. DIN -	0.00	0.00	0.00	0.00	0.00	-	0.00	-	0.00	-
Max. DIN +	0.00	0.00	0.00	0.00	0.00	-	0.00	-	0.00	-
Max. DOC -	-	-	-	-	-	-	-	-	-	-
Max. DOC +	-	-	-	-	-	-	-	-	-	-
Max. DON -	1.69	0.06	-8.02	1.61	0.99	-	0.98	-	1.00	-
Max. DON +	1.70	0.03	-3.27	1.60	0.98	-	0.98	-	1.00	-
Max. AA-	-	-	-	-	-	-	-	-	-	-
Max. AA+	-	-	-	-	-	-	-	-	-	-
AA synth. eff -	-	-	-	-	-	-	-	-	-	-
AA synth. eff +	-	-	-	-	-	-	-	-	-	-
C:N ON -	0.00	0.00	0.75	0.00	-7.17	-	0.00	-	0.00	-
C:N ON +	0.00	0.00	-4.55	-0.01	-4.78	-	0.00	-	0.00	-
C:N X+	0.00	0.00	-0.37	0.00	3.95	-	0.00	-	0.00	-
ON eff. -	1.69	1.62	-2.95	0.75	-4.78	-	-4.10	-	0.00	-
OC eff. -	0.00	0.00	-7.17	0.00	0.00	-	-0.04	-	0.00	-
Maintenance -	-0.70	-0.03	1.61	-0.60	0.02	-	0.02	-	0.00	-
Maintenance +	-0.70	-0.04	2.26	-0.60	0.02	-	0.02	-	0.00	-

Chapter 5: Understanding the different physiologies of *Prochlorococcus* and SAR11: a theoretical morphosis of two models

5.1 Introduction

Prochlorococcus (Pro) and SAR11 coexist in near equal abundances in the oligotrophic subtropical gyres of the Atlantic Ocean. Ecologically their niches overlap, competing for similar resources (Gómez-Pereira et al., 2012, Mary et al., 2008b). Both however maintain certain distinct physiological strategies.

It is assumed here that coexistence occurs if Pro and SAR11 grow at the same specific rate, i.e. both cells have the same division interval of 0.20 d^{-1}. This is in accordance with ranges observed in the field (Goericke and Welschmeyer, 1993, Malmstrom et al., 2005). Other forcing agents such as viral lysis and predation are therefore assumed to affect Pro and SAR11 equally. Pro and SAR11 are both subject to viral lysis (Sullivan et al., 2003, Zhao et al., 2013) and predation (Hartmann et al., 2013). The relative rates of influence are however yet to be established.

The aim of this chapter is to investigate the dissimilar aspects of Pro and SAR11 physiology and metabolism and their influence on specific growth rate, and how differences balance to result in equal specific rates of growth. The results from Chapters 3 and 4 are also evaluated in order to understand the importance of photoheterotrophy for Pro and SAR11 growth rate relative to the other traits investigated.

Models describing the physiology and metabolism of Pro and SAR11 have been built, parameterised and investigated separately in Chapters 2, 3 and 4. Both are constrained to grow at the same specific rate. In order to address this chapter's aim, a theoretical morphosis of the models will be undertaken. The model parameterised for an individual Pro cell will be 'morphed' in a stepwise fashion into the model of an individual SAR11 cell in order to understand the relative contribution of physiological differences in influencing growth rate. Ambient conditions are taken to be non-limiting, identical to Experiment 1 for Pro (Section 3.2.1) and SAR11 (Section 4.2.1). Each stage of the theoretical morphosis is therefore used to test the relative effect of each Pro and SAR11 physiological trait of growth rate.

More specifically, the following physiological characteristics will be studied:

- Cell size and shape
- Carbon acquisition: photoautotrophy versus photoheterotrophy
- Elemental composition of biomass (C:N)
- Light harvesting physiology
- Diurnal and nocturnal growth

Starting with a model of Pro, these physiological properties will be changed one-by-one in the order given above to eventually match that of SAR11. This method provides a means of exploring how physiological differences balance to give comparable specific growth rates. These properties have been chosen for the following reasons.

5.1.1. Cell size and shape: nutrient uptake and photosynthetic rates

In an individual cell uptake processes occur across the cell membrane and are used to satisfy maintenance and growth related processes for the whole cell. Uptake depends on surface area (SA) and maintenance and growth are proportional to cell volume (V). It is assumed that surface area related processes (e.g. uptake) are proportional to L^2, whereas volume related processes (e.g. maintenance) are proportional to L^3, where L is the equivalent spherical diameter.

A cell's size and shape can both influence SA:V and may be important competitive traits at low nutrient concentrations, as in oligotrophic gyres. For small cells, the smaller nutrient fluxes through the membrane required to create a given fraction of the cell volume, increases the utility of low concentrations of nutrients to smaller relative to larger cells (Raven, 1998). Resources can therefore be acquired and used for metabolism and growth more effectively in smaller cells (Raven, 1998). Pro are spherical to first order (Partensky et al., 1999). SAR11 are cylindrical and roughly one eighth of the volume of Pro (Rappé et al., 2002). Both the size and shape difference between Pro and SAR11 may therefore be critical in governing the uptake and synthesis of substrates, ultimately influencing the specific rate of growth.

The rate of photosynthetic carbon reduction in single cells may also vary with cell size (Finkel et al., 2009). Theoretically, smaller cells with a greater SA:V may have a higher specific photosynthetic rate. An artefact of pigment organisation in photosynthetic cells called the "package effect" means smaller cells have reduced resource costs for harvesting photons and

transformation into chemical energy than larger cells (Raven, 1998). SA:V based scaling is therefore assumed for the photosynthetic rate in Pro too. The method through which size and shape differences are applied in the model is provided in Section 5.2.1.

5.1.2. Carbon acquisition: photoautotrophy versus photoheterotrophy

The physiological strategies for acquiring organic carbon for energy and biomass synthesis are different for Pro and SAR11. Pro can synthesise carbohydrate (CHO) via photosynthetic (photoautotrophic) carbon reduction (Partensky et al., 1999). SAR11 cannot reduce carbon but can uptake reduced carbon forms from the environment as dissolved organic carbon (DOC) (Schwalbach et al., 2010). The maximum rate of photosynthetic carbon fixation per hour in Pro is approximately three times greater than the maximum rate of photoheterotrophic DOC uptake in SAR11 (Section 2.3.1.6). The availability of organic carbon relative to sources of nitrogen may influence the stoichiometry of biomass synthesis (Goldman and Dennett, 1991, Goldman et al., 1987, Goldman and Dennett, 2000), which has been demonstrated for Pro and SAR11 in Chapters 3 and 4. Differences in the rate and manner of carbon acquisition may therefore also influence the specific growth rate. The method through which the difference in carbon acquisition strategy is implemented is given in Section 5.2.2.

5.1.3. The elemental content of biomass (C:N)

The elemental content of biomass defines the relative quantity of carbon and nitrogen (C:N) in synthesised biomass both for maintenance turnover and new growth. The C:N of Pro (9.2) is almost twice that of SAR11 (5.0) (Section 2.3.2). As a consequence, SAR11 requires a greater quantity of nitrogen for every mole of carbon biomass synthesised than Pro. As Pro and SAR11 uptake dissolved organic nitrogen (DON) and dissolved inorganic nitrogen (DIN) at rates which may scale with differences in SA:V, and acquire carbon (CHO/DOC) at different rates, the net requirement of carbon and nitrogen (C:N) for synthesis using these substrates may influence the specific rate of growth. The method through which the difference in structural C:N is applied in the model is given in Section 5.2.3.

5.1.4. Light harvesting physiology

Resource acquisition in Pro and SAR11 is both facilitated (photoautotrophy in Pro) and enhanced (photoheterotrophy in Pro and SAR11) through phototrophy, which is therefore dependent on the cell's light harvesting system. Pro harvest solar energy primarily using derivatives of chlorophyll a and b (divinyl chlorophyll-a and chlorophyll-b, referred to from here-on-in as chl-a) (Partensky et al., 1999), whereas SAR11 uses a proteorhodopsin (PR)

proton pump (Giovannoni et al., 2005a). The light harvesting dynamics (electron turnover) of these two pigment types when fitted to a Michaelis-Menten model show dramatically different half saturation constants. The difference in light harvesting physiology may therefore be an important factor in influencing the specific growth rate. The method through which the difference in light harvesting system is applied in the model is given in Section 5.2.4.

5.1.5. Diurnal and nocturnal growth

Pro are considered to grow during the diurnal period only (Zubkov, 2014). Due to their small size the cells have minimal storage capacity for photosynthetically generated CHO (Maranon et al., 2013) which they depend upon entirely for growth as obligate photoautotrophs (Partensky et al., 1999). SAR11 can grow in both light and dark conditions, using harvested solar energy as facultative photoheterotrophs only. The method through which diel patterns of growth are incorporated into the model is given in Section 5.2.5.

5.2. Method

Starting with the Pro model, the physiological differences will be incorporated step-by-step, with the theoretical morphosis ending with the SAR11 model. Each step is therefore part of a cumulative process, keeping the changes implemented in the previous steps. For each step, growth rate will be analysed at the optimum light investment for maximum growth rate (β_{opt}), in accordance with the assumption that an organism will optimally balance its use of resources to maximise growth rate, also assumed in Chapters 3 and 4. Suboptimum dynamics are not evaluated. The following sections will describe how the theoretical morphosis will be applied. The reasons for the chosen order of the morphosis will be given in Section 5.2.6.

5.2.1. Cell size and shape

The first step incorporates the size difference only and converts a Pro cell to a spherical cell with the volume of SAR11, based on that of its equivalent spherical diameter. The cell type created in the first step will be referred to as SAR11-S1. The second step incorporates the difference in shape and converts the shrunk Pro shaped cell, SAR11-S1, to a SAR11 shaped cylinder and will be referred to as SAR11-S2. In order to incorporate the consequence of differences in cell size and shape between Pro and SAR11 in the model it is assumed that the maximum rates of uptake and synthesis (Section 2.3.1) vary with SA:V (Section 5.1.1).

To describe changes necessary in the model, the dimensions (SA and V) of Pro and SAR11 will first be given. Then the theory behind the coefficients used to implement the scaling of the maximum rates with SA:V will be explained. Application of the coefficients in the model for theoretical morphosis will finally be presented.

5.2.1.1. Cell dimensions

Measurements of Pro dimensions grown in cultures give a range of 0.5-0.8 µm for length and 0.4-0.6 µm width of the coccoid cell (Morel et al., 1993) with an equivalent spherical diameter (D_P) of 0.5-0.7 µm (Partensky et al., 1999) (volume 0.113 µm^3). For simplicity we take the cell to be spherical to first order, with a diameter of 0.6 µm.

SAR11 cells are crescent-cylinder-shaped and estimates of dimensions on cultured cells are 0.37-0.89 µm for length with a diameter of 0.12-0.20 µm (Rappé et al., 2002). Here we take the cells to be cylinders with an average length (l) of 0.63 µm and average diameter (D_c) of 0.16 µm (volume 0.013 µm^3). The equivalent spherical diameter of any given volume (V) is given as:

$$D = 2\left(\sqrt[3]{\frac{3V}{4\pi}}\right) \quad [5.1]$$

where D is the equivalent spherical diameter. The equivalent spherical diameter of SAR11 (D_S) is 0.3 µm, i.e approximately half that of Pro.

5.2.1.2. The difference in SA:V for SAR11-S1 and SAR11-S2

To calculate the SA and V of Pro and the SAR11-S1 sphere the following formulae are used:

$$SA\ sphere = 4\pi\left(\frac{D_{P/S}}{2}\right)^2 \quad [5.2]$$

$$V\ sphere = \frac{4}{3}\pi\left(\frac{D_{P/S}}{2}\right)^3 \quad [5.3]$$

where $D_{P/S}$ is the equivalent spherical diameter of Pro (D_P) and SAR11 (D_S). The SA:V of Pro ($SA{:}\,V_P$) and SAR11-S1 ($SA{:}\,V_S$) based on the average equivalent spherical diameter calculations are $SA{:}\,V_P$ = 10 µm^{-1} and $SA{:}\,V_S$ = 20 µm^{-1}.

For calculating the SA and V of the cylindrical SAR11-S2 the following formulae are used:

$$SA\ cylinder = 2\pi\left(\frac{D_c}{2}\right)^2 + 2\pi\left(\frac{D_c}{2}\right)l \quad [5.4]$$

$$V\ cylinder = \pi\left(\frac{D_c}{2}\right)^2 l \quad [5.5]$$

where D_c is the diameter of the cylinder's end faces and l is the length of a cylinder. The SA:V of SAR11-S2 ($SA{:}V_{SC}$) considering the SAR11 size and shape dimensions as mentioned above is $SA{:}V_{SC}$ = 28 μm^{-1}. Table 5.1 gives the equivalent spherical diameters, surface areas, volumes and SA:V for Pro, SAR11-S1 and SAR11-S2.

5.2.1.3. Scaling model rates using SA:V

In the model, substrates are taken up across the surface area (SA) of the cell at a given absolute rate ($\dot{U}$) in units of mols C hr^{-1} or mols N hr^{-1}. All fluxes in the present model, whether proportional to surface area (uptake) or volume (V) (maintenance and growth), are given relative to 1 mole of carbon biomass. As such, the normalised rate processes ($\dot{J}$) are equal to $\frac{\dot{U}}{V}$ given that structural biomass scales with volume. Substrate uptake across the surface area can be written in terms of either cell surface area or volume, so

$$\dot{U} = \dot{J}.V = SA.c \quad [5.6]$$

where c is the uptake rate per unit surface area. This assumption allows for the influence of size and shape differences between Pro and SAR11 on resource acquisition rates to be calculated if it is assumed that c is the same for Pro and SAR11, then

$$\frac{\dot{J}_P.V_P}{SA_P} = \frac{\dot{J}_S.V_S}{SA_S} \quad [5.7]$$

The subscripts P and S correspond to Pro and SAR11, respectively. So,

$$J_S = \left(\frac{SA_S}{V_S}\right)\left(\frac{V_P}{SA_P}\right)\dot{J}_P \quad [5.8]$$

Therefore there is a factor,

$$\delta_{size/shape} = \left(\frac{SA_S}{V_S}\right)\left(\frac{V_P}{SA_P}\right) \quad [5.9]$$

which can be used to scale maximum rates parameterised for Pro to maximum rates according to the change in size and shape, and therefore greater SA:V of SAR11. The coefficient used in the first step of the theoretical morphosis, reducing Pro to a sphere the same volume as SAR11 creating SAR11-S1, will use the coefficient δ_{size} given as,

$$\delta_{size} = \left(\frac{\pi {D_S}^2}{(\pi {D_S}^3)/6}\right)\left(\frac{(\pi {D_P}^3)/6}{\pi {D_P}^2}\right) = 2.0 \quad [5.10]$$

The coefficient used in the second step of the theoretical morphosis to reduce Pro to a cylinder of equal volume to SAR11, creating SAR11-S2, will use the coefficient δ_{shape} given as,

$$\delta_{shape} = \left(\frac{\pi D_C\left(\frac{D_C}{2}+l\right)}{\pi\left(\frac{{D_C}^2}{4}\right)l}\right)\left(\frac{(\pi {D_P}^3)/6}{\pi {D_P}^2}\right) = 2.8 \quad [5.11]$$

5.2.1.4. Application of the scaling coefficients to the maximum rate parameters

The maximum rate parameters in the model that are considered to be dependent on the cells surface area are DON uptake ($\dot{J}_{DON,U_m}$), DIN uptake ($\dot{J}_{DIN,U_m}$), CHO synthesis ($\dot{J}_{CHO,S_m}$) and amino acid (AA) synthesis ($\dot{J}_{AA,S_m}$) synthesis. The maximum rate of AA synthesis is dependent upon the value of the maximum rate of CHO synthesis and so scales with SA:V too. The influence of the size dependent "package effect" is implicit in the scaling of the maximum rate of photosynthetic CHO synthesis. A summary of the theoretical morphosis and maximum rate parameters for Pro, SAR11-S1 and SAR11-S2 created using δ_{size} and δ_{shape} are provided in Table 5.2.

5.2.2. Carbon acquisition: photoautotrophy versus photoheterotrophy

The rate of carbon acquisition is changed from that parameterised for photoautotrophy in Pro to that of photoheterotrophy in SAR11. The cell type created in this stage of the theoretical morphosis is referred to as SAR11-S3. It is assumed that the parameterisation (SU) that combines DIC with light to produce CHO in Pro also represents light enhanced uptake of DOC in SAR11. In order to create SAR11-S3, the maximum rate of CHO synthesis for Pro, which is 0.080 mol C (mol C)$^{-1}$ hr^{-1} is changed to the maximum rate of DOC uptake for SAR11, which is 0.025 mol C (mol C)$^{-1}$ hr^{-1} (Section 2.3.1.6), summarised in Table 5.2.

5.2.3. Elemental composition of biomass (C:N)

The parameter φX defines the C:N of synthesised biomass (Section 2.3.2). This parameter is changed from the C:N of Pro (9.2) to the C:N of SAR11 (5.0) in order to create SAR11-S4, summarised in Table 5.2.

5.2.4. Light harvesting physiology

The differences in light harvesting physiology between Pro and SAR11 are represented by different values for the half saturation irradiance (Section 2.3.1.1). The half saturation irradiance of 40 µmol photons m^{-2} s^{-1} for Pro is changed to 2700 µmol photons m^{-2} s^{-1} for SAR11 in the fifth stage of the theoretical morphosis in order to create SAR11-S5, summarised in Table 5.2.

5.2.5. Diurnal and nocturnal growth

Nocturnal (in addition to diurnal) growth is incorporated into the model using additional formulae, which have been explained in detail in Section 2.2.5. In short, the formulae allow SAR11 to take up nutrients during the diurnal and nocturnal periods. A 12:12 light:dark cycle is assumed so that SAR11 grows over a 24 hour period, with growth at night being constant and independent of parameter β. This stage marks the completion of the theoretical morphosis creating SAR11 from Pro, summarised in Table 5.2.

5.2.6. The order of steps for the theoretical morphosis

Physical differences in size and shape are considered first, followed by carbon acquisition strategy, biomass C:N, light harvesting physiology and lastly the diel growth pattern. The differences in physiology controlling the rates of resource acquisition are incorporated first so that carbon and nitrogen uptake for SAR11 is established prior to the evaluation of the effect of biomass C:N. The C:N defines the net requirement of carbon and nitrogen for biomass synthesis, which one would intuitively expect to co-evolve with the physiology for carbon and

nitrogen acquisition. To incorporate the differences in C:N immediately after changes to uptake provides a platform to examine how the different rates of carbon and nitrogen uptake of Pro and SAR11, which may be a function of cell size, shape and strategy of carbon acquisition, combine with the relative requirements of carbon and nitrogen for biomass synthesis to affect growth rate.

Light harvesting physiology and nocturnal growth are incorporated last for convenience. The formulae used to describe nocturnal growth also modify the half saturation irradiance, which is the parameter that is changed to represent differences in light harvesting physiology (Section 5.2.4). It is therefore essential that these two physiological differences are analysed next to each other.

5.2.7. Experimental conditions

The theoretical morphosis is carried out in the ambient conditions used in Experiment 1 for both Pro (Section 3.3.1) and SAR11 (Section 4.3.1) using the default parameter set, described as non-limiting conditions. The range of environmental conditions explored in the previous chapters that gave rise to different physiological dynamics of photoheterotrophic growth and nutrient fluxes are not evaluated.

5.3. Results

5.3.1. The effect of cell size and shape (SAR11-S1 and SAR11-S2)

5.3.1.1. Growth rate and uptake of carbon and nitrogen

Simulating a decrease in cell size to a sphere of equal volume to SAR11 (SAR11-S1) results in an increase in the specific growth rate from 0.20 d^{-1} to 0.43 d^{-1} at β_{opt} (Figure 5.1). The increase in growth rate is by a factor of 2.15, whereas the increases in uptake and synthesis according to the increase in SA:V, conferred by the decrease in cell size, are by a factor of 2.0 (Figure 5.1). The growth rate of SAR11-S1 at β_{opt} is 7.5 % greater than the increase in SA:V.

Simulating a decrease in cell size and change in shape from a Pro sphere to the cylindrical dimensions of SAR11 (SAR11-S2) results in an increase in the specific growth rate from 0.20 d^{-1} to 0.61 d^{-1} at β_{opt} (Figure 5.1). Growth rate increases by a factor of 3.05 at β_{opt}, yet the increases in uptake and synthesis, conferred by the decrease in size and change in shape are by a factor of 2.8 (Figure 5.1). The growth rate of SAR11-S2 at β_{opt} is 8.9 % greater than the increase in SA:V relative to Pro. The results from the model suggest that if uptake and synthesis rates scale with SA:V, the potential increase in the cell's specific growth rate is greater than would be predicted by the difference in SA:V alone.

Considering the two steps seperately, simulating a reduction in cell size in SAR11-S1 increases the specific growth rate by 0.23 d^{-1} at β_{opt} relative to Pro (Figure 5.1). Incorporating the change in cell shape, results in an additional increase in the specific growth rate by 0.18 d^{-1} for SAR11-S2, relative to that of SAR11-S1. Being cylindrical therefore increases the cells specific growth rate almost as much as the change in size.

5.3.1.2. The fate carbon and nitrogen

Maintenance is assumed to be a biomass specific process, i.e. proportional to volume, and will not change with changing SA:V. As a result, when synthesis and uptake rates increase as the size and shape change to SAR11-S1 and SAR11-S2, carbon and nitrogen increase in availability for growth after the fixed maintenance requirements have been met (Figure 5.2). The fraction of the total carbon flux used in maintenance decreases from ~3 % in Pro to ~1 % in SAR11-S1 and to less than 1 % in SAR11-S2 (Figure 5.2). The fraction of the total nitrogen flux used for maintenance decreases from ~10 % in Pro to ~5 % in SAR11-S1 and to ~3 % in SAR11-S2 (Figure 5.2).

The other fluxes of carbon and nitrogen shown in Figure 5.2 do not contribute to the greater increase in growth rate. AA synthesis increases in proportion to SA:V and, therefore, so does carbon dioxide release through it's production. Respiration at the constant specific maintenance rate is unchanging, and respiration at growth increases in direct proportion to the increase in growth rate. The contributions of each synthesis pathway (sparing pathway and deamination pathway, Equations 2.2.3a and 2.2.3b) for maintenance and growth for Pro, SAR11-S1 and SAR11-S2 are relatively unchanging (see step 3). This is because the relative delivery of ON and OC to maintenance and growth do not change signifcantly with increasing SA:V (Figure 5.1). Therefore, ammonium release through maintenance does not change signficantly. Ammonium release through new biomass synthesis increases in proportion to the rate of growth. The relative release of excess carbon and nitrogen also do not change signficantly (Figure 5.2).

5.3.2. The effect of carbon acquisition strategy (SAR11-S3)

5.3.2.1. Growth rate

Changing the maximum rate of carbon acqusition from that parameterised for photoautotrophy in Pro to that parameterised for photoheterotrophy in SAR11, results in a growth rate of 0.22 d^{-1} at β_{opt} for SAR11-S3 (Figure 5.3). The growth rate of SAR11-S3 at β_{opt} is 36.1 % of the growth rate of SAR11-S2. The inability to acquire carbon at the rate of Pro

through photoautotrophy strongly limits the growth rate of SAR11-S3 relative to that of SAR11-S2.

Interestingly, the growth rate of SAR11-S3 is remarkably similar to that of Pro, being greater by only 10.0 % (Figure 5.3). The lower rate of carbon acqusition through photoheterotrophic DOC uptake in SAR11-S3 is approximately balanced by the greater uptake rate of DIN and DON conferred by the increased SA:V.

5.3.2.2. The uptake of carbon and nitrogen

The rate of carbon acqusition through DOC uptake in SAR11-S3 (2.40 x 10^{-2} mol C (mol C)$^{-1}$ hr^{-1}) is 30.8 % of the rate of CHO synthesis in Pro (7.77 x 10^{-2} mol C (mol C)$^{-1}$ hr^{-1}) at β_{opt} (Figure 5.3). The reduced rate of carbon acqusition through photoheterotrophic DOC uptake in SAR11-S3 limits the rate at which AA can be synthesised, and therefore, the rate of DIN assimilation (Figure 5.3). The rate of AA synthesis in SAR11-S3 is 73.2 % of the rate for Pro. However, although the rate of AA synthesis is reduced in SAR11-S3 relative to Pro, the greater rate of DON uptake confered by increased SA:V, which is not effected by the change in the rate of carbon acqusition, means total ON available for maintenance and growth is 35.8 % greater in SAR11-S3 than Pro (Figure 5.3). OC delivery to maintenance and growth in SAR11-S3 is 24.6 % that of Pro. Similar growth rates between Pro and SAR11-S3 are achieved despite the signficiant difference in the relative delivery of OC and ON to maintenance and growth (Figure 5.3).

The rate of carbon acqusition in SAR11-S3 is 11.0 % of the rate for SAR11-S2. The rate of AA synthesis in SAR11-S3 is 26.2 % of the rate for SAR11-S2 and, because the rates of DON uptake in both model types are the same, total ON delivery to maintenance and growth in SAR11-S3 is 48.5 % that of SAR11-S2. OC delivery for maintenance and growth in SAR11-S3 is only 8.8 % of the rate for SAR11-S2 as a large fraction of the total DOC flux is used for AA synthesis. The results suggest that the rate of carbon acqusition is an important influence on SAR11 growth rate by limting both ON (by limitng DIN assimilation) and OC availability for maintenance and growth.

5.3.2.3. The fate of carbon and nitrogen

Changing the rate of carbon acquisition alters the relative delivery of ON and OC to maintenance and growth for SAR11-S3 compared to that of Pro (and SAR11-S2) (Figure 5.3). This influences the relative contribution of the deamination and sparing pathways (Equations

2.2.3a and 2.2.3b) to maintenance and growth and therefore the relative fates of carbon and nitrogen.

Firstly, Pro and SAR11-S2 deliver similar relative quantities of ON and OC to maintenance and growth although the absolute rates are greater in the latter cell type (Figure 5.1). The fraction of maintenance and growth via the sparing and deamination pathways are therefore similar for these two cell types (Figure 5.4). The relative fates of carbon and nitrogen do not change significantly, although the percentage of the total carbon and nitrogen fluxes used in maintenance does change (Figure 5.2), as discussed in Section 5.3.1.

The fraction of synthesis via the sparing pathway for Pro (and SAR11-S2) is significantly greater than the deamination pathway, due to the larger delivery of OC than ON to maintenance and growth (Figure 5.3). Upon the transition to heterotrophic DOC uptake in SAR11-S3, the relative delivery of OC to ON decreases (Figure 5.3) and as a consequence the fraction of synthesis via the deamination pathway increases from 7 % to % 23 % for maintenance and 7 % to 28 % for growth (Figure 5.4). This shift in metabolism influences the relative fates of carbon and nitrogen (Figure 5.5).

The most notable changes in the fate of the carbon and nitrogen fluxes for SAR11-S3 are those of ammonium release, excess carbon and maintenance (Figure 5.5). The total uptake rate of nitrogen in SAR11-S3 is 3.05 x 10^{-3} mol N (mol C)$^{-1}$ hr^{-1}, which is 36.2 % greater than Pro at 2.24 x 10^{-3} mol N (mol C)$^{-1}$ hr^{-1}. As a result of the greater fraction of biomass synthesis via the deamination pathway (Figure 5.4), however, the rate of ammonium release in SAR11-S3 is 0.76 x 10^{-3} mol N (mol C)$^{-1}$ hr^{-1}, 4.8 fold greater than Pro at 0.16 x 10^{-3} mol N (mol C)$^{-1}$ hr^{-1}, and represents ~25 % of the total nitrogen flux in SAR11-S3 compared to ~7 % in Pro (Figure 5.5), even though the two cell types grow at similar rates (Figure 5.3). Despite the fact that SAR11-S3 grows at 36.2 % the rate of SAR11-S2, with total carbon and nitrogen uptake rates that are 14.3 % and 48.6 % that of SAR11-S2, respectively, ammonium release in SAR11-S3 is 1.5 fold greater than SAR11-S2 (Figure 5.5). The rate of carbon acquisition in SAR11-S3 nots only limits the rate of DIN assimilation into AA (Figure 5.3) but also increases the dependency of SAR11-S3 on ON as a source of energy, resulting in a greater rate of ammonium release.

The total uptake rate of carbon in SAR11-S3 is 3.22 x 10^{-2} mol C (mol C)$^{-1}$ hr^{-1}, 39.0 % of the rate of total carbon uptake in Pro at 8.36 x 10^{-2} mol C (mol C)$^{-1}$ hr^{-1}and 13.8 % the rate of SAR11-S2 at 23.4 x 10^{-2} mol C (mol C)$^{-1}$ hr^{-1}. With the lower rate of carbon acquisition, the rate of excess carbon release decreases in SAR11-S3 relative to SAR11-S2 and Pro. Excess carbon release decreases to a rate of 8.62 x 10^{-3} mol C (mol C)$^{-1}$ hr^{-1} in SAR11-S3 (where it accounts for

27 % of the total carbon flux), 14.9 % of the rate for Pro (where it accounts for ~71 % of the total carbon flux) and 5.3 % of the rate for SAR11-S2 (where it accounts for ~71 % of the total carbon flux) (Figure 5.5).

With the decline in the total rates of carbon and nitrogen uptake upon transition to cell type SAR11-S3, the percentage that maintenance makes up of the total carbon flux increases to 7 %, compared to 3 % in Pro and less than 1 % in SAR11-S2 (Figure 5.5). 7 % of the total nitrogen flux is now used for maintenance in SAR11-S3 compared to 10 % in Pro and 4 % in SAR11-S2 (Figure 5.5). The reduced rate of carbon acquisition via DOC uptake offsets the benefit that increased SA:V confers by increasing the fraction of the total carbon and nitrogen fluxes used in maintenance.

5.3.3. The effect of biomass C:N (SAR11-S4)

5.3.3.1. Growth rate

Changing the biomass C:N from 9.2 (Pro and SAR11-S3) to 5.0 (SAR11-S4) in the fourth step of the theoretical morphosis results in a growth rate of 0.15 d^{-1} for SAR11-S4 at β_{opt}, which is 68.0 % the rate of SAR11-S3 at β_{opt} and 75.0 % the rate of Pro at β_{opt} (Figure 5.6).

5.3.3.2. The uptake of carbon and nitrogen

The uptake rates of carbon and nitrogen are not affected in this stage of the morphosis and are therefore in accordance with the previous step (Figure 5.6).

5.3.3.3. The stoichiometry of synthesis

Figure 5.7 shows the stoichiometry of biomass synthesis for the deamination pathway and sparing pathway according to Equations 2.2.3a and 2.2.3b for SAR11-S3 and SAR11-S4. The stoichiometry of synthesis per mole of carbon is the same for Pro and SAR11-S3 as both cell types have the same biomass C:N. The plots show the total quantity of carbon and nitrogen substrates required to generate one mole of carbon biomass. Metabolic by-products of carbon and nitrogen are given.

Considering the sparing pathway first, changing the C:N of biomass from 9.2 (Pro and SAR11-S3) to 5.0 (SAR11-S4) increases the quantity of nitrogen in every one mole of carbon biomass synthesised from 0.11 mol N (mol C)$^{-1}$ in SAR11-S3 (and Pro) to 0.20 mol N (mol C)$^{-1}$ in SAR11-S4 (Figure 5.7). Nitrogen is sourced from ON and bound to its carbon at the fixed C:N. As a result, the quantity of ON required for synthesis increases from 0.47 mol C (mol C)$^{-1}$ for SAR11-S3 (and Pro) to 0.86 mol C (mol C)$^{-1}$ for SAR11-S4 (Figure 5.7). As ON also contains

carbon, less carbon needs to be sourced from OC in order to synthesis each mole of carbon biomass via the sparing pathway. SAR11-S3 (and Pro) requires 0.57 mol C (mol C)$^{-1}$ whereas SAR11-S4 requires 0.18 mol C (mol C)$^{-1}$ of OC (Figure 5.7). As the costs of synthesis are fixed per unit carbon, respiration is the same for SAR11-S3 and SAR11-S4 at 0.04 mol C (mol C)$^{-1}$.

ON provides all carbon, nitrogen and energy for biomass synthesis via the deamination pathway (Figure 5.7). In order to synthesise one mole of carbon biomass, 1.04 mol C (mol C)$^{-1}$ of ON is used in both SAR11-S3 (and Pro) and SAR11-S4, with the remaining 0.04 mol C (mol C)$^{-1}$ respired due to the costs of synthesis (Figure 5.7). As ON contains nitrogen bound to carbon at the same fixed C:N regardless of organism, both SAR11-S3 (and Pro) and SAR11-S4 use the same quantity of nitrogen substrate at 0.24 mol N (mol C)$^{-1}$, despite the fact that the cell types have different biomass C:N and therefore nitrogen requirements. A different quantity of nitrogen is therefore released as ammonium in order to stoichiometrically balance synthesis. SAR11-S3 (and Pro) releases 0.13 mol N (mol C)$^{-1}$ as ammonium, whilst SAR11-S4 releases 0.04 mol N (mol C)$^{-1}$ as ammonium (Figure 5.7). The lower C:N of SAR11-S4 biomass means the cell will incorporate a greater fraction of nitrogen bound to ON via the deamination pathway, releasing less ammonium into the environment per mole of carbon biomass synthesised.

5.3.3.4. The fate of carbon and nitrogen

By incorporating the C:N of SAR11 in the fourth step in the theoretical morphosis, the relative contribution of the sparing pathway to biomass synthesis in SAR11-S4 increases relative to SAR11-S3 (Figure 5.8), despite the fact that the rates of uptake and synthesis are unchanging (Figure 5.6). The sparing pathway contributes 90 % to maintenance and growth in SAR11-S4 compared to 77 % and 71 % to maintenance and growth in SAR11-S3, respectively (Figure 5.8).

The uptake rate of DOC is the same for SAR11-S3 and SAR11-S4 but it can be used to synthesise a greater number of units of carbon biomass in SAR11-S4 via the sparing pathway, where a greater amount of carbon is sourced from ON (Figure 5.7). As a result, a greater number of binding sites at the synthesis machinery for maintenance and growth (synthesising units) can be filled by OC and less by ON in SAR11-S4, increasing the prevalence of the sparing pathway. When the size, shape, carbon acquisition rate and C:N differences are incorporated, the fraction of synthesis via the sparing and deamination pathways are similar for Pro and SAR11-S4. The sparing pathway contributes 93 % to maintenance and 94 % to growth in Pro, and in SAR11-S4 the sparing pathway satisfies 90.0 % for both maintenance and growth (Figure 5.8).

The total rates of carbon and nitrogen uptake are the same for SAR11-S3 and SAR11-S4 (Figure 5.3.3.5). However, the decrease in biomass C:N results in a greater rate of nitrogen turnover in maintenance at 4.2 x 10^{-3} mol N (mol C)$^{-1}$ hr^{-1} in SAR11-S4, compared to 2.3 x 10^{-3} mol N (mol C)$^{-1}$ hr^{-1} in both SAR11-S3 and Pro. Nitrogen used in maintenance now represents 14 % of the total nitrogen flux in SAR11-S4 compared to 7 % in SAR11-S3 and 10 % in Pro (Figure 5.9). The carbon maintenance turnover rate and fraction of the total carbon flux is unchanging but still represents a greater fraction of the total carbon flux than Pro, in accordance with Step 3.

Although growth rate decreases in SAR11-S4 relative to SAR11-S3 (Figure 5.6), the fraction of nitrogen incorporated into new growth increases from 62 % in SAR11-S3 to 83 % of the total nitrogen flux in SAR11-S4, which is similar to that of Pro (81 %). As a consequence of increased nitrogen assimilation into biomass per mole of carbon biomass synthesised via the deamination pathway (Figure 5.7), the rate of ammonium release decreases to 0.016 x 10^{-3} mol N (mol C)$^{-1}$ hr^{-1}, representing only 2 % of the total nitrogen flux in SAR11-S4 compared to 25 % in SAR11-S3 and 7 % in Pro. The reduced rate of carbon acquisition via DOC uptake in SAR11 relative to CHO synthesis in Pro, now does not result in a high rate of ammonium release, which is the case for the previous step when the C:N is that of Pro.

The fraction of excess carbon release increases to 45 % of the total carbon flux in SAR11-S4 compared to 27 % in SAR11-S3. The increased requirement for nitrogen per mole of carbon biomass synthesised reduces the percentage of the total carbon flux that can be assimilated into biomass in SAR11-S4 relative to SAR11-S3 and so growth rate declines.

5.3.4. The effect of the light harvesting systems (SAR11-S5)

5.3.4.1. Growth rate

When incorporating the light harvesting system of SAR11 in the fifth stage of the theoretical morphosis, the growth rate of SAR11-S5 is 0.09 d^{-1}, 45.0 % the growth rate of Pro and 75.0 % that of SAR11-S4 (Figure 5.10).

5.3.4.2. Uptake of carbon and nitrogen

The transition mimicking a change from chl-a to a PR based light harvesting system results in a decrease in the rates of uptake and synthesis relative to those of SAR11-S4 (Figure 5.10). The rates of DOC and DON uptake are affected by the change of light harvesting system to a similar extent and are 50.4 % and 56.7 % that of SAR11-S4 in the previous step, respectively. The rate of AA synthesis and therefore DIN assimilation is less affected by the change in light harvesting

system and is 79.3 % the rate of AA synthesis in SAR11-S4. The decrease in AA in synthesis is less than that of DOC and DON uptake because DOC is used dynamically in bacteria and in the model. As total ON declines, an increasing fraction of DOC is used for AA synthesis to counteract it. As a result, total ON delivery to maintenance and growth is 65.2 % that of SAR11-S4, whereas OC delivery is only 38.0 % that of SAR11-S4 (Figure 5.10).

Despite the transition to the PR light harvesting system, the DON uptake rate is 58.4 % greater in SAR11-S5 than Pro (Figure 5.10). This suggests that the benefits that size and shape confer to DON uptake may outweigh the limitations that light harvesting may have on uptake. The rate of DOC uptake in SAR11-S5 is 15.6 % the rate of CHO synthesis in Pro but AA synthesis does not decline to the same extent (58.0 % that of Pro). DOC is used dynamically, which means an increased fraction of total DOC is used of AA synthesis. ON delivery to maintenance and growth is 88.6 % the rate of Pro, whereas OC in SAR11-S5 is 9.3 % that of Pro (Figure 5.10).

5.3.4.3. Energy harvesting by each light harvesting system

The amount of energy harvested from each pigment system is modelled using a functional response. The functional response for each light harvesting system differs only by the value of the half saturation irradiance (Figure 5.11).

At 500 µmol photons m^{-2} s^{-1}, the irradiance used in the present study, the functional response value for the proteorhodopsin pigment system is 17 % that of the chl-a pigment system (Figure 5.11). For each value of light investment β, and whether harvested solar energy is directed to CHO synthesis/DOC uptake or DON uptake, the amount of energy received by SAR11-S5 to enhance each processes is a maximum of 17 % that of Pro and SAR11-S4 (Figure 5.11). The reduced uptake and rates of synthesis in SAR11-S5 are a consequence of this reduction in the available harvested solar energy.

5.3.4.4. The fate of carbon and nitrogen

The greater relative decrease in the OC flux compared to ON (Figure 5.10) results in a greater fraction of maintenance and growth being satisfied by the deamination pathway compared to the previous step (SAR11-S4) and Pro (Figure 5.12). The change is only by ~3 %, however.

The total carbon uptake rate in SAR11-S5 is 0.017 mol C $(\text{mol C})^{-1}$ hr^{-1}, which is 52.2 % that of SAR11-S4 and 20.7 % that of Pro (Figure 5.13). The total nitrogen uptake rate in SAR11-S5 is 2.0×10^{-3} mol N $(\text{mol C})^{-1}$ hr^{-1}, which is 65.1 % that of SAR11-S4 and 88.6 % that of Pro. A consequence of the decline in the total carbon flux is that maintenance now accounts for 12 %

of the total in SAR11-S5, compared to 7 % in SAR11-S4 and 3 % in Pro (Figure 5.13). The fraction of excess carbon also decreases, accounting for 30 % in SAR11-S5 compared to 45 % in SAR11-S4 and 71 % in Pro. A consequence of the decrease in the total nitrogen flux in SAR11-S5 is that maintenance now accounts for 21 % the total nitrogen flux compared to 14 % in SAR11-S4 and 10 % in Pro. Although the fraction of synthesis via the deamination pathway has increased slightly in SAR11-S5, ammonium release is only a minor component of the total nitrogen flux in SAR11-S5 (3 %) and SAR11-S4 (2 %). The change in excess nitrogen release is negligible (Figure 5.13).

5.3.5. The effect of nocturnal growth (SAR11): morphosis complete

5.3.5.1. Growth rate

Both Pro and SAR11 are taken to grow at 0.20 d^{-1} at β_{opt} (Figure 5.14). This stage completes the theoretical morphosis. Pro grows at 0.20 (12 hours)$^{-1}$ in a day at β_{opt}. During the day, SAR11 grows at 0.11 (12 hours)$^{-1}$ at β_{opt}, which is 55.0 % the rate of Pro d^{-1}. During the night, SAR11 grows at 0.09 (12 hours)$^{-1}$, 45.0 % the rate of Pro d^{-1} (Figure 5.14).

5.3.5.2. The uptake of carbon and nitrogen

Incorporating nocturnal growth in the final stage of the morphosis alters the rates of uptake and synthesis per hour relative to the previous step (SAR11-S5) during the day (Figure 5.15). This is because the nocturnal growth model constrains uptake rates to field data (discussed in Section 2.2.5). The change in uptake and synthesis rates are, however, small and do not represent a change in physiological strategy between Pro and SAR11 (Figure 5.15). Hence, the final stage of the morphosis will evaluate the influence of additional growth during the night, constrained by incorporating the nocturnal growth model (Section 2.2.5). A detailed comparision of SAR11-S5 and SAR11 will not be given.

During a 12 hour sunlit day, Pro synthesises CHO at 5.3 times the rate that SAR11 uptakes DOC per hour. When including DOC that is taken up at night (when Pro is inactive), Pro synthesises CHO at only 2.7 times the rate that SAR11 takes up DOC over 24 hours (Figure 5.15). Pro synthesises AA at 1.6 times the rate of SAR11 during the day. When considering the sum of both growth periods, SAR11 synthesises AA at 1.25 times the rate of Pro over 24 hours (5.15). SAR11 is therefore responsible for a greater quantity of DIN uptake over a 24 hour period than Pro. SAR11 uptakes DON at a rate 2.0 times greater than Pro during the day. Over 24 hours SAR11 is responsible for 3.5 times more DON uptake than Pro (Figure 5.15).

The sum of carbon and nitrogen compounds acquired by Pro and SAR11 (Figure 5.16) demonstrates a significant difference in the role that these organisms play in the processing of carbon and nitrogen, whilst growing at the same specific rate. Pro processes 0.97 mol C (mol C)$^{-1}$ d^{-1}, 96.4 % of which is carbon reduced through photosynthesis. 0.47 mol C (mol C)$^{-1}$ d^{-1} is processed by SAR11, comprised of 73 % DOC and 27 % DON (Figure 5.16). Pro may therefore process roughly twice as much carbon as SAR11 but through conversion of inorganic carbon to organic, whereas SAR11 processes organic only. SAR11 processes 0.052 mol N (mol C)$^{-1}$ d^{-1}, 55.4 % of which is from DON and 44.6 % of which is DIN (Figure 5.16). Pro processes 0.028 mol N (mol C)$^{-1}$ d^{-1}, roughly half that of SAR11, 30.0 % of which is sourced from DON and 70.0 % from DIN (Figure 5.16).

5.3.5.3. The fate of carbon and nitrogen

A detailed analysis of the fate of carbon and nitrogen for Pro and SAR11 per hour is given in Chapters 3 and 4, respectively. The influence of the additional growth period on our understanding of the fate of carbon and nitrogen per day will however be discussed.

Whilst growing at the same rate per day, Pro and SAR11 maintain the same amount of carbon biomass per hour at 0.21 x 10^{-2} mol C (mol C)$^{-1}$ hr^{-1} (Figure 5.17) during the diurnal period, accounting for 3 % and 10 % of the total carbon flux, respectively (Figure 5.18). For the same period SAR11 maintains 0.42 x 10^{-3} mol N (mol C)$^{-1}$ hr^{-1}, 18 % of the total nitrogen flux, compared to 0.23 x 10^{-3} mol N (mol C)$^{-1}$ hr^{-1} in Pro (Figure 5.17), which accounts for 10 % of the total nitrogen flux (Figure 5.18). It is assumed for simplicity that Pro only maintains biomass during the day whereas SAR11 maintains during the day and night. Carbon turnover for SAR11 over 24 hours is 0.05 mol C (mol C)$^{-1}$ d^{-1}, twice that of Pro at 0.025 mol C (mol C)$^{-1}$ d^{-1}. SAR11 however turns over 3.7 times more nitrogen per 24 hours than Pro at 0.01 mol N (mol C)$^{-1}$ d^{-1} compared to 0.0027 mol N (mol C)$^{-1}$ d^{-1} in Pro (Figure 5.17).

Because SAR11 synthesises 1.25 times more AA over 24 hours than Pro (Figure 5.15), the cell also respires 1.25 fold more carbon dioxide through it's synthesis at 0.05 mol C (mol C)$^{-1}$ d^{-1} compared to 0.04 mol C (mol C)$^{-1}$ d^{-1} in Pro (Figure 5.17). As a result of both increased respiration at AA synthesis and increased maintainance turnover per day in SAR11, total respiration is 1.2 fold greater in SAR11 at 0.06 mol C (mol C)$^{-1}$ d^{-1} compared to 0.05mol C (mol C)$^{-1}$ d^{-1} in Pro (Figure 5.17).

The rate of excess carbon release in Pro is 0.06 mol C (mol C)$^{-1}$ hr^{-1}, 8.5 fold greater than SAR11 at 6.8 x 10^{-3}mol C (mol C)$^{-1}$ hr^{-1} during the diurnal period (Figure 5.17), which

accounts for 71 % and 33 % of the total carbon flux, respectively (Figure 5.18) . When considering that released over 24 hours, Pro releases 0.69 mol C (mol C)$^{-1}$ d^{-1}, 4.5 fold more than SAR11 at 0.16 mol C (mol C)$^{-1}$ d^{-1}. The majority of carbon in Pro is however fixed and therefore Pro contributes to the pool of organic carbon. SAR11 however uptakes and releases from and to the same pool. Excess nitrogen is a negligible fraction of the total nitrogen flux for both Pro and SAR11 and will not be discussed in detail.

During the diurnal period Pro releases 0.16 x 10^{-3} mol N (mol C)$^{-1}$ hr^{-1} of ammonium, which is 2.6 fold more than SAR11, which releases 0.64 x 10^{-4} mol N (mol C)$^{-1}$ hr^{-1} (Figure 5.17), accounting for 7 % and 3 % of the total nitrogen flux, respectively (Figure 5.18) . Over 24 hours Pro releases 2.0 x 10^{-3} mol N (mol C)$^{-1}$ d^{-1}, which is only 1.4 fold more than SAR11, releasing 1.4 x 10^{-3} mol N (mol C)$^{-1}$ d^{-1} (Figure 5.17).

Pro and SAR11 both grow at 0.2 mol C (mol C)$^{-1}$ d^{-1} but SAR11 requires 0.040 mols N (mol C)$^{-1}$ d^{-1}, which is 1.8 times more than Pro that needs at only 0.022 mols N (mol C)$^{-1}$ d^{-1} (5.17).

5.3.6. Additional morphoses

Additonal morphoses have been conducted in order to examine physiological differences from other perspectives. First, SAR11 uptake and synthesis rates have been scaled so that the cell is spherical but of the same volume as SAR11 (SAR11-SM) and spherical and of the same volume as Pro (SAR1-LG). SAR11-SM grows at 0.13 d^{-1} (Figure 5.19). Shape alone therefore allows SAR11 to grow at a rate 1.5 times faster than an equivalent spherical cell of equal volume (SAR11-SM). SAR11-LG grows at 0.04 d^{-1} (Figure 5.19). Hence, SAR11's size and shape allows it to grow at a rate 5.0 times faster than an equivalent cell the same shape and volume as Pro (SAR11-LG).

Second, the Pro model has been modified so that it uptakes DOC at a rate equivalent to SAR11 (but scaled according to the increase in size and change in shape of Pro), instead of synthesising CHO through photosynthesis (Pro-DOC). Pro-DOC grows at a rate of 0.06 d^{-1} (Figure 5.19), which suggest that that photosynthetic carbon reduction may allow Pro to grow at 3.3 times the rate of an equivalent cell that uptakes organic carbon heterotrophically (Pro-DOC).

5.3.7. Results summary

The influence of each physiological property on growth rate is summarised in Figure 5.20. In step 1 (SAR11-S1), changing the volume of Pro to the same volume of SAR11 increases growth rate 2.15 fold to 0.43 d^{-1}. The additional change in shape to that of a SAR11 cyclinder (SAR11-S2) increases growth rate 3.05 fold relative to Pro to 0.61 d^{-1}. Changing the carbon acqusition strategy from photoautotrophic CHO synthesis to photoheterotrophic DOC uptake (SAR11-S3) decrease the growth rate to 0.22 d^{-1}, which is 10 % greater than Pro and 36.1 % that of SAR11-S2. Cell size and shape and carbon acqusition strategy have the greatest influence on cell growth rate. Decreasing the biomass C:N (SAR11-S4) decreases growth rate to 0.15 d^{-1}, 75.0 % that of Pro and 68.0 % that of SAR11-S3. The incoporation of the proteorhodopsin light harvesting system (SAR11-S5) further decreases growth rate compared to light harvesting using the chlorophyll pigment system. SAR11-S5 grows at 0.09 d^{-1}, 45.0 % that of Pro and 75.0 % that of SAR11-S4. SAR11 grows at 55 % the rate of Pro over the 12 hour day growth period, with nocturnal growth accounting for the remaining 45 %.

5.4. Discussion

This study has shown how the physiological differences of Pro and SAR11 in size, shape (SA:V), carbon acquisition rate, biomass C:N, light harvesting system and diel growth period balance when both organisms grow at the same specific rate. The physiological properties that have the greatest influence on growth rate in order of significance are SA:V, the rate of carbon acquisition, growth period, biomass C:N and light harvesting system (Figure 5.20). The following is a discussion of the importance of each physiological property in influencing the growth rates of Pro and SAR11. The importance of photoheterotrophy for the growth rate of Pro and SAR11 relative to the other physiological traits investigated in the theoretical morphosis will also be discussed.

5.4.1. Cell size and shape

The results from the model suggest that the size and cylindrical dimensions of SAR11 are one of the cell's most critical physiological properties (relative to the other properties investigated here), contributing to its ability to maintain the same growth rate as Pro in the subtropical oceans. Shape alone theoretically confers a 1.5 fold greater growth rate than an equivalent spherical cell the same volume of SAR11 (SAR11-SM) (Figure 5.19). Combined the smaller size and shape of SAR11 confers a five-fold greater rate of growth than an equivalent cell, spherical

in shape and the volume of Pro (SAR11-LG) (Figure 5.19). Conversely, the larger, spherical shape of Pro may be the most significant constraint on the cell's specific growth rate (relative to the other properties investigated here). The theoretical decrease in cell volume and the additional change in shape to that of a cylinder, demonstrated in steps 1 (SAR11-S1) and 2 (SAR11-2) of the theoretical morphosis, results in a 2.15 and 3.05 fold increase in the specific growth rate of Pro, respectively (Figure 5.1).

The results from the model demonstrate that growth rate does not increase in direct proportion to an increase in SA:V but is greater than would be predicted by simply increasing SA:V (Figure 5.1). This is a result of the assumption that a cell must maintain its entire biovolume, making maintenance turnover a volume specific process. As such, when SA:V changes, the fixed maintenance rate per unit volume does not change. A consequence of this is that in smaller, irregularly shaped cells, smaller nutrient fluxes per unit membrane are required to attain a given fraction of the cell's specific growth rate (Raven, 1998) and fixed specific maintenance rate. The rate of maintenance turnover in Pro and SAR11 is, however, not well established and is a poorly constrained parameter in the present study, based only on the rate of leucine turnover (Section 2.3.2). This reinforces the need for maintenance rate measurements, as discussed in Chapters 3 and 4. It is shown here, however, that if a cell maintains some fixed volume specific quantity, the benefits that being smaller and irregular in shape confer to growth rate, may be greater than predicted by a change in SA:V alone.

It remains to be established empirically whether maintenance rates scale with volume as it is assumed here. Some processes, which are considered to be critical components of maintenance for cells growing in oligotrophic waters, tend be to be associated with the cell's membrane and therefore might scale with surface area. Such processes include maintaining ion gradients across the cell's membrane during periods of senescence, maintaining extracellular membrane associated enzymes to digest ambient refractory DOM (Del Giorgio and Cole, 1998) and maintaining membrane associated light harvesting pigments. It is therefore possible that the maintenance scales in a manner between surface area and volume. If this is the case, the additional increase in growth rate beyond the increase in SA:V will be diminished.

The scaling coefficients implicitly assume that rates of uptake and synthesis scale with volume to the power 2/3 (Section 5.2.1). Studies suggest this is the case for phytoplankton size classes, although some suggest a scaling exponent greater than 2/3 for uptake and metabolic rates suggesting that nutrient uptake and metabolic rates may be limited by some volumetric

process (reviewed by Finkel et al. (2009)). Non-scalable components such as nitrogen rich nucleic acids may make up an increasing fraction of cell volume in small cells (Raven, 1998). This is supported by the observation that small cells become more nitrogen rich with decreasing size (Maranon et al., 2013). A smaller fraction of the cytoplasm would then be available for the machinery involved in metabolism and growth and uptake and synthesis rates may begin to be limited by volumetric processes rather that surface area limitation. In the extreme case where maintenance rates scale with surface area, and uptake and synthesis rates scale with volume, then the influence that differences in SA:V may have on the growth rate of Pro and SAR11, shown here, will not occur. Therefore, the influence that a change in SA:V may have on the growth rates of Pro and SAR11 discussed in this chapter may be an upper estimate.

Morphing the Pro and SAR11 models to their counterpart's respective size and shape demonstrates that both properties may be equally as important in influencing the cell's specific growth rate (Figure 5.1). In the case of Pro, it is interesting to ask what the selection criteria are for being spherical and of larger volume than SAR11, when a decrease in size and change in shape to that of SAR11 are equally as beneficial to growth rate. In terms of the physiological characteristics investigated here, both light harvesting and nutrient harvesting physiology benefit from a smaller cell size and elongated cell shape (Naselli-Flores et al., 2007). It is likely then that Pro morphology is related to an aspect of cellular physiology that is not investigated here. It is not clear, however, what selective advantage there may be from maintaining a spherical morphology as most literature studies discuss the benefits of non-uniform cell shape (reviewed by Young (2006)). As one possibility, Stanca et al. (2013) observed a predominance of spherical cells in warmer, nutrient poor regions, which are characteristic of subtropical gyres where Pro abounds. It was suggested that any decrease in SA:V by being spherical relative to irregular shaped cells and influence on light and nutrient harvesting physiology may be offset by their mixotrophic nutritional strategy. More work is clearly needed to understand the selective value of maintaining a spherical shape in Pro and more generally phytoplankton.

The results presented here suggest that empirical studies that attempt to relate cell size to metabolic rate in order to explain allometric scaling relationships in single celled organisms (Maranon et al., 2013) may be misleading when shape differences are not considered. Such investigations could benefit from considering organism SA:V.

5.4.2. Carbon acquisition: photoautotrophy versus photoheterotrophy

Converting the carbon acquisition rate from that parameterised for CHO synthesis in Pro to DOC uptake in SAR11 in step 3 of the theoretical morphosis, results in the greatest change in growth rate of any single step in this study. The three fold increase in growth rate conferred by the increase in the cell's SA:V (in SAR11-S2) is almost completely offset when the rate of carbon acquisition changes from that provided by photoautotrophy to photoheterotrophy, with SAR11-S3 growing at 0.22 d^{-1}, just 10 % greater than Pro. In addition, it was shown that a Pro cell acquiring carbon via heterotrophic DOC uptake (Pro-DOC) may only grow at 0.06 d^{-1}, which is 30 % of the growth rate of a standard Pro cell (Figure 5.19).

The difference in the rate of carbon acquisition between Pro and SAR11 demonstrates a critical difference in the cell's ability to assimilate DIN into AA. SAR11 may theoretically outcompete Pro for DIN uptake based on increased SA:V. However, despite the increased SA:V remaining for SAR11-S3, the change in carbon acquisition to the rate parameterised for photoheterotrophic DOC uptake results in a significant decline in the rate of AA synthesis per hour, to 26.2 % of the rate for SAR11-S2 and 73.2 % of the rate for Pro (Figure 5.3). Despite the reduced SA:V of Pro relative to SAR11, the greater rate of carbon acquisition via photosynthesis means the cell is better equipped than SAR11 to assimilate limiting concentrations of DIN in oligotrophic waters. DIN assimilation may therefore be partially limited by carbon availability through DOC uptake in SAR11. The view that SA:V is the critical physiological property conferring a competitive advantage for nutrient uptake in smaller relative to larger cells (Raven et al., 2013) may be too simplistic when nutrient uptake is limited by differences in physiology not related to SA:V. In the case of DIN assimilation this is the rate at which carbon is acquired.

In the model, DIN assimilation will decrease with the lower rate of carbon acquisition in SAR11 (Figure 5.3) even if a significant fraction of the total carbon flux is still released as excess (Figure 5.4). This is a consequence of how co-limitation is represented here using SUs. The assimilation of co-limiting compounds at an SU is dictated by the relative arrival rates of the co-limiting compounds, the affinity of compounds for the SU and reaction stoichiometry. In this study the same affinity is assumed for DIN and CHO/DOC, and stoichiometry is fixed and assumed equal for both Pro and SAR11 (Section 2.2.2). Different relative arrival rates of DIN and CHO/DOC therefore control substrate assimilation into AA. The model results suggests that an uptake rate of DOC with significant excess is required in order to assimilate enough DIN in addition to DON uptake in order for SAR11 to grow at 0.20 d^{-1}. There is, however, no direct

evidence to confirm that the AA synthesis system in Pro and SAR11 follows the principles set out in SU theory, which are based on queuing theory (Kooijman, 1998). If AA synthesis follows SU theory, then competition for limiting concentrations of DIN in oligotrophic ecosystems may be partially mediated by differences in cell SA:V but also by the rate of carbon acquisition.

5.4.3. Biomass C:N

The effect that the difference in biomass C:N between Pro and SAR11 has on growth rate is small relative to the difference in SA:V and rate of carbon acquisition (Figure 5.20). However, the large size of Pro may provide the volume to house photosynthetic machinery in order to acquire carbon at a high rate through photosynthesis (Raven et al., 2013), in addition to limiting the influence than non-scalable components may have on biomass C:N. The combination of both the superior properties of carbon acquisition and high biomass C:N, may more than offset the limitations imposed on growth rate by the larger size and lower SA:V, relative to SAR11.

Conversely, if the increased SA:V of SAR11 is intrinsically linked to the low biomass C:N and low rate of carbon acquisition then it may be an inferior strategy to being bigger whilst maintaining a higher rate of carbon acquisition and higher biomass C:N of Pro. Despite this negative effect on growth rate, the combination of resource acquisition strategy with the lower biomass C:N allows SAR11 to use DOC and DON more efficiently (Figure 5.7). As a result, a SAR11 cell with a C:N of 5.0 releases ammonium at a lower rate than it would do with a C:N of 9.2 (that of Pro) (Figure 5.9) and, therefore, does not convert DON into a chemical species that may be utilised by another microbial competitor.

5.4.4. Light harvesting system

Changing the pigment system from that parameterised for chl-a in Pro to PR in SAR11 reduces available solar energy that may be used for resource acquisition in the model. This model dynamic mimics the lower net energy harvesting through PR in SAR11 relative to chl-a in Pro (Kirchman and Hanson, 2012). Chl-a is clearly a superior light harvesting system relative to PR (Kirchman and Hanson, 2012), however, comparison of the pigment systems is not straight forward. The ability to harvest solar energy using chl-a is intrinsically linked to carbon acquisition in step 3 of the morphosis. As a result the significant benefit that Pro gains in growth rate through its strategy of carbon acquisition cannot be addressed in isolation and should be evaluated with reference to the energy source that drives the reduction of carbon.

In reference to SAR11, although the PR system has clear benefits to SAR11 growth rate and ultimately survival (Chapter 4), there are many other functions of PR pigments, such as light sensing for depth location and photoregulation of cellular energetics (Fuhrman et al., 2008), which may further confer increased fitness to the cell and influence the interpretation and comparison of PR with chl-a.

Additional uses of solar energy beyond that modelled here such as ATP uptake (Gómez-Pereira et al., 2012) may also influence conclusions drawn on the benefit of harvesting solar energy using PRs.

The representation of the light harvesting system in the present study is therefore highly simplified. The reader is referred to a more detailed analysis and comparison of the chl-a and PR light harvesting system (Kirchman and Hanson, 2012).

5.4.5. Diel growth pattern

The ability of SAR11 to uptake nutrients at night provides just under half of the biomass required to grow at the same specific rate of growth as Pro at 0.20 d^{-1}.

It has been observed however that Pro can uptake DOC from the ambient pool via mixotrophic metabolism (del Carmen Muñoz-Marín et al., 2013). If this mode of metabolism allows Pro to uptake additional nitrogen resources and grow in the absence of sunlight then this may facilitate nocturnal growth, which is independent of photosynthetic carbon fixation. Further work is needed to assess nocturnal activity in Pro in order to evaluate the importance of differences in growth period between Pro and SAR11 in influencing growth rate.

5.4.6. Photoheterotrophic metabolism in Pro and SAR11

It has previously been demonstrated in this thesis that photoheterotrophic light use can increase the growth rate of Pro by ~50 % (Chapter 3) and SAR11 by ~6 % (Chapter 4) in the same non-limiting conditions used throughout the theoretical morphosis (Figure 5.20). For Pro, although photoheterotrophic light use has a significant effect on growth rate, the results suggest that it is of secondary importance relative to the rate of photosynthetic carbon fixation for maintaining the same growth rate as SAR11 and therefore coexistence and survival in oligotrophic subtropical ecosystems. The benefit that photoheterotrophic light use in Pro confers to growth rate is in a similar order to that of the ability to synthesise biomass with a high C:N, relative to that of SAR11. Interestingly, a Pro cell that grows by photoautotrophy alone does so at a rate of 0.13 d^{-1} according to the present study, which is similar to the

growth rate of SAR11 during the day (0.11 d^{-1}). Photoheterotrophic light use in Pro therefore approximately balances with SAR11's ability to grow during the night.

For SAR11, the ability to use light energy photoheterotrophically to enhance the uptake of DOM is minimal in its effect on growth rate relative to the influence of increased SA:V and the ability to uptake resources at night, relative to Pro. It has however been demonstrated that photoheterotrophic light use may confer significant benefits to SAR11 growth with the effect being greatest during DOC and DIN limitation (Chapter 4), conditions which SAR11 populations growing in the Sargasso Sea may be subject to (Morris et al., 2002, Carlson and Ducklow, 1996). The effect of photoheterotrophy relative to other physiological traits investigated here may therefore benefit from an evaluation of their importance in multiple environmental settings, similar to those investigated in Chapters 3 and 4 in this thesis.

5.4.7. A view on traits and trade-offs

The theoretical morphosis of the Pro and SAR11 models investigated the influence of their physiological traits on growth rate, although no explicit trade-offs between them were assumed. Trade-offs between traits do, however, exists in microbial physiological. Empirical analyses demonstrate trade-offs between the phytoplankton maximum nutrient uptake rate and half saturation constant (Litchman et al., 2007). Modelling studies further demonstrate that a trade-off may exist between resource investment in nutrient and light harvesting machinery in phytoplankton (Bruggeman and Kooijman, 2007). The morphotypes simulated in each stage of the morphosis technique (Table 5.2) may indicate that certain constraints or trade-offs may exists for Pro and SAR11 traits, despite the fact that the trade-offs are not represented explicitly. For example, SAR11-S2 is a Pro cell the size and shape of SAR11 with a growth rate three fold faster than Pro (Figure 5.20). It is interesting to ask, what physiological constraints exist in nature that prohibit the emergence of SAR11-S2. I.e what stops Pro decreasing in size and changing shape to that of SAR11? Presumably being larger, despite the theoretical limitations on light and nutrient harvesting, benefits Pro in some way. The large size may be essential for housing the photosynthetic machinery for carbon acquisition, which is the single most advantageous trait for Pro growth rate. The theoretical morphosis technique can therefore be employed as a strategy to investigate the fitness theoretical morphotypes in order to design hypotheses about the existence of trade-offs in nature.

5.5. Summary

For SAR11, the cell size, cylindrical shape and conferred increased in SA:V, relative to Pro, collectively have the greatest positive influence on the cell's growth rate. The ability to take up nutrients during the nocturnal period further confers a physiological benefit to SAR11 with the effect being secondary to that of SA:V. These physiological properties offset the inferior properties of carbon acquisition through DOC uptake, low biomass C:N and proteorhodopsin light harvesting system, relative to that of Pro. The effect of photoheterotrophic DOM uptake on SAR11 growth rate relative to the influence of increased SA:V and nocturnal growth is small in the conditions investigated here. For Pro, the ability to synthesis CHO at a high rate relative to DOC uptake in SAR11 has the most significant positive influence on the cell's growth rate. In addition to the high C:N and chl-a based pigment system, these physiological properties offset the inferior properties of reduced SA:V and inability to uptake nutrients and grow during the nocturnal period, relative to SAR11. Photoheterotrophic light use in Pro is of secondary importance compared to that of photosynthesis for achieving a growth rate that allows it to compete with SAR11 in subtropical gyre ecosystems. However, it ranks in its influence on growth rate in a similar way to that of the ability to synthesis biomass with a high C:N, relative to that of SAR11 and may offset its inability to growth at night.

5.6. Tables

Table 5.1 Dimensions of Pro and SAR11

	Measurements based on equivalent spherical diameter				Measurements based on cylinder dimensions		
	Dia. (μm)	SA (μm^2)	Vol (μm^3)	SA:V (μm^{-1})	Dim. (μm)	SA (μm^2)	SA:V (μm^{-1})
Pro	0.6	1.13	0.113	10	-	-	-
SAR11	0.3	0.26	0.013	20	0.16 x 0.63	0.36	28

Table 5.2 Parameters set for each stage of the theoretical morphosis and additional morphoses

Morphotype	Description	Maximum rates (mol C (mol C)$^{-1}$ hr^{-1} *mol N (mol C)$^{-1}$ hr^{-1})					C:N (mol C (mol N)$^{-1}$)		Half sat. flux (μmols photons m^{-2} s^{-1})		Diel growth pattern	
		Max. CHO synth.	Max. DON uptake	Max. DIN uptake *	Max. AA synth.	Max. DOC uptake	Pro C:N	SAR11 C:N	Pro pigments	SAR11 pigments	Day model	Night model
Pro-PH (First stage)	Pro with photoheterotrophic capacity	0.080	0.0030	0.0022	0.053		9.2	-	40	-	Day model only	
SAR11-S1	Converting cell volume	0.160	0.0060	0.0044	0.106		9.2	-	40	-	Day model only	
SAR11-S2	Converting cell shape	0.224	0.0084	0.0057	0.148		9.2	-	40	-	Day model only	
SAR11-S3	Converting the carbon acquisition system	-	0.0084	0.0057	0.015	0.023	9.2	-	40	-	Day model only	
SAR11-S4	Converting the biomass C:N	-	0.0084	0.0057	0.015	0.023	9.2	5.0	40	-	Day model only	
SAR11-S5	Converting the light harvesting system	-	0.0084	0.0057	0.015	0.023	-	5.0	40	2700	Day model only	
SAR11-PH (Final stage)	Converting the diel growth pattern	-	0.0084	0.0057	0.015	0.023	-	5.0	-	-	Dark model inclusion*	
Additional morphoses												
SAR11-SM	SAR11 as a sphere with SAR11 volume	-	0.006	0.0044	0.0083	0.012	-	5.0	-	-	Dark model inclusion	
SAR11-LG	SAR11 as a sphere with Pro volume	-	0.003	0.0022	0.0059	0.0088	-	5.0	-	-	Dark model inclusion	
Pro-DOC	Pro acquiring carbon via DOC uptake	-	0.003	0.0022	0.0059	0.0088	9.2	-	40	-	Day model only	

5.7. Figures

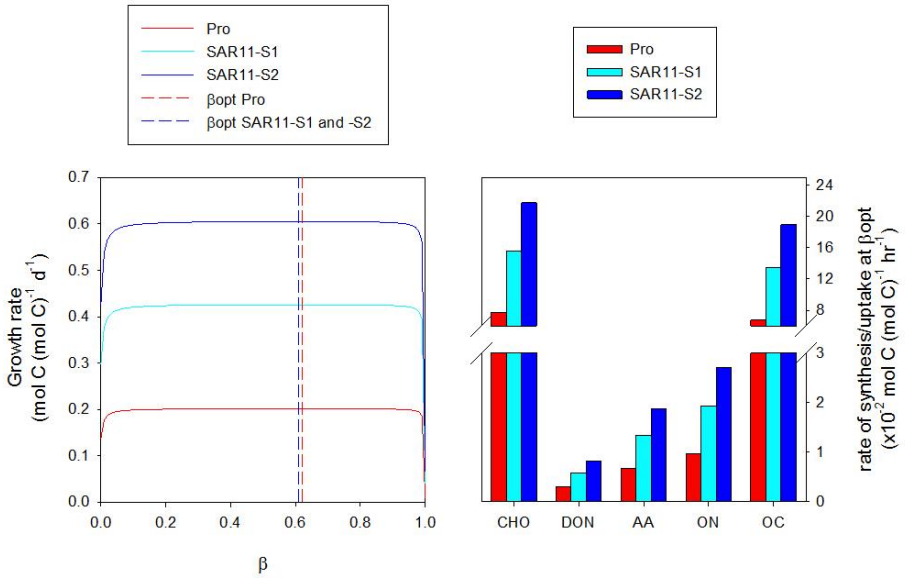

Figure 5.1 The variation of Pro, SAR11-S1 and SAR11-S2 growth rate with β (left). The vertical dashed line show the position of β_{opt} for each cell type. The uptake of carbon and nitrogen by Pro, SAR11-S1 and SAR11-S2 per hour at β_{opt} (right).

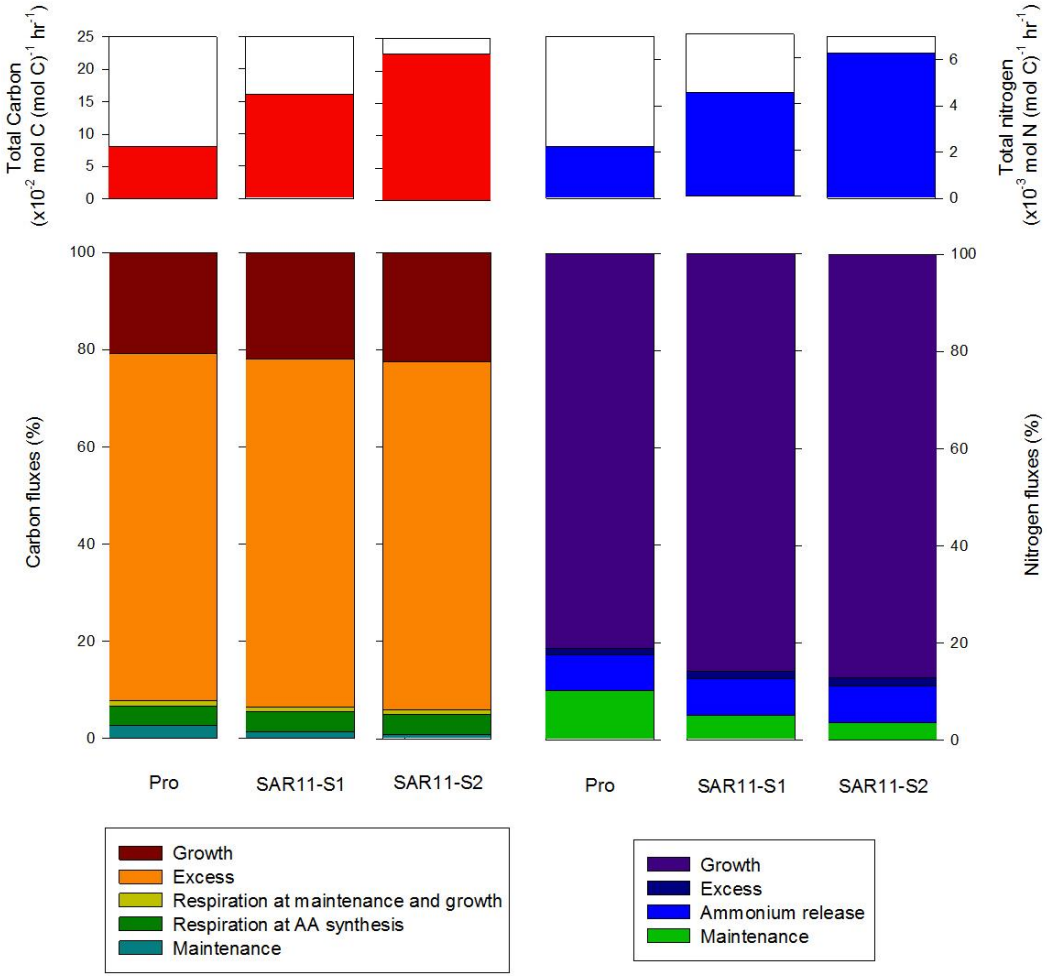

Figure 5.2 The total (top) and fate of (bottom) of carbon (left) and nitrogen (right) in Pro, SAR11-S1 and SAR11-S2 at β_{opt}. Processes are specified in the keys at the bottom of the figure.

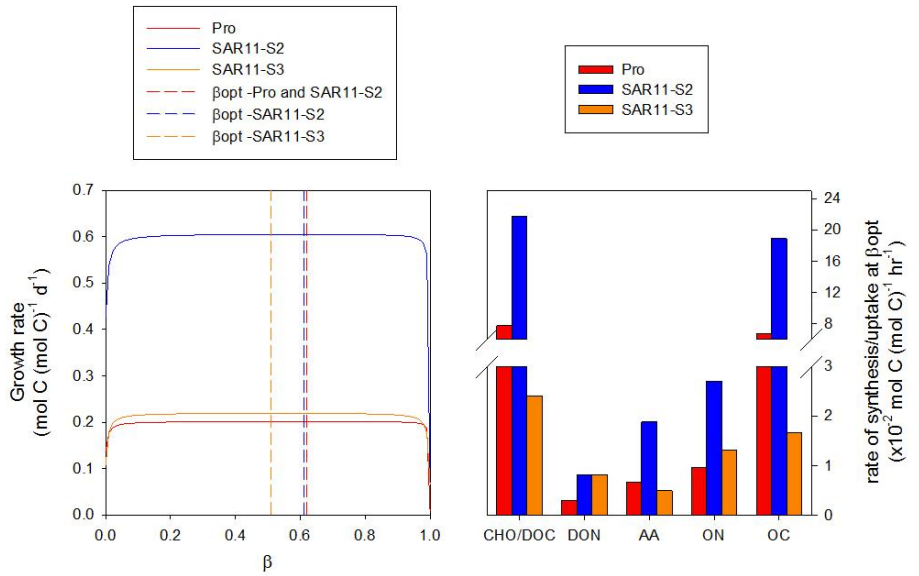

Figure 5.3 The variation of Pro, SAR11-S2 and SAR11-S3 growth rate with β (left). The vertical dashed lines show the position of β_{opt} for each cell type. The uptake of carbon and nitrogen by Pro, SAR11-S2 and SAR11-S3 per hour at β_{opt} (right).

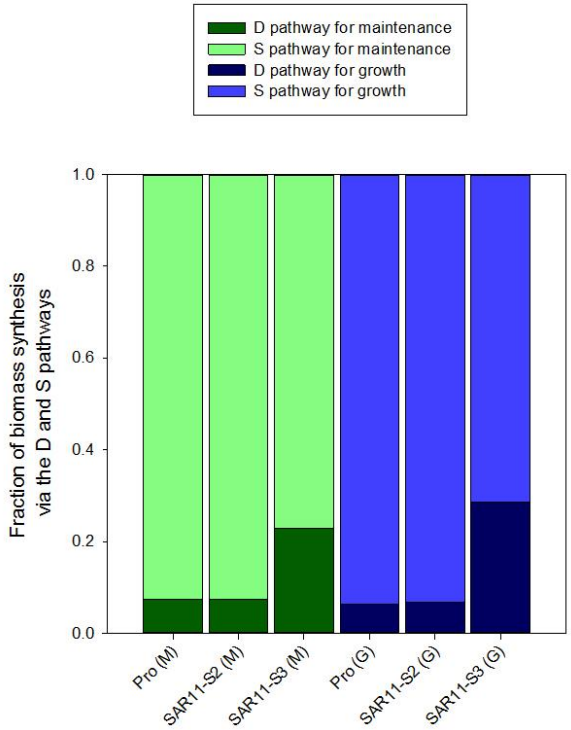

Figure 5.4 The fraction of biomass synthesis for maintenace (M) and growth (G) via the deamination (D) pathway and sparing (S) pathway for Pro, SAR11-S2 and SAR11-S3 at β_{opt}.

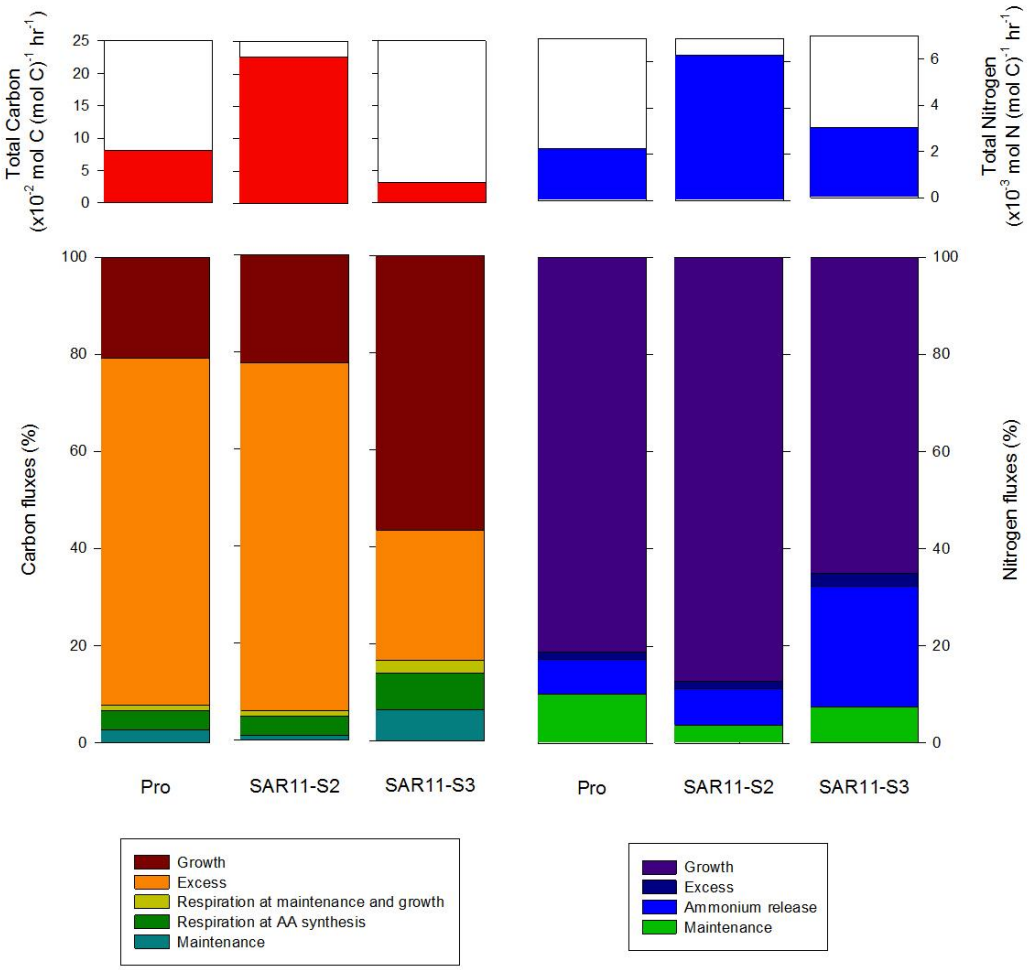

Figure 5.5 The total (top) and fate of (bottom) of carbon (left) and nitrogen (right) in Pro, SAR11-S2 and SAR11-S3 at β_{opt}. Processes are specified in the keys at the bottom of the figure.

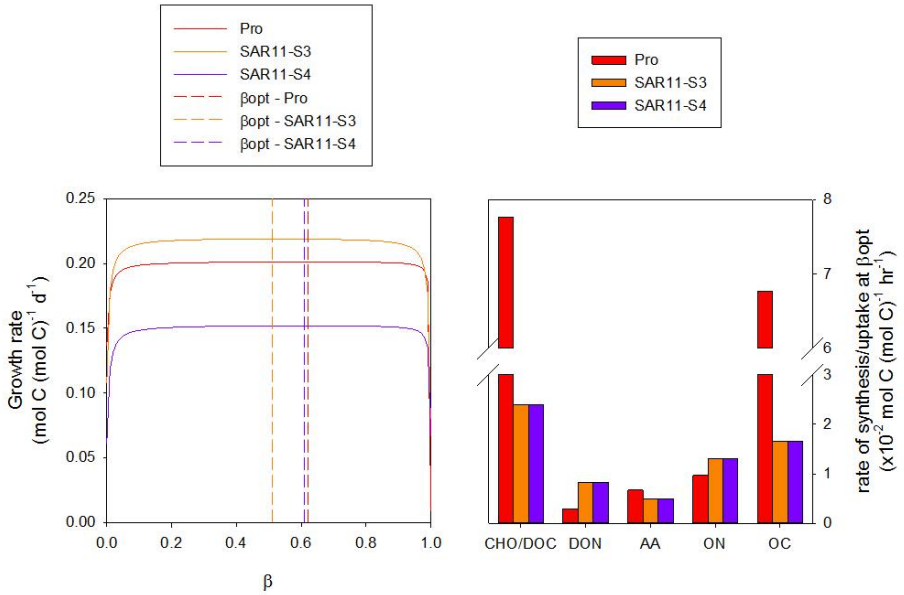

Figure 5.6 The variation of Pro, SAR11-S3 and SAR11-S4 growth rate with β (left). The vertical dashed lines show the position of β_{opt} for each cell type. The uptake of carbon and nitrogen by Pro, SAR11-S3 and SAR11-S4 per hour at β_{opt} (right).

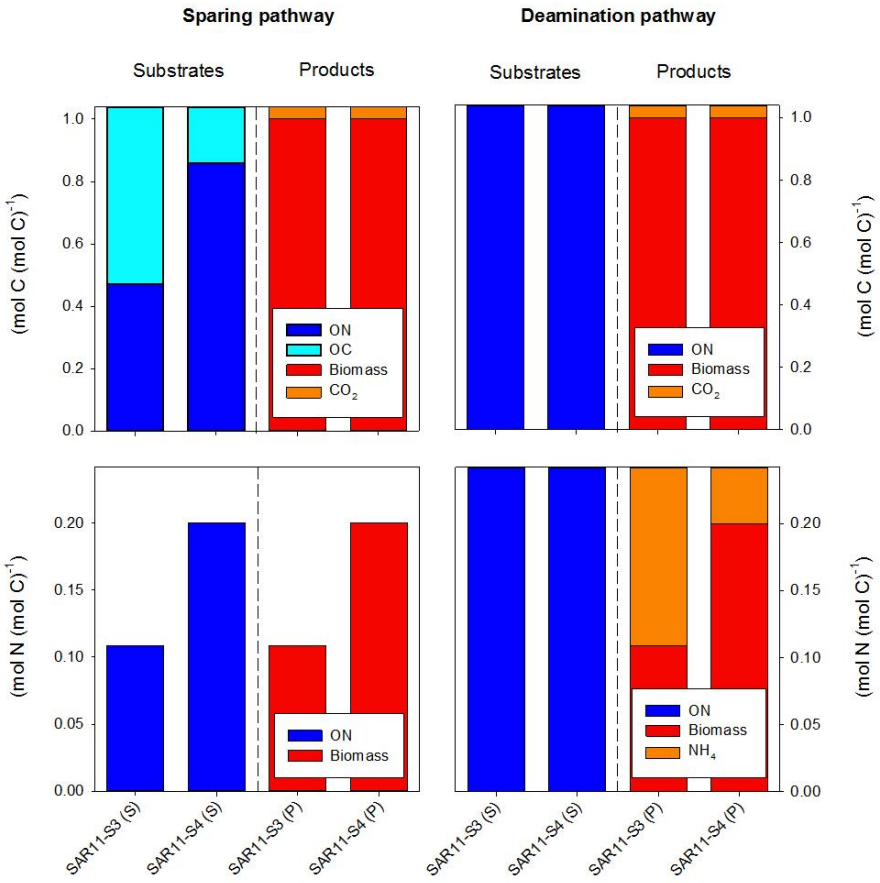

Figure 5.7 The stoichiometry of biomass synthesis for the sparing (S) and deamination (D) pathways for SAR11-S3 (and Pro) and SAR11-S4. Substrates (S) and products (P) of the synthesis process are separated by the vertical dashed line for each plot. Stoichiometric balance of carbon is given in the top plots and balance of nitrogen in the bottom.

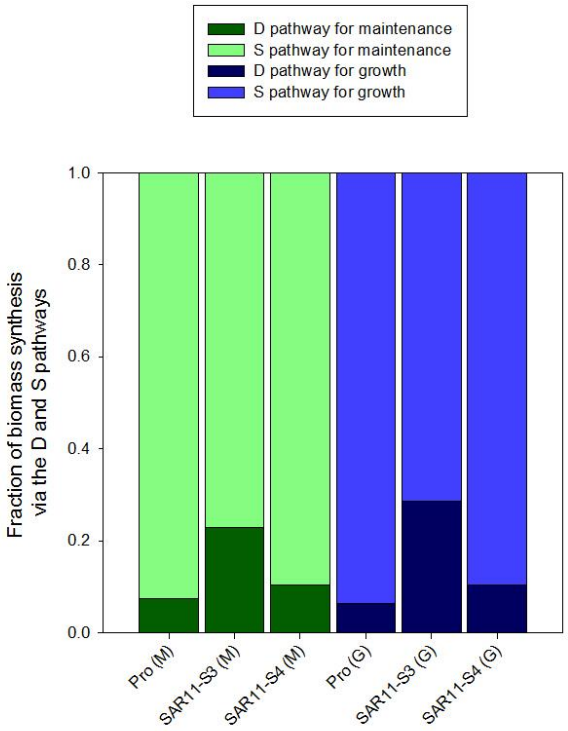

Figure 5.8 The fraction of biomass synthesis for maintenace and growth via the deamination (D) pathway and sparing (S) pathway for Pro, SAR11-S3 and SAR11-S4 at β_{opt}.

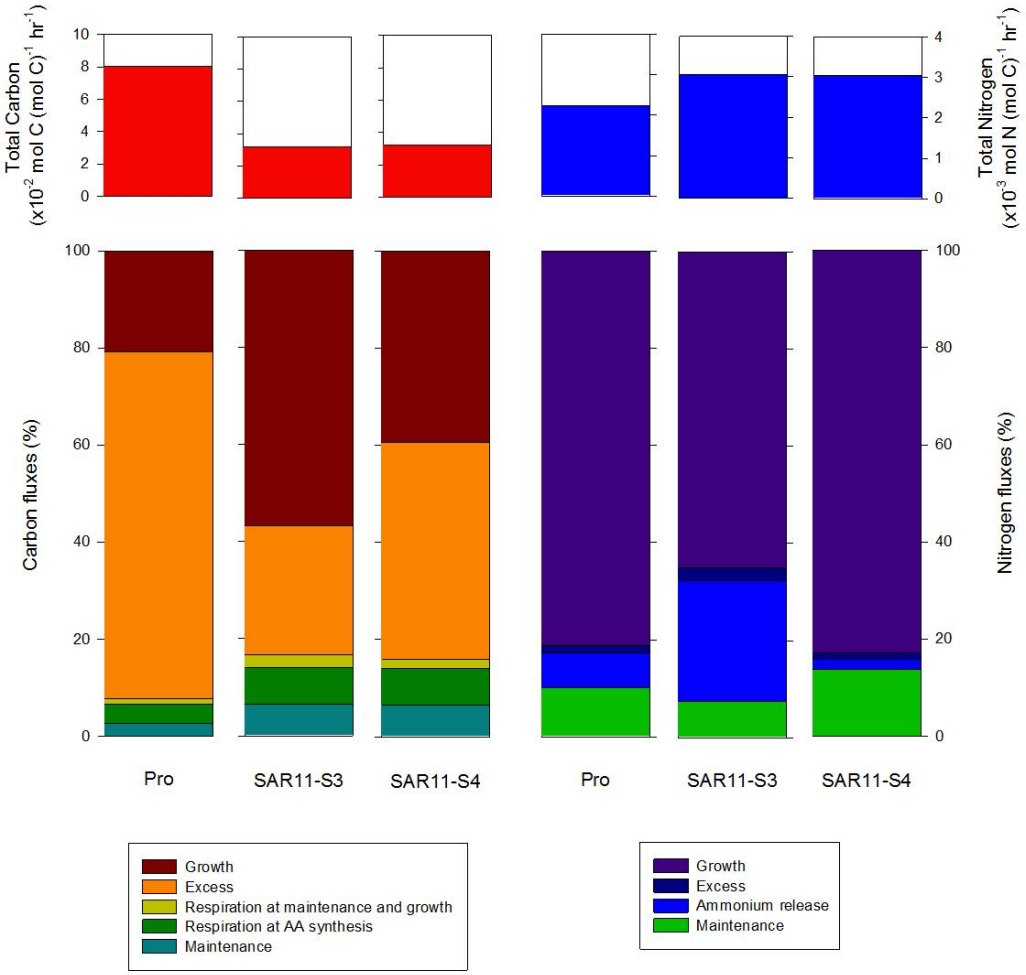

Figure 5.9 The total (top) and fate of (bottom) of carbon (left) and nitrogen (right) in Pro, SAR11-S3 and SAR11-S4 at β_{opt}. Processes are specified in the keys at the bottom of the figure.

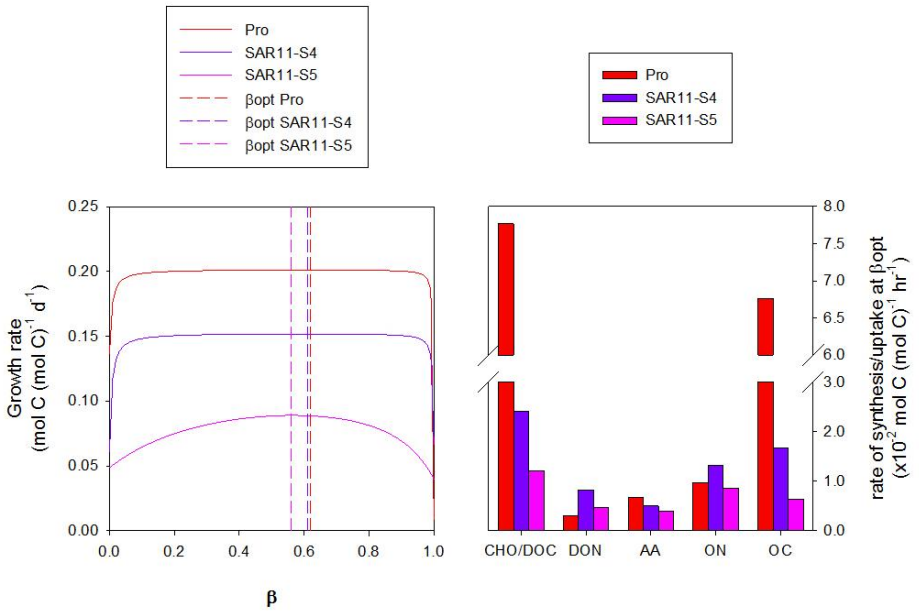

Figure 5.10 The variation of Pro, SAR11-S4 and SAR11-S5 growth rate with β (left). The vertical dashed lines show the position of β_{opt} for each cell type. The uptake of carbon and nitrogen by Pro, SAR11-S4 and SAR11-S5 per hour at β_{opt} (right).

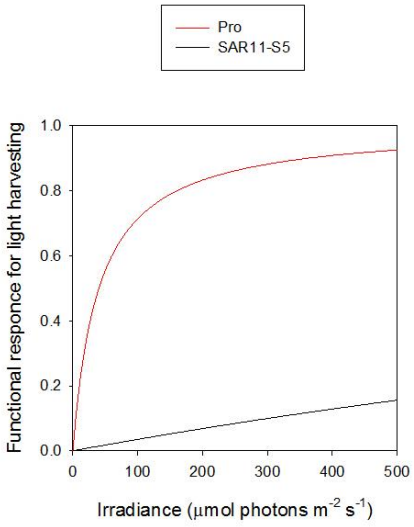

Figure 5.11 The functional response for light harvesting parameterised for chlorophyll-a repesentative of Pro and SAR11-S4, and proteorhodopsin representative of SAR11-S5.

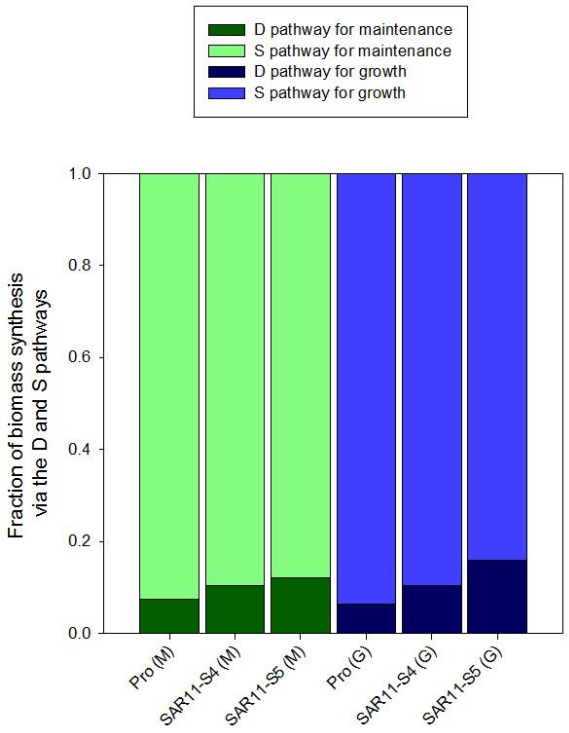

Figure 5.12 The fraction of biomass synthesised for maintenance (M) and growth (G) via the deamination (D) pathway and sparing (S) pathway for Pro, SAR11-S4 and SAR11-S5 at β_{opt}.

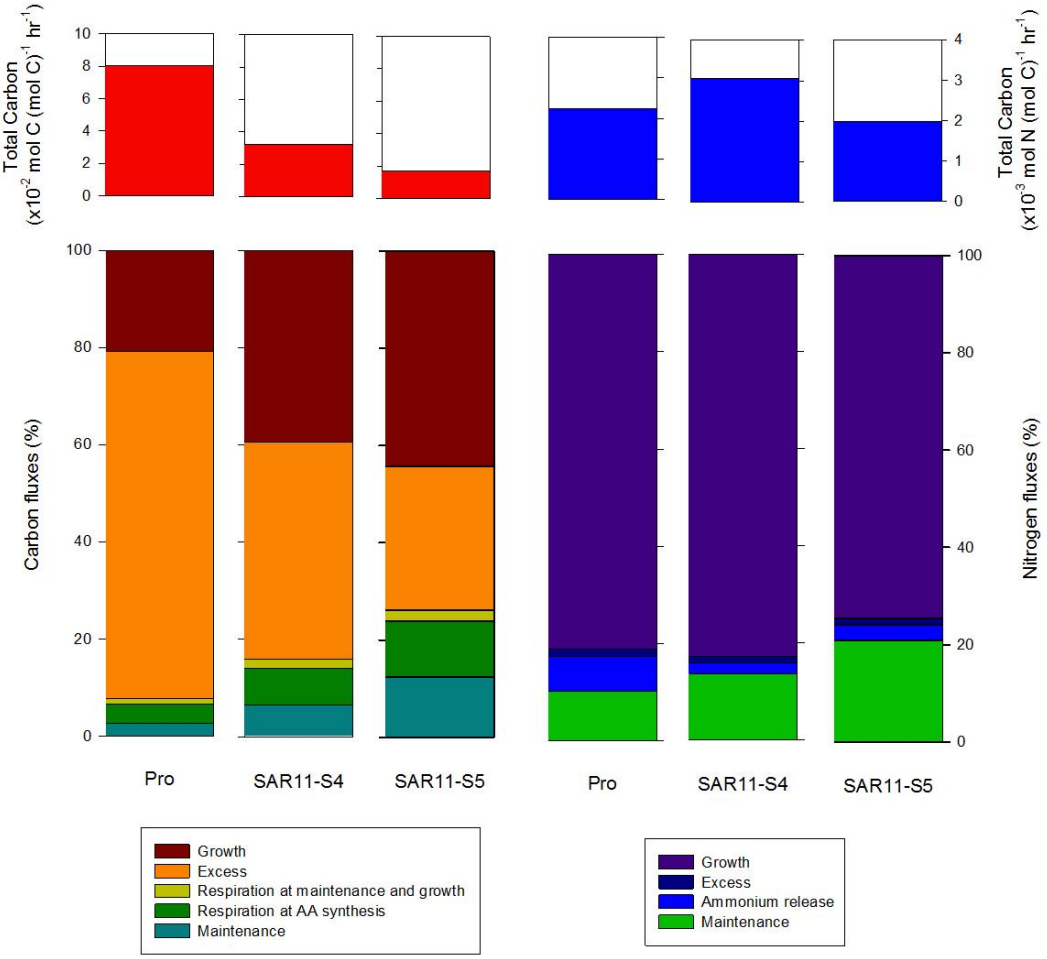

Figure 5.13 The total (top) and fate of (bottom) of carbon (left) and nitrogen (right) in Pro, SAR11-S4 and SAR11-S5 at β_{opt}. Processes are specified in the keys at the bottom of the figure.

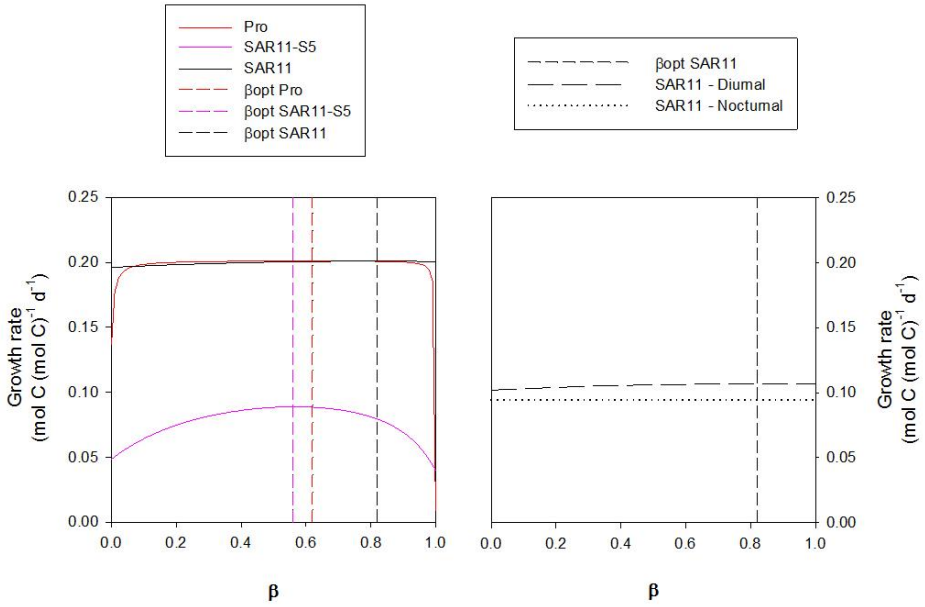

Figure 5.14 The growth rate of Pro, SAR11-S5 and SAR11 with changing β (left). The growth rate of SAR11 during the 12 hour diurnal period and 12 hour nocturnal period (right). The vertical dashed lines show the position of β_{opt} for each cell type.

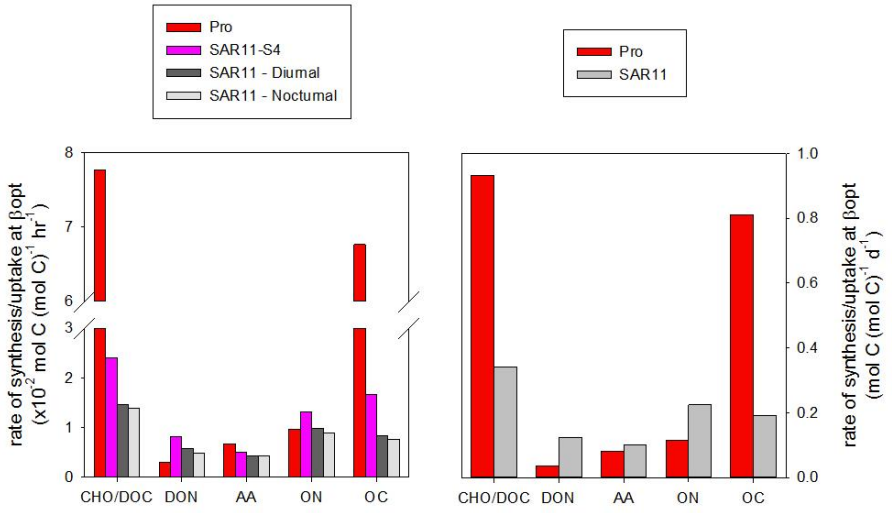

Figure 5.15 The hourly (left) and daily (right) uptake of carbon and nitrogen for Pro, SAR11-S5 and SAR11 at β_{opt}.

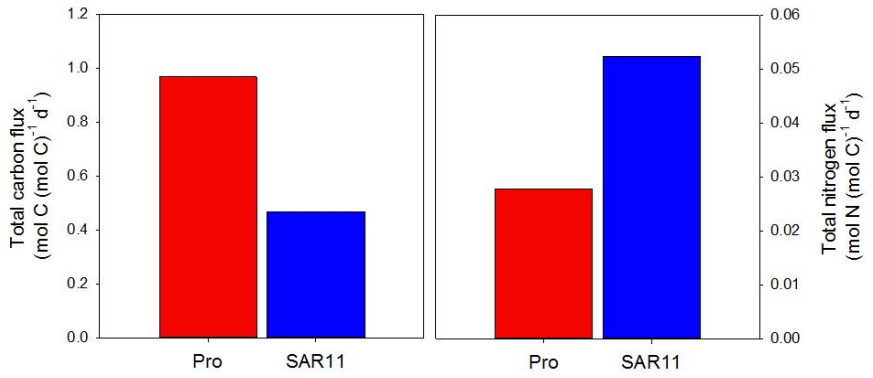

Figure 5.16 Total carbon (left) and nitrogen (right) fluxes for Pro and SAR11.

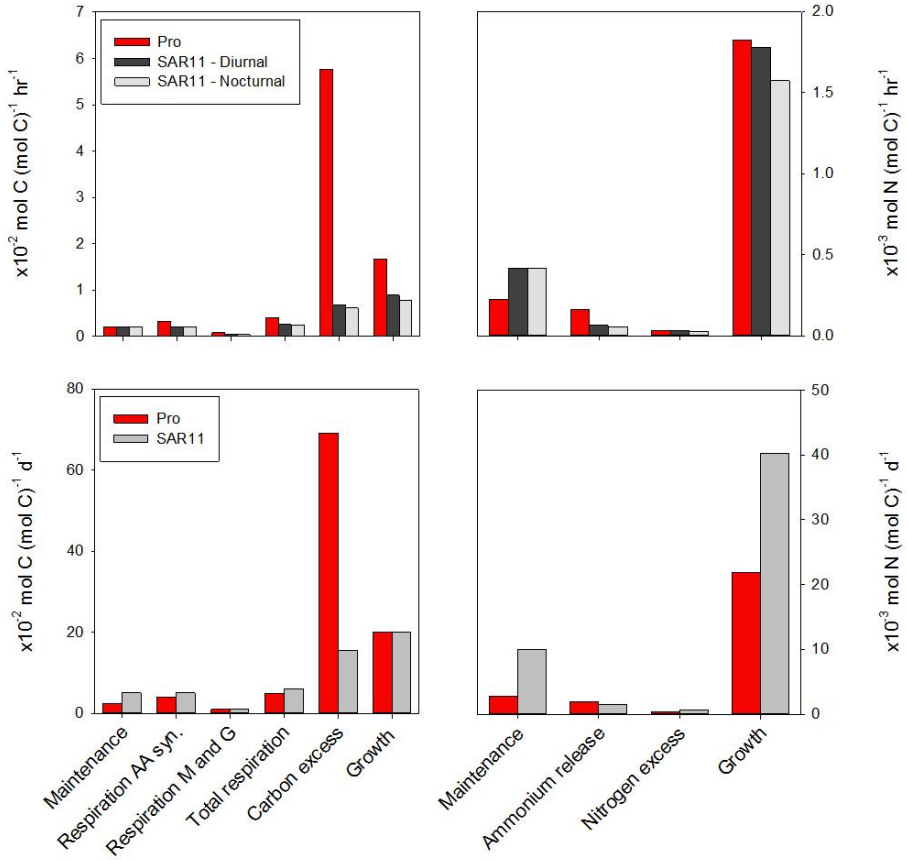

Figure 5.17 The fate of carbon (left) and nitrogen (right) for Pro and SAR11 during the diurnal and nocturnal periods per hour (top) and the total rates per day (bottom) at β_{opt}. M and G represent maintenance and growth, respectively.

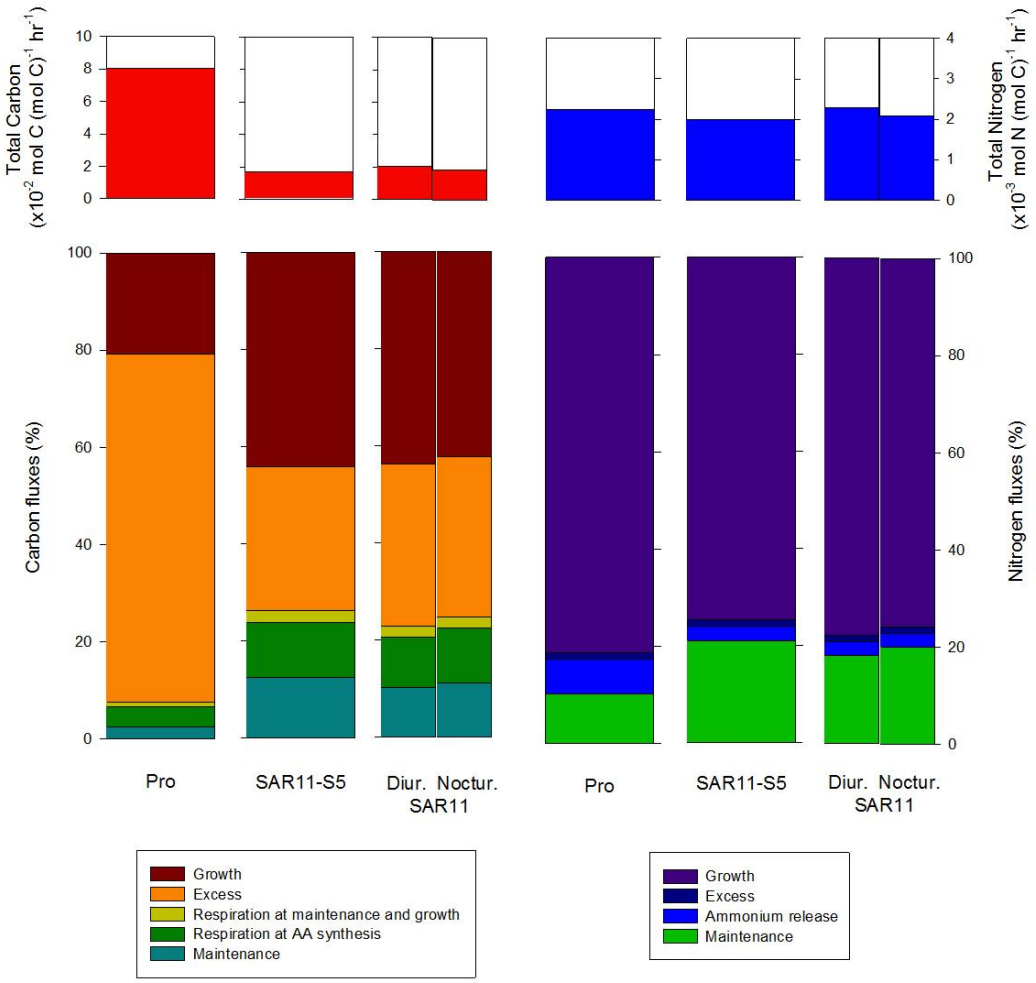

Figure 5.18 The total (top) and fate of (bottom) of carbon (left) and nitrogen (right) for Pro, and SAR11-S5 and SAR11 during the diurnal and nocturnal growth periods at β_{opt}. Processes are specified in the keys at the bottom of the figure.

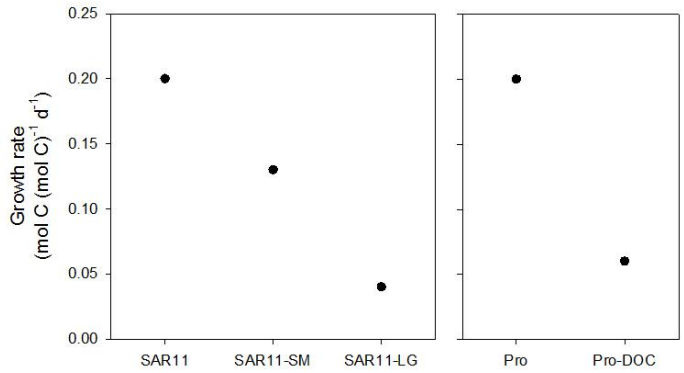

Figure 5.19 The growth rate of SAR11, SAR11-SM, SAR11-LG (left), Pro and Pro-DOC at β_{opt} (right).

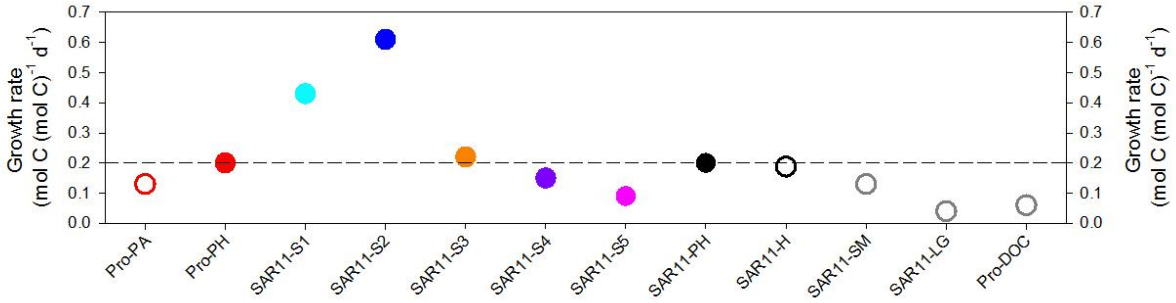

Figure 5.20 A summary of the change in growth rate throughout the theoretical morphosis for each cell type at β_{opt}. Pro-PA and SAR11-H, i.e. cell types that cannot grow by photoheterotrophy are also included for comparison. The additional morphoses (Figure 5.19) are also included. The horizontal dashed line shows the growth rate of Pro and SAR11 of 0.20 d^{-1}.

Chapter 6: Discussion

The aim of the work presented in this thesis was to investigate the influence of photoheterotrophic light use on the growth rate of Pro and SAR11 and the consequence for their processing of carbon and nitrogen (Chapters 3 and 4). As part of this I also explored how dissimilar aspects of Pro and SAR11 physiology balance to allow for equal growth rates, providing the cells with the ability to coexist in the oligotrophic ocean.

Chapter 6 summarises the main findings of this thesis (Section 6.1) and puts them in the wider context of ocean modelling and empirical analyses (Section 6.2). Finally the limitations of the approach, with suggestions for further research, are discussed (Section 6.3).

6.1. Summary of findings

6.1.1. Photoheterotrophy and the growth of *Prochlorococcus*

It has been shown in this work that the ability to partition harvested solar energy between photosynthesis and photoheterotrophy can increase the growth rate of Pro by up to ~50 % relative to an equivalent photoautotroph in non-limiting conditions. In DIN limiting conditions, Pro can survive on DON as the sole nitrogen source when taken up photoheterotrophically. Furthermore, the results from the model suggest that the use of harvested solar energy for photosynthesis and photoheterotrophy enhances growth rate over a broad irradiance range. The ability to direct harvested solar energy to cellular destinations in addition to that of photosynthesis may be critical to Pro survival, in part driving their distribution and abundance in the ocean.

Balancing solar energy use between photosynthesis and photoheterotrophy does not affect DIN assimilation in any experimental condition. DIN is the primary nitrogen source (70 % of total nitrogen uptake in non-limiting conditions) for Pro growth, and across a broad irradiance range DIN uptake is relatively unchanging. DON is an essential source of nitrogen (30 % of total nitrogen uptake in non-limiting conditions) for Pro growth.

In low irradiance conditions (~3-30 µmol photons m^{-2} s^{-1}) the joint use of solar energy reduces carbon fixation in Pro by up to ~20 % relative to an equivalent photoautotroph. In the same irradiance conditions Pro not only competes with other microbes for DON but the trade-off for light use also reduces the rate of excess carbon release. If Pro is an important source of DOC for heterotrophic competitors, then in low irradiance conditions photoheterotrophy may

have a dual effect on competition: decreasing DON availability through uptake and decreasing DOC availability through a decline in release.

6.1.2. Photoheterotrophy and the growth of SAR11

Photoheterotrophic light use increases the growth rate of SAR11 by between ~6 % and ~21 % relative to an equivalent cell that cannot harvest solar energy, the effect being dependent on the relative availability of ambient nutrients. The results show that when DIN and DOC are limiting, conditions which have been demonstrated for oligotrophic bacterioplankton where SAR11 populations dominate (Carlson and Ducklow, 1996, Morris et al., 2002), the ability to enhance DON uptake photoheterotrophically results in the biggest increase in growth rate. Such significant changes in growth rate may be critical to the survival of SAR11, in part governing their distribution and abundance in the open ocean.

DOC limitation (Carlson and Ducklow, 1996, Morris et al., 2002) is the most significant constraint on SAR11 growth rate relative to DIN and DON limitation. Photoheterotrophic DON uptake significantly relieves the effect of DOC limitation on the growth of SAR11.

Respiration in SAR11 is increased by up to ~10 % in conditions (DON limitation) that increase the cells dependency on synthesised AA for growth, which has a high cost on carbon for DIN assimilation. Photoheterotrophic light use, however, does not have a strong influence on BGE in any of the conditions investigated. The range of BGE estimates for SAR11 in the present study (56 % to 94 %) is significantly greater than field estimates from the open ocean for bacterioplankton populations dominated by SAR11 (1-10 %) (Hansell et al., 1995, Alonso and Pernthaler, 2006, Del Giorgio et al., 2011). This difference highlights the need for further work to understand the energetic sinks in open ocean bacterioplankton metabolism in order to model respiration and BGE more accurately (Section 6.3.3).

A decrease in the availability of DOC means SAR11, and bacterioplankton in general, are increasingly dependent on DON as a source of energy, the mobilisation of which results in ammonium release. In DOC limiting conditions, photoheterotrophic light use enhances SAR11 growth rate significantly and in turn increases the release of ammonium by up to ~20 %, which may be important for DIN limited photoautotrophic growth in the open ocean.

6.1.3. Balancing contrasts in *Prochlorococcus* and SAR11 physiologies

The larger SA:V of SAR11 relative to Pro approximately doubles the cells growth rate, with shape and size contributing equally for increased nutrient harvesting ability. If maintenance is

fixed and biomass specific, the benefit of being smaller and irregular in shape may confer a greater increase to growth rate than would be expected based on differences in SA:V alone.

Although one might expect SAR11 to outcompete Pro for DIN based on the difference in SA:V, the greater rate of carbon acquisition in Pro through photosynthesis allows the cell to assimilate DIN at a significantly greater rate than SAR11. This suggests that DIN assimilation in SAR11 is limited by the strategy for carbon acquisition. Interestingly, the benefit that photosynthesis confers to growth rate almost completely balances the limitations imposed by the lower SA:V in Pro relative to SAR11.

If the larger size of Pro is essential for housing the photosynthetic machinery (Stoecker, 1998) essential for carbon acquisition, and allows for a greater C:N than SAR11 due to the reduced imposing effects of non-scalable nitrogen rich components (Maranon et al., 2013, Raven, 1994) then being larger and spherical, with its associated physiological benefits of carbon acquisition and biomass C:N, confers a greater benefit to growth rate than being smaller and cylindrical in shape.

During the day SAR11 is physiologically inferior to Pro and needs to grow at night to provide just under half of the biomass required to grow at the same rate as Pro per 24 hours.

Photoheterotrophic light use in Pro and SAR11 increases the growth rate by ~50 % (Chapter 3) and by ~6 % (Chapter 4), respectively, relative to non-photoheterotrophic cells in equivalent conditions to that assumed for the theoretical morphosis. Relative to the effect that the high rate of photosynthetic carbon acquisition has on Pro growth rate, photoheterotrophic light use is of secondary importance. However, photoheterotrophy in Pro confers a similar benefit to growth rate as the ability to take up nutrients at night in SAR11. Photoheterotrophic light use in SAR11 results in the smallest change in growth rate relative to the influence of other physiological traits investigated here, relative to Pro. The importance on the availability of ambient DIN and DON for the influence of photoheterotrophy on SAR11 growth was not, however, considered in the theoretical morphosis.

6.2. Wider context

6.2.1. Photoheterotrophy in ecosystem models

Arguments for including the behaviour of Pro and SAR11 populations in marine ecosystem models are compelling. Both Pro and SAR11 dominate the oligotrophic subtropical gyres

numerically (Partensky et al., 1999, Morris et al., 2002, Chisholm et al., 1988) and metabolically (Zubkov, 2014, Mary et al., 2008b, Gómez-Pereira et al., 2012, Alonso and Pernthaler, 2006, Malmstrom et al., 2005, Malmstrom et al., 2004), which cover over 40 % of the planet's surface (Polovina et al., 2008). Pro contributes significantly to carbon reduction, (Zubkov, 2014) with some strains capable of both primary (growth on new nitrogen, i.e. nitrate of allochthonous origin) and regenerated (growth on recycled nitrogen, i.e. nitrogen of autochthonous origin) production (Martiny et al., 2009), and so potentially to the export of carbon to the deep ocean (Johnson and Lin, 2009). SAR11 dominates the bacterioplankton processing of DOM in the microbial food web and so plays a critical part in the release of carbon dioxide (Del Giorgio and Duarte, 2002) and regeneration of ammonium (Azam et al., 1983). Both cell types also compete for DIN and DON (Garcia-Fernandez et al., 2004, García-Fernández and Diez, 2004, Sowell et al., 2008, Gómez-Pereira et al., 2012) and release significant amounts of DOC and DON into the water column (Kujawinski, 2011, Kujawinski et al., 2009, Karl et al., 1998, Bertilsson et al., 2005).

The results presented in this thesis, summarised in Section 6.1, suggest that the photoheterotrophy of both Pro and SAR11 should be included when modelling ecosystems dominated by these organisms. The growth rate of Pro and SAR11 and key processes involving carbon and nitrogen are changed significantly by this mode of metabolism. The behaviour and outcome of ecosystem model simulations that address questions pertinent the cycling carbon and nitrogen in subtropical oligotrophic gyres may be influenced by photoheterotrophy.

The models of Fasham et al. (1990) and Taylor and Joint (1990) were the first to include a representation of bacterioplankton and the cycling of DOM, with the former extending the classic nutrient-phytoplankton-zooplankton-detritus (NPZD) modelling framework to nutrient-phytoplankton-zooplankton-detritus-bacteria (NPZDB). Since then NPZDB models have been used extensively, as reviewed by Christian and Anderson (2002). However, of these models, few separate the DOM pool into DOC and DON incorporating carbon and nitrogen stoichiometry (Anderson and Williams, 1998, Moloney and Field, 1991, Vallino, 2000). None consider the mixotrophy of bacterioplankton or have included photoheterotrophy.

An informative model to consider is that of the model of Anderson and Williams (1998) which extends the NPZDB framework by separating DOM into DOC and DON. A highly simplified schematic of the key connective flows of phytoplankton and bacterioplankton with ambient DIN, DOC and DON represented in the Anderson and Williams (1998) model is shown in Figure 6.1.

Phytoplankton acquire carbon through the photosynthetic reduction of DIC and source nitrogen from the DIN pool (Figure 6.1a). Phytoplankton also release fixed carbon directly to the ambient DOC pool through leakage. Bacterioplankton acquire carbon from the DOC and DON pools and nitrogen from the DIN and DON pools (Figure 6.1b). In addition, respiratory carbon dioxide release feeds back to DIC and ammonium regeneration feeds back to DIN (Figure 6.1a). The results from Chapters 3 and 4 suggest that the connective flows for communities dominated by Pro and SAR11 may not be sufficient. Such models should be modified to include photoheterotrophy for both phytoplankton and bacterioplankton due to the influence of photoheterotrophic light use on growth rate and the processing of carbon and nitrogen. Figure 6.1b shows the modified connective flows, highlighted in Chapters 3 and 4 that may be important for modelling communities that are dominated by Pro and SAR11. The twin use of light energy in Pro may enhance/facilitate uptake from the DON pool. The bacterioplankton component also interacts with the DON pool and will therefore compete with phytoplankton for DON. The rate of DOC release from Pro, which feeds into the pool of carbon available for bacterioplankton, may decrease at low irradiance if the trade-off for light use significantly reduces carbon fixation in Pro. The use of harvested solar energy in SAR11 may increase the uptake DIN, DOC and DON. In addition, the release of carbon dioxide to the DIC pool and ammonium to the DIN pool may be enhanced through photoheterotrophic light use. The dynamics of all these flux changes will be dependent on the size of bioavailable ambient pools.

Including the photoheterotrophy of Pro and SAR11 in an ecosystem model may be particularly relevant to simulating the cycling of carbon and nitrogen in the Sargasso Sea where Pro and SAR11 dominate the primary producing and bacterioplankton community, respectively. Bissett et al. (1999) have previously modelled this system and found that Pro begins to dominate the primary producer community in the nutrient depleted waters after the spring bloom and continue to do so throughout the summer. In the Bissett et al. (1999) model simulation, the bacterioplankton community, which is dominated by SAR11 (Morris et al., 2002), are carbon limited and remineralise a significant fraction of the DON pool to ammonium, which is rapidly utilised by Pro as a primary nitrogen source. The model presented in this thesis demonstrates that under similar carbon limiting conditions, photoheterotrophic light use in SAR11 increases growth rate and as a consequence increases the rate of ammonium release by up to ~ 20 %. If photoheterotrophy in the SAR11 enriched bacterioplankton community was included in the Bissett et al. (1999) model, it may result in an enhanced supply rate of nitrogen to the surface waters of the Sargasso Sea, increasing Pro

growth rate and the summer standing stocks of Pro in the model. In addition, the Bissett et al. (1999) model does not allow for photoheterotrophy in the Pro dominated phytoplankton community either. The ability of Pro to utilise solar energy for DON uptake, which does not influence DIN assimilation according to this thesis, may further increase nitrogen availability to Pro in the surface waters of the Sargasso Sea and increase the population growth rate and therefore the summer standing stocks of Pro and associated primary production in the Bissett et al. (1999) model.

Incorporating the photoheterotrophic metabolism of Pro and SAR11 into marine ecosystem models may help to refine our ability to simulate and forecast open ocean biogeochemistry. State-of-the-art marine biogeochemical models that consider the growth dynamics and nutrient utilisation characteristics of primary and secondary producers typically represent the bacterioplankton component of the ecosystem with a simple remineralisation parameter (Darwin and MEDUSA models) or a single bacterial functional type (ERSEM). It is argued that this representation is sufficient to first order as open ocean bacterioplankton respire the majority of carbon consumed (Tom Anderson pers. comm.). However, as it has been shown here (Chapters 3 and 4) and elsewhere (Vallino et al., 1996), the role that bacterioplankton play in the processing of key elements such as carbon and nitrogen can be dynamic and dependent on variable ambient conditions and critically, photoheterotrophic light use.

In order to incorporate the dynamics of Pro and SAR11 (photoheterotrophic) growth and nutrient utilisation characteristics (demonstrated in this thesis) into a state-of-the-art marine biogeochemical model a number of modifications need to be made. Firstly, the programming language used here (Powersim Studio 8) must be translated to a platform amenable for integration into the biogeochemical ecosystem model. Fortran is appropriate. In addition, the model formulae contain 10 state variables that are computationally expensive to simulate: four define the system used to synthesis AA and a further six to represent maintenance and growth (Chapter 2). Steady-state solutions can be used in place of the coupled differential equations to significantly reduce computations costs. The analysis of the entire axis β may also be unnecessary. If it is assumed that Pro and SAR11 both dynamically optimise their use of light to maximise growth rate (instead of having a fixed β), the model simulation could consider only β_{opt} and a limited number of values either side. As the shift of β_{opt} is predictable with changing ambient conditions (Chapters 3 and 4) a script can be included that will allow the model to only simulate a single value for β_{opt} and the new β_{opt}

that may occur at the next time point in the simulation. Such changes will aid in the integration of the current model system into a sophisticated complex ecosystem model. It is important to note that knowledge of ambient DIN, DON and DOC pools need to be understood more fully to incorporate bacterioplankton dynamics into ecosystem models in general.

6.2.2. Interpreting *Prochlorococcus* and SAR11 physiological traits

Photoheterotrophic light use may influence the abundance and distribution of Pro and SAR11. However, the importance of photoheterotrophy to growth rate in Pro is secondary relative to the benefits conferred by the cells high rate of carbon acquisition through photosynthesis. For SAR11, photoheterotrophic light use has a relatively small influence on growth rate compared to the cells high SA:V relative to Pro.

In addition to the role of photoheterotrophy the results from the theoretical morphosis demonstrate that SAR11's small size and cylindrical shape are critical physiological characteristic allowing the cell to thrive and coexist with Pro in the subtropical oligotrophic gyres with size equally as important as shape for fitness. This has implications for investigating allometric relationships in unicellular metabolism and physiology. Owing to the significant diversity in the size and shape of phytoplankton (Hutchinson, 1961) and prokaryotes (Young, 2006, Young, 2007), analyses of allometric scaling relationships with physiological parameters such as metabolic rate , growth rate and nutrient uptake rate in microbes, may benefit by considering an evaluation of SA:V based on cell size and shape. However, such investigations generally consider cell volume only and therefore neglect the influence that shape may have on SA:V and scaling relationships with physiological parameters (e.g. Maranon et al., 2013).

The suggestion that cell size is the microbial master trait is therefore challenged. Pro and SAR11 dominate the subtropical oligotrophic gyres in near equal abundances, and therefore are equally as successful, whilst having significantly different SA:V due to size and shape differences. Here it is shown that being larger, with the capacity to synthesise CHO photosynthetically and synthesise a high biomass C:N, confers greater benefits to fitness for Pro than greater SA:V relative to SAR11.

6.2.3. Photoheterotrophy in broader oceanographic contexts

It was described in Section 1.3 how photoheterotrophic metabolism in marine prokaryotes is not confined to the subtropical gyres but is also observed in marine temperate (Cottrell et al., 2008, Straza and Kirchman, 2011, Michelou et al., 2007), arctic (Cottrell and Kirchman, 2009) and freshwater systems (Martinez-Garcia et al., 2012). The results from this study are also

theoretically applicable to these environments. The models presented here (Chapter 2) are parameterised primarily using data from empirical studies conducted in the North Atlantic subtropical gyre. However, the use of mass specific units for all fluxes in the models means ambient pool sizes and, therefore, any nutritional differences between oligotrophic and eutrophic systems whether marine or freshwater are ignored. Both Pro and SAR11 have also been shown to grow photoheterotrophically in arctic (Cottrell and Kirchman, 2009) and temporal eutrophic systems (Cottrell et al., 2008; Lami et al., 2009). Analyses of the influence of photoheterotrophy in systems with different nutritional status' may be refined from the use of case specific parameters sets, although the results presented here to first order can be considered generally representative. Case specific parameter sets should first consider resource acquisition parameters as the remaining parameters are mostly based on theoretical considerations and generalised (Chapter 2). Pro and SAR11 are the most abundant organisms on the planet and are ubiquitously distributed (Morris et al., 2002; Partensky et al., 1999). The results from this thesis may therefore be globally applicable.

6.2.4. DEB theory and other approaches to modelling mixotrophy

The approach described in Chapter 2 was effective in quantifying the influence of photoheterotrophic light use on the growth rate of Pro and SAR11 and their processing of carbon and nitrogen. Other DEB models have been built to investigate, for example, evolutionary branching points in a population of mixotrophs (Troost et al., 2005a and b) and the vertical partitioning of mixotrophic strategies in a one dimensional (Kooijman et al. 2002) and a realistic physico-chemical setting, based on the Bermuda Atlantic time series (BATS) (Bruggeman, 2009). However, these mixotroph models differ from the one used here by not considering the dual use of limiting resources for maintenance and growth (Kuiper et al., 2005). This component of the modelled system is critical for understanding how photoheterotrophy influences Pro and SAR11 growth rate and elemental fluxes in variable environments (Chapters 3 and 4) and would have not been captured using previous approaches.

Critically the DEB theory approach allowed for the treatment of light as a resource analogous to nutrients, which provided the ability to investigate the consequences of partitioning a light flux between metabolic processes. Other approaches to modelling mixotrophy, such as that taken by Flynn et al. (2010), describing the mixotrophic metabolism of a "perfect beast", does not allow for the treatment of light in the same way as DEB theory. DEB theory, therefore, provides a unique opportunity to investigate the dynamic use of solar

energy in photoheterotrophic microbes and phototrophs in general. Furthermore, the approach taken by Flynn et al. (2010) describes the differences in organism physiology by using different model structures. The assumption of a fundamental model structure in DEB theory where differences between organisms are described using different parameter values, was an essential model characteristic that allowed for an investigation into the influence of different physiological strategies on the growth rate of Pro and SAR11 (Chapter 5).

6.3. Limitation and suggestions for future work

6.3.1. Moving on from an individual cell approach

Photoheterotrophic light use may increase the intrinsic growth rate of Pro and SAR11 and influence the processing of carbon and nitrogen in oligotrophic gyres. The approach taken in this thesis of modelling processes at the level of the individual organism was a useful first step in understanding the influence of photoheterotrophy on Pro and SAR11 metabolism. However, the interactions of these microbes in their ecosystem, particularly their competition for shared resources and biochemical feedbacks cannot be evaluated using this method. More specifically, Pro and SAR11 both compete for nitrogen from the ambient DIN and DON pools, and both excrete metabolic waste products into the DIC, DIN, DOC and DON pools with varying magnitude (Section 6.1). It is possible that interactions via these pools may influence the extrapolation of conclusions drawn in this thesis to the consequences at an ecosystem or basin scale. The impact of this limitation is difficult to predict without building a model capable of representing their competition.

A model chemostat is a tool which may be employed as an informative next step to investigate these interactions (Follows pers. comm). The chemostat model could contain populations of Pro and SAR11, based on the individual models developed in this thesis. Mass fluxes in the models of individual cells described in this thesis are specified as rates relative to everyone mol of carbon structure, given as mol C (mol C)$^{-1}$ hr^{-1}. To change the models of individual Pro and SAR11 cells to populations that grow in size, the specific rates (mol C (mol C)$^{-1}$ hr^{-1}) for each model can first be multiplied by the known carbon content of Pro and SAR11 cells (units mol C cell^{-1}) to obtain rates per cell (units mol C cell^{-1} hr^{-1}). The cell specific rates for Pro and SAR11 can then be multiplied by their population densities (units cells mL^{-1}) to produce the population specific measure of growth (units mol C mL^{-1} hr^{-1}), which can be converted to a cell population (cells mL^{-1}) by dividing by the mol C cell^{-1} for Pro and SAR11.

The chemostat has an equal in and out flow, to allow the quantity of seawater to remain constant inside the tank. Nutrients are added to the inflowing water and dissolved compounds (nutrients and metabolic excretion products) and a fraction of the Pro and SAR11 populations are removed in the outflowing stream. By changing the flow rate and upstream nutrient concentrations, the environment within the chemostat can be controlled to explore how competition affects growth rate. As a first experiment, one population of Pro and one of SAR11, each with the β_{opt} found for the non-limiting conditions in Experiment 1 where both Pro and SAR11 grow at 0.20 d^{-1} can be allowed to interact with the ambient pools. This approach can be used to understand how competition influences Pro and SAR11 growth rate, which in isolation should be identical.

As a further step, multiple populations of Pro and SAR11, each with a different value of β could be allowed to compete. This strategy, inspired by oceanographic studies based on resource competition theory (Follows et al., 2007), will allow the chemostat environment to select the best population(s) of Pro and SAR11, based on light investment strategy (β) for the given environment. The model can then be used to explore how the relative abundance of Pro and SAR11 populations, each with a different value of β, varies with ambient nutrient concentrations and competition. This approach could investigate how competition influences β_{opt} compared to modelled scenarios where competition is not considered, i.e. in Chapters 3 and 4 of this thesis.

6.3.2. Incorporating a quantitative description of light harvesting

Chapter 3 highlighted the potential for a decrease in carbon reduction in Pro by up to ~20 % at low irradiance when light energy is directed to photoheterotrophic DON uptake. As Pro plays a significant role in open ocean carbon fixation (Goericke and Welschmeyer, 1993, Zubkov, 2014) photoheterotrophic light use may be important for our understanding of oceanic metabolic balance and its capacity to respond to anthropogenic carbon dioxide release. However, the quantitative value of this result is limited. The harvesting of solar energy in both the Pro and SAR11 models is described using a simple functional response (Section 2.2.1.1) and does not include quantitative detail on harvested solar energy and corresponding the electron flux available and used for photoautotrophy and photoheterotrophy. As a result, the trade-off for solar energy use is conceptual. The specific change in fluxes as a result of the solar energy trade-off, although following a realistic functional response, may not be quantitatively accurate. Incorporating harvested solar energy or irradiance sourced electrons as a model currency to develop a model based on detailed stoichiometry of electron fluxes required to

facilitate known CHO synthesis and DON uptake rates would be useful to gain a more accurate quantitative understanding of the influence of the trade-off for light use on carbon reduction in Pro. The bioenergetic model quantifying the net energy gain in chlorophyll and PR light harvesting systems, developed by Kirchman and Hanson (2012), provides the opportunity to incorporate physiological detail in light harvesting and corresponding electron fluxes. With this model in place of the current functional response, light energy stoichiometry can be built into model based on biochemical theory (White, 2007). It is important to note that it may be challenging to incorporate electron fluxes as a currency into the model presented here due to the difficulties in measuring energy harvesting and storage (Zubkov, 2009).

6.3.3. A more sophisticated description of maintenance and predicting bacterial growth efficiency

The model estimates significantly higher BGE for SAR11 (56 % to 94 %) than measured for bacterioplankton populations in oligotrophic subtropical ecosystems (1-10 %) (Hansell et al., 1995, Alonso and Pernthaler, 2006, Del Giorgio et al., 2011). High respiration rates that result in low BGE in oceanic bacterioplankton are a consequence of high maintenance demands (Del Giorgio and Cole, 1998). Energy requiring processes for maintenance pertinent to open ocean bacterioplankton such as SAR11 may include, high transport costs for nutrient uptake, high exo-enzymatic activity and maintenance of the proton motive force (Del Giorgio and Cole, 1998). None of these processes are, however, described in the model used in this thesis. To incorporate this physiological detail it is not sufficient to modify the maintenance rate parameter in the model as synthesised maintenance biomass is organic. Although increasing the maintenance rate will decrease growth rate at the same ambient conditions, the respiration rate will not change as the cost for biomass synthesis is fixed per unit carbon whether for maintenance or growth. Therefore, BGE will decrease but the change will not represent increased maintenance energy sinks through carbon dioxide respiration. Knowledge of the maintenance requirements specific to SAR11 are absent from the literature. Further field work is required on the processes that result in carbon dioxide respiration and the influence on BGE for SAR11 (and Pro) and more generally for oligotrophic bacterioplankton populations. Such information is essential for understanding whether the open ocean acts as a sink or source of carbon dioxide, where lower BGE estimates point towards it being the latter.

6.3.4. Ammonium release by Pro

Bacterioplankton tend not to release ammonium as long as a carbon source is present (Goldman and Dennett, 1991, Goldman et al., 1987, Goldman and Dennett, 2000). However,

the Pro model releases between ~7 % and 20 % of nitrogen as ammonium (depending on environmental conditions) even when carbon, acquired through photosynthesis, is available. In addition, when irradiance and therefore carbon is limiting, AA which are synthesised at a high cost on carbon are then mobilised as a source of energy resulting in ammonium release, which is physiologically unrealistic. It is recognised that Pro physiology may be significantly different from the heterotrophic bacterioplankton populations, upon which our understanding of the dynamics of ammonium regeneration is based (Goldman and Dennett, 1991, Goldman et al., 1987, Goldman and Dennett, 2000). Nevertheless, an interesting future avenue to explore with the model would be to modify the representation of biomass synthesis in the Pro model, via the sparing and deamination pathways, so that synthesis occurs via the sparing pathway only. The new formulation should be similar to that used to describe AA synthesis currently in the model, where DIN is incorporated with 100 % efficiency and CHO is used as a source of carbon and energy. A similar representation is used by Troost et al. (2005). The incorporation of a greater fraction of total nitrogen uptake when Pro no longer excretes ammonium may influence growth rate and the quantity of solar energy directed to enhance nitrogen uptake via photoheterotrophy.

6.3.5. Maximum rates of uptake

In order to estimate certain parameters a number of assumptions were made. For Pro, it was assumed that the maximum rates of CHO synthesis and DON uptake correspond to situations where the growth rate of the cell is 0.20 d^{-1}, allowing for an estimation of the maximum rate of DIN uptake (Section 2.3.1.4). Due to the significant variation in the observed rates of DON uptake (Gómez-Pereira et al., 2012, Mary et al., 2008a), CHO synthesis and growth rate (Goericke and Welschmeyer, 1993, Zubkov, 2014, Jardillier et al., 2010, Partensky et al., 1999) in Pro, ideally this physiological data should be obtained in the future from a single study, preferably from multiple such studies.

6.4. Conclusion

Experimental evidence increasingly demonstrates that photosynthesis is not the only conduit through which solar energy is channelled to support life on Earth. Photoheterotrophic light use in the two most abundant organisms on our planet, Pro and SAR11, appears to be an essential tool for survival, influencing their distribution and abundance in the open ocean. The construction of two models describing the physiology and metabolism of individual Pro and SAR11 cells and, uniquely, their multiple uses of solar energy, were used to investigate the importance of photoheterotrophic light use for Pro and SAR11 growth rate. The method was

effective in demonstrating that multiple light uses can significantly increase the growth rate of Pro and SAR11 relative to equivalent cell types without the capacity for photoheterotrophy. The effect is critically dependent on the availability of ambient resources.

The results also impact our understanding of how carbon and nitrogen are processed through these abundant organisms, influencing DOM cycling, carbon fixation, respiration and nutrient remineralisation. These results support the requirement for the development of ecosystem models that incorporate photoheterotrophic light use in the bacterioplankton and picophytoplankton components when investigating regions dominated by Pro and SAR11, namely the oligotrophic subtropical gyres.

The theoretical morphosis from Pro to SAR11 carried out in this thesis disentangled the interacting physiological traits that influence their growth rate and ability to coexist in the oligotrophic subtropical gyre ecosystems. This work demonstrated that size is not the only key physiological property exploited to survive and dominate oligotrophic ecosystems. For SAR11, shape is also key for nutrient acquisition. For Pro, the larger size may be essential for housing photosynthetic machinery and maintaining a high biomass C:N, which collectively have a greater positive influence on Pro growth rate than morphology alone does for SAR11. In addition, SAR11 must grow at night in order to balance the significantly superior diurnal growth mode in Pro. Photoheterotrophic light use is of secondary importance for growth rate relative to photosynthesis in Pro and morphology in SAR11. Photoheterotrophy in Pro approximately balances with the ability of SAR11 to grow at night. The benefits that photoheterotrophy confer to SAR11 growth rate are minimal relative to the other physiological properties investigated here.

The work presented in this thesis hopefully marks the start of what will be a fascinating and fruitful field of research modelling the multiple uses of solar energy by microorganisms in the ocean. Illuminating how the planet's two most abundant inhabitants, Pro and SAR11, use solar energy and the consequence for ocean biogeochemistry is paramount for understanding how sunlight influences elemental cycles in the Earth system.

6.5. Figures

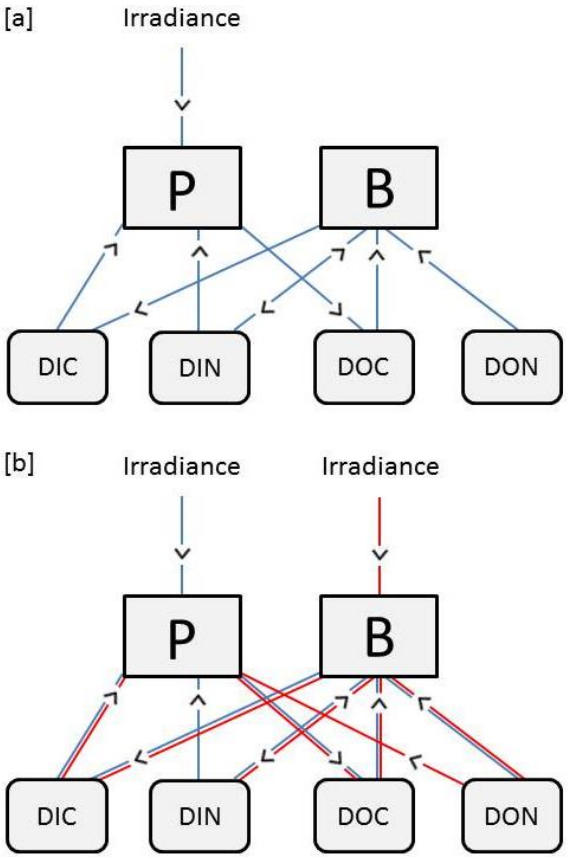

Figure 6.1 [a] A simplified description of the interactions of phytoplankton (P) and bacterioplankton (B) with dissolved inorganic carbon (DIC) and nitrogen (DIN) and dissolved organic carbon (DOC) and nitrogen (DON) based on Anderson and Williams (1998). The schematic omits interactions not associated with phytoplankton and bacterioplankton. [b] The additional red lines show where photoheterotrophic light use influences interactions with ambient pools if Pro and SAR11 are the dominant organisms in the P and B boxes, respectively.

7. Bibliography

AKSNES, D. L. & EGGE, J. K. 1991. {A} theoretical model for nutrient uptake in phytoplankton. *{M}arine {E}cology {P}rogress {S}eries,* 70**,** 65-72.

ALONSO, C. & PERNTHALER, J. 2006. Roseobacter and SAR11 dominate microbial glucose uptake in coastal North Sea waters. *Environmental microbiology,* 8**,** 2022-2030.

ANDERSON, T. & WILLIAMS, P. L. B. 1998. Modelling the seasonal cycle of dissolved organic carbon at Station E 1 in the English Channel. *Estuarine, Coastal and Shelf Science,* 46**,** 93-109.

AZAM, F., FENCHEL, T., FIELD, J. G., GRAY, J. S., MEYER, L. A. & THINGSTAD, F. 1983. The ecological role of water-column microbes in the sea. *Mar. Ecol. Prog. Ser.,* 10**,** 257-263.

BAILEY, S., MELIS, A., MACKEY, K. R., CARDOL, P., FINAZZI, G., VAN DIJKEN, G., BERG, G. M., ARRIGO, K., SHRAGER, J. & GROSSMAN, A. 2008. Alternative photosynthetic electron flow to oxygen in marine Synechococcus. *Biochimica et Biophysica Acta (BBA)-Bioenergetics,* 1777**,** 269-276.

BATTCHIKOVA, N., EISENHUT, M. & ARO, E.-M. 2011. Cyanobacterial NDH-1 complexes: novel insights and remaining puzzles. *Biochimica et Biophysica Acta (BBA)-Bioenergetics,* 1807**,** 935-944.

BEJA, O., ARAVIND, L., KOONIN, E. V., SUZUKI, M. T., HADD, A., NGUYEN, L. P., JOVANOVICH, S. B., GATES, C. M., FELDMAN, R. A., SPUDICH, J. L., SPUDICH, E. N. & DELONG, E. F. 2000. Bacterial Rhodopsin: Evidence for a New Type of Phototrophy in the Sea. *Science,* 289**,** 1902-1906.

BEJA, O., SPUDICH, E. N., SPUDICH, J. L., LECLERC, M. & DELONG, E. F. 2001. Proteorhodopsin phototrophy in the ocean. *Nature,* 411**,** 786-789.

BÉJÀ, O. & SUZUKI, M. T. 2008. Photoheterotrophic marine prokaryotes. *Microbial Ecology of the Oceans, Second Edition***,** 131-157.

BENNER, R. & BIDDANDA, B. 1998. Photochemical Transformations of Surface and Deep Marine Dissolved Organic Matter: Effects on Bacterial Growth. *Limnology and Oceanography,* 43**,** 1373-1378.

BERTILSSON, S., BERGLUND, O., KARL, D. M. & CHISHOLM, S. W. 2003. Elemental composition of marine Prochlorococcus and Synechococcus: Implications for the ecological stoichiometry of the sea. *Limnology and Oceanography,* 48**,** 1721-1731.

BERTILSSON, S., BERGLUND, O., PULLIN, M. J. & CHISHOLM, S. W. 2005. Release of dissolved organic matter by Prochlorococcus. *Vie et Milieu,* 55**,** 225-231.

BERUBE, P. M., BILLER, S. J., KENT, A. G., BERTA-THOMPSON, J. W., ROGGENSACK, S. E., ROACHE-JOHNSON, K. H., ACKERMAN, M., MOORE, L. R., MEISEL, J. D., SHER, D., THOMPSON, L. R., CAMPBELL, L., MARTINY, A. C. & CHISHOLM, S. W. 2014. Physiology and evolution of nitrate acquisition in Prochlorococcus. *ISME J*.

BILLER, S. J., BERUBE, P. M., LINDELL, D. & CHISHOLM, S. W. 2015. Prochlorococcus: the structure and function of collective diversity. *Nat Rev Micro,* 13**,** 13-27.

BRUGGEMAN, J. & KOOIJMAN, S. A. L. M. 2007. A Biodiversity-Inspired Approach to Aquatic Ecosystem Modeling. *Limnology and Oceanography,* 52**,** 1533-1544.

BRYANT, D. A. & FRIGAARD, N.-U. 2006. Prokaryotic photosynthesis and phototrophy illuminated. *Trends in microbiology,* 14**,** 488-496.

CALOW, P. 1977. Conversion efficiencies in heterotrophic organisms. *Biological Reviews,* 52**,** 385-409.

CAPONE, D. G. 2000. The marine microbial nitrogen cycle. *Microbial ecology of the oceans. Wiley-Liss***,** 455-493.

CARDOL, P., FORTI, G. & FINAZZI, G. 2011. Regulation of electron transport in microalgae. *Biochimica et Biophysica Acta (BBA)-Bioenergetics,* 1807**,** 912-918.

CARINI, P., STEINDLER, L., BESZTERI, S. & GIOVANNONI, S. J. 2012. Nutrient requirements for growth of the extreme oligotroph 'Candidatus Pelagibacter ubique'HTCC1062 on a defined medium. *The ISME journal,* 7**,** 592-602.

CARINI, P., STEINDLER, L., BESZTERI, S. & GIOVANNONI, S. J. 2013. Nutrient requirements for growth of the extreme oligotroph /`Candidatus Pelagibacter ubique/' HTCC1062 on a defined medium. *ISME J,* 7**,** 592-602.

CARLSON, C. A. & DUCKLOW, H. W. 1996. Growth of bacterioplankton and consumption of dissolved organic carbon in the Sargasso Sea. *Aquatic Microbial Ecology,* 10**,** 69-85.

CASEY, J. R., LOMAS, M. W., MANDECKI, J. & WALKER, D. E. 2007. Prochlorococcus contributes to new production in the Sargasso Sea deep chlorophyll maximum. *Geophysical Research Letters,* 34.

CHISHOLM, S. W., OLSON, R. J., ZETTLER, E. R., GOERICKE, R., WATERBURY, J. B. & WELSCHMEYER, N. A. 1988. A novel free-living prochlorophyte abundant in the oceanic euphotic zone. *Nature,* 334**,** 340-343.

CHURCH, M. J., DUCKLOW, H. W. & KARL, D. M. 2004. Light Dependence of [3H]Leucine Incorporation in the Oligotrophic North Pacific Ocean. *Appl. Environ. Microbiol.,* 70**,** 4079-4087.

CHURCH, M. J., DUCKLOW, H. W., LETELIER, R. M. & KARL, D. M. 2006. Temporal and vertical dynamics in picoplankton photoheterotrophic production in the subtropical North Pacific Ocean. *Aquatic Microbial Ecology,* 45**,** 41-53.

COTTRELL, M. T. & KIRCHMAN, D. L. 2009. Photoheterotrophic microbes in the Arctic Ocean in summer and winter. *Applied and environmental microbiology,* 75**,** 4958-4966.

COTTRELL, M. T., MICHELOU, V. K., NEMCEK, N., DITULLIO, G. & KIRCHMAN, D. L. 2008. Carbon cycling by microbes influenced by light in the Northeast Atlantic Ocean. *Aquatic microbial ecology,* 50**,** 239-250.

DE VRIES, F., BRUNSTING, A. & VAN LAAR, H. 1974. Products, requirements and efficiency of biosynthesis a quantitative approach. *Journal of theoretical Biology,* 45**,** 339-377.

DEL CARMEN MUÑOZ-MARÍN, M., LUQUE, I., ZUBKOV, M. V., HILL, P. G., DIEZ, J. & GARCÍA-FERNÁNDEZ, J. M. 2013. Prochlorococcus can use the Pro1404 transporter to take up glucose at nanomolar concentrations in the Atlantic Ocean. *Proceedings of the National Academy of Sciences,* 110**,** 8597-8602.

DEL GIORGIO, P. A. & COLE, J. J. 1998. Bacterial growth efficiency in natural aquatic systems. *Annual Review of Ecology and Systematics,* 29**,** 503-541.

DEL GIORGIO, P. A., CONDON, R. H., BOUVIER, T., LONGNECKER, K., BOUVIER, C., SHERR, E. & GASOL, J. M. 2011. Coherent patterns in bacterial growth, growth efficiency, and leucine metabolism along a northeastern Pacific inshore-offshore transect.

DEL GIORGIO, P. A. & DUARTE, C. M. 2002. Respiration in the open ocean. *Nature,* 420**,** 379-384.

DUARTE, C. M., REGAUDIE-DE-GIOUX, A., ARRIETA, J. M., DELGADO-HUERTAS, A. & AGUSTÍ, S. 2013. The Oligotrophic Ocean Is Heterotrophic*. *Marine Science,* 5.

DUCKLOW, H. W. & DONEY, S. C. 2013. What is the metabolic state of the oligotrophic ocean? A debate. *Annual review of marine science,* 5**,** 525-533.

DUHAMEL, S., BJÖRKMAN, K. M. & KARL, D. M. 2012. Light dependence of phosphorus uptake by microorganisms in the subtropical North and South Pacific Ocean. *Aquatic Microbial Ecology,* 67**,** 225-238.

EVANS, C., GÓMEZ-PEREIRA, P. R., MARTIN, A. P., SCANLAN, D. J. & ZUBKOV, M. V. 2015. Photoheterotrophy of bacterioplankton is ubiquitous in the surface oligotrophic ocean. *Progress in Oceanography*.

FALKOWSKI, P. G. & RAVEN, J. A. 2013. *Aquatic photosynthesis*, Princeton University Press.

FASHAM, M., DUCKLOW, H. & MCKELVIE, S. 1990. A nitrogen-based model of plankton dynamics in the oceanic mixed layer. *Journal of Marine Research,* 48**,** 591-639.

FIELD, C. B., BEHRENFELD, M. J., RANDERSON, J. T. & FALKOWSKI, P. 1998. Primary Production of the Biosphere: Integrating Terrestrial and Oceanic Components. *Science,* 281**,** 237-240.

FIELD, K., GORDON, D., WRIGHT, T., RAPPE, M., URBACK, E., VERGIN, K. & GIOVANNONI, S. 1997. Diversity and depth-specific distribution of SAR11 cluster rRNA genes from marine planktonic bacteria. *Applied and Environmental Microbiology,* 63**,** 63-70.

FINKEL, Z. V., BEARDALL, J., FLYNN, K. J., QUIGG, A., REES, T. A. V. & RAVEN, J. A. 2009. Phytoplankton in a changing world: cell size and elemental stoichiometry. *Journal of Plankton Research***,** fbp098.

FOLLOWS, M. J. & DUTKIEWICZ, S. 2010. Modeling Diverse Communities of Marine Microbes. *Annual Review of Marine Science,* 3**,** 427-451.

FOLLOWS, M. J., DUTKIEWICZ, S., GRANT, S. & CHISHOLM, S. W. 2007. Emergent Biogeography of Microbial Communities in a Model Ocean. *Science,* 315**,** 1843-1846.

FUHRMAN, J. A., SCHWALBACH, M. S. & STINGL, U. 2008. Proteorhodopsins: an array of physiological roles? *Nat Rev Micro,* 6**,** 488-494.

FUKUDA, R., OGAWA, H., NAGATA, T. & KOIKE, I. 1998. Direct determination of carbon and nitrogen contents of natural bacterial assemblages in marine environments. *Applied and environmental microbiology,* 64**,** 3352-3358.

GARCIA-FERNANDEZ, J. M., DE MARSAC, N. T. & DIEZ, J. 2004. Streamlined Regulation and Gene Loss as Adaptive Mechanisms in Prochlorococcus for Optimized Nitrogen Utilization in Oligotrophic Environments. *Microbiol. Mol. Biol. Rev.,* 68**,** 630-638.

GARCÍA-FERNÁNDEZ, J. M. & DIEZ, J. 2004. Adaptive mechanisms of nitrogen and carbon assimilatory pathways in the marine cyanobacteria Prochlorococcus. *Research in microbiology,* 155**,** 795-802.

GIOVANNONI, S. J., BIBBS, L., CHO, J.-C., STAPELS, M. D., DESIDERIO, R., VERGIN, K. L., RAPPE, M. S., LANEY, S., WILHELM, L. J., TRIPP, H. J., MATHUR, E. J. & BAROFSKY, D. F. 2005a. Proteorhodopsin in the ubiquitous marine bacterium SAR11. *Nature,* 438**,** 82-85.

GIOVANNONI, S. J., BRITSCHGI, T. B., MOYER, C. L. & FIELD, K. G. 1990. Genetic diversity in Sargasso Sea bacterioplankton.

GIOVANNONI, S. J., TRIPP, H. J., GIVAN, S., PODAR, M., VERGIN, K. L., BAPTISTA, D., BIBBS, L., EADS, J., RICHARDSON, T. H. & NOORDEWIER, M. 2005b. Genome streamlining in a cosmopolitan oceanic bacterium. *science,* 309**,** 1242-1245.

GIOVANNONI, S. J. & VERGIN, K. L. 2012. Seasonality in ocean microbial communities. *Science,* 335**,** 671-676.

GOERICKE, R. & WELSCHMEYER, N. A. 1993. The marine prochlorophyte Prochlorococcus contributes significantly to phytoplankton biomass and primary production in the Sargasso Sea. *Deep Sea Research Part I: Oceanographic Research Papers,* 40**,** 2283-2294.

GOLDMAN, J. & DENNETT, M. 1991. Ammonium regeneration and carbon utilization by marine bacteria grown on mixed substrates. *Marine Biology,* 109**,** 369-378.

GOLDMAN, J. C., CARON, D. A. & DENNETT, M. R. 1987. Regulation of gross growth efficiency and ammonium regeneration in bacteria by substrate C: N ratio. *Limnology and Oceanography***,** 1239-1252.

GOLDMAN, J. C. & DENNETT, M. R. 2000. Growth of marine bacteria in batch and continuous culture under carbon and nitrogen limitation. *Limnology and Oceanography,* 45**,** 789-800.

GÓMEZ-CONSARNAU, L., AKRAM, N., LINDELL, K., PEDERSEN, A., NEUTZE, R., MILTON, D. L., GONZÁLEZ, J. M. & PINHASSI, J. 2010. Proteorhodopsin phototrophy promotes survival of marine bacteria during starvation. *PLoS biology,* 8**,** e1000358.

GÓMEZ-CONSARNAU, L., GONZÁLEZ, J. M., COLL-LLADÓ, M., GOURDON, P., PASCHER, T., NEUTZE, R., PEDRÓS-ALIÓ, C. & PINHASSI, J. 2007. Light stimulates growth of proteorhodopsin-containing marine Flavobacteria. *Nature,* 445**,** 210-213.

GÓMEZ-PEREIRA, P. R., HARTMANN, M., GROB, C., TARRAN, G. A., MARTIN, A. P., FUCHS, B. M., SCANLAN, D. J. & ZUBKOV, M. V. 2012. Comparable light stimulation of organic nutrient uptake by SAR11 and Prochlorococcus in the North Atlantic subtropical gyre. *The ISME journal,* 7**,** 603-614.

GRAZIANO, L., GEIDER, R., LI, W. & OLAIZOLA, M. 1996. Nitrogen limitation of North Atlantic phytoplankton: Analysis of physiological condition in nutrient enrichment experiments. *Aquatic Microbial Ecology,* 11**,** 53-64.

GROB, C., OSTROWSKI, M., HOLLAND, R. J., HELDAL, M., NORLAND, S., ERICHSEN, E. S., BLINDAUER, C., MARTIN, A. P., ZUBKOV, M. V. & SCANLAN, D. J. 2013. Elemental composition of natural populations of key microbial groups in Atlantic waters. *Environmental microbiology,* 15**,** 3054-3064.

HANSELL, D. A., BATES, N. R. & GUNDERSEN, K. 1995. Mineralization of dissolved organic carbon in the Sargasso Sea. *Marine Chemistry,* 51**,** 201-212.

HARTMANN, M., GOMEZ-PEREIRA, P., GROB, C., OSTROWSKI, M., SCANLAN, D. J. & ZUBKOV, M. V. 2014. Efficient CO2 fixation by surface Prochlorococcus in the Atlantic Ocean. *ISME J,* 8**,** 2280-2289.

HARTMANN, M., ZUBKOV, M. V., SCANLAN, D. J. & LEPÈRE, C. 2013. In situ interactions between photosynthetic picoeukaryotes and bacterioplankton in the Atlantic Ocean: evidence for mixotrophy. *Environmental Microbiology Reports,* 5**,** 835-840.

HERRERO, A., MURO-PASTOR, A. M. & FLORES, E. 2001. Nitrogen control in cyanobacteria. *Journal of Bacteriology,* 183**,** 411-425.

HILL, P. G., WARWICK, P. E. & ZUBKOV, M. V. 2013. Low microbial respiration of leucine at ambient oceanic concentration in the mixed layer of the central Atlantic Ocean. *Limnology and oceanography,* 58**,** 1597-1604.

HUTCHINSON, G. E. 1961. The paradox of the plankton. *American Naturalist***,** 137-145.

JARDILLIER, L., ZUBKOV, M. V., PEARMAN, J. & SCANLAN, D. J. 2010. Significant CO2 fixation by small prymnesiophytes in the subtropical and tropical northeast Atlantic Ocean. *The ISME journal,* 4**,** 1180-1192.

JOHNSON, Z. I. & LIN, Y. 2009. Prochlorococcus: Approved for export. *Proceedings of the National Academy of Sciences,* 106**,** 10400-10401.

KARL, D. M. 2002. Nutrient dynamics in the deep blue sea. *TRENDS in Microbiology,* 10**,** 410-418.

KARL, D. M. 2014. Solar energy capture and transformation in the sea. *Elementa: Science of the Anthropocene,* 2**,** 000021.

KARL, D. M., HEBEL, D. V., BJÖRKMAN, K. & LETELIER, R. M. 1998. The role of dissolved organic matter release in the productivity of the oligotrophic North Pacific Ocean.

KETTLER, G. C., MARTINY, A. C., HUANG, K., ZUCKER, J., COLEMAN, M. L., RODRIGUE, S., CHEN, F., LAPIDUS, A., FERRIERA, S., JOHNSON, J., STEGLICH, C., CHURCH, G. M., RICHARDSON, P. & CHISHOLM, S. W. 2007. Patterns and Implications of Gene Gain and Loss in the Evolution of <italic>Prochlorococcus</italic>. *PLoS Genet,* 3**,** e231.

KIRCHMAN, D. L. & HANSON, T. E. 2012. Bioenergetics of photoheterotrophic bacteria in the oceans. *Environmental Microbiology Reports***,** n/a-n/a.

KOLBER, Z. S., PLUMLEY, F. G., LANG, A. S., BEATTY, J. T., BLANKENSHIP, R. E., VANDOVER, C. L., VETRIANI, C., KOBLIZEK, M., RATHGEBER, C. & FALKOWSKI, P. G. 2001. Contribution of Aerobic Photoheterotrophic Bacteria to the Carbon Cycle in the Ocean. *Science,* 292**,** 2492-2495.

KOLBER, Z. S., VAN DOVER, C. L., NIEDERMAN, R. A. & FALKOWSKI, P. G. 2000. Bacterial photosynthesis in surface waters of the open ocean. *Nature,* 407**,** 177-179.

KOOIJMAN, S. A. L. M. 1998. The Synthesizing Unit as model for the stoichiometric fusion and branching of metabolic fluxes. *Biophysical Chemistry,* 73**,** 179-188.

KOOIJMAN, S. A. L. M. 2010. *Dynamic Energy Budget Theory for Metabolic Organisation*, Cambridge University Press.

KOOIJMAN, S. A. L. M., DIJKSTRA, H. A. & KOOI, B. W. 2002. Light-induced Mass Turnover in a Mono-species Community of Mixotrophs. *Journal of Theoretical Biology,* 214**,** 233-254.

KUIJPER, L. D. J., ANDERSON, T. R. & KOOIJMAN, S. A. L. M. 2004. C and N gross growth efficiencies of copepod egg production studied using a Dynamic Energy Budget model. *Journal of Plankton Research,* 26**,** 213-226.

KUJAWINSKI, E. B. 2011. The impact of microbial metabolism on marine dissolved organic matter. *Annual review of marine science,* 3**,** 567-599.

KUJAWINSKI, E. B., LONGNECKER, K., BLOUGH, N. V., VECCHIO, R. D., FINLAY, L., KITNER, J. B. & GIOVANNONI, S. J. 2009. Identification of possible source markers in marine dissolved organic matter using ultrahigh resolution mass spectrometry. *Geochimica et Cosmochimica Acta,* 73**,** 4384-4399.

LAMI, R., COTTRELL, M. T., CAMPBELL, B. J. & KIRCHMAN, D. L. 2009. Light-dependent growth and proteorhodopsin expression by Flavobacteria and SAR11 in experiments with Delaware coastal waters. *Environmental Microbiology,* 11**,** 3201-3209.

LINDELL, D., ERDNER, D., MARIE, D., PRÁŠIL, O., LE GALL, F., RIPPKA, R., PARTENSKY, F., SCANLAN, D. J. & POST, A. F. 2002. NITROGEN STRESS RESPONSE OF PROCHLOROCOCCUS STRAIN PCC 9511 (OXYPHOTOBACTERIA) INVOLVES CONTRASTING REGULATION OF ntcA AND amt11. *Journal of phycology,* 38**,** 1113-1124.

LITCHMAN, E., KLAUSMEIER, C. A., SCHOFIELD, O. M. & FALKOWSKI, P. G. 2007. The role of functional traits and trade-offs in structuring phytoplankton communities: scaling from cellular to ecosystem level. *Ecology Letters,* 10**,** 1170-1181.

LIU, H., CAMPBELL, L., LANDRY, M., NOLLA, H., BROWN, S. & CONSTANTINOU, J. 1998. Prochlorococcus and Synechococcus growth rates and contributions to production in the Arabian Sea during the 1995 Southwest and Northeast Monsoons. *Deep Sea Research Part II: Topical Studies in Oceanography,* 45**,** 2327-2352.

LIU, H., HA, N. & L, C. 1997. Prochlorococcus growth rate and contribution to primary production in the equatorial and subtropical North Pacific Ocean. *Aquatic Microbial Ecology,* 12**,** 39-47.

LIU, H., LANDRY, M. R., VAULOT, D. & CAMPBELL, L. 1999. Prochlorococcus growth rates in the central equatorial Pacific: An application of the ƒmax approach. *Journal of Geophysical Research: Oceans (1978–2012),* 104**,** 3391-3399.

LONGHURST, A., SATHYENDRANATH, S., PLATT, T. & CAVERHILL, C. 1995. An estimate of global primary production in the ocean from satellite radiometer data. *Journal of Plankton Research,* 17**,** 1245-1271.

LÓPEZ-LOZANO, A., DIEZ, J., EL ALAOUI, S., MORENO-VIVIÁN, C. & GARCÍA-FERNÁNDEZ, J. M. 2002. Nitrate is reduced by heterotrophic bacteria but not transferred to Prochlorococcus in non-axenic cultures. *FEMS microbiology ecology,* 41**,** 151-160.

MACKENZIE, T. D., BURNS, R. A. & CAMPBELL, D. A. 2004. Carbon status constrains light acclimation in the cyanobacterium Synechococcus elongatus. *Plant physiology,* 136**,** 3301-3312.

MALMSTROM, R. R., COTTRELL, M. T., ELIFANTZ, H. & KIRCHMAN, D. L. 2005. Biomass Production and Assimilation of Dissolved Organic Matter by SAR11 Bacteria in the Northwest Atlantic Ocean. *Appl. Environ. Microbiol.,* 71**,** 2979-2986.

MALMSTROM, R. R., KIENE, R. P., COTTRELL, M. T. & KIRCHMAN, D. L. 2004. Contribution of SAR11 Bacteria to Dissolved Dimethylsulfoniopropionate and Amino Acid Uptake in the North Atlantic Ocean. *Appl. Environ. Microbiol.,* 70**,** 4129-4135.

MARAÑÓN, E., CERMEÑO, P., FERNÁNDEZ, E., RODRÍGUEZ, J. & ZABALA, L. 2004. Significance and mechanisms of photosynthetic production of dissolved organic carbon in a coastal eutrophic ecosystem. *Limnology and Oceanography,* 49**,** 1652-1666.

MARANON, E., CERMENO, P., LÓPEZ-SANDOVAL, D. C., RODRÍGUEZ-RAMOS, T., SOBRINO, C., HUETE-ORTEGA, M., BLANCO, J. M. & RODRIGUEZ, J. 2013. Unimodal size scaling of

phytoplankton growth and the size dependence of nutrient uptake and use. *Ecology letters,* 16**,** 371-379.

MÅRDÉN, P., NYSTRÖM, T. & KJELLEBERG, S. 1987. Uptake of leucine by a marine Gram-negative heterotrophic bacterium during exposure to starvation conditions. *FEMS microbiology letters,* 45**,** 233-241.

MARTINEZ-GARCIA, M., SWAN, B. K., POULTON, N. J., GOMEZ, M. L., MASLAND, D., SIERACKI, M. E. & STEPANAUSKAS, R. 2012. High-throughput single-cell sequencing identifies photoheterotrophs and chemoautotrophs in freshwater bacterioplankton. *The ISME journal,* 6**,** 113-123.

MARTINY, A. C., KATHURIA, S. & BERUBE, P. M. 2009. Widespread metabolic potential for nitrite and nitrate assimilation among Prochlorococcus ecotypes. *Proceedings of the National Academy of Sciences,* 106**,** 10787-10792.

MARY, I., HEYWOOD, J., FUCHS, B., AMANN, R., TARRAN, G., BURKILL, P. & ZUBKOV, M. 2006. SAR11 dominance among metabolically active low nucleic acid bacterioplankton in surface waters along an Atlantic meridional transect. *Aquatic microbial ecology,* 45**,** 107-113.

MARY, I., TARRAN, G. A., WARWICK, P. E., TERRY, M. J., SCANLAN, D. J., BURKILL, P. H. & ZUBKOV, M. V. 2008a. Light enhanced amino acid uptake by dominant bacterioplankton groups in surface waters of the Atlantic Ocean. *FEMS microbiology ecology,* 63**,** 36-45.

Light enhanced amino acid uptake by dominant bacterioplankton groups in surface waters of the Atlantic Ocean, 2008b. Directed by MARY, I., TARRAN, G. A., WARWICK, P. E., TERRY, M. J., SCANLAN, D. J., BURKILL, P. H. & ZUBKOV, M. V.: Blackwell Publishing Ltd.

MCDONALD, A. E., IVANOV, A. G., BODE, R., MAXWELL, D. P., RODERMEL, S. R. & HÜNER, N. P. 2011. Flexibility in photosynthetic electron transport: the physiological role of plastoquinol terminal oxidase (PTOX). *Biochimica et Biophysica Acta (BBA)-Bioenergetics,* 1807**,** 954-967.

MICHELOU, V. K., COTTRELL, M. T. & KIRCHMAN, D. L. 2007. Light-Stimulated Bacterial Production and Amino Acid Assimilation by Cyanobacteria and Other Microbes in the North Atlantic Ocean. *Appl. Environ. Microbiol.,* 73**,** 5539-5546.

MOLONEY, C. L. & FIELD, J. G. 1991. The size-based dynamics of plankton food webs. I. A simulation model of carbon and nitrogen flows. *Journal of Plankton Research,* 13**,** 1003-1038.

MOORE, L. R., ANTON, F. P., ROCAP, G. & CHISHOLM, S. W. 2002. Utilization of Different Nitrogen Sources by the Marine Cyanobacteria Prochlorococcus and Synechococcus. *Limnology and Oceanography,* 47**,** 989-996.

MOORE, L. R. & CHISHOLM, S. W. 1999. Photophysiology of the Marine Cyanobacterium Prochlorococcus: Ecotypic Differences among Cultured Isolates. *Limnology and Oceanography,* 44**,** 628-638.

MOORE, L. R., ROCAP, G. & CHISHOLM, S. W. 1998. Physiology and molecular phylogeny of coexisting Prochlorococcus ecotypes. *Nature,* 393**,** 464-467.

MOREL, A., AHN, Y.-H., PARTENSKY, F., VAULOT, D. & CLAUSTRE, H. 1993. Prochlorococcus and Synechococcus: A comparative study of their optical properties in relation to their size and pigmentation. *Journal of Marine Research,* 51**,** 617-649.

MORITA, R. Y. 1997. Bacteria in oligotrophic environments.

MORRIS, R. M., RAPPE, M. S., CONNON, S. A., VERGIN, K. L., SIEBOLD, W. A., CARLSON, C. A. & GIOVANNONI, S. J. 2002. SAR11 clade dominates ocean surface bacterioplankton communities. *Nature,* 420**,** 806-810.

NASELLI-FLORES, L., PADISÁK, J. & ALBAY, M. 2007. Shape and size in phytoplankton ecology: do they matter? *Hydrobiologia,* 578**,** 157-161.

OBERNOSTERER, I., REITNER, B. & HERNDL, G. J. 1999. Contrasting Effects of Solar Radiation on Dissolved Organic Matter and Its Bioavailability to Marine Bacterioplankton. *Limnology and Oceanography,* 44**,** 1645-1654.

OGAWA, T. & MI, H. 2007. Cyanobacterial NADPH dehydrogenase complexes. *Photosynthesis research,* 93**,** 69-77.

PAERL, H. W. 1991. Ecophysiological and Trophic Implications of Light-Stimulated Amino Acid Utilization in Marine Picoplankton. *Appl. Environ. Microbiol.,* 57**,** 473-479.

PARTENSKY, F., HESS, W. R. & VAULOT, D. 1999. Prochlorococcus, a Marine Photosynthetic Prokaryote of Global Significance. *Microbiol. Mol. Biol. Rev.,* 63**,** 106-127.

POLOVINA, J. J., HOWELL, E. A. & ABECASSIS, M. 2008. Ocean's least productive waters are expanding. *Geophys. Res. Lett.,* 35**,** L03618.

RAPPÉ, M. S., CONNON, S. A., VERGIN, K. L. & GIOVANNONI, S. J. 2002. Cultivation of the ubiquitous SAR11 marine bacterioplankton clade. *Nature,* 418**,** 630-633.

RAVEN, J. 1998. The twelfth Tansley Lecture. Small is beautiful: the picophytoplankton. *Functional ecology,* 12**,** 503-513.

RAVEN, J. A. 1994. Why are there no picoplanktonic O2 evolvers with volumes less than 10− 19 m3? *Journal of plankton research,* 16**,** 565-580.

RAVEN, J. A., BEARDALL, J., LARKUM, A. W. & SÁNCHEZ-BARACALDO, P. 2013. Interactions of photosynthesis with genome size and function. *Philosophical Transactions of the Royal Society B: Biological Sciences,* 368**,** 20120264.

ROCAP, G., LARIMER, F. W., LAMERDIN, J., MALFATTI, S., CHAIN, P., AHLGREN, N. A., ARELLANO, A., COLEMAN, M., HAUSER, L. & HESS, W. R. 2003. Genome divergence in two Prochlorococcus ecotypes reflects oceanic niche differentiation. *Nature,* 424**,** 1042-1047.

SARMIENTO, J. L. 2013. *Ocean biogeochemical dynamics*, Princeton University Press.

SCHWALBACH, M., TRIPP, H., STEINDLER, L., SMITH, D. & GIOVANNONI, S. 2010. The presence of the glycolysis operon in SAR11 genomes is positively correlated with ocean productivity. *Environmental microbiology,* 12**,** 490-500.

SHIBA, T., SIMIDU, U. & TAGA, N. 1979. Distribution of Aerobic Bacteria Which Contain Bacteriochlorophyll a. *Appl. Environ. Microbiol.,* 38**,** 43-45.

SIMON, M. & AZAM, F. 1989. Protein content and protein synthesis rates of planktonic marine bacteria. *Marine ecology progress series. Oldendorf,* 51**,** 201-213.

SOUSA, T., DOMINGOS, T., POGGIALE, J.-C. & KOOIJMAN, S. 2010. Dynamic energy budget theory restores coherence in biology. *Philosophical Transactions of the Royal Society B: Biological Sciences,* 365**,** 3413-3428.

SOWELL, S. M., WILHELM, L. J., NORBECK, A. D., LIPTON, M. S., NICORA, C. D., BAROFSKY, D. F., CARLSON, C. A., SMITH, R. D. & GIOVANONNI, S. J. 2008. Transport functions dominate the SAR11 metaproteome at low-nutrient extremes in the Sargasso Sea. *The ISME journal,* 3**,** 93-105.

STANCA, E., CELLAMARE, M. & BASSET, A. 2013. Geometric shape as a trait to study phytoplankton distributions in aquatic ecosystems. *Hydrobiologia,* 701**,** 99-116.

STEINDLER, L., SCHWALBACH, M. S., SMITH, D. P., CHAN, F. & GIOVANNONI, S. J. 2011. Energy starved Candidatus Pelagibacter ubique substitutes light-mediated ATP production for endogenous carbon respiration. *PLoS One,* 6**,** e19725.

STOECKER, D. K. 1998. Conceptual models of mixotrophy in planktonic protists and some ecological and evolutionary implications. *European Journal of Protistology,* 34**,** 281-290.

STRAZA, T. R. & KIRCHMAN, D. L. 2011. Single-cell response of bacterial groups to light and other environmental factors in the Delaware Bay, USA. *Aquatic Microbial Ecology,* 62**,** 267-277.

SULLIVAN, M. B., WATERBURY, J. B. & CHISHOLM, S. W. 2003. Cyanophages infecting the oceanic cyanobacterium Prochlorococcus. *Nature,* 424**,** 1047-1051.

SUTTLE, C. A., FUHRMAN, J. A. & CAPONE, D. G. 1990. Rapid ammonium cycling and concentration-dependent partitioning of ammonium and phosphate: implications for carbon transfer in planktonic communities. *Limnology and Oceanography,* 35**,** 424-433.

TAYLOR, A. H. & JOINT, I. 1990. Steady-State Analysis of the' Microbial Loop' in Stratified Systems. *Marine Ecology Progress Series MESEDT,* 59.

TOLONEN, A. C., AACH, J., LINDELL, D., JOHNSON, Z. I., RECTOR, T., STEEN, R., CHURCH, G. M. & CHISHOLM, S. W. 2006. Global gene expression of Prochlorococcus ecotypes in response to changes in nitrogen availability. *Molecular systems biology,* 2.

TREUSCH, A. H., VERGIN, K. L., FINLAY, L. A., DONATZ, M. G., BURTON, R. M., CARLSON, C. A. & GIOVANNONI, S. J. 2009. Seasonality and vertical structure of microbial communities in an ocean gyre. *ISME J,* 3**,** 1148-1163.

TRIPP, H. J. 2013. The unique metabolism of SAR11 aquatic bacteria. *Journal of Microbiology,* 51**,** 147-153.

TROOST, T. A., KOOI, B. W. & KOOIJMAN, S. A. L. M. 2005. When do mixotrophs specialize? Adaptive dynamics theory applied to a dynamic energy budget model. *Mathematical Biosciences,* 193**,** 159-182.

VALLINO, J. 2000. Improving marine ecosystem models: use of data assimilation and mesocosm experiments. *Journal of Marine Research,* 58**,** 117-164.

VALLINO, J., HOPKINSON, C. & HOBBIE, J. 1996. Modeling bacterial utilization of dissolved organic matter: optimization replaces Monod growth kinetics. Limnol.

WALTER, J. M., GREENFIELD, D., BUSTAMANTE, C. & LIPHARDT, J. 2007. Light-powering Escherichia coli with proteorhodopsin. *Proceedings of the National Academy of Sciences,* 104**,** 2408-2412.

WATERBURY, J. B., STANLEY W, W., ROBERT R. L, G. & LARRY E, B. 1979. Widespread occurrence of a unicellular, marine, planktonic, cyanobacterium. Nature Publishing Group.

WHITE, D. 2007. *The physiology and biochemistry of prokaryotes*, Oxford University Press.

WILKEN, S., SCHUURMANS, J. M. & MATTHIJS, H. C. 2014. Do mixotrophs grow as photoheterotrophs? Photophysiological acclimation of the chrysophyte Ochromonas danica after feeding. *New Phytologist,* 204**,** 882-889.

WILLIAMS, P. J. L. B., QUAY, P. D., WESTBERRY, T. K. & BEHRENFELD, M. J. 2013. The Oligotrophic Ocean Is Autotrophic*. *Annual review of marine science,* 5**,** 535-549.

YOUNG, K. D. 2006. The selective value of bacterial shape. *Microbiology and molecular biology reviews,* 70**,** 660-703.

YOUNG, K. D. 2007. Bacterial morphology: why have different shapes? *Current opinion in microbiology,* 10**,** 596-600.

YURKOV, V. V. & BEATTY, J. T. 1998. Aerobic Anoxygenic Phototrophic Bacteria. *Microbiol. Mol. Biol. Rev.,* 62**,** 695-724.

ZEHR, J. P. & KUDELA, R. M. 2009. Photosynthesis in the open ocean. *Science,* 326**,** 945.

ZEHR, J. P. & KUDELA, R. M. 2011. Nitrogen cycle of the open ocean: from genes to ecosystems. *Annual review of marine science,* 3**,** 197-225.

ZHAO, Y., TEMPERTON, B., THRASH, J. C., SCHWALBACH, M. S., VERGIN, K. L., LANDRY, Z. C., ELLISMAN, M., DEERINCK, T., SULLIVAN, M. B. & GIOVANNONI, S. J. 2013. Abundant SAR11 viruses in the ocean. *Nature,* 494**,** 357-360.

ZINSER, E. R., JOHNSON, Z. I., COE, A., KARACA, E., VENEZIANO, D. & CHISHOLM, S. W. 2007. Influence of light and temperature on Prochlorococcus ecotype distributions in the Atlantic Ocean. *Limnology and Oceanography,* 52**,** 2205-2220.

ZUBKOV, M. V. 2009. Photoheterotrophy in marine prokaryotes. *Journal of Plankton Research,* 31**,** 933-938.

ZUBKOV, M. V. 2014. Faster growth of the major prokaryotic versus eukaryotic CO2 fixers in the oligotrophic ocean. *Nat Commun,* 5.

ZUBKOV, M. V., FUCHS, B. M., TARRAN, G. A., BURKILL, P. H. & AMANN, R. 2003. High Rate of Uptake of Organic Nitrogen Compounds by Prochlorococcus Cyanobacteria as a Key to Their Dominance in Oligotrophic Oceanic Waters. *Appl. Environ. Microbiol.,* 69**,** 1299-1304.

ZUBKOV, M. V., SLEIGH, M. A. & BURKILL, P. H. 2000. Assaying picoplankton distribution by flow cytometry of underway samples collected along a meridional transect across the Atlantic Ocean. *Aquatic Microbial Ecology,* 21**,** 13-20.

ZUBKOV, M. V., SLEIGH, M. A., TARRAN, G. A., BURKILL, P. H. & LEAKEY, R. J. G. 1998. Picoplanktonic community structure on an Atlantic transect from 50°N to 50°S. *Deep Sea Research Part I: Oceanographic Research Papers,* 45**,** 1339-1355.

ZUBKOV, M. V. & TARRAN, G. A. 2005. Amino acid uptake of Prochlorococcus spp. in surface waters across the South Atlantic Subtropical Front. *Aquatic Microbial Ecology,* 40**,** 241-249.

ZUBKOV, M. V., TARRAN, G. A. & FUCHS, B. M. 2004a. Depth related amino acid uptake by Prochlorococcus cyanobacteria in the Southern Atlantic tropical gyre. *FEMS microbiology ecology,* 50**,** 153-161.

Depth related amino acid uptake by Prochlorococcus cyanobacteria in the Southern Atlantic tropical gyre, 2004b. Directed by ZUBKOV, M. V., TARRAN, G. A. & FUCHS, B. M.: Blackwell Publishing Ltd.

ZUBKOV, M. V., TARRAN, G. A., MARY, I. & FUCHS, B. M. 2008. Differential microbial uptake of dissolved amino acids and amino sugars in surface waters of the Atlantic Ocean. *Journal of Plankton Research,* 30**,** 211-220.